

Seagrass as a Sustainable Alternative for Building Materials: Assessing its Feasibility, Processing Methods, and Performance in Construction

A dissertation submitted to attain the degree of
Doctor of Philosophy of the Faculty of Forest Sciences and Forest Ecology at the
University of Göttingen

Submitted by

Aldi Kuqo

M.Sc. in Industrial and Environmental Chemistry, University of Tirana

born in Pogradec, Albania

Göttingen 2023

Supervision Committee

Prof. Dr. Carsten Mai

Department of Wood Biology and Wood Products, Georg-August University of Göttingen, Göttingen, Germany

Prof. Dr. Kai Zhang

Department of Wood Technology and Wood-based Composites, Georg-August University of Göttingen, Göttingen, Germany

Dr. Tim Koddenberg

Department of Wood Biology and Wood Products, Georg-August University of Göttingen, Göttingen, Germany

Examination Committee

- **Prof. Dr. Carsten Mai**

Department of Wood Biology and Wood Products, Georg-August University of Göttingen, Göttingen, Germany

- **Prof. Dr. Kai Zhang**

Department of Wood Technology and Wood-based Composites, Georg-August University of Göttingen, Göttingen, Germany

- **Prof. Dr. Stergios Adamopoulos**

Department of Forest Biomaterials and Technology, Swedish University of Agricultural Sciences, Uppsala, Sweden

- **PD. Dr. Markus Euring**

Department of Wood Technology and Wood-based Composites, Georg-August University of Göttingen, Göttingen, Germany

- **Prof. Dr. Rupert Wimmer**

Institute of Wood Technology and Renewable Materials, University of Natural Resources and Life Sciences (BOKU), Vienna, Austria

Date of oral examination: **21.09.2023**

This cumulative dissertation describes the framework of the work and presents the research results in a short form. The detailed results have already been published in the following articles attached to the dissertation:

1. Kuqo, A., and Mai, C. (2021). Mechanical properties of lightweight gypsum composites comprised of seagrass *Posidonia oceanica* and pine (*Pinus sylvestris*) wood fibers. *Construction and Building Materials*, 282, 122714.
2. Mayer*, A. K., Kuqo*, A., Koddenberg, T., and Mai, C. (2022). Seagrass-and wood-based cement boards: A comparative study in terms of physico-mechanical and structural properties. *Composites Part A: Applied Science and Manufacturing*, 156, 106864. (*Co-first authors)
3. Kuqo, A., Koddenberg, T., and Mai, C. (2023). Use of dry mixing-spraying process for the production of geopolymer-bonded wood and seagrass fibreboards. *Composites Part B: Engineering*, 248, 110387.
4. Kuqo, A., Mayer, A. K., Amiandamhen, S. O., Adamopoulos, S., and Mai, C. (2023). Enhancement of physico-mechanical properties of geopolymer particleboards through the use of seagrass fibers. *Construction and Building Materials*, 374, 130889.
5. Kuqo, A., and Mai, C. (2022). Seagrass leaves: An alternative resource for the production of insulation materials. *Materials*, 15(19), 6933.
6. Kuqo, A., and Mai, C. (2023). Flexible Insulation Mats from *Zostera marina* Seagrass. *Journal of Natural Fibers*, 20(1), 2154303.

Acknowledgements

I would like to express my gratitude to Prof. Carsten Mai for his guidance, unwavering support, and invaluable insights throughout my doctoral studies. His expertise, dedication, and advice have played a pivotal role in shaping the trajectory of this research. I am also deeply thankful to my second supervisor, Prof. Kai Zhang, for his support throughout the course of this study. I would like to extend my appreciation to Tim Koddenberg and André Klüppel for their valuable contributions and assistance during various stages of this research. Their input and collaboration are greatly appreciated.

I am grateful to the German Academic Exchange Service (**DAAD**) for providing the financial support that made this study possible. Their support has been instrumental in enabling me to undertake this research endeavor.

I would like to express my heartfelt thanks to all my colleagues in the Department of Wood Biology and Wood Products. Their insightful discussions have been invaluable in shaping new ideas and approaches in this study.

Furthermore, I am grateful for the guidance provided by Prof. Nikolla Dhamo, my Master's thesis supervisor at the University of Tirana. His support was instrumental in developing the research proposal for my subsequent doctoral studies. I am also thankful to Prof. Pranvera Lazo and Prof. Teuta Dilo for their support during the application process for the DAAD scholarship. I would also like to extend my appreciation to my colleagues at the Department of Industrial Chemistry at the University of Tirana for their support.

Abstract

Seagrasses are vital contributors to the ecosystem, absorbing atmospheric CO₂ and generating oxygen for marine life. However, when they decompose, the accumulated biomass along the shores can lead to concerns like CO₂ and CH₄ emissions and eutrophication. Although seagrass remains are essential for local habitats, they hinder the scenic beauty of tourist beaches. Instead of landfilling this biomass, it can be transformed into building materials. This study aims to investigate the main characteristics of seagrass, suitable processing methods and combinations with several binders to produce building products.

Lightweight gypsum composite materials containing seagrass fibers (*Posidonia oceanica*) were prepared by casting. Seagrass fibers were added to the gypsum paste at a proportion of up to 6 wt%. The seagrass-based composites were compared with pure gypsum composites and those based on wood fibers. The results revealed that at a low proportion of fibers, seagrass had no significant effect on the bending and compression properties of the composites, unlike the wood fiber composites which exhibited increased strength even compared to pure gypsum ones. Still, the inclusion of seagrass fibers led to a significant increase in the roughness of the composites.

Further investigations focused on the production of fiberboards using seagrass fibers (*Posidonia oceanica*) as the raw material, both with Portland cement. A comparison was made between the seagrass-based cement boards and those made from wood particles. The chemical analysis of the raw materials and their effect on cement hydration was conducted prior to the production of boards. Cement powder was mixed with a large proportion of lignocellulosic material (up to 52 wt%). The blend was hot-pressed, conditioned for 28 days, and then cut into testing samples. Mechanical and physical tests were performed to evaluate the properties of the boards. Additionally, a structural analysis was carried out using a 3D digital microscope and micro-CT to examine the bonding and failure mechanisms of both intact and broken samples. The seagrass cement bonded boards exhibited much higher mechanical and physical performance compared to wood particleboards bonded with cement. The high strength and resistance to water and heat can be attributed to the morphology of the seagrass fibers, characterized by their long and flexible nature (high aspect ratio), as well as their chemical composition. Leachates released from seagrass fibers did not seem to significantly affect cement hydration, making them a compatible material for use in cement fiberboard production.

Geopolymer-bonded seagrass-based boards, similar to cement bonded boards, were produced using the dry mixing-spraying process and they were compared to boards made from wood fibers. This technique allowed for the mixing and pressing of large amounts of lignocellulosic materials to obtain strong boards. The objective of this part of the study was to produce geopolymer bonded boards with high lignocellulosic content, with proportions of up to 50 wt%. Mechanical tests, including bending strength, screw withdrawal test, and internal bond tests, were conducted, along with physical tests such as cone calorimetry, water absorption, and thickness swelling. The distribution of the binder and the effectiveness of the dry mixing process were assessed through microscopy techniques such as SEM, 3D microscope, and micro-CT. The results demonstrated that seagrass-based fiberboards exhibited significantly better performance compared to wood fiberboards. It was concluded that the adequacy of mixing was influenced by the size and morphology of the mixed aggregates.

Sandwich boards bonded with geopolymer binder were also produced using the dry mixing spraying process. When seagrass fibers were allocated in the outer parts of geopolymer bonded wood-based particleboards, they acted as reinforcements, resulting in an increase in the bending strength of the

boards. The performance of these boards was compared to that of commercial cement boards. Besides performing mechanical and physical tests, additional investigations were conducted to assess the mixing efficiency of metakaolin and the alkaline activator. This evaluation involved adding a colorant to the alkaline activator and subsequently using microscopy investigations to analyze the geopolymer paste. The incorporation of seagrass fibers appeared to enhance the bending strength of the geopolymer sandwich boards and provided a slight improvement in fire protection.

Insulation boards were manufactured using seagrass leaves and pMDI as a binder. Seagrass leaves from two species of seagrass were used in this study (*Posidonia oceanica* and *Zostera marina*). The mechanical and physical properties of the low-density boards (densities ranging from 80 to 200 kg m⁻³) were evaluated according to the standard requirements for insulation boards. Thermal conductivity measurements were conducted using a heat flow meter, and fire resistance was assessed through cone calorimetry and single flame tests. An economic analysis was performed to assess the production cost and profitability of seagrass insulation boards compared to those made from wood fibers. The seagrass leaves boards exhibited low thermal conductivity similar to wood fiber boards, as well as high fire resistance. Cost analysis indicated that seagrass leaves are a cost-effective alternative to wood fibers due to low raw material costs, minimal energy requirements for production, and the potential for reduced fire-retardant usage. Additionally, flexible mats were produced using *Zostera marina* and bicomponent fibers as a binding agent. The correlation between compression, internal bond strength, flexibility, and density was assessed through a vertical density profile analysis and microscopy analysis. These mats displayed high elasticity and a thermal conductivity ranging from 0.039 to 0.051 W m⁻¹K⁻¹.

Overall, the use of seagrass fibers and leaves to produce building materials appears to be a promising approach for its effective utilization. After the end of life, seagrass biomass can be further utilized, extending its life cycle and promoting sustainable practices in the construction industry.

Zusammenfassung

Seegräser leisten einen wichtigen Beitrag zum Ökosystem, indem sie CO₂ aus der Atmosphäre absorbieren und Sauerstoff für das Meeresleben erzeugen. Wenn sie sich jedoch zersetzen, kann die angesammelte Biomasse an den Ufern zu Problemen wie CO₂- und CH₄-Emissionen und Eutrophierung führen. Obwohl Seegrasreste für lokale Lebensräume wichtig sind, beeinträchtigen sie die landschaftliche Schönheit von Touristenstränden. Anstatt diese Biomasse zu deponieren, kann sie in Baumaterialien umgewandelt werden. Ziel dieser Studie ist es, die wichtigsten Eigenschaften von Seegras, geeignete Verarbeitungsmethoden und Kombinationen mit verschiedenen Bindemitteln zur Herstellung von Bauprodukten zu untersuchen.

Leichte Gipsverbundwerkstoffe, die Seegrasfasern (*Posidonia oceanica*) enthalten, wurden durch Gießen hergestellt. Seegrasfasern wurden in den Gipsbrei bis zu einem Anteil von 6 Gewichtsprozent zugegeben. Die seegrasbasierten Verbundwerkstoffe wurden mit reinen Gipsverbundwerkstoffen und solchen auf Holzfasernbasis verglichen. Die Ergebnisse zeigten, dass Seegras bei einem geringen Anteil an Fasern keinen signifikanten Einfluss auf die Biege- und Druckeigenschaften der Verbundwerkstoffe hatte, im Gegensatz zu den Holzfaserverbundwerkstoffen, die sogar im Vergleich zu reinen Gipswerkstoffen eine höhere Festigkeit aufwiesen. Dennoch führte die Beimischung von Seegrasfasern zu einer signifikanten Erhöhung der Rauheit der Verbundwerkstoffe.

Weitere Untersuchungen konzentrierten sich auf die Herstellung von Faserplatten unter Verwendung von Seegrasfasern (*Posidonia oceanica*) als Rohmaterial, sowohl mit Portlandzement. Es wurde ein Vergleich zwischen den seegrasbasierten Zementplatten und solchen aus Holzpartikeln angestellt. Vor der Herstellung der Platten erfolgte eine chemische Analyse der Rohmaterialien und deren Auswirkung auf die Zementhydratation. Zementpulver wurde mit einem großen Anteil lignozellulosischem Material (bis zu 52 Gewichtsprozent) gemischt. Die Mischung wurde heißgepresst, 28 Tage lang konditioniert und anschließend in Testproben geschnitten. Mechanische und physikalische Tests wurden durchgeführt, um die Eigenschaften der Platten zu bewerten. Zusätzlich wurde eine strukturelle Analyse mit einem 3D-Digitalmikroskop und einer micro-CT durchgeführt, um die Bindungs- und Versagensmechanismen sowohl intakter als auch gebrochener Proben zu untersuchen. Die seegrasgebundenen Zementplatten zeigten im Vergleich zu mit Zement gebundenen Holzspanplatten eine wesentlich höhere mechanische und physikalische Leistung. Die hohe Festigkeit und Beständigkeit gegenüber Wasser und Hitze kann auf die Morphologie der Seegrasfasern zurückgeführt werden, die durch ihre lange und flexible Natur (hoher Aspektverhältnis) sowie ihre chemische Zusammensetzung gekennzeichnet sind. Auslaugungen aus Seegrasfasern schienen die Zementhydratation nicht signifikant zu beeinflussen, was sie zu einem kompatiblen Material für die Verwendung in der Herstellung von Zementfaserplatten macht.

Geopolymer-gebundene, seegrasbasierte Platten wurden ähnlich wie zementgebundene Platten mit dem Trockenmisch-Sprühverfahren hergestellt und mit Platten aus Holzfasern verglichen. Diese Technik ermöglichte das Mischen und Pressen großer Mengen lignozellulosischer Materialien, um starke Platten zu erhalten. Ziel dieses Teils der Studie war es, geopolymergebundene Platten mit einem hohen lignozellulosischen Gehalt von bis zu 50 Gewichtsprozent herzustellen. Mechanische Tests, einschließlich Biegefestigkeit, Schraubenrückzugstest und Innenausreißfestigkeit, wurden durchgeführt, sowie physikalische Tests wie Kegelkalorimetrie, Wasseraufnahme und Dickenquellung. Die Verteilung des Bindemittels und die Effektivität des Trockenmischverfahrens wurden mit Hilfe von Mikroskopieverfahren wie SEM, 3D-Mikroskop und micro-CT bewertet. Die

Ergebnisse zeigten, dass seegrasbasierte Faserplatten im Vergleich zu Holzfaserplatten deutlich bessere Leistung aufwiesen. Es wurde festgestellt, dass die Eignung des Mischens von der Größe und Morphologie der gemischten Aggregate beeinflusst wurde.

Sandwichplatten, die mit geopolymerem Bindemittel hergestellt wurden, wurden ebenfalls mit dem Trockenmisch-Sprühverfahren produziert. Wenn Seegrasfasern in den äußeren Teilen der geopolymergebundenen Holzspanplatten eingesetzt wurden, wirkten sie als Verstärkungselemente und führten zu einer Erhöhung der Biegefestigkeit der Platten. Die Leistung dieser Platten wurde mit der von kommerziellen Zementplatten verglichen. Neben mechanischen und physikalischen Tests wurden zusätzliche Untersuchungen durchgeführt, um die Mischeffizienz von Metakaolin und dem alkalischen Aktivator zu bewerten. Diese Bewertung umfasste die Zugabe eines Farbstoffs zum alkalischen Aktivator und anschließende mikroskopische Untersuchungen der Geopolymerpaste. Die Einbindung von Seegrasfasern schien die Biegefestigkeit der Geopolymer-Sandwichplatten zu verbessern und eine leichte Verbesserung des Brandschutzes zu bieten.

Isolationsplatten wurden unter Verwendung von Seegrasblättern und pMDI als Bindemittel hergestellt. In dieser Studie wurden Seegrasblätter von zwei Seegrasarten verwendet (*Posidonia oceanica* und *Zostera marina*). Die mechanischen und physikalischen Eigenschaften der Platten mit geringer Dichte (Dichten im Bereich von 80 bis 200 kg m⁻³) wurden gemäß den Standards für Isolationsplatten bewertet. Die Wärmeleitfähigkeitsmessungen wurden mit einem Wärmeflussmessgerät durchgeführt, und der Brandschutz wurde durch Kegelkalorimetrie- und Einflammtests bewertet. Es wurde eine Wirtschaftsanalyse durchgeführt, um die Herstellungskosten und Rentabilität von Seegrasisolationsplatten im Vergleich zu solchen aus Holzfasern zu bewerten. Die Platten aus Seegrasblättern hatten eine niedrige Wärmeleitfähigkeit, ähnlich wie Holzfaserplatten, sowie eine hohe Feuerbeständigkeit. Die Kostenanalyse ergab, dass Seegrasblätter aufgrund geringer Rohstoffkosten, geringem Energiebedarf für die Produktion und dem Potenzial für eine reduzierte Verwendung von flammhemmenden Mitteln eine kostengünstige Alternative zu Holzfaserplatten darstellen. Zusätzlich wurden flexible Matten unter Verwendung von *Zostera marina* und Bicomponent-Fasern als Bindemittel hergestellt. Die Korrelation zwischen Kompression, interner Haftfestigkeit, Flexibilität und Dichte wurde durch eine vertikale Dichteprofilanalyse und eine Mikroskopieanalyse bewertet. Diese Matten wiesen eine hohe Elastizität und eine Wärmeleitfähigkeit von 0,039 bis 0,051 W m⁻¹K⁻¹ auf.

Insgesamt scheint die Verwendung von Seegrasfasern und -blättern zur Herstellung von Baumaterialien ein vielversprechender Ansatz für deren effektive Nutzung zu sein. Nach dem Ende der Lebensdauer kann die Seegras-Biomasse weiterverwendet werden, was ihren Lebenszyklus verlängert und nachhaltige Praktiken in der Bauindustrie fördert.

Table of Contents

Chapter 1

1. Introduction	1
1.1. Seagrasses and seagrass wracks	2
1.1.1. Seagrass wracks: The benefits and the problems they cause to the environment	4
1.1.2. Seagrass leaves and seagrass fibers	5
1.1.3. Seagrass wracks management strategies	5
1.2. Environmentally friendly composite building materials based on lignocellulosic materials ..	7
1.2.1. Wood and non-wood-based composites. Particleboards and fiberboards	7
1.2.2. Mineral binders and mineral bonded composites	8
1.2.3. Insulation from lignocellulosic sources	10
1.3. Current advances in seagrass utilization as a building material	11
1.4. Objectives and questions	13

Chapter 2

2. Materials and methods	15
2.1. Materials	15
2.2. Methods	16
2.2.1. Characterization of raw materials	16
2.2.2. Processing, production and conditioning	16
2.2.3. Characterization of final products	17

Chapter 3

3. Medium density fiberboards (MDF) based on seagrass fibers (unpublished results)	18
3.1. Materials and methods	18
3.2. Results and discussion	18

Chapter 4

4. Discussion	21
4.1. Size, morphology and chemical composition of seagrass leaves and fibers	21
4.2. Seagrass-based composites bonded with mineral binders	23
4.2.1. Seagrass-based gypsum composites	23
4.2.2. Seagrass-based cement boards	24
4.2.3. Geopolymer bonded seagrass-based fiberboards	26
4.3. Insulation materials from seagrass	27

4.4. Utilization of seagrass biomass: From the perspective of economy and environment..... 28

Chapter 5

5. Conclusion 30

Chapter 6

6. References.....33

Appendix.....41

Article 1.....41

Article 2.....51

Article 3.....64

Article 4.....75

Article 5.....88

Article 6.....106

Chapter 1

Introduction

Seagrasses are flowering plants that thrive in marine environments. They encompass a broad spectrum, from the elongated strap-like blades of eelgrass (*Zostera caulescens*) in the Sea of Japan, measuring over 4 meters in length, to the small, rounded leaves of sea vine (e.g., *Halophila decipiens*) found in the deep tropical waters of Brazil, measuring up to 2-3 centimeters. Extensive underwater meadows of seagrass adorn the coastlines of various regions worldwide, including Australia, Alaska, southern Europe, India, east Africa, the Caribbean islands, and other coastal areas.

Seagrasses can reproduce sexually or asexually. As flowering plants, they produce seeds, with pollen transported through the water to fertilize female flowers. Additionally, seagrasses can propagate through rhizome roots, enabling the emergence of new growth and the expansion of entire underwater meadows from a single plant (Short, 2003). Seagrasses have significant ecological importance as a food source and habitat for a diverse community of wildlife.

Seagrasses grow in coastal and marine habitats worldwide. These meadows exhibit varying sizes, ranging from small patches to expansive stretches covering several hectares. The coverage of seagrasses is influenced by numerous factors, including water depth, light availability, nutrient levels, sediment characteristics, and wave energy (De Boer, 2007; Short, 2003). Currently, the estimated total coverage of seagrasses is approximately 177,000 – 600,000 km² (McKenzie et al., 2020; Short, 2003). However, it is plausible that this value underestimates the actual global coverage, considering the presence of undocumented areas.

So far, there are 72 known species of seagrasses (Reynolds et al., 2018a). They are commonly divided into four main groups: *Zosteraceae*, *Hydrocharitaceae*, *Posidoniaceae* and *Cymodoceaceae*. Some of the most well-known species of seagrasses are:

- ***Zostera marina* and *Zostera japonica*:** *Zostera marina* seagrass is the most extensively distributed seagrass in the world (Olsen et al., 2004). *Zostera marina* can be mainly found in the northern hemisphere. It has long and narrow leaves which can grow up to a meter in length while their width can vary from several millimeters up to a centimeter (Figure 1 a). The blade-like leaves have a smooth surface and are green in color. The plant has a fibrous root, that can extend up to 15 cm into the sediment (Short, 1983). The chemical composition of *Zostera marina* depends on several factors such as the location and growth conditions. It consists of cellulose, hemicellulose, lignin, protein, and other minor components such as lipids (Davies et al., 2007). Davies et al., (2007) have indicated that *Zostera marina* leaves contain microscopic fibers (Figure 1 c) which can exhibit very high strength, similar to that of jute and sisal fibers. These tiny fibers could be considered as an interesting candidate for polymer reinforcement to form environmentally friendly composites.

Zostera japonica are quite similar type to *Zostera marina* seagrass in terms of structural form, but can vary significantly in size and productivity (Duarte, 1991). It is also referred to as the Japanese seagrass or the dwarf seagrass. This species is native to the seacoast of eastern Asia from

Russia to Vietnam (Short et al., 2007). It has also been reported that it can grow in some parts of the world beyond its natural habitat (on the western coast of North America) where it is considered an invasive species (Shafer et al., 2014).

- ***Posidonia oceanica* and *Posidonia australis*:** Seagrass *Posidonia oceanica* is found in the Mediterranean Sea and is the most common seagrass species in the region. It typically grows in shallow waters, up to a depth of around 40 meters. Its blade-like leaves can reach a length of up to a meter and a width of several centimeters (Figure 1 b). *Posidonia oceanica* meadows provide a habitat for a diverse range of marine species and significantly contribute to the coastal protection as they reduce erosion. The dense foliage of *Posidonia oceanica* contributes to significant oxygen production through photosynthesis. Additionally, the seagrass meadows act as carbon sinks, effectively storing carbon and helping mitigate climate change. Similarly to other types of seagrasses, *Posidonia australis* forms extensive underwater meadows along the coastlines of southern Australia, including shallow coastal waters, estuaries, and bays (Larkum et al., 2006). This seagrass species has a rhizomatous growth form, with long horizontal stems called rhizomes that enable vegetative spread and contribute to the stability of the meadows (Hemminga and Duarte, 2000; Vasapollo, 2009) (Figure 1 d).
- ***Cymodocea nodosa*:** *Cymodocea nodosa* or commonly referred as kelp grass is an important habitat for various sea animals. Its leaves are similar to *Zostera marina*. They can be 2 to 4 mm wide and up to 45 cm long (Borum and Greve, 2004). They are bright green in color and have a distinct central midrib (Duarte, 2002). *Cymodocea nodosa*, usually found in the Mediterranean basin, forms extensive underwater meadows in shallow coastal areas. Similarly to other species of seagrass, it shows a rhizomatous growth, with long creeping rhizomes that allow for vegetative expansion and the formation of interconnected meadows (Marbà et al., 2015).
- ***Thalassia testudinum*:** *Thalassia testudinum*, also referred to as turtle grass, are long, strap-like blade leaves. The leaves can reach lengths of up to one meter and are arranged in dense clusters from a branching rhizome. This species grows in coastal areas of the western Atlantic Ocean and the Caribbean Sea (Short et al., 2007; Wabnitz et al., 2008). The turtle grass is the major food source for various animals living in the sea, especially for green turtles (Moran, 2003). Generally, muddy and sandy substrates provide a suitable environment for this kind of seagrass (Heck, 1977). Another characteristic is that it can tolerate a wide range of salinity levels (Kahn and Durako, 2006).

1.1. Seagrasses and seagrass wracks

Despite being confined to a narrow belt around the shoreline of the world's oceans, where they cover less than 7 million km², vegetated coastal habitats support about 1 to 10 % of the global marine net primary production and generate a large organic carbon surplus of about 40 % of their net primary production (Duarte, 2017). According to Hemminga and Duarte (2000), the seagrasses represent a submarine carbon sink of 0.08×10^9 tons of carbon per year worldwide.

Often, seagrasses are referred to as the lungs of the sea (Reynolds et al., 2018b). The seagrass meadows act as primary producers, similar to forests on land, by photosynthesizing and converting carbon dioxide (CO₂) into oxygen (O₂) (Hori et al., 2019). They release oxygen into the water during photosynthesis, contributing to the oxygen levels of the surrounding aquatic environment (Larkum et

al., 2006; Short, 2003). Seagrass meadows provide essential habitat for numerous marine species. They can also help stabilize sediments, reduce coastal erosion, and improve water clarity by trapping suspended particles.

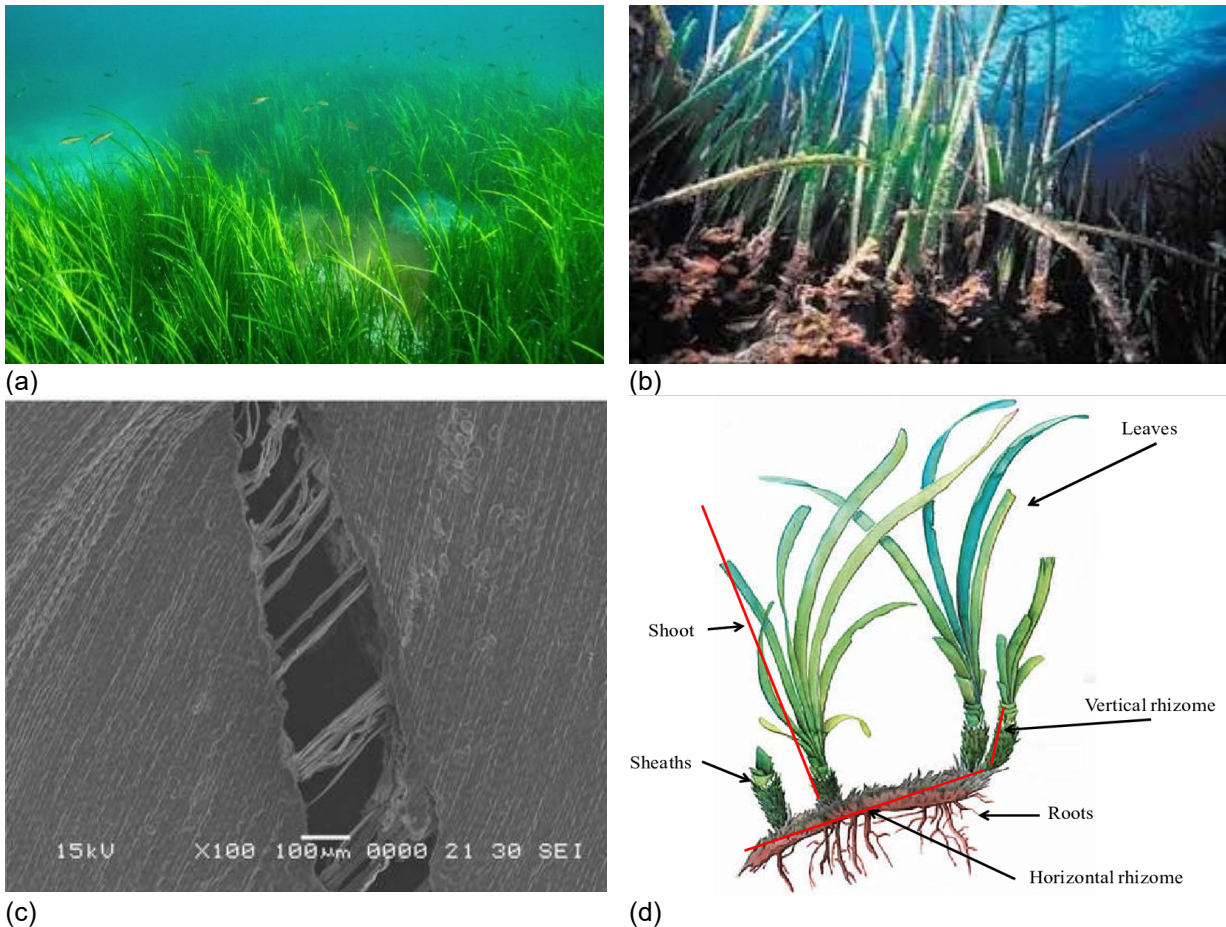


Figure 1. Seagrass *Zostera marina* (a), (source: Howarth et al., 2021). Seagrass *Posidonia oceanica* (b), (source: Bazairi et al., 2012). Microscopic fibers from *Zostera marina* (c), (source: Davies et al., 2007). Structure of *Posidonia oceanica* plant (d), (source: Vasapollo, 2009).

Seagrass meadows are highly sensitive to human activity and environmental changes. Pollution and climate change have been shown to negatively affect their health and survival (Björk et al., 2008). The presence and condition of seagrass meadows are often used as indicators of the overall health and ecological status of coastal areas, as they are very delicate to changes in water quality and habitat degradation (Marbà et al., 2013). Some anthropogenic threats of seagrass include:

- Coastal development and habitat destruction
- Pollution and nutrient runoff
- Dredging and coastal modification
- Overfishing and destructive fishing practices
- Climate change

Other issues concerning the seagrass meadows ecosystem is often their susceptibility to one another. Some seagrass species can be more susceptible to the impacts of invasive species compared to others. Invasive species are non-native organisms that can compete with native

species, disrupt their ecological processes, and negatively affect the balance of marine ecosystems (Çinar et al., 2014).

1.1.1. Seagrass wracks: The benefits and the problems they cause to the environment

During bad weather conditions, leaves break and the detached seagrass biomass is subsequently transported by wind and current dynamics to accumulate along the shores and form seagrass wracks (Jiménez et al., 2017; Mateo, 2010). A large amount of seagrass waste is deposited every year on the shorelines worldwide. It has been reported that more than 78 million tons of residual seagrass deposits accumulate annually (Masri et al., 2018). Other studies have estimated the total primary production of *Posidonia oceanica* in the Mediterranean basin alone to be in the range of $5 \times 10^6 - 5 \times 10^7$ tons per year (Pergent et al., 1997). The seagrass wrack plays an important role in sustaining the beach and marine environment as it brings ecological benefits (Vacchi et al., 2017). Some of the benefits include providing food and habitat to sandy beach fauna (Ince et al., 2007) and supplying nutrients for vegetation (Del Vecchio et al., 2017). Seagrass beds whose roots are bonded to the sand, seagrass leaves suspended in the water after they detach and wracks which act as physical barriers can altogether dissipate the sea current and prevent deterioration of the seashore (Infantes et al., 2022).

The lifespans of seagrass leaves are on average 90 days (Hemminga et al., 1999), while rhizome lifespans can last up to several years (Hemminga and Duarte, 2000). The decomposition rate of seagrass biomass depends on the species' chemistry such as the lignocellulose content. Because of the low proportion of lignin the leaves are usually more prone to decomposition compared to the rhizome and root tissues (Fourqurean and Schrlau, 2003; Infantes et al., 2022; Klap et al., 2000; Vichkovitten and Holmer, 2004). Moisture can accelerate the decomposition of plant wrack by facilitating the loss of soluble compounds through leaching and enhancing the activity of decomposers (Dick and Osunkoya, 2000; Nicastro et al., 2012), which ultimately results in the release of greenhouse gases flux (Liu et al., 2017; Liu et al., 2019; Sayer et al., 2011).

The effects of seagrass wrack lying onshore in rotting piles are multiple and include the hindering of tourism in the affected areas (Corraini et al., 2018), as well as the contribution to greenhouse gas emissions due to natural fermentation and degradation (Liu et al., 2019). The lignocellulosic biomass undergoes a microbial breakdown, emitting mainly gases such as carbon dioxide (CO₂) and methane (CH₄) into the atmosphere (Liu et al., 2019; Mainardis et al., 2021; Misson et al., 2020). Seagrass wrack is also a nuisance to humans due to the production of unpleasant odors when wrack biomass decompose on the shoreline resulting in the loss of beach amenity (Mainardis et al., 2021; Oldham et al., 2010). Another pressing problem of the shorelines containing seagrass wracks is eutrophication. The organic material that is washed ashore is rich in nutrients, and due to decomposition processes can encourage eutrophication (Chubarenko et al., 2021).

Beach wrack poses a challenge not only as an environmental issue but also as a social problem for local authorities, especially those whose economies depend on tourism. The management of beaches and their authorities are responsible for adhering to legal regulations, such as the removal of beach cast accumulations in accordance with Directive (EU) 2006/7/EC, which focuses on bathing water quality. Additionally, the Directive (EU) 2018/850 prohibits the storage of biodegradable waste. A common solution for managing seagrass wrack has been therefore its removal and disposal in landfills (Misson et al., 2020; Pfeifer, 2021).

1.1.2. Seagrass leaves and seagrass fibers

After the end of life, the green leaves of seagrass are transported and deposited on the shore to form banquettes. The banquettes of seagrass typically form due to natural processes such as wave action, currents, and storms that discharge and transport seagrass biomass. The banquettes can vary in size, ranging from small patches to extensive accumulations along shorelines.

A portion of seagrass leaves, along with other plant debris such as algae, rhizomes, and roots, can also accumulate on the seabed (Lefebvre et al., 2021) (Figure 2). The accumulation of organic matter on the shores has been extensively studied (Boudouresque et al., 2006; Gobert et al., 2003, 2006; Pergent et al., 1994). Over time, this litter can contribute to sediment formation across various marine habitats, ranging from beaches to deeper abyssal regions. Alternatively, it undergoes degradation processes mediated by macro- and microorganisms as well as abiotic factors (Pergent et al., 1994). For certain types of seagrasses, another form of the seagrass litter is usually found on the shores. Aegagropiles (Figure 2, left), also known as *Posidonia* balls, seagrass balls, or Neptune balls are rounded conglomerations of seagrass fibers that are found along seashores. They are formed through a natural process in which seagrass fibers derived from the rhizomes intertwine and accumulate over time. Aegagropiles are typically composed of dead seagrass fibers, along with sediment particles and other organic matter or plastic waste (Sanchez-Vidal et al., 2021). These high-density aegagropiles (on average 210 kg m⁻³), collected along the beaches of the Mediterranean Sea, are mainly ellipsoidal and are composed of several concentric layers that are distinguishable by their plant fibers and mineral particle concentrations as well as by their fiber types, orientation and degradation (Lefebvre et al., 2021).

Aegagropiles are primarily associated with the species *Posidonia oceanica*. They are commonly found in seagrass meadows dominated by *Posidonia oceanica* in the Mediterranean Sea. Other types of seagrasses however, derived from the same family (*Posidoniaceae*), have reportedly been shown to generate similar agglomerates. *Posidonia sinuosa*, *Posidonia angustifolia*, and *Posidonia australis* can also generate seagrass balls. In this study, fibers from seagrass balls will be referred to as **seagrass fibers**.

1.1.3. Seagrass wracks management strategies

The European Union (EU) Waste Framework Directive (2008) recognizes landfilling as the least effective method of managing waste biomass. To achieve sustainable management, a shift in paradigm is required: seagrass wrack should no longer be regarded as waste, but as a valuable resource (Figure 3).

Numerous studies have focused on finding effective ways to make use of seagrass wrack. Recent research conducted by Mainardis et al., (2021) has indicated that composting is a highly efficient method for utilizing organic seagrass residues. Meanwhile, other studies have explored the potential of seagrass for biogas production through anaerobic digestion (Balata and Tola, 2018; Misson et al., 2020).

Some researchers have taken a different approach to addressing the issue of seagrass waste management. Khiari and Belgacem (2017) investigated the possibility of producing cellulose pulps and paper. Although the potential for paper production using this raw material has been confirmed, the high content of mineral components may negatively affect the chemical recovery process in the papermaking and packaging industry. In this context, some studies have focused on Polyvinyl alcohol (PVA)–*Zostera marina* composites with seagrass content of up to 20%, demonstrating improved mechanical properties and potential applications in packaging, providing a cost-effective and highly

biodegradable alternative (Sapalidis et al., 2007). The potential use of *Posidonia oceanica* leaves in the industrial food packaging sector has also been suggested, with the incorporation of PHB (poly-3-hydroxybutyrate) as a binder (Sánchez-Safont et al., 2018). The study revealed that seagrass exhibited a reinforcing effect in terms of increased elastic modulus, although the resulting barrier properties and thermal stability decreased compared to neat PHB.

Voca et al., (2019) conducted research on the potential of seagrass waste for energy generation through incineration. The study found that seagrass remains have the potential to be a valuable source of energy, releasing approximately 9-11 MJ kg⁻¹. However, the high moisture content of the leaves and the large amount of ash produced are limiting factors for this application.

A small company in Germany (KS-VTCtech GmbH) operating in the area of bio-waste to energy conversion has suggested a possible solution for seagrass wrack utilization. It has been suggested that the thermal process can convert the seagrass biomass into a bio-coal which is comparable to lignite (brown coal). The treatment process imitates the natural carbonization of biomass, takes only a few hours and takes place in a reaction atmosphere of saturated steam at 220 °C and 23 bar (Chubarenko et al., 2021).

In other studies, seagrasses have been identified as a valuable food source for ruminant animals such as cattle and sheep (Torbatinejad et al., 2007). The quantity of major nutrients found in seagrass species like *Posidonia australis* makes it comparable to more common lignocellulosic feed sources for ruminants. However, due to its high ash content, it may not be viable to use seagrass as the sole dietary ingredient. Nevertheless, it could potentially be incorporated into their diet as a supplementary feed source. One of the most commonly investigated utilization methods of seagrass waste has been its conversion into functional materials for the construction sector. This practice will be elaborated upon in subsequent sections.

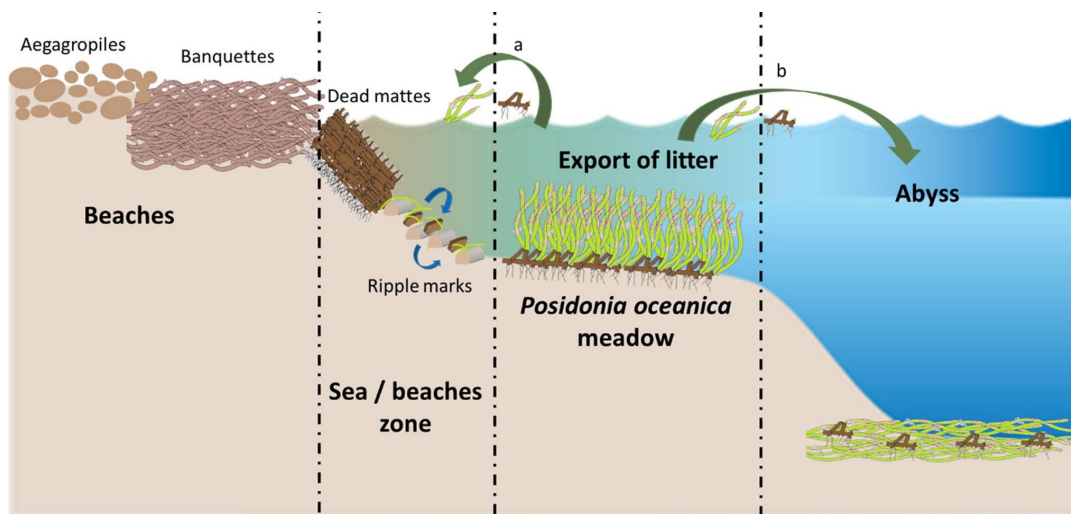


Figure 2. The export of *Posidonia oceanica* organs from the meadow, (source: Lefebvre et al., 2021).

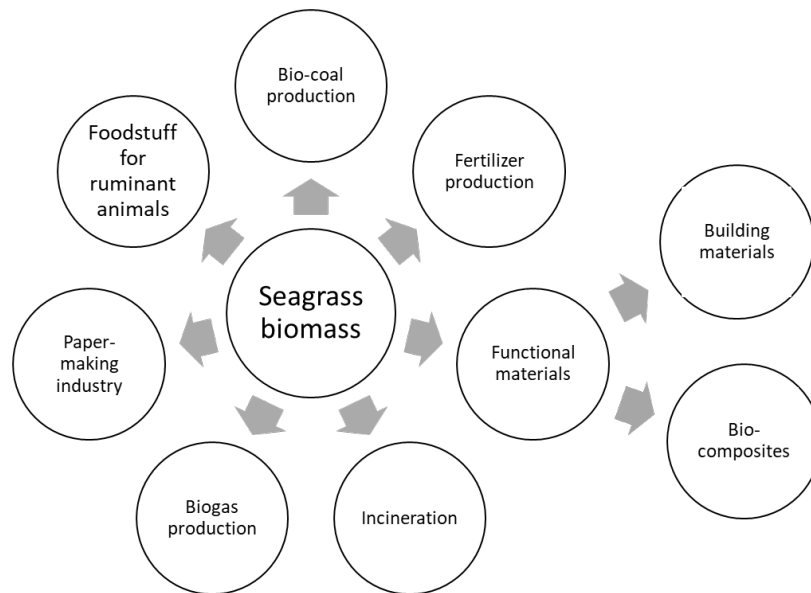


Figure 3. Possible application of seagrass wracks.

1.2. Environmentally friendly composite building materials based on lignocellulosic materials

This section provides a brief overview of the binders and lignocellulosic-based materials commonly used in the construction industry. It is divided into several subsections, focusing on wood-based panels, inorganic composites, and insulation materials. The binders described in these subsections will also be considered for their application in the production of seagrass-based composites.

1.2.1. Wood and non-wood-based composites. Particleboards and fiberboards

Currently there are several types of wood-based products in the market. These include particleboards, fiberboards, oriented strand boards, plywood and wood-plastic composites. Particleboards are engineered wood products made from wood particles or other lignocellulosic materials. Particleboards are produced by compressing and bonding small wood particles together with a synthetic resin or adhesive under high heat and pressure (Niemz et al., 2023). Wood aggregates having various morphologies like sawdust, wood chips, or even recycled wood fibers are used as raw materials. The advantages of these wood-based products are dimensional stability, uniformity, and consistent mechanical properties. They are mostly used in the construction industry and for various furniture applications due to their low density, high strength, their relatively low cost and ease of manufacturing.

Medium- (MDF) and high-density fiberboards (HDF) are very common and widely used building materials. For the MDF boards production, the raw material is wood fiber generated from a refining process. These engineered products are widely used as panels for wall division, ceilings, flooring and furniture manufacturing. The performance of these products depends on factors such as the type and size of particles/fibers, adhesive type and content, and manufacturing process (Niemz and Sandberg, 2022).

Several types of binders are used for production with the most common being UF, pMDI, MUF etc. Generally, low amounts of organic binders are sprayed onto the material and then they are pressed

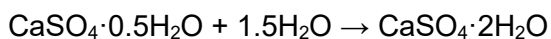
at elevated temperatures. In the industrial sector these amounts vary but usually lie in the proportions of 3 to 12 wt%, depending on the desired properties and the binder (Phanopoulos, n.d.). Although wood is considered a sustainable material, often, its high requirement for a preliminary processing has initiated the use of a wide range of lignocellulosic materials that have the potential to be good alternatives. As a replacement to wood, various non-wood lignocellulosic-based raw materials have been extensively investigated in recent decades (Battegazzore et al., 2018; Karimah et al., 2021; Nasir et al., 2019; Pugazhenthii and Anand, 2020). However, the lack of fiber consistency, limited availability, and technical performance of the produced boards are some of the challenges that need to be overcome for their industrial application in MDF production.

1.2.2. Mineral binders and mineral bonded composites

Mineral binders, also known as inorganic binders, play a crucial role in the production of construction materials by providing the necessary bonding and cohesion between particles. These binders typically comprise mineral-based substances that, when combined with an activator, undergo a chemical reaction (or activation) to form a solid and durable material. In addition to the binders themselves, the mixture often includes other additives, including chemicals that influence the solidification reaction, fillers and reinforcing materials like fibers, metallic rods, or meshes.

Mineral binders have been used not only to bond inorganic materials such as gravel or sand but also lignocellulosic materials. In our study, we focus on the investigation of various mineral binders and mineral bonded composites including:

- Gypsum: Gypsum is a mineral composed of calcium sulfate dihydrate ($\text{CaSO}_4 \cdot 2\text{H}_2\text{O}$). Initially, gypsum mineral is thermally treated at elevated temperatures and is converted to hemihydrate ($\text{CaSO}_4 \cdot 0.5\text{H}_2\text{O}$). The hemihydrate, also known as the “Plaster of Paris” can react with water to form again a dihydrate or simply gypsum ($\text{CaSO}_4 \cdot 2\text{H}_2\text{O}$). During hydration, the gypsum powder reacts with water and forms an interlocking network of gypsum crystals, transforming into a solid material. The chemical reaction can be represented by the following equation:



Gypsum is a relatively cheap binder that cannot only be obtained from gypsum mines but also from the desulfurization process in the power plants. The sulfur dioxide (SO_2) released from burning the coal is usually treated with a slurry of $\text{Ca}(\text{OH})_2$ or CaCO_3 and as a result large amount of synthetic (flue-gas-desulfurization - FGD) gypsum is formed.

Gypsum has been widely used as a building material because of its unique properties. It can be easily shaped, molded and modified to produce a wide range of products. It exhibits high fire resistance and favorable acoustic and thermal performance. Gypsum boards are commonly employed as interior panels, ceilings, and partitions. Prominent products derived from gypsum include plasterboards, gypsum blocks, and gypsum insulation. In addition to plasterboards, gypsum fiberboards have emerged as a noteworthy alternative. These fiberboards are manufactured by mixing gypsum with cellulose fibers and additives. They can provide enhanced strength, durability, and dimensional stability compared to traditional gypsum boards. Recent research has explored the incorporation of natural fibers as reinforcements for the production of eco-friendly gypsum fiberboards (Gigar et al., 2023; Jia et al., 2021). The addition of lignocellulosic material such as wood particles or fibers has shown to improve the thermal

insulation properties of gypsum bonded products such as gypsum bricks (Adamopoulos et al., 2015).

- Portland cement: Portland cement is produced by a high energy demanding process of milling the raw materials (limestone - CaCO_3 and clay – usually a mixture of SiO_2 - Al_2O_3 - Fe_2O_3), mixing them and burning them at very high temperatures (approximately 1450 °C). The high production temperature of Portland cement contributes significantly to CO_2 emissions (Andrew, 2018; Emmanuel et al., 2021; Provis and Van Deventer, 2009). When cement reacts with water, it undergoes a chemical process known as hydration, leading to the formation of calcium silicate hydrate (C-S-H) gel.

Cement powder has traditionally been utilized as a binder in the industrial production of cement-bonded particleboards and fiberboards. Initially, asbestos fibers were mixed with cement to produce fiberboards. However, due to health concerns, asbestos was replaced by cellulosic fibers.

Lignocellulosic materials have been traditionally used to produce cement bonded composites. Their function has been either to be used as fillers or as reinforcements for the cement matrix. A lot of research has been undertaken to investigate several natural fibers for the preparation of cement bonded composites (Junior et al., 2017; Onuaguluchi and Banthia, 2016). Much of the research however has been focused on the production of lignocellulosic-based composites containing a low proportion of aggregates (Makul, 2020; Onuaguluchi and Banthia, 2016). Investigating a production process that closely aligns with industrial processes has the potential to enhance the scalability of manufacturing industrial cement bonded panels from lignocellulosic materials. There are two primary mixing methods for producing cement-bonded particleboards or fiberboards, the Hatschek (wet) and the Elmendorf (dry) process (Marteinsson and Gudmundsson, 2018). In the wet process, a relatively low proportion of short fibers can be mixed with the binding agents as they tend to agglomerate (Junior et al., 2017). In the latter, the Elmendorf process, a higher amount of lignocellulosic material can be mixed, however, the aggregates such as wood chips and particles generally have a low aspect ratio and they are not flexible. Research has shown that these processes (as they are or modified) can be employed to produce cement bonded boards based on natural fibers or lignocellulose agro-industrial residues (Emmanuel et al., 2021; Junior et al., 2017).

- Geopolymer: A geopolymer is a 3D inorganic polymer that is formed by the reaction of aluminosilicate precursors with an alkaline activator solution. Geopolymers are typically formed by mixing materials such as metakaolin, fly ash, slag, or even clay with an alkaline solution. The reaction between the source materials (precursors) and the alkaline activator results in the formation of a three-dimensional network of linked polymer chains (Figure 4). The mechanism of geopolymerization is described briefly:

1. Dissolution: The alkaline solution dissolves the raw materials, releasing their silicate and aluminate components into the solution. The reactive components necessary for geopolymer formation are exposed.
2. Nucleation: The reactive components start to nucleate and polymerize forming oligomers. The Si-O and Al-O bonds are rearranged and linked together. This polycondensation reaction forms the backbone of the geopolymer structure.

3. Further polymerization: As the polymerization reaction progresses, the geopolymer chains continue to grow and interconnect, forming a three-dimensional network. The network becomes increasingly stable and rigid as more bonds are formed.
4. Curing: After the geopolymer mixture is cast or shaped, it undergoes a curing process to allow the geopolymerization reaction to complete and the structure to gain strength. Curing can occur at ambient or elevated temperatures, depending on the specific geopolymer system.

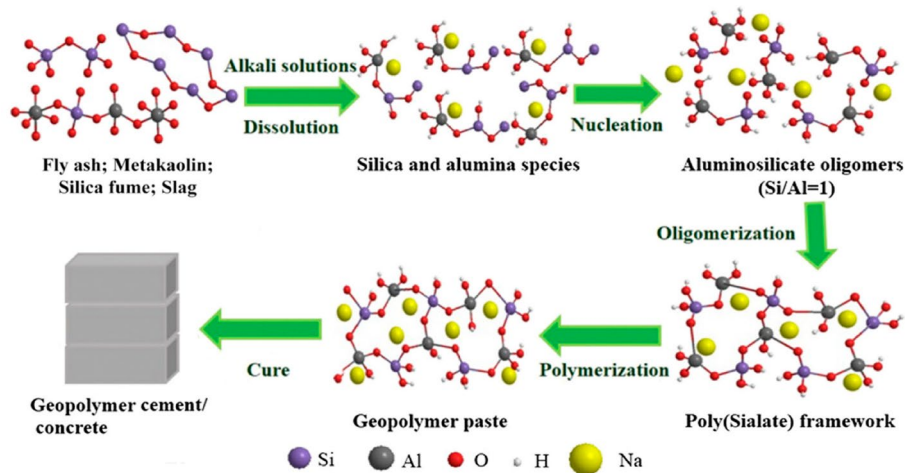


Figure 4. The mechanism of geopolymerization, (source: Zhuang et al., 2016).

Geopolymers are known for their high mechanical properties, high temperature resistance, and durability (Davidovits, 2005). They can be used as cementitious binders in construction materials, replacing traditional Portland cement-based materials. Apart from their properties, geopolymers offer a great advantage, which is the lower greenhouse gas emissions during production (Emmanuel et al., 2021; Provis and Van Deventer, 2009; Zhuang et al., 2016).

In recent studies, a lot of research has been conducted, dedicated to the use of geopolymer binder for the production of composites. A wide range of geopolymer bonded lignocellulosic-based materials have been studied so far. Most authors have focused on the production of geopolymer blocks which have been reinforced with several fibers at low proportions (Emmanuel et al., 2021; Ma et al., 2018). Geopolymers-wood composites are regarded as promising materials for construction (Furtos et al., 2022). However, previous reports have shown that an extensive addition of wood aggregates can worsen the mechanical properties of the composites (Sarmin and Welling, 2016). Nevertheless, by implementing an appropriate production method and utilizing suitable aggregates, it may be possible to incorporate a high amount of lignocellulosic material in the production of geopolymer composites. Natural fibers are potential candidates that have already been used to produce reinforced geopolymer composites (Korniejenko et al., 2016).

1.2.3. Insulation from lignocellulosic sources

Insulation materials are materials designed to reduce heat transfer. Their use is of significant importance as they can increase energy efficiency and comfort in a building by minimizing the heat transfer and maintaining consistent temperatures and also have a low environmental impact as the energy consumption for heating and cooling is lowered. Fiberglass, mineral wool, polyurethane foam, and expanded polystyrene are among the conventional thermal insulation materials. Apart from the

thermal efficiency these products also generally require a high amount of energy to be produced (Berge, 2009)

Wood fiber insulation has gained popularity as a sustainable solution in recent decades. Wood fiber insulation has the advantage of carbon storage, recyclability and high thermal insulation performance. However, the refining process of wood used in insulation production can sometimes have a high environmental impact and cost (Hill et al., 2018).

Wood thermal insulation boards are produced by blending wood fibers or particles with additives, such as binders and fire retardants. The mixture is formed into boards using heat and pressure in a hot press (Euring et al., 2015; Kirsch et al., 2018; Schubert et al., 2020). Apart from wood fibers, natural fibers have also been considered as ecological alternatives for being used as thermal insulators. The most important requirement for thermal insulation materials must fulfil a series of requirements such as low energy demand for production, affordable cost, high thermal performance, and desirable mechanical properties. Fire resistance is also a crucial consideration when working with lignocellulosic-based materials.

1.3. Current advances in seagrass utilization as a building material

One of the most common practices of utilizing seagrass waste is by converting it into a functional material for the construction sector. The seagrass *Zostera marina* (**leaves**) has been successfully used in the past to produce insulation quilts. In the Caribbean Sea, indigenous communities utilized dried eelgrass as a construction material for their huts due to its excellent insulating properties comparable to reed or straw. This traditional technology was later revived by Samuel Cabot, an American industrialist, in 1893. Cabot developed a novel insulating blanket known as Cabot-Quilt, which incorporated dried eelgrass enclosed between two layers of craft paper or asbestos. Marketed as highly resistant to decay, fire, and vermin, the Cabot-Quilt found its place within walls and floors, remaining a popular product until the 1940s (Bozsaky, 2010; Wyllie-Echeverria and Cox, 1999).

Significant research efforts have been devoted to exploring the utilization of seagrass leaves and fibers in the production of fiber/particleboards, employing various organic binders such as pMDI and epoxy resin. Maciá et al., (2016) conducted a study on medium density boards bonded with different types of polyurethane resins using *Posidonia oceanica* leaves. The study involved the production of boards with different densities and formulations, incorporating mixtures of wood and chopped leaves. Notably, a substantial amount of binder was employed in the formulations, ranging from 10 to 60 wt%.

Similarly, Rammou et al., (2021) investigated several mixtures of seagrass chopped leaves and wood particles. Although the dimensional stability of the resulting boards containing up to 50% seagrass showed improvements compared to pure particle boards, their mechanical performance fell short of meeting standard requirements. Other researchers, such as Ntalos and Sideras, (2014) have also suggested the use of seagrass leaves as a raw material in particleboard production, albeit in small proportions. In a separate study by Kuqo et al., (2019), boards made from unchopped seagrass leaves bonded with a pMDI binder achieved a density of 460 kg m⁻³ and a flexural strength of approximately 8 MPa, which still fell below the standard requirements.

The potential of utilizing *Posidonia oceanica* **fibers** in plastic reinforced composites was initially proposed by Khiari et al., (2011) marking an early contribution to this field. Their research highlighted the favorable mechanical properties and ease of processing, indicating the possibility of incorporating seagrass fibers into other polymeric matrices and providing a rational approach for valorizing

Posidonia oceanica residue. Since then, significant efforts have been made to effectively utilize seagrass fibers with various types of binders.

Garcia-Garcia et al., (2017) employed epoxy resin as a binder to produce high-strength reinforced plastic composites. The authors employed different pretreatment methods, including the highly effective silanization technique, to enhance the mechanical performance of epoxy resin-bonded boards. The binder content used in their study was 30 wt%. Furthermore, seagrass fibers have been successfully used to reinforce polyester matrix composites, resulting in a significant improvement in mechanical properties. Surface modification of the fibers was again employed to enhance the bonding between the matrix and the fibers.

In addition, promising results have been achieved by incorporating seagrass fibers into Polyethylene/Maleic Anhydride Grafted Polyethylene (PE/MA-g-PE) composites, with fiber surface modification also being conducted (Puglia et al., 2014). These studies collectively demonstrate the potential of seagrass fibers as reinforcing elements in various polymeric matrices, emphasizing the importance of fiber surface modification for enhancing interfacial adhesion and composite performance. Seagrass fibers have been extensively utilized as reinforcing elements in the preparation of biocomposites using various ecological binders. Rather than serving as fillers, seagrass fibers are commonly incorporated into polymer matrices such as Polyhydroxyalkanoates or wheat gluten (Ferrero et al., 2013; Seggiani et al., 2017, 2018).

Furthermore, seagrass fibers exhibit promising potential as insulation materials. Recent research has focused on the production of Airlaid Non-Woven boards using bicomponent fibers, resulting in insulation boards with densities ranging from 43 to 103 kg m⁻³ and low thermal conductivities ranging from 0.035 to 0.039 W m⁻¹K⁻¹ (Ayadi et al., 2020). The properties of flexible panels made from seagrass fibers have also been investigated in collaborative projects involving multiple companies and institutes (Gräbe et al., 2011). Recently, an innovative insulation product derived from seagrass fibers (*Posidonia oceanica* fibers) was patented and commercialized under the name Neptutherm. The seagrass fibers having a low uncompacted density can be simply blown into the facades, between the walls. Previous reports have shown that the uncompacted fibers (density: 65 – 75 kg m⁻³) can exhibit a very low thermal conductivity ranging from 0.039 – 0.046 W m⁻¹ K⁻¹ (Fachagentur nachwachsenden Rohstoffe e.V. (FNR). Dämmstoffe Aus Nachwachsenden Rohstoffen. Gülzow-Prüzen., 2019).

In addition to organic polymer-based matrices, inorganic matrices reinforced with seagrass fibers or leaves have gained attention. Composites combining seagrass fibers and Portland cement matrices have been extensively studied, with the aim of reinforcing the mineral matrices by incorporating small amounts of seagrass reinforcing fibers (Allegue et al., 2015; Benjeddou et al., 2022a; Hamdaoui et al., 2021; Kuqo et al., 2018). The results demonstrated that the addition of a low percentage of seagrass fibers (ranging from 0.5 to 1%) can increase the mechanical strength of the composites. Moreover, the density and thermal conductivity properties of the resulting blocks can be significantly reduced resulting in a lightweight, insulation product. In addition to cement, gypsum has been widely explored as a matrix in various studies (Guedri et al., 2023; Jedidi and Abroug, 2020). These investigations have shown that the incorporation of fibers at volumetric ratios of 5 to 10% can effectively reinforce gypsum blocks, leading to reduced thermal conductivity and the development of robust insulation materials.

Furthermore, mineral binders have been utilized not only to bond seagrass fibers but also seagrass leaves. Some researchers have taken a different approach by mixing seagrass leaves (instead of fibers) with cement or other mineral binders, such as lime. Lime bonded blocks incorporating chopped seagrass leaves were investigated by Stefanidou et al., (2021). The results demonstrated that, at low

proportions of seagrass aggregates, there could be an improvement in mechanical strength. However, the produced blocks exhibited a low strength, measuring less than 1 MPa, which falls significantly below the standard requirements. Similarly, when seagrass leaves were mixed with cement, low mechanical strengths of the composites were obtained (Mehrez et al., 2022).

Instead of manufacturing mineral matrix-seagrass composite blocks, Saval Pérez et al., (2014) attempted to produce cement bonded particle boards. These boards incorporated both chopped and unchopped seagrass leaves, with proportions ranging from 25 to 66.7 wt%. The boards exhibited satisfactory performance in terms of bending strength and modulus of elasticity, reaching approximately 4 N mm⁻² and 2000 N mm⁻², respectively. The authors also observed that in some cases, internal bonding (IB) values were very high, meeting the standard requirements for particleboards. Moreover, the fire resistance and other physical properties of the boards showed improvements. Notably, the boards containing seagrass leaves outperformed those with unchopped leaves. While these relatively high-density organically or minerally bonded seagrass-based materials may present an attractive alternative to conventional wood fiberboards/particleboards, their low mechanical properties remain a major drawback that limits their potential applications. Thus, a more comprehensive study focusing on the investigation of seagrass aggregates as a raw material, the production methods and their compatibility with several binders to produce a wide range of building materials is necessary. Based on what is presented above, this study would focus on the production of seagrass-based composites considering several aspects:

- Depending on the type, species, form, size and chemical composition of seagrass aggregates, the production of a range of materials where the full potential of seagrass can be achieved.
- Using non-conventional binders to form innovative composites from seagrass such as geopolymers.
- Production of composites containing very low amounts of binder. Thus, because of the low cost (as there is a low amount of costly binder included) could result in the production of building products that can potentially be produced on a large scale.
- Production of seagrass-based boards or reinforced blocks that have a very high performance in terms of mechanical strength and physical properties with the aim of fulfilling the standard requirements.

1.4. Objectives and questions

This work is intended to contribute to the development of building materials based on seagrass biomass. The main objective is to assess the possibility of using seagrass in the construction sector. Through comprehensive investigation, the aim is to determine the feasibility and suitability of seagrass fibers and leaves as a viable alternative to traditional construction materials. By examining the initial processing methods and mixing with various binders and by investigating the physical and mechanical properties and cost-effectiveness of the final products, this study seeks to provide effective ways for integrating the seagrass remains into sustainable building materials.

Within this framework, this work deals with the following questions:

- What are the main characteristics of seagrass leaves and fibers?
- What is the best approach for using different types (form and species) of seagrass to produce various materials for different applications?

- What is the compatibility of various binders (organic or inorganic) with different types of seagrass aggregates?
- How does the structure of a material influence its properties (structure – properties relationship)?
- Is the use of seagrass waste economically profitable?
- Which mixing methods would be most effective in evenly distributing the binders within the lignocellulosic aggregate to achieve optimal performance?

In this study, various mixing systems will be investigated (Figure 5) to explore the potential of utilizing **seagrass fibers** derived from *Posidonia oceanica* in combination with inorganic binders such as gypsum, Portland cement, and metakaolin activated by alkaline activator. The objective is to develop mineral bonded composites, specifically lightweight building blocks and separation panels suitable for interior and, occasionally, exterior applications.

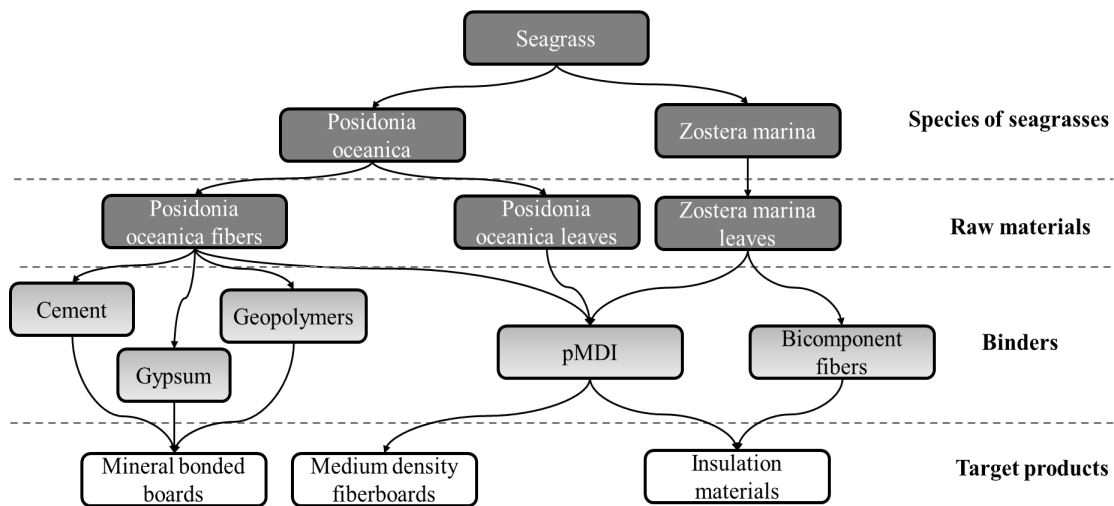


Figure 5. Schematic diagram showing the various mixing systems that are investigated in this study.

Additionally, a separate set of experiments will be conducted to produce medium density boards bonded with organic bonded pMDI (polymeric methylene diphenyl diisocyanate) using seagrass fibers. These boards are intended for interior applications such as dividing walls or furniture. Furthermore, insulation materials bonded with pMDI and Bicomponent fibers (BiCO) will also be manufactured. In this case, **seagrass leaves** will be used instead of seagrass fibers, as the insulation potential of the latter has already been extensively studied. Two seagrass species, *Posidonia oceanica* and *Zostera marina*, will be investigated for this purpose.

Chapter 2

Materials and methods

This chapter provides a short description of the materials used in the experiments and outlines the processing methods employed to produce the composites, as well as their subsequent characterization. More detailed information on the materials and methods used for each specific part is included in the corresponding sections of their respective articles.

2.1 Materials

Posidonia oceanica fibers were collected in the seashore of Durrës (Albania, Mediterranean Sea) in the autumn periods of 2019 and 2020. In their original form, the fibers are twisted into spherical clusters forming balls. Leaves of the Mediterranean seagrass *Posidonia oceanica* were also collected on the shore of Durrës, Albania (Figure 6). The relatively freshly washed-up seagrass was collected in December 2021. The leaves were dried and shaken several times to remove excess sand before further processing. *Zostera marina* leaves were provided by Seegrashandel GmbH (Westerau, Germany). They had been collected from the East Sea. After natural drying under ambient conditions, leaves with a length of 5 to 60 cm were cut to shorter lengths using an electric trimmer (Gardena, Ulm, Germany) to avoid problems during the spraying (mixing with the binder) process.

Other, mostly wood-based raw lignocellulosic materials were also used for the experiments mainly for reference purposes. Wood fibers (a mixture of spruce and pine wood fibers) for the production of reference boards were provided by GUTEX GmbH (Waldshut-Tiengen, Germany). *Pinus sylvestris* wood fibers used for insulation were provided by STEICO SE (Feldkirchen, Germany). The industrial wood particles used were provided by the Swiss Krono Group AG (Luzern, Switzerland). The moisture content of the afore-mentioned materials varied from 7 to 14%.



Figure 6. Seagrass wracks on the coast of Durrës, Albania.

Both organic and inorganic binding agents were utilized in this study. The production of medium-density fiberboards (MDF) and insulation boards involved the use of a low-temperature curing

polymeric methylene diphenyl diisocyanate (pMDI) resin (I-Bond WFI 4370, Huntsman, Everberg, Belgium) as a binder. Flexible mats, on the other hand, were produced using bicomponent fibers (Bico) from AL-Adhesion C (FiberVisions, Varde, Denmark) as a binding agent.

The mineral binding agents used in this research were Portland cement, gypsum powder as well as metakaolin powder and an alkaline activator for geopolymer preparation. The used cement was the commercial rapid curing variant CEM I 52,5R-HS/NA (Holcim GmbH, Sehnde, Germany). For composites bonded with gypsum, the commercial gypsum Knauf Goldband with a concentration (CaSO_4) > 85% (Knauf Gips KG, Iphofen, Germany) was used. The geopolymer matrix was formed as a result of the activation of Metamax metakaolin (BASF, Ludwigshafen, Germany) with the alkaline activator. The alkaline activator was prepared by mixing sodium silicate Na_2SiO_3 (Carl Roth GmbH + Co. KG, Karlsruhe, Germany) and sodium hydroxide (NaOH) technical grade 98% (AppliChem GmbH, Darmstadt).

2.2 Methods

2.2.1 Characterization of raw materials

Several imaging techniques were used for the determination of size distribution and gathering information on the morphology of the lignocellulosic aggregates. The aggregates were scanned using a flatbed scanner (Epson Perfection V850 Pro, Epson, Tokyo, Japan) and the high-resolution images were loaded FiberShape software (FibreShape PRO (X-shape, IST, Vilters, Switzerland). A dynamic image analyzer (Qicpic, Sympatec, Clausthal-Zellerfeld, Germany) was employed for determining the size and shape characteristics of fibers. Chemical characterization was performed using specific standard methods, including laboratory analytical procedures (LAP) from the National Renewable Energy Laboratory (NREL) and standards published by the Technical Association of the Pulp and Paper Industry (TAPPI) to determine the organic components of the biomasses.

2.2.2 Processing, production and conditioning

The preliminary mechanical processing of seagrass fibers is necessary for an adequate mixing of fibers with the binders. In the case of seagrass fibers, a mobile sawdust suction collector (Holzkraft ASA 163, Stürmer Maschinen GmbH, Hallstadt, Germany) was used to unravel them in a loose form without shortening and changing their morphological features.

The application of binder or mixing the raw materials depended on the type of binder to be used. For the application of organic binders such as pMDI, the raw material was vigorously stirred in an improvised gluing drum and the adhesive sprayed through a nozzle at a flow rate of approximately 0.1 to 0.15 g s^{-1} . For thorough mixing of bicomponent fibers with the seagrass leaves, they were put to a hammer mill (Electra SAS VS1, Poudenas, France).

When applying a mineral binder such as cement, gypsum or geopolymer the mixing process was more complex and will be described in the following chapter. An 80 L drum mixer (Atika, Altrad Lescha Atika GmbH, Burgau, Germany) was used for the mixing of fibers with the binders. The drum mixer ($\sim 50 \text{ rpm}$) was equipped with a modified agitator. In some cases, deagglomeration was necessary to break down the agglomerates of fibers. For this purpose, a gasoline-powered shredder (Güde GH650, Güde GmbH and Co. KG, Wolpertshausen, Germany) was used.

For the formation of boards and insulation mats a hot press (Joos HP-2000 lab, Gottfried Joos GmbH and Co.KG, Pfalzgrafenweiler, Germany) was employed. Depending on the activation temperature (or melting in the case of bicomponent fibers) and their density, the hot-pressing machine was operated at various temperatures, pressures and times.

Before the characterization of the produced seagrass-based boards and insulation mats, they were cut into various sample sizes. The samples were generally conditioned at 20 °C and 65% relative humidity. For specific tests such as fire and thermal conductivity tests, the samples were conditioned at 23 °C and a relative humidity of 50%.

2.2.3 Characterization of the final products

The mechanical properties of the produced boards were tested in accordance with European EN standards. A universal testing machine (ZwickRoell Zmartpro, ZwickRoell, Ulm, Germany) with a 10-kN load cell was employed for testing the boards. In most cases, bending, internal bond and compression strength were determined. On special occasions, further tests such as Brinell hardness, screw pull out resistance test were also carried out using the same device. The dynamic mechanical properties (Charpy impact resistance) of the boards were tested using a swinging pendulum impact tester (Resil Impact, CEAST, Martinsried, Germany).

The resistance to fire was examined using a mass loss calorimeter (MLC FTT, Fire Testing Technology, East Grinstead, UK) following the procedure described in *ISO 5660-1*, (2002). In the case of insulation boards, a further single flame test was carried out using a fire chamber device (Taurus Instruments AG, Weimar, Germany) according to *DIN EN ISO 11925-2*, (2010).

Water uptake and thickness swelling were determined according to the specified standards (*DIN EN 317*, 1993). The specimens were immersed in water for a specified period of time, they were removed and allowed to drain to remove excess water. Subsequently, the thickness and weight were measured.

For testing the thermal insulation properties (thermal conductivity) a 446 Lambda Eco-Line Heat Flow Meter (NETZSCH Group, Selb, Germany) was employed. The test procedure was in accordance with the standard *DIN EN 12667* (2001).

Structural and microscopy investigations were conducted to identify several morphological features of the raw materials and for the examination of bonding and fracture characteristics of the final products. The equipment most commonly used were the scanning electron microscope (SEM) Zeiss EVO LS 15 Microscope (Carl Zeiss Microscopy GmbH, Jena, Germany) and the digital 3D-reflected light microscope Keyence VHX-5000 (Keyence, Neu-Isenburg, Germany). For a more in-depth examination of composites, non-destructive imaging was accomplished by the commercial micro-CT system phoenix datos|x reconstruction© software (phoenix|x-ray, GE Sensing and Inspection Technologies GmbH, Wunstorf, Germany).

Chapter 3

Medium density fiberboards (MDF) based on seagrass fibers (unpublished results)

This chapter elaborates on the investigation of medium density fiberboards produced from seagrass fibers (*Posidonia oceanica* fibers). In addition, a series of boards made from Steico wood fibers (*Pinus sylvestris*) were also prepared as reference material. The boards were examined to assess their major mechanical properties and resistance to water.

3.1 Materials and methods

The collected seagrass balls went through a processing step to separate and loosen the fibers, as described in Section 2.2.2. Subsequently, seagrass-based Medium Density Fiberboard (MDF) was manufactured utilizing pMDI as a binder, following the same production method employed for pMDI insulation boards (spraying method, Section 2.2.2). A 6% proportion of pMDI was sprayed onto the fibers, and then they were pressed at 200 °C and 100 bar. The dimensions of the seagrass fiber-based MDF were 450 × 450 × 12 mm³, and their densities ranged from 400 to 700 kg m⁻³. The boards were cut to specific sample dimensions and conditioned for two weeks at a temperature of 20 °C and a relative humidity of 65%. Subsequently, the samples were tested for bending strength, internal bond, water absorption and thickness swelling, in accordance with EN 310, EN 319, and EN 317 standards, respectively. The seagrass-based boards are referred to as POF (*Posidonia oceanica* Fiber) boards, while the boards made from wood fibers are designated as WF (Wood Fiber) boards.

3.2 Results and discussion

The bending strength of the seagrass fiber-based (POF) MDF is lower in comparison to MDF made from pine wood fibers (Figure 7 a); it increases with the density of the boards. The strength difference between the two variants tends to decrease with higher density. The same trend is observed for the modulus of elasticity of the boards (Figure 7 b). Similarly, the internal bond strength of both POF- and WF-based boards seems to increase with the density of the boards. POF-based boards exhibit approximately 25 to 50% lower internal bond strengths than the respective WF boards (Figure 8). There are several potential reasons for the relatively lower mechanical performance of POF-based MDF. The relatively large seagrass fibers have a low surface area and possess a striped (channel-like) structure instead of a flat shape (Figure 11 a, section 4.1). Inorganic binders with a voluminous matrix are suitable for this structure, but not sprayed organic binders such as pMDI. When pMDI binder is sprayed onto the fibers, a portion of it is deposited within the fiber channels, not contributing to fiber bonding. This particular shape and the low surface area reduce the effective bonding area and, consequently, the strength of the boards. Another factor causing the low bending strength might be the presence of dust on the seagrass fibers. Seagrass fibers are collected from seashores and may contain sand particles. Additionally, during the untwisting process, some dust may be generated. The sprayed pMDI might settle on the particles present on the fiber surface, further reducing the effective bonding area of the fibers. Also, the individual tensile strength of seagrass fibers compared to wood fibers might be another reason that affects the bonding effectiveness and eventually the

board's mechanical performance. In terms of the internal bond strength, it is already known from the literature that the shorter the fibers the higher is the internal bond (Bütün Buschalsky and Mai, 2021).

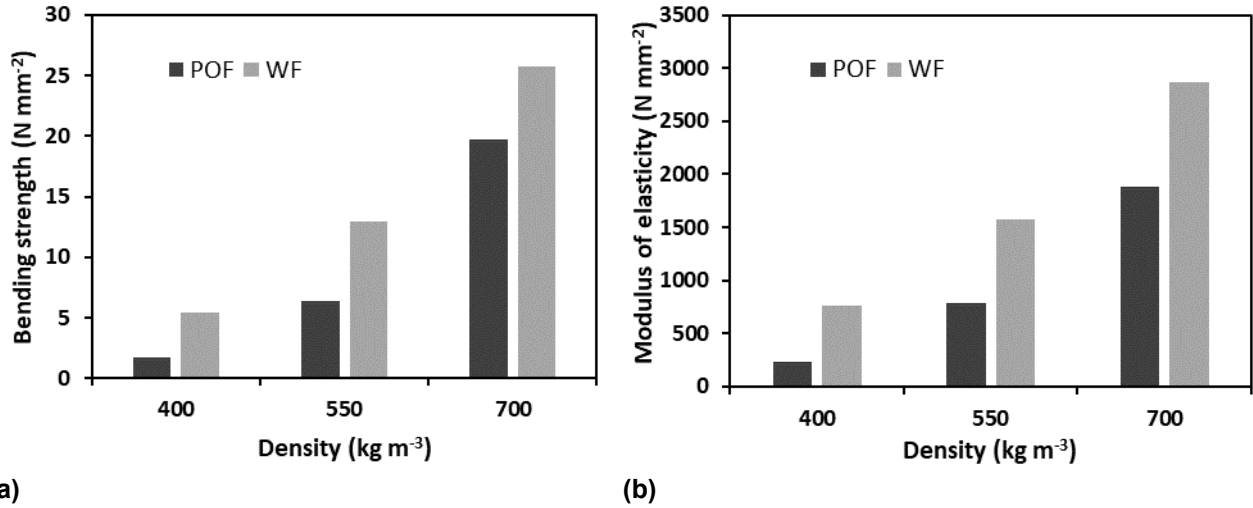


Figure 7. The bending strength (a) and the modulus of elasticity (b) of seagrass-based MDF (POF) and wood-based MDF (WF).

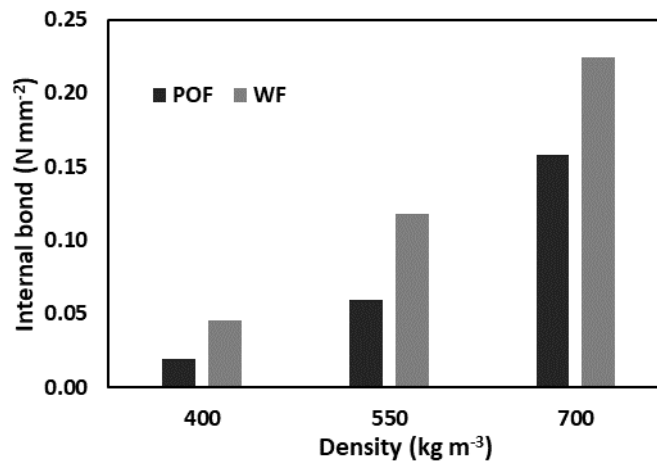


Figure 8. The internal bond strength of seagrass-based boards (POF) and wood fiber-based boards (WF) at different densities.

The water absorption (WA) of the samples tended to increase as the immersion time in water increased. WF boards exhibited significantly higher WA compared to POF boards (Figure 9). Additionally, there was a clear correlation between density and WA. Higher density was associated with lower WA, indicating that denser boards had lower water absorption. It appears that WF boards due to their structure characteristics and their hydrophilicity (associated with the chemical composition of wood fibers) display a higher affinity for water compared to POF boards.

The thickness swelling (TS) of the produced boards exhibited significant variation depending on the board type, density, and immersion duration (Figure 10). WF boards demonstrated lower TS values compared to POF boards. In the case of WF boards, TS tended to decrease with increasing density, while it increased with longer immersion periods in water. However, for POF boards, the results showed inconsistency. Initially, at a density of 400 kg m⁻³ the TS was relatively low.

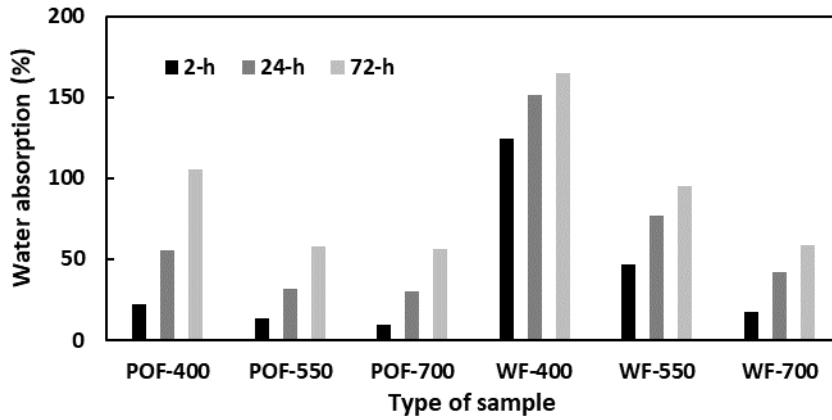


Figure 9. Water absorption of WF and POF boards with densities varying from 400 to 700 kg m⁻³.

As density increased, the boards exhibited higher water absorption, but at maximum density, the TS seemed to decrease again. It's important to note that this observation was primarily relevant for a 2-hour immersion period. However, for longer periods, water was found to penetrate inside the samples, resulting in increased TS.

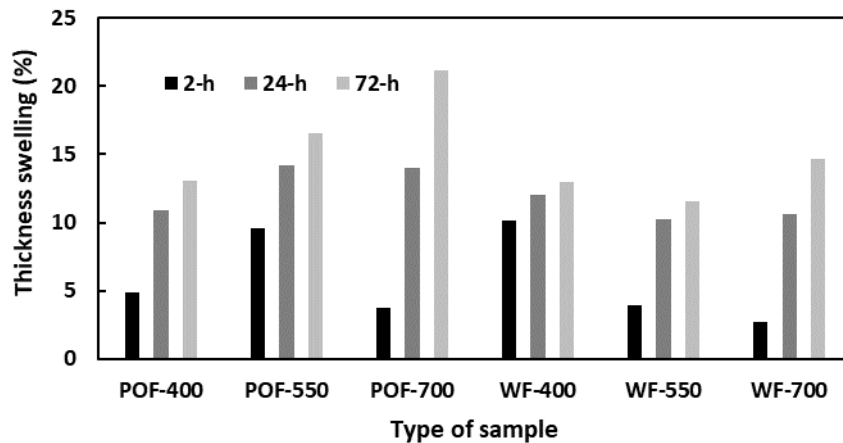


Figure 10. Thickness swelling of WF and POF boards with densities varying from 400 to 700 kg m⁻³.

The low density (400 kg m⁻³) allowed easier water penetration due to larger internal void spaces, which acted as pathways for water. As fibers swelled, they occupied the air voids inside the board. Conversely, as density increased (500 kg m⁻³), the TS increased due to fewer voids and greater fiber swelling caused by inter-fiber contact. In the case of high-density POF boards, the TS was very low after a 2-hour immersion but significantly increased after 72 hours. It appeared that not all fibers were fully wet during the initial 2-hour period due to the compact structure. However, after longer durations (24 and 72 hours), water managed to penetrate the internal structure, leading again to increased board swelling.

Chapter 4

Discussion

This chapter provides a discussion of the findings obtained in this study. It begins with an overview of the main results and includes an overall interpretation. The chapter is organized into several subsections that specifically address the key characteristics of the raw materials, the inorganically bonded composites, and the insulation materials. Furthermore, a brief discussion is included, focusing on the environmental and economic implications associated with the utilization of seagrass biomass.

4.1 Size, morphology and chemical composition of seagrass leaves and fibers

The dimensions and composition of lignocellulosic aggregates have a direct effect on the performance of final seagrass-based products. It is already known that the length and aspect ratio of aggregates can affect the mechanical properties of composites (Frybort et al., 2008). Furthermore, the size distribution influences the mixing of raw materials with the binder. Therefore, characterizing seagrass fibers in terms of size and shape can provide information to understand the properties of the produced composites.

The size of the leaves is mainly dependent on the degree of harshness of external factors and time. The longer the leaves are exposed to such factors, the higher their decomposition degree and the shorter they become. Additionally, factors such as the type of soil where the seagrass meadows grow and the time of the season when they are washed ashore can also impact the size of the leaves (Hemminga and Duarte, 2000). Seagrass fibers obtained from seagrass balls also exhibit a wide range of lengths (Lefebvre et al., 2021). During the collection and processing of seagrass balls, it was observed that larger balls tend to contain longer fibers. Also, the longer fibers were mostly situated in the exoteric part of the balls, whereas the inner part contained shorter fibers.

Given the numerous factors influencing the size of seagrass aggregates, they generally display a wide size distribution. Various techniques were employed to assess their length and other shape properties. For the determination of the mean geodesic length and thickness distribution, the seagrass aggregates were analyzed using image analysis methods (Table 1). The analysis showed that seagrass **fibers** can reach lengths of up to ~ 40 mm, while their thickness ranges from 45 to 500 μm . Seagrass **leaves**, on the other hand, are much larger in length compared to the fibers. Due to their size, it was not suitable to examine their length using the QICPIC device and the 3D microscope; they were only analyzed using the FiberShape. For the determination of thickness and width distribution of the leaves both FiberShape and 3D digital microscope were used. The results indicate that the leaves of *Posidonia oceanica* are wider and thicker compared to those of *Zostera marina*.

While there is no available literature on the length distribution of fibers, researchers have observed a wide thickness distribution ranging from 0.14 to 2.3 mm using a stereomicroscope (Lefebvre et al., 2021). It should be noted, however, that the untwisting method employed in our case, involving a rotor blade device, can impact the fiber size by potentially reducing their size.

Table 1. Size distribution of seagrass fibers and leaves.

Type of raw material	Object side	Used method to examine size of fibers		
		Static image analysis - FiberShape	Dynamic image analysis - Qicpic	3D optical microscope
<i>Posidonia oceanica</i> fibers	Length (mm)	0.1 – 33	2 – 42	2 – 36
	Thickness (mm)	0.02 – 0.5	0.045 – 0.2	0.03 – 0.12
<i>Posidonia oceanica</i> leaves	Length (mm)	45 – 100	n/a	n/a
	Width (mm)	1 – 9	n/a	7 – 12
	Thickness (mm)	n/a	n/a	0.15 – 0.3
<i>Zostera marina</i> leaves	Length (mm)	13.5 – 86	n/a	n/a
	Width (mm)	0.5 – 4.3	n/a	2.5 – 4.2
	Thickness (mm)	n/a	n/a	0.055 – 0.1

Seagrass fibers and leaves differ significantly not only in terms of size but also in terms of their morphology (Figure 11). Scanning electron micrographs revealed that seagrass fibers display a striped, channel-like structure (Figure 11 a). The thin and long fibers consist of fibrils linked together by a pectin and a lignin interphase (Allegue et al., 2015). Similar observations have been obtained by other authors, showing the structure of *Posidonia oceanica* fibers (Allegue et al., 2015; Khiari and Belgacem, 2017). Due to their shape and size, they are well-suited for bonding with bulky binders such as mineral pastes or bulky synthetic resins.

Similarly to previous investigations (Khiari and Belgacem, 2017), the scanning electron microscopy (SEM) images of seagrass leaves reveal an inherent porous structure (Figure 11 b, c). This porous structure is anticipated to exert a notable influence on the insulation properties of the leaves (**see Appendix, Article 5**).

Seagrass fibers exhibit significant differences in chemical composition compared to both types of seagrass leaves, characterized by a higher lignin content and lower proportion of extractives. In contrast, both types of leaves contain a high amount of extractives. It has been suggested that the variations in lignin and holocellulose content are likely influenced by climate conditions and soil chemical composition (Khiari and Belgacem, 2017). Additionally, seagrasses have a considerably high ash content, similar to that of rice and flax shives (Jongpradist et al., 2018; Ross and Mazza, 2010). The high ash content of seagrasses can be attributed to the specific chemical composition of the marine environment in which they have grown, as well as the potential contamination from sand particles (Cocozza et al., 2011; Voca et al., 2019). The ash content in seagrass may also be influenced by other external factors. Observations have shown that the ash content of seagrass is higher when it has been submerged in seawater, while for beach-dried seagrass is much lower (Voca et al., 2019).

The contribution of sand particles and salt on the ash content of seagrass fibers and leaves was determined by conducting a thorough washing of the raw material, followed by the ash content analysis (Table 2). The results show that 30 to 50% of the ash derives from the sand and salt settled on the surface of the seagrass leaves or fibers.

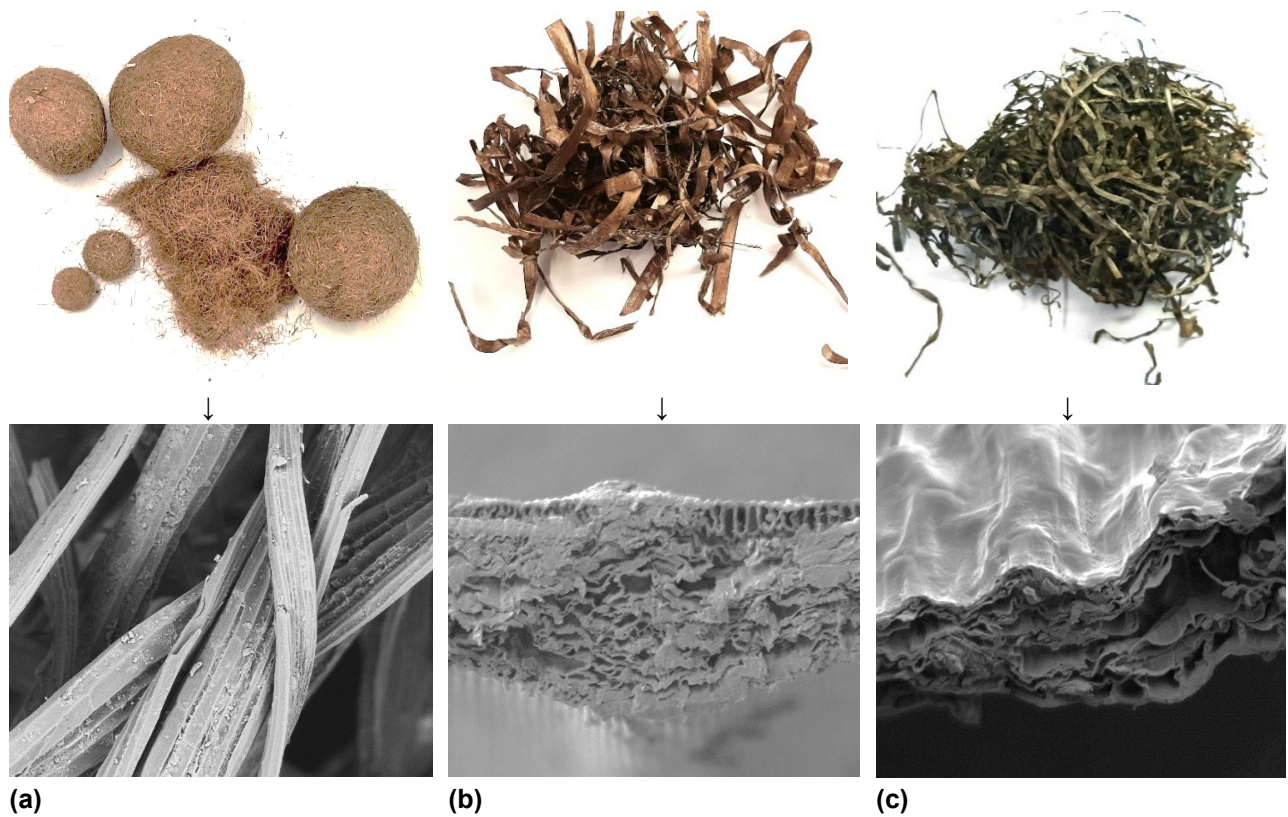


Figure 11. Seagrass fibers and leaves. *Posidonia oceanica* balls and fibers (a), *Posidonia oceanica* leaves (b), *Zostera marina* leaves (c). Corresponding SEM images illustrating the structure (bottom).

Table 2. Chemical composition of seagrass aggregates used in this study.

Raw material	HWE ^a (%)	CEE ^b (%)	Lignin (%)	Holocellulose (%)	Ash (%)	Ash after washing (%)
<i>Posidonia oceanica</i> fibers	5.8	2.1	35.4	53.7	12.9	8.7
<i>Posidonia oceanica</i> leaves	10.9	4.2	18.7	54.7	13.9	9.2
<i>Zostera marina</i> leaves	17.9	1.0	17.5	44.6	22.0	11.5

^aHWE indicates hot water extractives, ^bCEE indicates cyclohexane – ethanol extractives.

4.2 Seagrass-based composites bonded with mineral binders

4.2.1 Seagrass-based gypsum composites

Mixing the seagrass fibers with the gypsum paste was attainable up to a proportion of 6 wt% (**see Appendix, Article 1**). The proportion of fibers used to produce the composites in this study was significantly higher compared to that used in previous research (Guedri et al., 2023; Jedidi and Abroug, 2020). The seagrass fibers were well distributed into the gypsum paste. Although the homogeneity was adequate, the bending strength of the seagrass-based composites was lower compared to the reference gypsum sample. The low mechanical properties can be associated with the presence of small pores in the gypsum matrix. Due to the presence of pores, the stress applied on the material during the mechanical tests can be amplified. Geometric discontinuities cause an object to experience a localized increase in stress. Thus, the final product can fail more easily compared to a solid gypsum structure.

In a related study where *Posidonia oceanica* fibers were utilized as reinforcements in a gypsum matrix, higher compressive and bending strengths were achieved (Guedri et al., 2023; Jedidi and Abroug, 2020). However, it should be noted that the fabrication method and the type of gypsum used were different from that used in our study.

The impact bending resistance of seagrass-based gypsum composites was higher compared to the reference gypsum composite. This is attributed to the post-crack energy required to completely break the specimens. In contrast to the reference material, the long seagrass fibers in the seagrass-based composites required an additional amount of energy in order to completely pull out of the matrix. This energy is related to the friction between fibers and gypsum mortar when fiber sliding took place and the post-crack resistance. As it was mentioned earlier, the rough striped surface of seagrass fibers along with their length are responsible for the high friction required to pull them out (Figure 11 a). There have been no reports on the impact bending characterization for seagrass-based gypsum composites. However, authors consistently emphasize that the incorporation of seagrass fibers in a mineral matrix of composite materials generally leads to an increase in toughness and eventually a high impact resistance (Allegue et al., 2015; Hamdaoui et al., 2021; Jedidi and Abroug, 2020).

It should be noted that in order to produce fiber reinforced gypsum blocks with both acceptable mechanical properties and low density, it is important to carefully consider their fabrication process to reduce the presence of pores within the material. The reduction of pores could be achieved by using a vibrating device or compression. Additionally, incorporating small fibers such as wood fibers along with seagrass fibers can also be effective in improving the properties of the final product as they can further increase the degree of stress distribution.

4.2.2 Seagrass-based cement boards

In contrast to most previous studies that primarily focused on producing composites with low proportions of seagrass (Allegue et al., 2015; Benjeddou et al., 2022b; Hamdaoui et al., 2021), typically up to 5 wt%, our study aimed at producing boards with higher proportions of seagrass (22 to 52 wt%). Saval et al., (2014) have also conducted research on the production and analysis of cement bonded panels. Their study involved the fabrication of boards with varying proportions of seagrass material, ranging from 25 to 67 wt%.

The physical performance and mechanical strength of cement-bonded seagrass-based boards were high and, in many cases, compliant with standard requirements (**see Appendix, Article 2**). Specifically, water uptake and thickness swelling depended on the proportion of seagrass fibers in the board and its density. The higher the proportion of seagrass fibers, the higher the thickness swelling. Interestingly, for all proportions of seagrass fibers, the thickness swelling did not exceed the EN 634 standard value of 1.5%. According to previous reports, cement boards with thickness swelling lower than 1.5% can be used for exterior applications (Mngomezulu, 2019). In contrast, Saval et al., (2014) reported a range of 1.1% to 9.3% for the swelling thickness of their boards. It is important to note, however, that their panels had significantly lower densities compared to the boards produced for this study. As a result, it is expected that their boards would exhibit higher thickness swelling due to the presence of larger void spaces.

The fire resistance of cement-bonded seagrass-based boards was very high, despite the incorporation of a large amount of lignocellulosic material. The findings of our study (**see Appendix, Article 2**) are consistent with the findings reported by Saval et al., (2014) who also demonstrated the

non-flammable nature of seagrass-based boards. This outcome was anticipated, since cement is not flammable, it releases water upon combustion and oxygen cannot easily penetrate into the interior structure, thus protecting the organic aggregates. Furthermore, seagrass fibers are recognized for their fire resistance properties (Khiari and Belgacem, 2017; Kuqo et al., 2019). As demonstrated earlier (Table 2), seagrass contains substantial amounts of ash, indicating the presence of inorganic components.

In terms of mechanical and physical performance, cement-bonded fiberboards demonstrated satisfactory results as they surpassed the 9 N mm^{-2} standard requirement. In comparison to previous studies (Saval et al., 2014), where the bending strength was reported to be below 5 N mm^{-2} , our high-density seagrass-based boards achieved significantly higher values, ranging from 10 to 11 N mm^{-2} (**see Appendix, Article 2**).

Several factors appear to influence the performance of these boards:

1. **Mixing method:** The dry mixing method proved to be suitable for effectively mixing seagrass fibers, Portland cement, and water. Through the dry mixing process, an even distribution of all components was facilitated. During this process, the fibers were mixed with cement powder and water, ensuring that they were thoroughly dispersed and preventing any agglomeration or balling. Despite the inclusion of large amounts of seagrass fibers, certain mechanical properties, such as bending strength, remained high.

2. **Fiber length/aspect ratio:** The shape and size of fibers play a significant role in fiberboard performance. Comparative analysis was conducted between seagrass-based boards and those made from wood particles. Structural investigations, utilizing techniques like micro-CT and 3D microscopy, revealed distinct fracture mechanisms for the two board types. The differences in breaking behavior were attributed to variations in aggregate geometry. Seagrass fibers, being long and thin, require a considerable amount of energy for pull out. In contrast, less energy is needed for the delamination of wood particles.

3. **Low inhibition effect on cement hydration:** Preliminary examinations focused on the impact of polysaccharides or hemicellulose released from seagrass fibers on cement hydration were also carried out (**see Appendix, Article 2**). Compared to pine wood particles, seagrass had a minimal effect on cement hydration and subsequently a minimal reduction of mechanical strength. It is known that certain sugars can hinder the hydration of cement, leading to reduced hydration products and lower mechanical properties of the cement matrix (Bishop and Barron, 2006). In the case of seagrass fibers mixed with cement paste, it has been observed that the leached sugars do not significantly impede cement hydration, positively affecting its overall performance.

4. **Flexibility and roughness of seagrass fibers:** Seagrass fibers are known to have high flexibility (Lefebvre et al., 2021). The flexibility plays a vital role in facilitating the mixing process with the binder and also impacts the performance of the boards. The ability of the fibers to effectively fill the voids within the matrix during compaction enhances the overall bonding and performance of the cement composite materials. In addition to flexibility, the surface roughness of seagrass fibers has been identified as another influential factor in the performance of cement bonded composites (Allegue et al., 2015; Guedri et al., 2023). As depicted in Figure 11 a, seagrass fibers exhibit a rough surface texture. This high surface roughness contributes to increased frictional forces within the composite, leading to enhanced pull resistance and improved mechanical properties.

4.2.3 Geopolymer bonded seagrass-based fiberboards

Geopolymers are more environmentally friendly than Portland cements due to reduced CO₂ emissions, lower energy consumption and utilization of waste materials such as fly ash or slag (Emmanuel et al., 2021; Provis and Van Deventer, 2009). The use of geopolymer binder can enhance the eco-friendliness of construction materials. Prior to the beginning of this study, no research had been conducted on seagrass-based geopolymer composites.

By employing the dry mixing-spraying process, it is possible to incorporate high proportions of seagrass fibers into geopolymer-bonded fiberboards (**see Appendix, Article 3**). In contrast, when utilizing the conventional casting method, the maximum amount of seagrass fibers in the mixture cannot exceed 6 wt%. Moreover, the resulting composites from the casting method tend to be brittle and susceptible to dynamic impact stresses due to the high proportion of mineral matrix (**see Appendix, Article 1**). On the other hand, the dry mixing-spraying process includes a series of operations that facilitate uniform binder distribution and the production of high-strength fiberboards.

The successful distribution of the raw components consisting of the geopolymer binder leads to the production of boards with high bending strength. The highest strength is achieved when the proportion of seagrass fibers is 40 wt%. If the fiber proportion is lower (e.g., 30 wt%), the boards become brittle, and the likelihood of crack generation and propagation increases, resulting in rapid failure. When the proportion of incorporated fibers exceeds 40 wt%, the amount of binder required for solid bonding becomes insufficient, resulting in lower strength. As expected, similar to Portland cement boards, an increase in the fiber content leads to a decrease in the modulus of elasticity and internal bond strength of the boards. Moreover, the resistance of the boards to fire and water tend to decrease as the proportion of seagrass fibers increases. As indicated by micro-CT, the proper encapsulation of the lignocellulosic aggregates remains a crucial factor in achieving high physical and mechanical performance.

The reinforcing capability of seagrass fibers was further investigated by combining them with wood particles to produce seagrass-based sandwich particleboards. While seagrass fibers are readily available on the shores of the Mediterranean Sea, the collection and transportation costs can be significantly high. Utilizing seagrass fibers efficiently (e.g. using lower amounts of expensive seagrass fibers) and involving a much cheaper lignocellulosic material such as wood chips or particles can result in a more cost-effective approach for board production. Therefore, a small amount of seagrass fibers was used to produce the sandwich particleboards by allocating them to the outer layers (**see Appendix, Article 4**).

The thin seagrass-based layer increases the bending strength and the toughness of boards. Compared to wood particles, seagrass can better distribute applied stress, reducing the likelihood of crack formation. These fibers, being thin and long, are oriented perpendicular to the direction of the load, enabling them to absorb a significant amount of energy before breaking or pulling out. Although some of the properties are improved, some others such as the modulus of elasticity or the internal bond strength of seagrass-based sandwich boards are worse than the ones of pure particleboards. This lower internal bond strength can be attributed to inadequate interlocking between the seagrass fibers (in the outer layers) and the wood particles (in the inner layer).

4.3 Insulation materials from seagrass

Seagrass leaves-pMDI bonded boards exhibit good thermal insulation properties, comparable to or even better than the reference wood insulation fiberboards (**see Appendix, Article 5**). Both types of studied seagrass, namely *Posidonia oceanica* leaves and *Zostera marina* leaves, demonstrate good insulation performance. The thermal conductivity of seagrass leaves boards is significantly lower compared to wood fiber boards, particularly at high densities ranging from 150 to 200 kg m⁻³.

Seagrass leaves boards exhibit a thermal conductivity ranging from 0.039 to 0.051 W m⁻¹K⁻¹, which is consistent with findings reported in previous studies (Jones and Brischke, 2017). The thermal insulation effect of seagrass leaves in composites has been emphasized in prior research. Mehrez et al., (2022) found out that incorporating *Posidonia oceanica* leaves into cement paste, up to a 30% proportion, can significantly reduce thermal conductivity. Nevertheless, the obtained thermal conductivity values remain relatively high (0.091 W m⁻¹K⁻¹), which is expected due to the use of cement as the matrix material, which is known for its high thermal conductivity (Xu and Chung, 2000).

Several factors contribute to the high insulation performance of seagrass leaves-based insulation boards. Firstly, the morphology and chemical composition of the leaves directly influence their insulation ability. As previously demonstrated, the leaves possess a spongy internal structure that acts as an insulating layer on its own (Figure 11 b, c). Secondly, the preferred horizontal orientation of seagrass leaves achieved during the pressing process influences the direction of heat transfer. The seagrass leaves-based boards consist of multiple individual layers bonded together. Heat primarily is conducted through the solid material along the horizontal direction since the leaves are directed that way. Because of this preferential positioning of leaves, the heat transfer in the vertical direction is minimal. The presence of voids between the layers of seagrass leaves further disrupts the heat transfer through conduction.

The results of cone calorimetry and single flame tests demonstrate that seagrass leaves-based boards exhibit high fire resistance. The heat release and mass loss rate of the boards are lower compared to wood fiber insulation boards. The boards also do not ignite when a single flame is applied. The high flame and heat resistance of seagrass leaves-based boards can be attributed to their structure and chemical composition. Chemical analysis results revealed that seagrass leaves contain a significant proportion of mineral constituents, such as silica (SiO₂), sodium chloride (NaCl), and trace minerals (Khiari and Belgacem, 2017). When exposed to intense heat, a protective layer forms on the surface of the specimens, acting as insulation for the inner organic material. This behavior is similar to rice husk-based materials, where the silica layer provides a shielding effect by reradiating heat from external sources (Zhao et al., 2009). Given their flame-shielding properties, seagrass leaves could potentially be used as fire protection coatings. Their broad leaf structure and ability to insulate make them suitable for attaching to existing wooden structures to protect against thermal flux. Furthermore, their appealing brownish appearance could enhance the interior decoration. Based on the single flame test results, seagrass leaves-based insulation boards can be classified as fire resistance class B, C, or D. On the other hand, some wood fiber boards failed the flame test and fell into class E.

One weakness of seagrass leaves-based insulation boards lies in their mechanical performance, which is significantly lower compared to wood fiber insulation boards. During production, seagrass leaves are arranged horizontally, and some leaves tend to fold, resulting in the formation of large voids within the board structure. These voids contribute to the low compression and internal bond

strength of the boards. Additionally, the individual tensile strength of seagrass leaves is not as high as that of wood fibers, leading to failure under low applied stresses. Investigating processing techniques such as the production of multilayered insulation boards bonded together and modifying the vertical density profile could potentially lead to stronger boards, particularly with improved internal bond. Another approach would be the incorporation of stiff fibers, including seagrass fibers which could serve as reinforcements.

Seagrass leaves are large aggregates with a flat surface and relatively low surface area, unlike wood fibers. This characteristic suggests that the amount of organic binder sprayed onto the leaves could be reduced without significantly affecting the board's performance. It is hypothesized that seagrass leaves can effectively attach to each other, even with a small amount of binder, maintaining their strength and reducing production costs. However, further investigations are required to verify these assumptions.

Besides pMDI, other binders can also be used for insulation board production, depending on various factors, including the intended application. Bendable mats are necessary for insulating rounded areas or when installing them in rafters. Flexible insulation mats made from *Zostera marina* and bicomponent fibers were produced by thoroughly mixing the raw materials and hot-pressing (**see Appendix, Article 6**). These mats exhibited a low thermal conductivity, similar to wood fiber insulation mats.

Earlier studies have also investigated mats composed of washed *Zostera marina* leaves; however, the authors did not disclose the binders used and neither the used binder proportions. The results revealed that these mats exhibited a very low thermal conductivity of $0.036 \text{ W m}^{-1}\text{K}^{-1}$ (Pedersen and Ransby, 2005). The slightly higher thermal conductivity observed in our case may be attributed to the addition of bicomponent fibers, the presence of dirt and salts on the leaves (since they are not washed) and the morphology of milled leaves (a hammer mill was used for the mixing of BiCO fibers and seagrass leaves and significantly affected their morphology). It is also important to consider the density as well when assessing the thermal conductivity (In the aforementioned research, authors produced low density mats).

The fire resistance of seagrass-based mats is significantly higher than that of wood fiber due to the reasons mentioned earlier. Flexible mats offer high elasticity and mechanical stability (adequate internal bond) due to the interconnection of bicomponent fibers during the hot-pressing process, where the fibers melt and link with each other. Fire and mechanical performance results are consistent with those obtained by Pedersen and Ransby (2005), especially at high densities.

4.4 Utilization of seagrass biomass: From the perspective of economy and environment

Seagrasses have been used by humans for many centuries. They have been used to fertilize fields, insulate houses, weave furniture, thatch roofs, make bandages, and fill mattresses and even car seats (Reynolds et al., 2018b). But it's what they do in their native habitat that has the biggest benefits for humans and the ocean. Seagrasses support commercial fisheries and biodiversity, clean the surrounding water and help to take carbon dioxide out of the atmosphere. Because of these benefits, seagrasses are believed to be the third most valuable ecosystem in the world. It is claimed that one hectare of seagrass is estimated to be worth over \$19,000 per year (Reynolds et al., 2018b).

Similar to seagrass meadows, the presence of seagrass remains along the shores, offers several benefits to the surrounding ecosystem. Seagrass wracks serve as a natural barrier, protecting the shores from erosion caused by waves and currents. Despite the proposal of various management strategies for seagrass wracks, utilizing this lignocellulosic biomass in the construction industry appears to be a particularly promising approach to maximize its overall value throughout its lifecycle. However, to minimize its environmental impact, careful administration of seagrass wrack is necessary. Therefore, it is recommended that the use of seagrass in the building materials sector should be accompanied by ecological restoration efforts along the shores. After its initial use as a building material, seagrass biomass can then be further utilized for other purposes, such as composting or anaerobic digestion to produce eco-friendly fuels. This comprehensive approach ensures the sustainable use of seagrass and enhances its environmental benefits (Mainardis et al., 2021).

The utilization of seagrass biomass for industrial applications relies on the availability and cost of the raw material. From a technical point of view, *Posidonia oceanica* fibers have been identified as suitable for producing building materials. Seagrass fibers can be mainly found along the Mediterranean coasts, as they are derived specifically from *Posidonia oceanica*. The annual generation volume of seagrass balls (fibers) remains uncertain, with various reports indicating a range between 6000 and 15000 tons per year (Sanchez-Vidal et al., 2021). However, this quantity may be relatively low for the needs of large companies. Moreover, seagrass fibers are collected in the form of seagrass balls, which are widely distributed throughout the Mediterranean basin. The extensive distribution of seagrass increases collection costs, as equipment needs to be transported to multiple areas throughout the year to gather the seagrass. Additionally, the transportation of seagrass to a specific mainland site can further contribute to the overall costs. For the production of building materials from seagrass fibers, small enterprises operating in coastal areas with high seagrass abundance offer the most effective approach. Seagrass fibers bonded with Portland cement or geopolymer can be utilized to construct exterior and interior panels near building sites located along the Mediterranean Sea's seashore.

In contrast to seagrass fibers, waste seagrass leaves can be abundantly found. It has been reported that approximately 78 million tons of seagrass biomass accumulate annually (Masri et al., 2018). Researchers have made numerous attempts to utilize these leaves for the production of mineral-bonded inorganic materials, such as cement or lime composites (Mehrez et al., 2022; Saval et al., 2014; Stefanidou et al., 2021). However, the resulting products exhibit low mechanical properties, often making them unsuitable for structural or non-structural applications. On the other hand, seagrass leaves can be effectively used to manufacture insulation products at low costs. The raw material expenses primarily include collection, transportation, cleaning, and drying. In fact, an analysis of the economic feasibility shows that seagrass insulation boards could be up to 30% cheaper than corresponding wood fiber insulation boards (**see Appendix, Article 5**). Besides, coastal communities would be willing to cover the costs associated with the removal of waste seagrass biomass. Considering the relatively low cost of the raw materials and the high performance of seagrass leaves in terms of thermal application and fire behavior it seems that their use offers both environmental benefits, increased sustainability and economic advantages.

Chapter 5

Conclusion

The utilization of seagrass remains from wrack (dead leaves and fibers) in the production of building materials not only contributes to the reduction of greenhouse gas emissions but is also an effective measure to avoid costly landfilling. This study aimed to investigate the potential utilization of seagrass biomass in the construction sector by producing composites using various binders and examining their properties.

Seagrass fibers exhibit an appropriate shape, size distribution, and chemical composition for effective mixing and bonding with mineral binders to form solid composites. The incorporation of seagrass in gypsum matrices reduces the bending and compression strength of the resulting composites, but it enhances their impact bending strength. The major reason for the lower mechanical performance is attributed to the presence of pores in the gypsum composites. The addition of wood fibers on the other hand seems to significantly increase the mechanical properties while making the gypsum composites lighter.

Seagrass-based cement bonded boards containing large amounts of fibers were compared with the corresponding cement particleboards. The results revealed that seagrass-based boards have significantly higher mechanical properties, as well as enhanced resistance to heat and water. The flexural strengths of seagrass-based cement bonded boards range from 6 to 11 N mm⁻². Micro-CT analysis conducted for structural investigation demonstrated that the mechanical performance is greatly influenced by the bonding type and fracture mechanism. Additionally, the chemical composition of the aggregates plays a vital role in the development of hydration reactions in cement. The inhibitory effect of seagrass leachates on cement paste has a lesser effect compared to that of used wood particles (*Pinus sylvestris*).

In addition to Portland cement, geopolymer also seems to be a suitable binder for bonding seagrass fibers. The seagrass-based boards perform better than the wood-fiber boards in terms of mechanical strength, primarily due to the even distribution of the geopolymer binder within the boards. This distribution is influenced not only by the mixing process but also by the size of the aggregates used. It is worth noting that, in addition to the mechanical performance, other physical properties such as fire and water resistance are heavily influenced by the proper distribution of the binder. The binder not only bonds the lignocellulosic aggregates together but also contributes to adequate encapsulation, enhancing protection against external conditions. The main reason that influences the effectiveness of mixing is the size and, consequently, the specific surface area of the fibers being mixed. Larger fibers have a smaller surface area, making it easier for the binder to bond and cover them.

Sandwich boards based on seagrass fibers (allocated in the outer part) and wood particles in the core bonded with geopolymer also showed enhanced performance compared to pure geopolymer particleboards. The seagrass fibers act as reinforcements, increasing the bending strength of the boards. Besides, the resulting boards exhibited a slightly enhanced heat protection. However, other

properties such as internal bond strength and resistance to water were negatively affected. The inadequate bonding between the seagrass fiber-layer and wood particle-layer may contribute to the worsening of these properties. Further investigations into the production method are recommended to improve the bonding between the two layers (the core composed of wood particles and the outer layers consisting of seagrass fibers).

Based on the results obtained from testing pMDI-bonded MDF fiberboards based on seagrass fibers, it is shown that although fiberboards exhibited satisfactory strength, it was significantly lower when compared to boards made from wood fibers. The lower performance can be attributed to factors such as the individual strength of seagrass fibers, their shape and size, and the limited effectiveness of the binder used in the production process when compared to wood-based fiberboards.

Using seagrass leaves (*Posidonia oceanica* and *Zostera marina*) for insulation board production appears to be one of the best solutions for their effective utilization. The boards exhibit interesting properties, such as very low thermal conductivity (similar or lower to that of wood fiber boards) and high fire resistance, albeit with moderate mechanical strength. The low thermal conductivity of seagrass leaves boards is attributed to the chemical composition and the morphological characteristics of aggregates. During the pressing process, the leaves are arranged horizontally, resulting in predominantly horizontal heat conduction rather than vertical. Additionally, digital microscopy images revealed an internal spongy structure within the leaves, which acts as an additional insulating layer when heat is transferred from leaf to leaf. The results obtained by the cone calorimetry and single flame test showed that insulation boards made of seagrass leaves have very high resistance to fire attributed to their mineral content. The simplified economic analysis conducted to assess the production cost and profitability of seagrass insulation boards indicated that they can be up to 30% cheaper compared to wood-based insulation boards. This cost advantage stems from the absence of high-cost refining processes required for seagrass leaves. Additionally, the inherent fire resistance of seagrass eliminates the need for adding expensive fire retardants to the boards, further contributing to cost savings.

Seagrass leaves also hold potential for use as a decorative and fire-resistant coating for conventional wood-based particleboards and fiberboards. However, further research is necessary to assess the impact of the top seagrass layer on mechanical properties (especially on internal bond strength) and other physical properties like water absorption and thickness swelling.

The most effective approach for the proper utilization of seagrass biomass involves combining multiple practices such as ecological restoration of seagrass wracks and composting or biogas production. Referring to the results of this work, a new seagrass remains management strategy is proposed. After the collection of seagrass waste, its utilization in construction and subsequent use in other areas emerges as a more promising management strategy. By implementing sustainable and environmentally friendly management practices, starting with ecological restoration, the impact of seagrass removal from shores for flora, fauna, and land stability, particularly in terms of erosion protection can be minimized.

Based on the obtained results, it appears that utilizing organic adhesives like pMDI and UF may not be the most effective method for bonding seagrass fibers due to their unique structure. As mentioned earlier, when compared to wood-based boards, seagrass fiber boards exhibit lower strength. Instead a bulkier adhesive would be more suitable for bonding. Similarly, the use of seagrass leaves in the production of cement-bonded composites is not recommended due to insufficient interlocking and

incompatibility with the inorganic matrix, resulting in low mechanical performance. Although there have been attempts to incorporate seagrass leaves as reinforcing aggregates in inorganic matrices, their mechanical performance remains low. Therefore, mixing them with mineral-based binders such as gypsum, cement, lime, or clay to create mineral bonded materials is not recommended.

Chapter 6

References

- Abteilung Kompetenz-und Informationszentrum Wald und Holz (KIWUH) (last) (Ed.). (2019). *Fachagentur Nachwachsende Rohstoffe e.V. (FNR). Dämmstoffe aus Nachwachsenden Rohstoffen. Gülzow-Prüzen*. [FNR report]. FNR.
- Adamopoulos, S., Foti, D., Voulgaridis, E., & Passialis, C. (2015). Manufacturing and properties of gypsum-based products with recovered wood and rubber materials. *BioResources*, *10*(3), 5573–5585.
- Allegue, L., Zidi, M., & Sghaier, S. (2015). Mechanical properties of *Posidonia oceanica* fibers reinforced cement. *Journal of Composite Materials*, *49*(5), 509–517.
- Andrew, R. M. (2018). Global CO₂ emissions from cement production. *Earth System Science Data*, *10*(1), 195–217.
- Ayadi, M., Zouari, R., Segovia, C., Baffoun, A., Msahli, S., & Brosse, N. (2020). *Development of airlaid non-woven panels for building's thermal insulation*. 110–117.
- Balata, G., & Tola, A. (2018). Cost-opportunity analysis of the use of *Posidonia oceanica* as a source of bio-energy in tourism-oriented territories. The case of Alghero. *Journal of Cleaner Production*, *172*, 4085–4098.
- Battegazzore, D., Alongi, J., Duraccio, D., & Frache, A. (2018). Reuse and valorisation of hemp fibres and rice husk particles for fire resistant fibreboards and particleboards. *Journal of Polymers and the Environment*, *26*, 3731–3744.
- Bazairi, H., Bianchi, C. N., Boudouresque, C.-F., Buia, M. C., Clabaut, P., Harmelin-Vivien, M. L., Mateo, M. A., Montefalcone, M., Morri, C., & Orfanidis, S. (2012). *Les herbiers de Magnoliophytes marines de Méditerranée: Résilience et contribution à l'atténuation des changements climatiques*.
- Benjeddou, O., Jedidi, M., Khadimallah, M. A., Ravindran, G., & Sridhar, J. (2022a). Effect of *Posidonia oceanica* Fibers Addition on the Thermal and Acoustic Properties of Cement Paste. *Buildings*, *12*(7), 909.
- Berge, B. (2009). *The ecology of building materials*. Routledge.
- Bishop, M., & Barron, A. R. (2006). Cement hydration inhibition with sucrose, tartaric acid, and lignosulfonate: Analytical and spectroscopic study. *Industrial & Engineering Chemistry Research*, *45*(21), 7042–7049.
- Björk, M., Short, F., Mcleod, E., & Beer, S. (2008). *Managing seagrasses for resilience to climate change* (Issue 3). Iucn.
- Borum, J., & Greve, T. (2004). The four European seagrass species. *European Seagrasses: An Introduction to Monitoring and Management*, *1*.
- Boudouresque, C. F., Bernard, G., Bonhomme, P., Charbonnel, E., Diviacco, G., Meinesz, A., Pergent, G., Pergent-Martini, C., Ruitton, S., & Tunesi, L. (2006). *Préservation et conservation des herbiers à *Posidonia oceanica**. Ramoge.
- Bozsaky, D. (2010). The historical development of thermal insulation materials. *Periodica Polytechnica Architecture*, *41*(2), 49–56.

- Bütün Buschalsky, F. Y., & Mai, C. (2021). Repeated thermo-hydrolytic disintegration of medium density fibreboards (MDF) for the production of new MDF. *European Journal of Wood and Wood Products*, 79(6), 1451–1459.
- Chubarenko, B., Woelfel, J., Hofmann, J., Aldag, S., Beldowski, J., Burlakovs, J., Garrels, T., Gorbunova, J., Guizani, S., & Kupczyk, A. (2021). Converting beach wrack into a resource as a challenge for the Baltic Sea (an overview). *Ocean & Coastal Management*, 200, 105413.
- Çinar, M. E., Arianoutsou, M., Zenetos, A., & Golani, D. (2014). Impacts of invasive alien marine species on ecosystem services and biodiversity: A pan-European review. *Aquatic Invasions*, 9(4), 391–423.
- Cocozza, C., Parente, A., Zaccone, C., Mininni, C., Santamaria, P., & Miano, T. (2011). Comparative management of offshore posidonia residues: Composting vs. Energy recovery. *Waste Management*, 31(1), 78–84.
- Corraini, N. R., de Lima, A. de S., Bonetti, J., & Rangel-Buitrago, N. (2018). Troubles in the paradise: Litter and its scenic impact on the North Santa Catarina island beaches, Brazil. *Marine Pollution Bulletin*, 131, 572–579.
- Davidovits, J. (2005). *Geopolymer, green chemistry and sustainable development solutions: Proceedings of the world congress geopolymer 2005*. Geopolymer Institute.
- Davies, P., Morvan, C., Sire, O., & Baley, C. (2007). Structure and properties of fibres from sea-grass (*Zostera marina*). *Journal of Materials Science*, 42, 4850–4857.
- De Boer, W. (2007). Seagrass–sediment interactions, positive feedbacks and critical thresholds for occurrence: A review. *Hydrobiologia*, 591, 5–24.
- Del Vecchio, S., Jucker, T., Carboni, M., & Acosta, A. T. (2017). Linking plant communities on land and at sea: The effects of *Posidonia oceanica* wrack on the structure of dune vegetation. *Estuarine, Coastal and Shelf Science*, 184, 30–36.
- Dick, T. M., & Osunkoya, O. O. (2000). Influence of tidal restriction floodgates on decomposition of mangrove litter. *Aquatic Botany*, 68(3), 273–280.
- DIN EN 317. (1993). Particleboards and fibreboards; determination of swelling in thickness after immersion in water.
- DIN EN ISO 11925-2. (2010). Reaction to Fire Tests-Ignitability of Products Subjected to Direct Impingement of flame-Part 2: Single Flame Source Test
- Duarte, C. M. (1991). Allometric scaling of seagrass form and productivity. *Marine Ecology Progress Series*. Oldendorf, 77(2), 289–300.
- Duarte, C. M. (2002). The future of seagrass meadows. *Environmental Conservation*, 29(2), 192–206.
- Duarte, C. M. (2017). Reviews and syntheses: Hidden forests, the role of vegetated coastal habitats in the ocean carbon budget. *Biogeosciences*, 14(2), 301–310.
- Emmanuel, O. U., Kuqo, A., & Mai, C. (2021). Non-Conventional Mineral Binder-Bonded Lignocellulosic Composite Materials: A Review. *BioResources*, 16(2).
- Euring, M., Kirsch, A., & Kharazipour, A. (2015). Hot-Air/Hot-Steam Process for the Production of Laccase-Mediator-System Bound Wood Fiber Insulation Boards. *BioResources*, 10(2).
- European Parliament. Directive 2008/98/EC of the European Parliament and of the Council of 19 November 2008 on Waste and Repealing Certain Directives. 2008. (2008). European Parliament. <https://eur-lex.europa.eu/legal-content/EN/TXT/PDF/?uri=CELEX:02008L0098-20180705&from=EN>

- Ferrero, B., Boronat, T., Moriana, R., Fenollar, O., & Balart, R. (2013). Green composites based on wheat gluten matrix and *Posidonia oceanica* waste fibers as reinforcements. *Polymer Composites*, 34(10), 1663–1669.
- Fourqurean, J. W., & Schrlau, J. E. (2003). Changes in nutrient content and stable isotope ratios of C and N during decomposition of seagrasses and mangrove leaves along a nutrient availability gradient in Florida Bay, USA. *Chemistry and Ecology*, 19(5), 373–390.
- Frybort, S., Mauritz, R., Teischinger, A., & Müller, U. (2008). Cement bonded composites-A mechanical review. *BioResources*, 3(2), 602–626.
- Furtos, G., Molnar, L., Silaghi-Dumitrescu, L., Pascuta, P., & Korniejenko, K. (2022). Mechanical and thermal properties of wood fiber reinforced geopolymer composites. *Journal of Natural Fibers*, 19(13), 6676–6691.
- Garcia-Garcia, D., Quiles-Carrillo, L., Montanes, N., Fombuena, V., & Balart, R. (2017). Manufacturing and characterization of composite fibreboards with *Posidonia oceanica* wastes with an environmentally-friendly binder from epoxy resin. *Materials*, 11(1), 35.
- Gigar, F. Z., Khennane, A., Liow, J., & Tekle, B. H. (2023). *Effect of Wood/Binder Ratio, Slag/Binder Ratio, and Alkaline Dosage on the Compressive Strength of Wood-Geopolymer Composites* (A. Ilki, D. Çavunt, & Y. S. Çavunt, Trans.). 658–667.
- Gobert, S., Cambridge, M., Velimirov, B., Pergent, G., Lepoint, G., Bouquegneau, J.-M., Dauby, P., Pergent-Martini, C., & Walker, D. (2006). Biology of *Posidonia*. *Seagrasses: Biology, Ecology and Conservation*, 387–408.
- Gobert, S., Kyramarios, M., Lepoint, G., Pergent-Martini, C., & Bouquegneau, J.-M. (2003). Variations à différentes échelles spatiales de l'herbier à *Posidonia oceanica* (L.) Delile; effets sur les paramètres physico-chimiques du sédiment. *Oceanologica Acta*, 26(2), 199–207.
- Gräbe, G., Woidasky, J., Meier, R., & Greiner A. (2011). *Herstellung ressourceneffizienter und klimaneutraler hochwertiger technischer Dämmstoff-Produkte – Posidonia-Dämmstoff*. Umwelttechnik in Baden-Württemberg Herstellung.
- Guedri, A., Yahya, K., Hamdi, N., Baeza-Urrea, O., Wagner, J.-F., & Zagrarni, M. F. (2023). Properties Evaluation of Composite Materials Based on Gypsum Plaster and *Posidonia Oceanica* Fibers. *Buildings*, 13(1), 177.
- Hamdaoui, O., Limam, O., Ibos, L., & Mazioud, A. (2021). Thermal and mechanical properties of hardened cement paste reinforced with *Posidonia-Oceanica* natural fibers. *Construction and Building Materials*, 269, 121339.
- Heck, K. (1977). Comparative species richness, composition, and abundance of invertebrates in Caribbean seagrass (*Thalassia testudinum*) meadows (Panamá). *Marine Biology*, 41, 335–348.
- Hemminga, M. A., & Duarte, C. M. (2000). *Seagrass ecology*. Cambridge University Press.
- Hemminga, M., Marba, N., & Stapel, J. (1999). Leaf nutrient resorption, leaf lifespan and the retention of nutrients in seagrass systems. *Aquatic Botany*, 65(1–4), 141–158.
- Hill, C., Norton, A., & Dibdiakova, J. (2018). A comparison of the environmental impacts of different categories of insulation materials. *Energy and Buildings*, 162, 12–20.
- Hori, M., Bayne, C. J., & Kuwae, T. (2019). Blue carbon: Characteristics of the ocean's sequestration and storage ability of carbon dioxide. *Blue Carbon in Shallow Coastal Ecosystems: Carbon Dynamics, Policy, and Implementation*, 1–31.
- Howarth, Leigh et, Reid, G.K., & Lewis-McCrea, L. (2021). *Managing Aquaculture and Eelgrass Interactions in Nova Scotia* [BOOK].

- Ince, R., Hyndes, G. A., Lavery, P. S., & Vanderklift, M. A. (2007). Marine macrophytes directly enhance abundances of sandy beach fauna through provision of food and habitat. *Estuarine, Coastal and Shelf Science*, 74(1–2), 77–86.
- Infantes, E., Hoeks, S., Adams, M. P., van der Heide, T., van Katwijk, M. M., & Bouma, T. J. (2022). Seagrass roots strongly reduce cliff erosion rates in sandy sediments. *Marine Ecology Progress Series*, 700, 1–12.
- ISO 5660-1. (2002). Heat release, smoke production and mass loss rate.
- Jedidi, M., & Abroug, A. (2020). Valorization of Posidonia oceanica Balls for the Manufacture of an Insulating and Ecological Material. *Jordan Journal of Civil Engineering*, 14(3).
- Jia, R., Wang, Q., & Feng, P. (2021). A comprehensive overview of fibre-reinforced gypsum-based composites (FRGCs) in the construction field. *Composites Part B: Engineering*, 205, 108540.
- Jiménez, M. A., Beltran, R., Traveset, A., Calleja, M. L., Delgado-Huertas, A., & Marbà, N. (2017). Aeolian transport of seagrass (Posidonia oceanica) beach-cast to terrestrial systems. *Estuarine, Coastal and Shelf Science*, 196, 31–44.
- Jones, D., & Brischke, C. (2017). *Performance of bio-based building materials*. Woodhead Publishing.
- Jongpradist, P., Homtragoon, W., Sukkarak, R., Kongkitkul, W., & Jamsawang, P. (2018). Efficiency of rice husk ash as cementitious material in high-strength cement-admixed clay. *Advances in Civil Engineering*, 2018.
- Junior, H. S., Fiorelli, J., & Dos Santos, S. F. (2017). *Sustainable and nonconventional construction materials using inorganic bonded fiber composites*.
- Kahn, A. E., & Durako, M. J. (2006). Thalassia testudinum seedling responses to changes in salinity and nitrogen levels. *Journal of Experimental Marine Biology and Ecology*, 335(1), 1–12.
- Karimah, A., Ridho, M. R., Munawar, S. S., Adi, D. S., Damayanti, R., Subiyanto, B., Fatriasari, W., & Fudholi, A. (2021). A review on natural fibers for development of eco-friendly bio-composite: Characteristics, and utilizations. *Journal of Materials Research and Technology*, 13, 2442–2458.
- Khiari, R., & Belgacem, M. (2017). Potential for using multiscale Posidonia oceanica waste: Current status and prospects in material science. *Lignocellulosic Fibre and Biomass-Based Composite Materials*, 447–471.
- Khiari, R., Marrakchi, Z., Belgacem, M. N., Mauret, E., & Mhenni, F. (2011). New lignocellulosic fibres-reinforced composite materials: A stepforward in the valorisation of the Posidonia oceanica balls. *Composites Science and Technology*, 71(16), 1867–1872.
- Kirsch, A., Ostendorf, K., & Euring, M. (2018). Improvements in the production of wood fiber insulation boards using hot-air/hot-steam process. *European Journal of Wood and Wood Products*, 76, 1233–1240.
- Klap, V. A., Hemminga, M. A., & Boon, J. J. (2000). Retention of lignin in seagrasses: Angiosperms that returned to the sea. *Marine Ecology Progress Series*, 194, 1–11.
- Korniejenko, K., Frączek, E., Pytlak, E., & Adamski, M. (2016). Mechanical properties of geopolymer composites reinforced with natural fibers. *Procedia Engineering*, 151, 388–393.
- Kuqo, A., Boci, I., Vito, S., & Vishkulli, S. (2018). Mechanical properties of lightweight concrete composed with Posidonia oceanica fibres. *Zaštita Materijala*, 59(4), 519–523.
- Kuqo, A., Korpa, A., & Dharmo, N. (2019). Posidonia oceanica leaves for processing of PMDI composite boards. *Journal of Composite Materials*, 53(12), 1697–1703.

- Larkum, A. W., Orth, R. J., & Duarte, C. M. (2006). Seagrasses: Biology, ecology and conservation. *Phycologia*, 45(5), 5.
- Larkum, A. W., Orth, R. J., Duarte, C. M., Borum, J., Sand-Jensen, K., Binzer, T., Pedersen, O., & Greve, T. M. (2006). Oxygen movement in seagrasses. *Seagrasses: Biology, Ecology and Conservation*, 255–270.
- Lefebvre, L., Compère, P., Léonard, A., Plougonven, E., Vandewalle, N., & Gobert, S. (2021). Mediterranean aegagropiles from *Posidonia oceanica* (L.) Delile (1813): A first complete description from macroscopic to microscopic structure. *Marine Biology*, 168(3), 37.
- Liu, S., Jiang, Z., Deng, Y., Wu, Y., Zhao, C., Zhang, J., Shen, Y., & Huang, X. (2017). Effects of seagrass leaf litter decomposition on sediment organic carbon composition and the key transformation processes. *Science China Earth Sciences*, 60, 2108–2117.
- Liu, S., Trevathan-Tackett, S. M., Lewis, C. J. E., Ollivier, Q. R., Jiang, Z., Huang, X., & Macreadie, P. I. (2019). Beach-cast seagrass wrack contributes substantially to global greenhouse gas emissions. *Journal of Environmental Management*, 231, 329–335.
- Ma, C.-K., Awang, A. Z., & Omar, W. (2018). Structural and material performance of geopolymer concrete: A review. *Construction and Building Materials*, 186, 90–102.
- Maciá, A., Baeza, F., Saval, J., & Ivorra, S. (2016). Mechanical properties of boards made in biocomposites reinforced with wood and *Posidonia oceanica* fibers. *Composites Part B: Engineering*, 104, 1–8.
- Mainardis, M., Magnolo, F., Ferrara, C., Vance, C., Misson, G., De Feo, G., Speelman, S., Murphy, F., & Goi, D. (2021). Alternative seagrass wrack management practices in the circular bioeconomy framework: A life cycle assessment approach. *Science of the Total Environment*, 798, 149283.
- Makul, N. (2020). Modern sustainable cement and concrete composites: Review of current status, challenges and guidelines. *Sustainable Materials and Technologies*, 25, e00155.
- Marbà, N., Arias-Ortiz, A., Masqué, P., Kendrick, G. A., Mazarrasa, I., Bastyan, G. R., Garcia-Orellana, J., & Duarte, C. M. (2015). Impact of seagrass loss and subsequent revegetation on carbon sequestration and stocks. *Journal of Ecology*, 103(2), 296–302.
- Marbà, N., Krause-Jensen, D., Alcoverro, T., Birk, S., Pedersen, A., Neto, J. M., Orfanidis, S., Garmendia, J. M., Muxika, I., & Borja, A. (2013). Diversity of European seagrass indicators: Patterns within and across regions. *Hydrobiologia*, 704, 265–278.
- Marteinsson, B., & Gudmundsson, E. (2018). Cement Bonded Particle Boards with Different Types of Natural Fibres—Using Carbon Dioxide Injection for Increased Initial Bonding. *Open Journal of Composite Materials*, 8(01), 29.
- Masri, M. A., Younes, S., Haack, M., Qoura, F., Mehler, N., & Brück, T. (2018). A Seagrass-Based Biorefinery for Generation of Single-Cell Oils for Biofuel and Oleochemical Production. *Energy Technology*, 6(6), 1026–1038. <https://doi.org/10.1002/ente.201700604>
- Mateo, M. A. (2010). Beach-cast *Cymodocea nodosa* along the shore of a semienclosed bay: Sampling and elements to assess its ecological implications. *Journal of Coastal Research*, 26(2), 283–291.
- McKenzie, L. J., Nordlund, L. M., Jones, B. L., Cullen-Unsworth, L. C., Roelfsema, C., & Unsworth, R. K. (2020). The global distribution of seagrass meadows. *Environmental Research Letters*, 15(7), 074041.
- Mehrez, I., Hachem, H., Gheith, R., & Jemni, A. (2022). Valorization of *Posidonia-Oceanica* leaves for the building insulation sector. *Journal of Composite Materials*, 56(13), 1973–1985.

- Misson, G., Mainardis, M., Incerti, G., Goi, D., & Peressotti, A. (2020). Preliminary evaluation of potential methane production from anaerobic digestion of beach-cast seagrass wrack: The case study of high-adriatic coast. *Journal of Cleaner Production*, 254, 120131.
- Mngomezulu, L. B. (2019). *Phosphate-bonded composite products: The influence of filler materials, biomass type, and processing method on panel properties*.
- Moran, K. L. (2003). *Simulated green turtle grazing: Effects on structure and productivity in seagrass (Thalassia testudinum) beds in the central Bahamas*. University of Florida.
- Nasir, M., Khali, D., Jawaid, M., Tahir, P., Siakeng, R., Asim, M., & Khan, T. (2019). Recent development in binderless fiber-board fabrication from agricultural residues: A review. *Construction and Building Materials*, 211, 502–516.
- Nicastro, A., Onoda, Y., & Bishop, M. J. (2012). Direct and indirect effects of tidal elevation on eelgrass decomposition. *Marine Ecology Progress Series*, 456, 53–62.
- Niemz, P., Teischinger, A., & Sandberg, D. (2023). *Springer Handbook of Wood Science and Technology*. Springer.
- Ntalos, G., & Sideras, A. (2014). The usage of Posidonia oceanica as a raw material for wood composite and thermal energy production. *Journal of International Scientific Publications: Materials, Methods and Technologies*, 8, 605–611.
- Oldham, C., Lavery, P. S., McMahon, K., Pattiaratchi, C., & Chiffings, T. (2010). Seagrass wrack dynamics in Geographe Bay, Western Australia. *Report to Western Australian Department of Transport, and Shire of Bussleton*, 214.
- Olsen, J. L., Stam, W. T., Coyer, J. A., Reusch, T. B., Billingham, M., Boström, C., Calvert, E., Christie, H., Granger, S., & Lumiere, R. L. (2004). North Atlantic phylogeography and large-scale population differentiation of the seagrass *Zostera marina* L. *Molecular Ecology*, 13(7), 1923–1941.
- Onuaguluchi, O., & Banthia, N. (2016). Plant-based natural fibre reinforced cement composites: A review. *Cement and Concrete Composites*, 68, 96–108.
- Pedersen, C., & Ransby, E. (2005). Production and properties of insulation mats made from sea grass. *Hørsholm: SBI*.
- Pergent, G., Rico-Raimondino, V., & Pergent-Martini, C. (1997). Fate of primary production in Posidonia oceanica meadows of the Mediterranean. *Aquatic Botany*, 59(3–4), 307–321.
- Pergent, G., Romero, J., Pergent-Martini, C., Mateo, M.-A., & Boudouresque, C.-F. (1994). Primary production, stocks and fluxes in the Mediterranean seagrass Posidonia oceanica. *Marine Ecology Progress Series*, 139–146.
- Pfeifer, L. (2021). “Neptune Balls” Polysaccharides: Disentangling the Wiry Seagrass Detritus. *Polymers*, 13(24), 4285.
- Phanopoulos, C. (n.d.). *Polyurethanes and Isocyanates used as adhesives in*.
- Provis, J. L., & Van Deventer, J. S. J. (2009). *Geopolymers: Structures, processing, properties and industrial applications*. Elsevier.
- Pugazhenthii, N., & Anand, P. (2020). A Review on Mechanical Properties of Medium Density Fiberboard Prepared from Different Fiber Materials. *Proceedings of ICDMC 2019: Design, Materials, Cryogenics, and Constructions*, 321–333.
- Puglia, D., Petrucci, R., Fortunati, E., Luzi, F., Kenny, J., & Torre, L. (2014). Revalorisation of Posidonia oceanica as reinforcement in polyethylene/maleic anhydride grafted polyethylene composites. *J. Renew. Mater*, 2(1), 66–76.

- Rammou, E., Mitani, A., Ntalos, G., Koutsianitis, D., Taghiyari, H. R., & Papadopoulos, A. N. (2021). The potential use of seaweed (*Posidonia oceanica*) as an alternative lignocellulosic raw material for wood composites manufacture. *Coatings*, *11*(1), 69.
- Reynolds, P. L., Duffy, E., & Knowlton, N. (2018b). Seagrass and seagrass beds. *Ocean Portal*.
- Ross, K., & Mazza, G. (2010). Characteristics of lignin from flax shives as affected by extraction conditions. *International Journal of Molecular Sciences*, *11*(10), 4035–4050.
- Sánchez-Safont, E. L., Aldureid, A., Lagarón, J. M., Gámez-Pérez, J., & Cabedo, L. (2018). Biocomposites of different lignocellulosic wastes for sustainable food packaging applications. *Composites Part B: Engineering*, *145*, 215–225.
- Sanchez-Vidal, A., Canals, M., De Haan, W. P., Romero, J., & Veny, M. (2021). Seagrasses provide a novel ecosystem service by trapping marine plastics. *Scientific Reports*, *11*(1), 1–7.
- Sapalidis, A. A., Katsaros, F. K., Romanos, G. E., Kakizis, N. K., & Kanellopoulos, N. K. (2007). Preparation and characterization of novel poly-(vinyl alcohol)–*Zostera* flakes composites for packaging applications. *Composites Part B: Engineering*, *38*(3), 398–404.
- Sarmin, S. N., & Welling, J. (2016). Lightweight geopolymer wood composite synthesized from alkali-activated fly ash and metakaolin. *Jurnal Teknologi*, *78*(11).
- Saval, J., Lapuente, R., Navarro, V., & Tenza-Abril, A. (2014). Fire-resistance, physical, and mechanical characterization of particleboard containing Oceanic *Posidonia* waste. *Materiales de Construcción*, *64*(314), e019–e019.
- Saval Pérez, J. M., Lapuente Aragón, R., Navarro Miquel, V. P., & Tenza-Abril, A. J. (2014). *Fire-resistance, physical, and mechanical characterization of particleboard containing Oceanic Posidonia waste*.
- Sayer, E. J., Heard, M. S., Grant, H. K., Marthews, T. R., & Tanner, E. V. (2011). Soil carbon release enhanced by increased tropical forest litterfall. *Nature Climate Change*, *1*(6), 304–307.
- Schubert, M., Luković, M., & Christen, H. (2020). Prediction of mechanical properties of wood fiber insulation boards as a function of machine and process parameters by random forest. *Wood Science and Technology*, *54*, 703–713.
- Seggiani, M., Cinelli, P., Balestri, E., Mallegni, N., Stefanelli, E., Rossi, A., Lardicci, C., & Lazzeri, A. (2018). Novel sustainable composites based on poly (hydroxybutyrate-co-hydroxyvalerate) and seagrass beach-CAST fibers: Performance and degradability in marine environments. *Materials*, *11*(5), 772.
- Seggiani, M., Cinelli, P., Mallegni, N., Balestri, E., Puccini, M., Vitolo, S., Lardicci, C., & Lazzeri, A. (2017). New bio-composites based on polyhydroxyalkanoates and *posidonia oceanica* fibres for applications in a marine environment. *Materials*, *10*(4), 326.
- Shafer, D. J., Kaldy, J. E., & Gaeckle, J. L. (2014). Science and management of the introduced seagrass *Zostera japonica* in North America. *Environmental Management*, *53*, 147–162.
- Short, F., Carruthers, T., Dennison, W., & Waycott, M. (2007). Global seagrass distribution and diversity: A bioregional model. *Journal of Experimental Marine Biology and Ecology*, *350*(1–2), 3–20.
- Short, F. T. (1983). The seagrass, *Zostera marina* L.: Plant morphology and bed structure in relation to sediment ammonium in Izembek Lagoon, Alaska. *Aquatic Botany*, *16*(2), 149–161.
- Short, F. T. (2003). *World atlas of seagrasses*. Univ of California Press.

- Stefanidou, M., Kamperidou, V., Konstantinidis, A., Koltsou, P., & Papadopoulos, S. (2021). Use of *Posidonia oceanica* fibres in lime mortars. *Construction and Building Materials*, *298*, 123881.
- Torbatinejad, N. M., Annison, G., Rutherford-Markwick, K., & Sabine, J. R. (2007). Structural constituents of the seagrass *Posidonia australis*. *Journal of Agricultural and Food Chemistry*, *55*(10), 4021–4026.
- Vacchi, M., De Falco, G., Simeone, S., Montefalcone, M., Morri, C., Ferrari, M., & Bianchi, C. N. (2017). Biogeomorphology of the Mediterranean *Posidonia oceanica* seagrass meadows. *Earth Surface Processes and Landforms*, *42*(1), 42–54.
- Vasapollo, C. (2009). *Spatio-temporal variability of plant features and motile invertebrates in Posidonia oceanica seagrass meadows*.
- Vichkovitten, T., & Holmer, M. (2004). Contribution of plant carbohydrates to sedimentary carbon mineralization. *Organic Geochemistry*, *35*(9), 1053–1066.
- Voca, N., Grubor, M., Peter, A., & Kricka, T. (2019). Evaluation of *Posidonia oceanica* waste as a biomass source for energy generation. *Bioenergy Research*, *12*(4), 1104–1112.
- Wabnitz, C. C., Andréfouët, S., Torres-Pulliza, D., Müller-Karger, F. E., & Kramer, P. A. (2008). Regional-scale seagrass habitat mapping in the Wider Caribbean region using Landsat sensors: Applications to conservation and ecology. *Remote Sensing of Environment*, *112*(8), 3455–3467.
- Wyllie-Echeverria, S., & Cox, P. A. (1999). The seagrass (*Zostera marina* [Zosteraceae]) industry of Nova Scotia (1907-1960). *Economic Botany*, 419–426.
- Xu, Y., & Chung, D. (2000). Effect of sand addition on the specific heat and thermal conductivity of cement. *Cement and Concrete Research*, *30*(1), 59–61.
- Zhao, Q., Zhang, B., Quan, H., Yam, R. C., Yuen, R. K., & Li, R. K. (2009). Flame retardancy of rice husk-filled high-density polyethylene ecocomposites. *Composites Science and Technology*, *69*(15–16), 2675–2681.
- Zhuang, X. Y., Chen, L., Komarneni, S., Zhou, C. H., Tong, D. S., Yang, H. M., Yu, W. H., & Wang, H. (2016). Fly ash-based geopolymers: Clean production, properties and applications. *Journal of Cleaner Production*, *125*, 253–267.

Appendix

Article 1

Mechanical properties of lightweight gypsum composites comprised of seagrass *Posidonia oceanica* and pine (*Pinus sylvestris*) wood fibers – Article 1

Aldi Kuqo *, Carsten Mai

*Corresponding author, email: akuqo@uni-goettingen.de

Wood Biology and Wood Products, Burckhardt Institut, Georg-August-Universität Göttingen, BÜsgenweg 4, 37077 Göttingen

Authorship (according to Clement, 2014)

	Conceptualization (30%)	Practical work (30%)	Writing/Editing (30%)	Administration (10%)	Contribution
A. Kuqo	60%	100%	70%	20%	71%
C. Mai	40%	0%	30%	80%	29%

Ideas: Design of the investigation / Experimental planning / Interpretation of the data

Work: Execution of the experiment / Data collection and analysis

Writing: Drafting the article / Critical, substantive revision / Reviewing the final version

Administration: Resource management and ensuring scientific integrity before, during, and after publication

Published in Construction and Building Materials, 282, 122714.

Published in February 2021

DOI: <https://doi.org/10.1016/j.conbuildmat.2021.122714>

Mechanical properties of lightweight gypsum composites comprised of seagrass *Posidonia oceanica* and pine (*Pinus sylvestris*) wood fibers



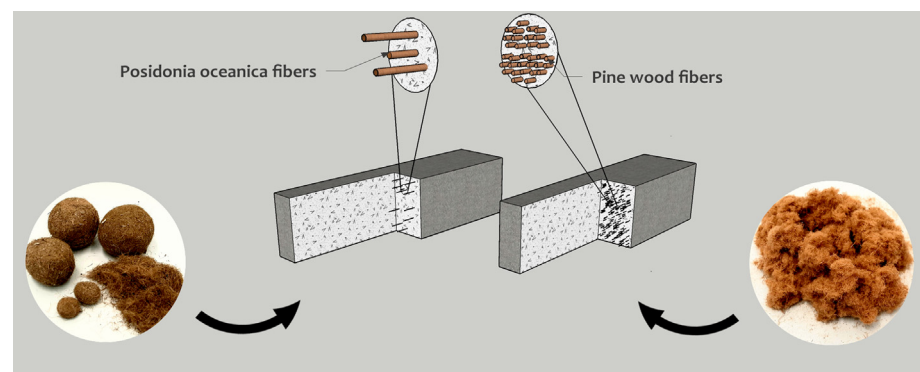
Aldi Kuqo*, Carsten Mai

Wood Biology and Wood Products, Burckhardt Institute, Georg-August University of Göttingen, Büsingenweg 4, 37077 Göttingen, Germany

HIGHLIGHTS

- Seagrass (*Posidonia oceanica*) and pine wood (*Pinus sylvestris*) fibers used as reinforcing components in plaster.
- Incorporation of wood fibers improves mechanical properties of plaster.
- Addition of seagrass and wood fibers enhances plaster toughness.
- The number and length of the added fibers influences the fracture mechanism of the plaster.

GRAPHICAL ABSTRACT



ARTICLE INFO

Article history:

Received 16 October 2020
Received in revised form 16 January 2021
Accepted 14 February 2021

Keywords:

Gypsum composites
Mechanical properties
Posidonia oceanica
Pine wood fibers
Seagrass

ABSTRACT

Considering the current environmental awareness and the increasing interest in advanced and sustainable materials, the use of natural fibers has become a common practice owing to their appealing characteristics. This study assesses the mechanical properties with respect to bending and compression, impact bending resistance as well as the hardness of gypsum plaster composed with the Mediterranean seagrass (*Posidonia oceanica*) and pine wood (*Pinus sylvestris*) fibers. The addition of fibers from 1 to 6 wt% led to a reduction of density from 5% to 30%, respectively. In terms of mechanical properties, composites containing up to 2% wood fiber develop enhanced flexural and compression strength by 28% and 4% respectively; however, a further addition worsened these properties. Composites comprised of seagrass yielded a decrease in strength; yet, the fracture energy absorbed by the material before it completely lost its load-bearing capacity increased. Correspondingly, the impact resistance of the seagrass composites was 57% higher than that of unreinforced plaster. Surface hardness tests indicated that the smaller wood fibers are more effective in transferring the load on a small scale and therefore can improve localized strength compared to larger seagrass fibers. The addition of seagrass and wood fibers presents a sustainable and ecological way to improve the major properties of gypsum products.

© 2021 Elsevier Ltd. All rights reserved.

1. Introduction

As one of the most common indoor building materials, gypsum plays a significant part in construction especially as a finishing

material. It is a low-cost product with the ability to shape in various forms giving aesthetically pleasing lining as well as having several other properties such as good thermal insulation and the ability to regulate the humidity in the interior [1]. Gypsum products, however, require adequate mechanical and physical properties depending on their application, which cannot always be guaranteed.

* Corresponding author.

E-mail addresses: akuqo@uni-goettingen.de (A. Kuqo), cmai@gwdg.de (C. Mai).

Although conventional gypsum plasterboard has an acceptable compressive resistance, it often lacks the tensile and bending strength required in building for the interior. In order to overcome this limitation, a wide variety of reinforcing agents such as synthetic and natural fibers have been employed. Synthetic polymeric fibers, basalt fibers, and mainly fiberglass have been largely used as reinforcing meshes as well as in dispersed form in the gypsum matrix [2–7]. The obtained reinforced composites exhibited improved stiffness dissipation capacity and superior impact resistance. The reinforcement increases the ductility of the composite owing to the absorption of a large amount of energy by fibers [7]. Apparently, fibers, which in most cases have a higher tensile strength than the gypsum matrix, may contribute to the improvement of the mechanical performance of the composite through the distribution of applied stress load [8].

Natural fibers have gained attention as a potential replacement of the conventional synthetic ones, considering both the environmental awareness, the low cost, and their attractive features such as the combination of mechanical and physical-thermal properties. Traditional natural fibers such as palm fibers, jute, sisal, and others have been widely used and proved to positively affect the properties of plasterboards [2,9–14]. Particularly, hemp has been studied and considered as a promising candidate. Lucolano et al. investigated hemp fibers, concluding that their addition can enhance the mechanical properties of the reinforced plasterboard even at high temperatures [15,16].

In addition to these natural fibers, wood, both particles (chips) and fibers, have been used as substitutes for synthetic reinforcing/filling agents. Particles are processed by chipping large wood parts into smaller ones, whereas fibers are manufactured by using a high-cost refining process. A decrease in density and an improvement of hygrothermal properties were noticed due to the addition of sawdust and/or fibers to the gypsum paste; flexural and compressive strength, however, considerably decreased [17–20]. Similar results were obtained by using wood fibers, although, in some cases, when small amounts were added, mechanical performance reportedly improved [21].

In the last decades, due to the increasing demand for natural-based composites, much research has been carried out to investigate local, non-conventional alternatives for their utilization in construction.

Posidonia oceanica seagrasses are aquatic flowering plants, endemic to the Mediterranean Sea. They play a crucial role in the marine habitats across the seashores as they protect the thalassic environment and provide food for the sea fauna. After stormy weather conditions, however, leaves detach from the main plant and accumulate in the shoreline. Beach wracks (seagrass remains) in the coastal shores are a longstanding problem as their decomposition is the source of unpleasant smells and as they present an unattractive appearance especially in the touristic season. In addition, the removal of this undesirable lignocellulosic waste incurs a considerable cost for seaside communities. The seagrass is divided into two parts, the brownish leaves and the balls composed of fibrous material known as egargopili or *Posidonia oceanica* balls.

Posidonia oceanica fibers have been studied in the last decade as a response to the demand for new environmentally and sustainable materials. As has been previously reported, they possess interesting physical and mechanical properties which make them propitious for various applications [22]. A lot of research has been conducted with respect to polymer bio-composites using seagrass fibers [23,24]. Seagrass composites display satisfying mechanical performance and present a feasible and valuable solution to the present-day management problem associated with the accumulation of seagrass wastes on the seashore. Additionally, utilization of seagrass in mineral (cement) bonded composites, revealed an increase of flexural and compressive strength up to a specific

seagrass fiber content, whereas density was significantly lower than that of pure cement blocks [25,26].

The main objective of the present study was to assess the major mechanical properties of gypsum composites consisting of *Posidonia oceanica* fibers and to compare them with pine wood fibers as eco-friendly and cost-effective solutions.

2. Experimental work

2.1. Materials

Posidonia oceanica fibers (POF) were randomly collected in the coastal area of Durres (Albania) in November 2019. Fibers were interconnected, forming balls with various equivalent diameters varying from 4 to 15 cm (Fig. 1 a). POF balls were put in a mobile sawdust suction collector in order to unravel fibers without shortening and changing their morphological features. *Pinus sylvestris* wood fibers (WF) used for insulation (Fig. 1 b) were provided by STEICO SE (Feldkirchen, Germany). The compressed and agglomerated wood fibers were processed in a hammer mill (Electra SAS VS1, Poudenas, France) in order to split and increase their bulk volume. This step was undertaken as a way of preventing the balling effect during mixing.

The commercial gypsum Knauf Goldband with a concentration (CaSO_4) > 85% (Knauf Gips KG, Iphofen, Germany) for interior application was used as a binding agent in this study. It meets all the requirements in accordance with the characteristics defined in the EN 13279-1 [27].

2.2. Methods

2.2.1. Fibershape analysis

Preliminary characterization of fiber morphology was performed to evaluate the length distribution of POF and WF. A small amount of fibers was weighted (0.25 g for POF and 0.10 g for WF) then, using a sieve, they were carefully distributed into the scanner glass. Fibers were placed and scattered in such a way, so they do not superimpose on each other. This step is of a high importance since superimposed objects often appear larger than their actual size while two attached fibers/particles will be counted as a single one. A scanner (Epson Perfection V850 Pro, Epson, Tokyo, Japan) was employed for capturing high resolution images. Photographs were then analyzed with FibreShape PRO (X-shape, IST, Vilters, Switzerland).

2.2.2. Preparation of fiber reinforced composites

Prior to mixing fibers with the gypsum paste, their moisture content was determined via a thermogravimetric approach and the equivalent dry mass for the mixture was established. The water: gypsum ratio changed with the added amount of fibers as they increasingly absorb water and affect the workability of the paste.

Gypsum was mixed with water using a low-speed electric mixer (Heidolph d744.01, Heidolph Instruments, Schwabach, Germany) for approximately 1 min. Subsequently, the fibers were slowly added in order to avoid agglomeration and achieve full dispersion in the matrix. The mixing period, following the addition of fibers, lasted roughly 5 to 15 min depending on the amount of added fibers. The homogeneous paste was molded in prismatic molds which were previously coated with a release agent and left for 12 h to set. In the next step, the specimens were unmolded, dried at 40 °C for 48 h, and then stored in a climatic chamber ($T = 23$ °C, $\text{RH} = 50\%$). For each type of composite, three gypsum – fiber mixtures, and for each mixture three standardized specimens were prepared (in total 9 specimens).



Fig. 1. *Posidonia oceanica* fibers and balls (a) and pine wood fibers (b).

Table 1

The design of the mixture for the preparation of composites containing *Posidonia oceanica* fibers (POF-C) and wood fibers (WF-C).

Type of composite	Amount of WF (wt %)	Amount of POF (wt %)	Water : Gypsum ratio
REF-C	–	–	0.60
WF1-C	1	–	0.62
WF2-C	2	–	0.64
WF4-C	4	–	0.70
WF6-C	6	–	0.80
POF1-C	–	1	0.62
POF2-C	–	2	0.64
POF3-C	–	4	0.70
POF4-C	–	6	0.80
POF-WF-C	1	1	0.64

2.2.3. SEM investigation

Scanning electron microscope images of the broken samples were taken using a Zeiss EVO LS 15 Microscope (Carl Zeiss Microscopy GmbH, Jena, Germany).

2.2.4. Flexural and compressive strength

Modulus of rupture (MOR) was assessed in a three-point bending test (Fig. 5 a.) according to the European standard EN 13279-2 [28]. For this purpose, a universal testing machine (ZwickRoell Zmartpro, ZwickRoell, Ulm, Germany) with a 10 kN load cell was utilized at a constant displacement rate of 1 mm min⁻¹. The samples displayed dimensions of 160 × 40 × 40 mm³ and the effective span between supports was 100 mm (Fig. 6 a). Along with flexural strength, Young Modulus was determined by the three-points bending test as well. After testing, the half-broken samples were used for the compression test.

For the compression test, a universal testing machine (ZwickRoell Zmartpro, ZwickRoell, Ulm, Germany) with a 10 kN load cell was employed, operating with a displacement speed of 0.7 mm min⁻¹. In order to guarantee a compressive surface of 1600 mm² (in accordance with the standard), two prismatic metal bars with dimensions of 40 × 40 × 8 mm³ were attached to the movable crosshead and the table. Half-broken samples were checked for possible fractures and then were placed over and precisely fitted to the prismatic bars.

2.2.5. Impact bending test

The Charpy - notched impact strength was determined using a swinging pendulum impact tester (Resil Impact, CEAST, Martinsried, Germany) following a slight variation of the procedure described in ISO 179 [29] for long fiber reinforced composites using

planned specimens with dimensions of 10 × 15 × 110 mm³. The support span for the bending test was 60 mm.

2.2.6. Brinell hardness test

Brinell hardness was determined according to the European standard EN 13279-2 [28] utilizing a universal testing machine (ZwickRoell Zmartpro, ZwickRoell, Ulm, Germany) with a 10 kN load cell and a displacement speed of 0.5 mm min⁻¹. A 10 mm diameter steel sphere was used as an indenter applying 200 N force (a 100 N load was used in case of less dense samples) on the surface of the sample with dimensions of 40 × 40 × 40 mm³ (in total 9 specimens for each type of composite).

3. Results and discussion

3.1. Fiber length distribution

For the fiber length distribution, approx. 49.7 × 10³ seagrass fibers (POF) and 137.2 × 10³ wood fibers (WF) were measured. Taking in consideration the initial weighted amount for the test and the number of measured objects for each type of fiber it can be asserted that the number of fibers per unit of weight (g) was much greater in case of WF than that of POF. Boxplots show a rough geodesic length distribution to illustrate POF and WF assessed by FibreShape (Fig. 2). Therein, whiskers represent the first and the last decile (10th and 90th percentile) whereas filled boxes (P10-P50 and P50-P90) represent the interval between them. The mean length for POF was 4.8 mm, but only 0.7 mm for WF. Comparing the 50th and 90th percentiles between the two

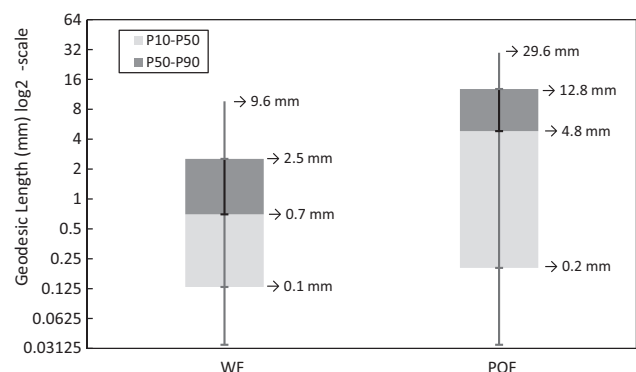


Fig. 2. Geodesic fiber length distribution of *Posidonia oceanica* fibers (POF) and wood fibers (WF) assessed by FibreShape. *P10-P50 and P50-P90 represent the intervals of the 10th to 50th percentile and the 50th to 90th Percentile respectively.

types of fibers (the dark grey area in the boxplot), POF were on average 5 to 6 times longer than WF.

3.2. Phenomena during mixing and curing of the composites

Even though no specific tests were undertaken to investigate various occurrences in the preparation process, some differences were observed between WF and POF during mixing. In both cases, the addition of the cellulosic fibers worsens the workability of the paste making it harder to stir. The excessive volume of water, necessary to maintain the workability of the paste-mixtures was proportional to the amount of added fibers. This relationship, however, appeared to be exponential rather than linear.

As mentioned above, the addition of cellulosic fibers was undertaken at slow speed due to the undesirable balling effect which generates agglomeration and causes evident fluctuations in density and strength of the boards. POF turned out to be more prone to agglomerate than WF and to form balls during mixing. Longer POF were more prone to agglomeration than shorter WF.

During curing, significant dissimilarities were noticed concerning the contraction of the gypsum paste. Caliper measurements indicated that the gypsum - wood fiber mixtures containing high amount of fibers had a greater tendency to shrink than the gypsum - seagrass mixture and the pure gypsum paste. Concrete values of drying shrinkage for gypsum mixtures containing the maximal amount of fibers are 0.29% and 0.65% for POF6-C and WF6-C respectively, while pure gypsum pastes shrank by 0.19%. According to previous studies, the addition of plant fibers to cement mortar can increase its drying shrinkage [30]. Research has shown that drying shrinkage depends on the type and amount of lignocellulosic fibers, their surface characteristics and moisture absorption behavior [31].

The increased drying shrinkage of pine WF6-C compared to others can be attributed, along with the aforementioned factors, to the small dimensions of the hydrophilic wood fibers which results in a higher surface area. This is a positive trait for the composites containing *Posidonia oceanica* fibers (POF-C), as high shrinkage is usually undesirable in the manufacturing process.

3.3. SEM investigation

Scanning electron micrographs indicated a weak adhesion of the fibers to the matrix caused mostly by their morphological features and the lack of surface roughness. In addition, the SEM images revealed the presence of voids and pores in the gypsum matrix, which can negatively affect the interaction. The images display the dissimilarities between fibers and their lack of compatibility with the gypsum matrix (Fig. 3). The hill-like structures of the POF surface (Fig. 3 b) affect the interconnection of the fibers with the gypsum matrix negatively (the relatively big, calcium sulfate hemihydrate crystals) as they reduce the number of bonding sites with the matrix. This results in low pull out resistance (Fig. 3 c, d).

3.4. Density

Densities of prepared specimens varied from 655 kg m^{-3} to 934 kg m^{-3} (Table 2). The addition of fibers caused a decrease in density. Additionally, the densities of POF-C were, on average, slightly lower than those of wood fiber-composites (WF-C) with the same amount of added fibers. Lower densities imply that the material has a declined thermal conductivity compared to the reference products (pure gypsum plasterboards) making it propitious for insulation purposes.

3.5. Flexural and compressive strength

Flexural strength varies from 0.73 N mm^{-2} to 1.39 N mm^{-2} for WF-C and 0.50 N mm^{-2} to 0.88 N mm^{-2} for POF-C, while the reference specimens (REF-C) had a mean bending strength of 1.09 N mm^{-2} (Fig. 4). WF-C, at first, experienced an approx. 28% increase in strength up to fiber content of 2%, and then, it decreased with the further addition of fibers. On the other hand, the strength of composites containing POF constantly decreased with increasing amounts of fibers. Correspondingly, compressive strength exhibited the same trends as bending strength (Table 2). Composites containing small amounts of POF and WF (1 wt% for each type of fiber) exhibited a 13% reduction in density while their flexural strength reached 1.08 N mm^{-2} .

The density of the material had a significant influence on the mechanical properties. Both compressive and tensile load (flexural load can be expressed as tensile load in the tensile zones, mainly the cores of the sample) can be divided by the specimen's cross-sectional area. As the cross-sectional area is decreased due to the presence of pores, voids, and micro-cracks in the internal structure, the applied load is amplified. By using POF and WF as reinforcing agents, the applied load is transmitted to and distributed among the fibers to the matrix phase to a larger degree reducing the chance of stress concentration and eventually crack occurrence. The same amount of pine wood fibers having small sizes creates more bridging connections than seagrass fibers; these connections can better transfer and distribute the applied load to the inner structure of the composite (Fig. 5).

Aside from the decreased cross-sectional area for the transfer of load within the matrix, porosity can affect the transmission of the matrix and the fiber as well. A less densified vicinity of the fiber region can attenuate the adherence between fiber and matrix and, thus, facilitating the pullout process. Pulled out fibers from the bending test specimen are shown in Fig. 6 b. In addition to density reduction, an influential factor for the worsening of the mechanical properties is the mixtures' water : gypsum ratio, which was increased up to 25%.

The load-displacement diagram (Fig. 7) indicated that adding of WF and especially POF enhanced the ductility compared to the reference plaster (REF-C). The initial linear response of the fiber-reinforced plaster corresponds to the perfect interconnection of the fiber and the gypsum matrix. In this stage, there is an elastic reaction to loading and no cracking occurs. This part also reflects the modulus of elasticity (MOE), which in the case of REF-C ends with the maximal value (Table 2). A slight reduction in MOE was noticed in composites containing 1 and 2% WF, even though their flexural strength was higher. This minor decrease is attributed to two reasons: The amount of fibers increases the porosity and cracking of the gypsum matrix takes place more easily. Subsequently, small fibers are engaged in the transfer of the compression load, preventing further increase in the rate of displacement with the applied load. In contrast, the MOE values of POF-C are evidently lower because the increase of porosity has a stronger effect than the transfer of applied force.

In the second stage, following the elastic part, at a specific point on the ascending curve, the response became nonlinear because some parts of the fiber began to de-bond and propagate along with the embedded length. In the third stage (the post-crack region) a further debonding and fiber sliding took place. In this stage, there was an evident difference between the curves of POF-C and WF-C composites in the load-displacement diagram.

While composites containing WF experience an instantaneous drop in load-bearing ability, due to the fiber's small size, composites containing POF can maintain higher load-bearing capacity due to the friction and mechanical interlocking between the gypsum matrix and the long fibers.

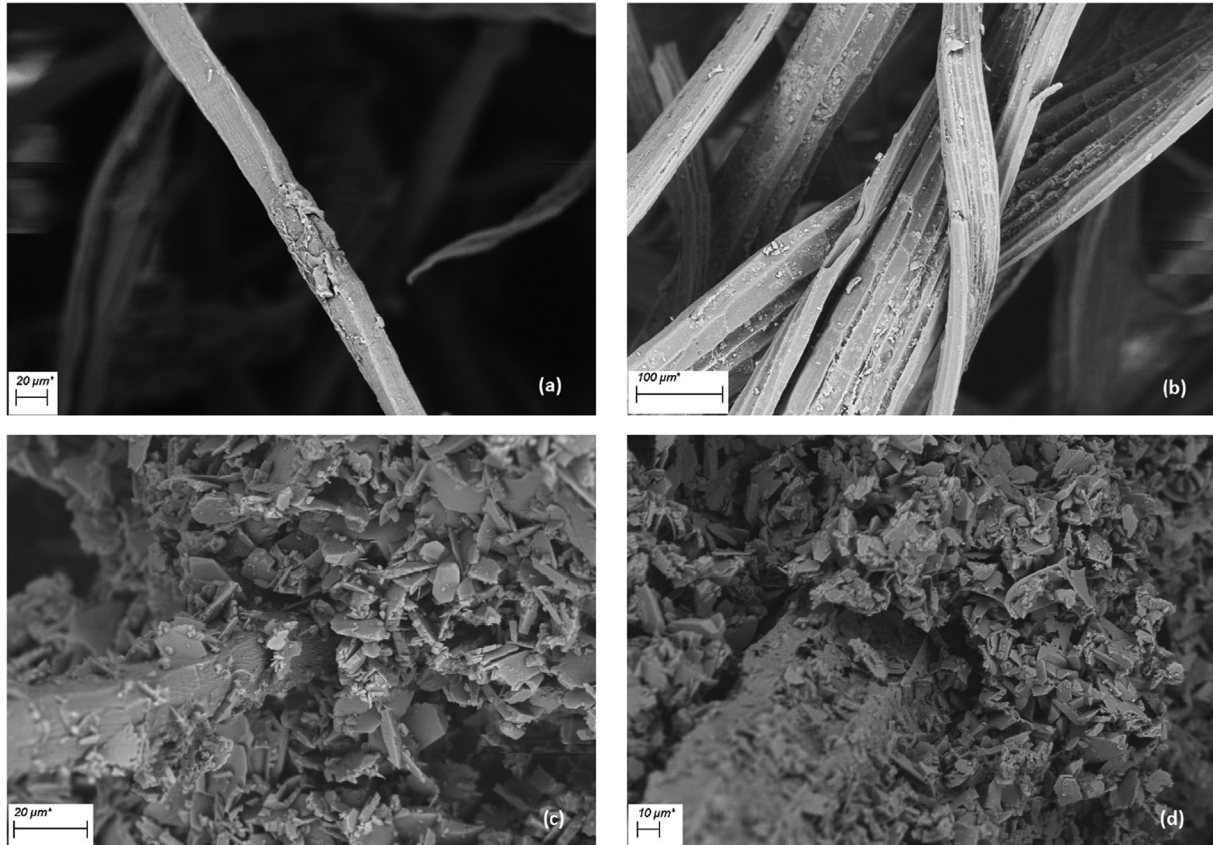


Fig. 3. SEM images of (a) single pine wood fibers, (b) single *Posidonia oceanica* seagrass fibers, (c) structure of WF-C showing WF – matrix connection and (d) structure of POF-C showing POF – matrix connection.

Table 2

Density, modulus of elasticity (MOE) and compression strength of *Posidonia oceanica* fiber composites (POF-C) and wood fiber (WF-C) composites.

Type of Composite	Density (kg m ⁻³)	Modulus of elasticity (N mm ⁻²)	Compression strength (N mm ⁻²)
REF-C	934 ± 6	562 ± 54	2.51 ± 0.02
WF1-C	895 ± 69	489 ± 86	2.49 ± 0.47
WF2-C	894 ± 17	538 ± 69	2.61 ± 0.12
WF4-C	713 ± 22	123 ± 19	1.33 ± 0.23
WF6-C	685 ± 29	93 ± 25	0.79 ± 0.08
POF1-C	853 ± 33	355 ± 40	2.07 ± 0.13
POF2-C	812 ± 13	194 ± 28	1.48 ± 0.08
POF4-C	723 ± 26	109 ± 27	0.85 ± 0.15
POF6-C	655 ± 33	70 ± 19	0.52 ± 0.08
POF-WF-C	811 ± 28	188 ± 22	1.93 ± 0.14

Mean values and standard deviations (±) of 9 (3 sets × 3 samples) replicates for each type of composite

3.6. Impact resistance and absorbed energy

The addition of fibers increased the impact resistance and thus indicated higher ductility as the fibers can absorb more energy while REF-C (0 wt% fibers) exhibited a brittle behavior (Fig. 8). Mean values varied from 0.63 kJ m⁻² for REF-C to 1.40 kJ m⁻² for composites with 4% POF. While the static bending strength was higher for WF-C, the impact bending resistance appeared to be higher for POF-C composites. This difference is attributed to the post-crack energy required to completely break the specimens. Aside from this, the impact bending strength is equivalent to the toughness (at static bending it is given by the total area under the load–displacement curve in Fig. 7). Regarding POF-WF-C (data not presented in the diagram), the impact bending resistance is

substantially higher (approx. 40%) compared to the REF-C reaching a value of 1.02 kJ m⁻².

In contrast to WF-C the long seagrass fibers in the POF-C required an additional amount of energy in order to completely pull out of the matrix (Fig. 9). This energy is related to the friction between fibers and gypsum mortar when fiber sliding took place.

3.7. Brinell surface hardness

Similar to bending and compression strength, composites containing 2% WF displayed the highest Brinell hardness (Table 3), whereas further addition of fibers had negative effects. On the other hand, the addition of POF, irrespective of the amount, considerably reduced hardness.

The decrease in hardness is due to the reduction of density and eventually the increase in porosity in the inner structure of the gypsum specimen. On the other hand, a minor addition of WF enhanced hardness even though the density of the samples was slightly lower. This indicates that the addition of small WF can increase the surface strength of the composite. The same amount of POF did not act in the same way as WF did. Compared to WF, large POF do not affect the transfer of the applied load from the indenter to the inner part but, instead, they mostly affect hardness by increasing the porosity and the number of voids in the gypsum composite.

The surface hardness, as well as most of the mechanical properties, have a direct dependency on the number of the pores and distribution of fibers in the inorganic matrix. The surface hardness of REF-C (Fig. 10 a) was relatively high because of the low number of pores in the matrix. Indenter caused only localized damage, crushing only the part that is completely in contact with it. A slight

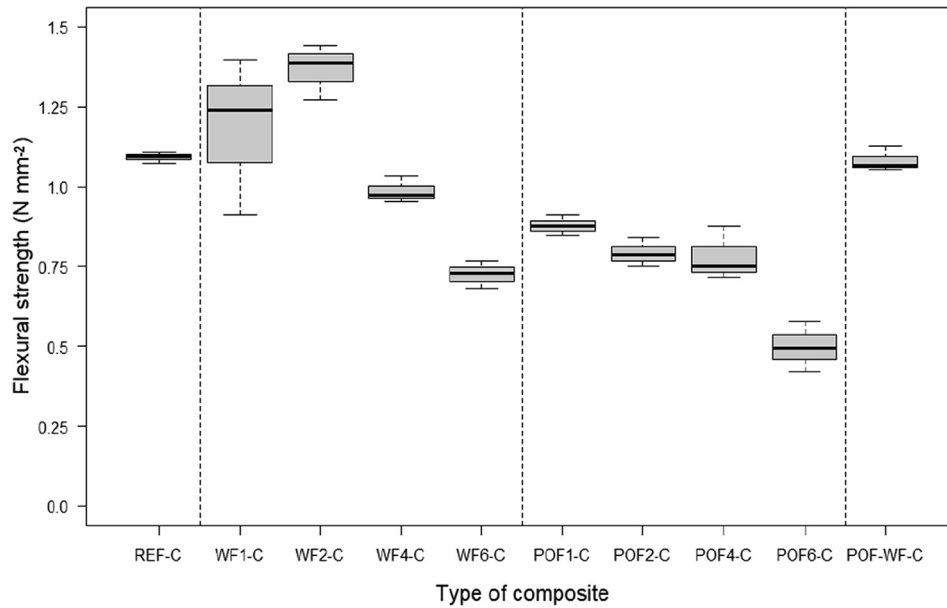


Fig. 4. Flexural strength of reference specimen (REF-C), *Posidonia oceanica* fiber – gypsum composite (POF-C) and wood fiber – gypsum composite (WF-C) and the mixture (POF-WF-C) containing various amounts of fibers as specified in Table 1.

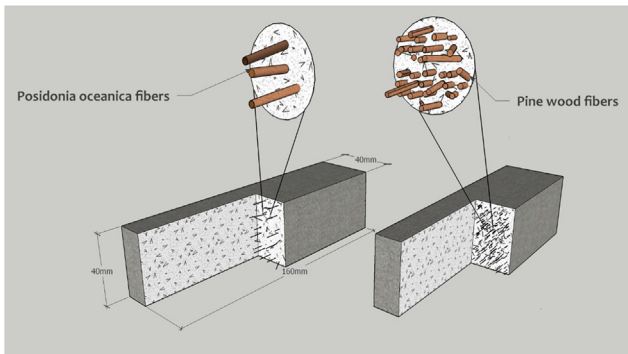


Fig. 5. Illustration of specimens containing large *Posidonia oceanica* fibers and small pine wood fibers.

addition of wood fibers increased porosity and mechanical strength of the composite (WF1-C). Black arrows (Fig. 10 b) show the damaged area from the indenter. Compared to REF-C, WF1-C has wider damaged area indicating that an enlarged volume of

fiber–matrix was engaged for the transfer along the spherical indenter. The anisotropic distribution of small fibers may induce increased reinforcement as the fibers might be able to transmit the bearing load to the other parts of the structure. Further addition of fibers can worsen mechanical properties to a great extent. Composites containing a high amount of fibers are shown in the images below (Fig. 10 c, d). Similarly, with WF1-C, composites containing 6%wt fibers exhibit an extended damaged area along the indenter. This region appears to have a brownish color because of the high concentration of fibers (the broken gypsum matrix particles were removed when the cut was made) and is indicated by black arrows.

4. Conclusion

The effect of the incorporation of two natural fibers, seagrass (*Posidonia oceanica*) and pine wood (*Pinus sylvestris*) on the mechanical properties of gypsum was investigated in this article. Gypsum plasters containing wood fibers can be used for interior applications requiring better flexural performance. Further, lower bulk densities suggest that composites can be used as thermal

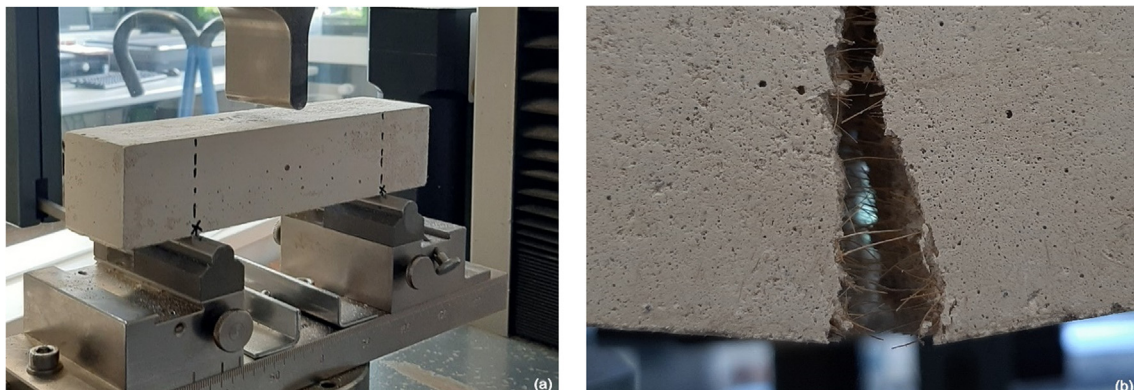


Fig. 6. Setup of three-point bending test (a), pulled out fibers under bending stress (b).

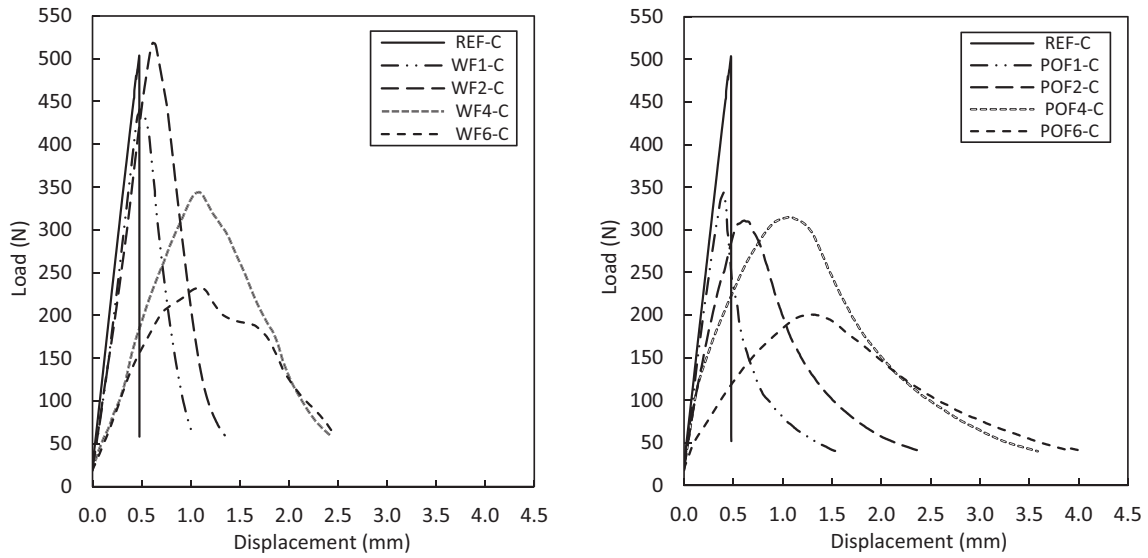


Fig. 7. Applied load versus displacement for *Posidonia oceanica* fiber – gypsum composites (POF-C) and for wood fiber – gypsum composites (WF-C).

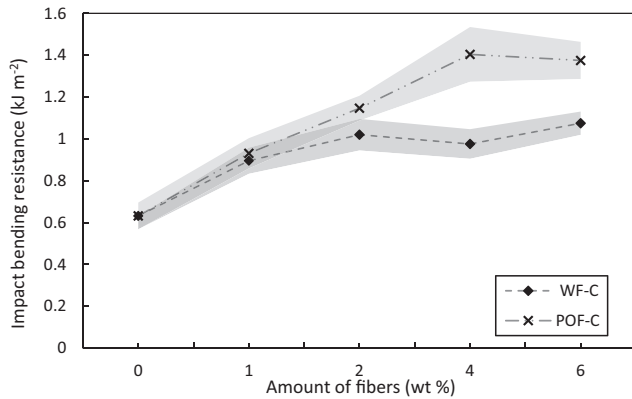


Fig. 8. Impact bending resistance for REF-C (0 wt% amount of fibers), *Posidonia oceanica* fiber – gypsum composites (POF-C) and for wood fiber – gypsum composites (WF-C), the grey-shaded area represents standard deviation).

Table 3

Brinell hardness of gypsum composites.

Type of Composite	Surface hardness (N mm^{-2})
REF-C	5.0 ± 0.1
WF1-C	5.4 ± 0.6
WF2-C	5.7 ± 0.3
WF4-C	2.0 ± 0.1
WF6-C	1.7 ± 0.3
POF1-C	3.2 ± 0.2
POF2-C	2.6 ± 0.2
POF4-C	1.7 ± 0.1
POF6-C	1.3 ± 0.1
POF-WF-C	3.3 ± 0.2

Mean values and standard deviations (\pm) of 9 (3 sets \times 3 samples) replicates for each type of composite

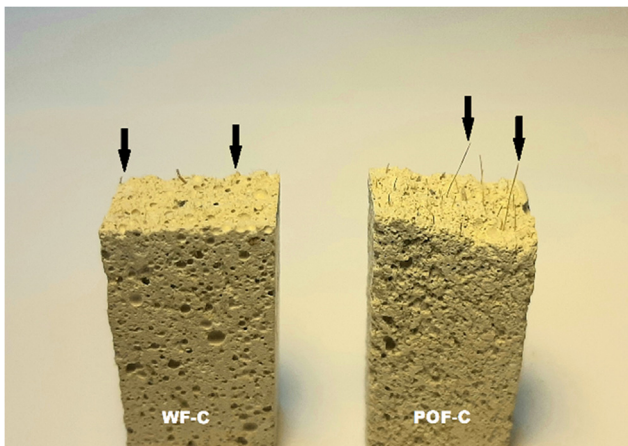


Fig. 9. Broken unnotched Charpy test specimens for wood fiber composites (WF-C, left) and for seagrass fiber composites (POF-C, right). Black arrows indicate the presence of fibers.

insulating blocks, partition blocks, and non-load-bearing wall panels. In terms of mechanical performance, composites containing up to 2% wood fibers (WF-C) develop enhanced flexural strength, compression strength, and surface hardness, however, a further addition can worsen these properties due to the increase of porosity. The behavior of plaster changed from brittle to non-linear one when fibers were added. The number of fibers that are equivalent to load transfer sites, and their length, variously influenced mechanical properties. The addition of low-cost seagrass can make the material more ductile as it may absorb more mechanical energy until failure. A combination of low amounts of WF and POF in the composite (WF-POF-C) reduces density, increases toughness, even though the material itself can maintain similar flexural properties as the unreinforced plaster (REF-C). In the case of lightweight gypsum composites, where the porosity was high and the connection between fibers and matrix was poor, the factor that predominated in mechanical strength was the number of fibers (transfer sites) rather than their length.

Since the dumping of seagrass, a waste lignocellulosic material found on the Mediterranean seashores does not provide the optimal solution, its utilization as a reinforcement or as a filler can bear numerous advantages in the local building sector. Gypsum mortar reinforced with seagrass and refined wood fibers present a sustainable and eco-friendly alternative for the construction industry and can be of particular interest for application in highly seismic areas.

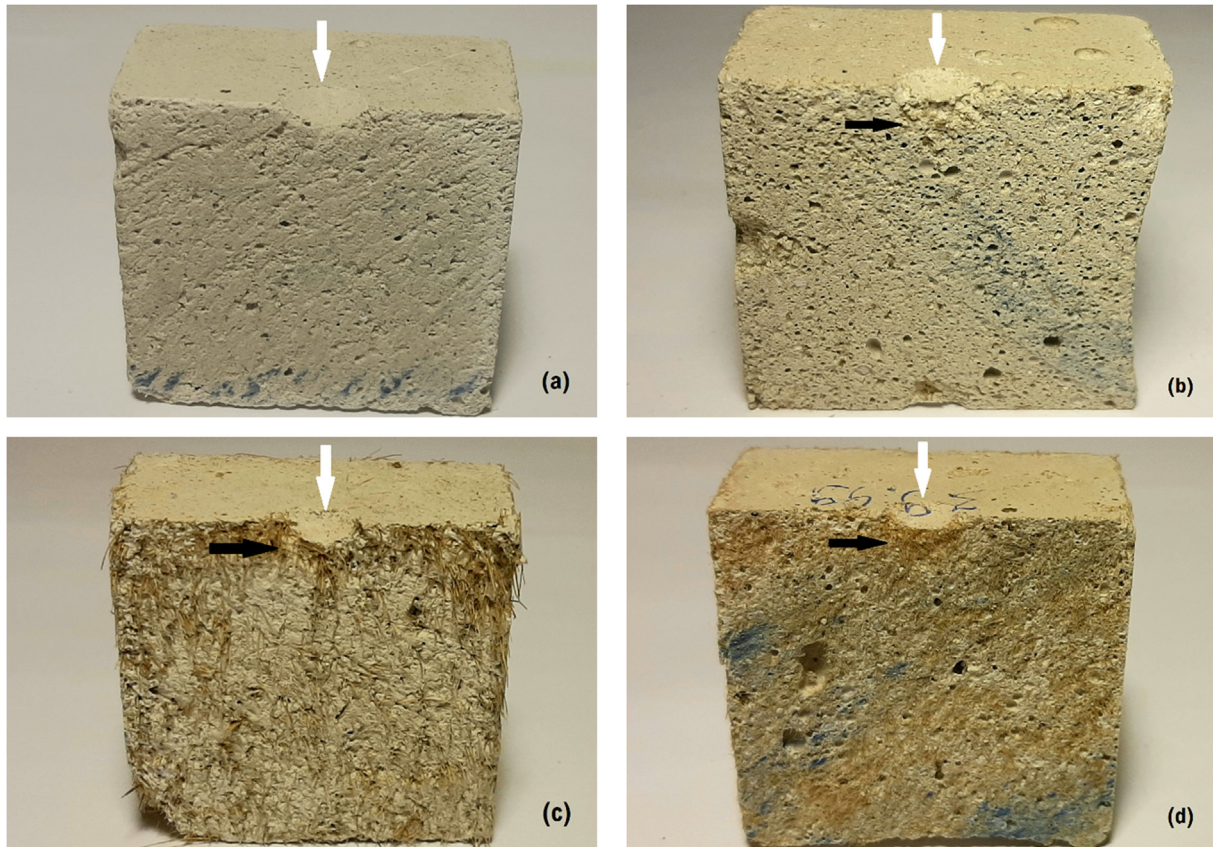


Fig. 10. Cross sections of tested surface hardness cubic specimens for REF-C (a), WF1-C (b), POF6-C (c), WF6-C (d).

CRedit authorship contribution statement

Aldi Kuqo: Conceptualization, Methodology, Data curation, Writing - original draft, Investigation, Validation, Writing - review & editing. **Carsten Mai:** Conceptualization, Methodology, Investigation, Supervision, Validation, Writing - review & editing.

Declaration of Competing Interest

The authors declare that they have no known competing financial interests or personal relationships that could have appeared to influence the work reported in this paper.

Acknowledgements

This work was supported by DAAD (German Academic Exchange Service). Funding was provided through the funding programme: Research Grants - Doctoral Programmes in Germany, DAAD.

References

- [1] Ji Hun Park, Yujin Kang, Jongki Lee, Seunghwan Wi, Jae D. Chang, Sumin Kim, Analysis of walls of functional gypsum board added with porous material and phase change material to improve hygrothermal performance, *Ener. and Build.* 183 (2019) 803–816, <https://doi.org/10.1016/j.enbuild.2018.11.023>.
- [2] Manjit Singh, Mridul Garg, Gypsum-based fibre-reinforced composites: an alternative to timber, *Constr. Build. Mater.* 8 (1994) 155–160, [https://doi.org/10.1016/S0950-0618\(09\)90028-9](https://doi.org/10.1016/S0950-0618(09)90028-9).
- [3] Cong Zhu, Jianxin Zhang, Jiahui Peng, Wenxiang Cao, Jiansen Liu, Physical and mechanical properties of gypsum-based composites reinforced with PVA and PP fibers, *Constr. and Build. Mater.* 163 (2018) 695–705, <https://doi.org/10.1016/j.conbuildmat.2017.12.168>.
- [4] Kang Liu, Wu Yu-Fei, Xin-Liang Jiang, Shear strength of concrete filled glass fiber reinforced gypsum walls, *Mater. and Struct.* 41 (2008) 649–662, <https://doi.org/10.1617/s11527-007-9271-8>.
- [5] S.A.Y. Yildizel, Material Properties of Basalt-Fiber-Reinforced Gypsum-Based Composites Made with Metakaolin and Silica Sand, *Mechan. of Comp. Mater.* 56 (2020) 379–388, <https://doi.org/10.1007/s11029-020-09889-z>.
- [6] Nelson Flores Medina, M. MarBarbero-Barrera, Mechanical and physical enhancement of gypsum composites through a synergic work of polypropylene fiber and recycled isostatic graphite filler, *Constr. Build. Mater.* 131 (2017) 165–177, <https://doi.org/10.1016/j.conbuildmat.2016.11.073>.
- [7] Nelson Flores Medina, M. Mar Barbero-Barrera, Mechanical and physical enhancement of gypsum composites through a synergic work of polypropylene fiber and recycled isostatic graphite filler, *Constr. and Build. Mater.* 131 (2017) 165–177, <https://doi.org/10.1016/j.conbuildmat.2016.11.073>.
- [8] Ibrahim Bilici, Celal U. Deniz, Beytullah Oz, Thermal and mechanical characterization of composite produced from recycled PE and flue gas desulfurization gypsum, *Jour. Comp. Mater.* 53 (2019) 3325–3333, <https://doi.org/10.1177/0021998319827097>.
- [9] F. Suárez, L. Felipe-Sesé, F.A. Díaz, J.C. Gálvez, M.G. Alberti, On the fracture behaviour of fibre-reinforced gypsum using micro and macro polymer fibres, *Constr. Build. Mater.* 244 (2020), <https://doi.org/10.1016/j.conbuildmat.2020.118347>.
- [10] A. Elsaid, M. Dawood, C Bobko Seracino, Mechanical properties of kenaf fiber reinforced concrete, *Constr. Build. Mater.* 25 (2011) 1991–2001, <https://doi.org/10.1016/j.conbuildmat.2010.11.052>.
- [11] Wail N. Al-Rifaie, Maamoon Al-Niami, Mechanical performance of date palm fibre-reinforced gypsums, *Innov. Infrastruct. Solut.* 1 (18) (2016) 1–7, <https://doi.org/10.1007/s41062-016-0022-y>.
- [12] Jorge Segura Alcaraz, Isaac Montava Belda, Ernesto Julia Sanchis, Jose M. Gadea Borrell, Mechanical properties of plaster reinforced with yute fabrics. *Composites Part B*, 178 (2019) 107390. <https://doi.org/10.1016/j.compositesb.2019.107390>
- [13] Naiiri Fatma, Lamis Allegue, Mehdi Salem, Redouane Zitoune, Mondher Zidi, The effect of doum palm fibers on the mechanical and thermal properties of gypsum mortar, *J. Comp. Mater.* 53 (19) (2019) 2641–2659.
- [14] Fabio Iucolano, Domenico Caputo, Flavio Leboffe, Barbara Liguori, Mechanical behavior of plaster reinforced with abaca fibers, *Constr. Build. Mater.* 99 (2015) 184–191, <https://doi.org/10.1016/j.conbuildmat.2015.09.020>.
- [15] Fabio Iucolano, Luca Boccarusso, Antonio Langella, Hemp as eco-friendly substitute of glass fibres for gypsum reinforcement: Impact and flexural

- behavior, *Composites Part B* 175 (2019), <https://doi.org/10.1016/j.compositesb.2019.107073>.
- [16] Fabio Iucolano, Barbara Liguori, Paolo Aprea, Domenico Caputo, Thermo-mechanical behaviour of hemp fibers-reinforced gypsum plasters, *Constr. Build. Mater.* 185 (10) (2018) 256–263, <https://doi.org/10.1016/j.conbuildmat.2018.07.036>.
- [17] M.J. Morales-Conde, C. Rodríguez-Liñán, M.A. Pedreño-Rojas, Physical and mechanical properties of wood-gypsum composites from demolition material in rehabilitation works, *Constr. and Build. Mater.* 114 (2016) 6–14, <https://doi.org/10.1016/j.conbuildmat.2016.03.137>.
- [18] Stergios Adamopoulos, Dafni Foti, Elias Voulgaridis, Costas Passialis, Manufacturing and Properties of Gypsum-Based Products with Recovered Wood and Rubber Materials, *BioResources*. 10 (2015) 5573–5585.
- [19] Markéta Hošťálková, Nikola Vavřínová, Veronika Longauerová, Mechanical properties of the gypsum composite reinforcement with wooden fibers, *Int. Rev. Appl. Sci. Eng.* 10 (1) (2019) 15–21, <https://doi.org/10.1556/1848.2019.0003>.
- [20] Hamed Ramezania, Sina Shahdabb, Ali Nouric, Study on effects of wood fiber content on physical, mechanical, and acoustical properties of wood-fiber-filled gypsum composites, *Mater. Res.* 15 (2012) 236–241, <https://doi.org/10.1590/S1516-14392012005000018>.
- [21] Rodríguez-Liñán Carmen, María J. Morales-Conde, P. Rubio-De-Hita, F. Pérez-Gálvez, A. Pedreño Rojas Manuel, The Influence of Natural and Synthetic Fibre Reinforcement on Wood-Gypsum Composites, *The Open Construction and Building Technology Journal* 11 (2017) 350–362, <https://doi.org/10.2174/1874836801711010350>.
- [22] R. Khiari, M.N. Belgacem. Potential for using multiscale *Posidonia oceanica* waste: current status and prospects in material science, in: B.S. Naheed Saba, Mohammad Jawaid, Paridah Md. Tahir, *Lignocellulosic Fibre and Biomass-Based Composite Materials* (Eds), Woodhead Publishing, Duxford, 2017, pp 447–471. <https://doi.org/10.1016/B978-0-08-100959-8.00021-4>
- [23] Maurizia Seggiani, Patrizia Cinelli, Norma Mallegni, Elena Balestri, Monica Puccini, Sandra Vitolo, Claudio Lardicci, Andrea Lazzeri New Bio-Composites Based on Polyhydroxyalkanoates and *Posidonia oceanica* Fibres for Applications in a Marine Environment. *Materials*. 10 (2017).1-13. <https://doi.org/10.3390/ma10040326>
- [24] Daniel Garcia-Garcia, Luis Quiles-Carrillo, Nestor Montanes, Vicent Fombuena, Rafael Balart, Manufacturing and Characterization of Composite Fibreboards with *Posidonia oceanica* Wastes with an Environmentally-Friendly Binder from Epoxy Resin, *Materials*. 11 (2018) 1–15, <https://doi.org/10.3390/ma11010035>.
- [25] L. Allegue, M. Zidi, S. Sghaier, Mechanical properties of *Posidonia oceanica* fibers reinforced cement, *J. Comp. Mater.* 49 (2014) 509–517.
- [26] Aldi Kuqo, Ilirjana Boci, Sonila Vito, Sidorela Vishkulli, Mechanical properties of lightweight concrete composed with *Posidonia Oceanica* fibres, *Zastita Materijala* 59 (2018) 519–523, <https://doi.org/10.5937/zasmat1804519K>.
- [27] BS EN 13279-1: Gypsum binders and gypsum plasters – Part 1: Definitions and requirements, 2008.
- [28] BS EN 13279-2: Gypsum binders and gypsum plasters – Part 2: Test methods, 2014.
- [29] DIN EN ISO 179-1: Kunststoffe – Bestimmung der Charpy-Schlageigenschaften – Deutsche Fassung EN ISO 179-1:2010.
- [30] Romildo D. Toledo Filho, Khosrow Ghavami, Miguel A. Sanjuán, George L. England. Free, restrained and drying shrinkage of cement mortar composites reinforced with vegetable fibres, 27, (2005), 537-546. <https://doi.org/10.1016/j.cemconcomp.2004.09.005>
- [31] S. Parveen, S. Rana, R. Fangueiro, Macro- and nanodimensional plant fiber reinforcements for cementitious composites, in: H. Savastano Junior, J. Fiorelli, F. d. Santos (Eds), *Sustainable and Nonconventional Construction Materials using Inorganic Bonded Fiber Composites*, Woodhead Publishing Series in Civil and Structural Engineering, Duxford, 2017, pp. 343–382, <http://dx.doi.org/10.1016/B978-0-08-102001-2.00020-6>

Article 2

Seagrass- and wood-based cement boards: A comparative study in terms of physico-mechanical and structural properties – Article 2

Aaron Kilian Mayer[†], Aldi Kuqo[†], Tim Koddenberg, Carsten Mai^{*}

[†]First-Co authors

^{*}Corresponding author, email: cmai@gwdg.de

Wood Biology and Wood Products, Burckhardt Institut, Georg-August-Universität Göttingen, BÜsngenweg 4, 37077 Göttingen

Authorship (according to Clement, 2014)

	Conceptualization (30%)	Practical work (30%)	Writing/Editing (30%)	Administration (10%)	Contribution
A. K. Mayer	40%	45%	35%	10%	37%
A. Kuqo	40%	45%	35%	10%	37%
T. Koddenberg	0%	10%	15%	0%	7.5%
C. Mai	20%	0%	15%	80%	18.5%

Ideas: Design of the investigation / Experimental planning / Interpretation of the data

Work: Execution of the experiment / Data collection and analysis

Writing: Drafting the article / Critical, substantive revision / Reviewing the final version

Administration: Resource management and ensuring scientific integrity before, during, and after publication

Published in Composites Part A: Applied Science and Manufacturing 156 : 106864

Published in February 2022

DOI: <https://doi.org/10.1016/j.compositesa.2022.106864>



Seagrass- and wood-based cement boards: A comparative study in terms of physico-mechanical and structural properties

Aaron Kilian Mayer¹, Aldi Kuqo¹, Tim Koddenberg, Carsten Mai^{*}

Wood Biology and Wood Products, Burckhardt Institute, Georg-August University of Göttingen, Büsingenweg 4, Göttingen 37077, Germany

ARTICLE INFO

Keywords:

- A. Natural fibres
- A. Reinforced cement/plaster
- B. Debonding
- D. CT analysis

ABSTRACT

The inclusion and management of local, natural resources in the construction sector are on the rise as a result of the undisputed essentiality of sustainability. This study aims to assess and compare cement-bonded boards containing seagrass fibers (*Posidonia oceanica*) and pine wood particles (*Pinus sylvestris*) in terms of their compatibility with cement, their physico-mechanical properties, and their microstructure using X-ray micro-computed tomography and 3D-reflected light microscopy. Seagrass-based cement boards comply with the DIN EN 634 surpassing the stated MOR value of 9 N mm^{-2} . The thickness swelling of all seagrass-based cement boards was between 0.2 and 1.2%, indicating a possible outdoor application. The structural characterization and the study of the degree of compatibility showed that the size, geometry, and chemical composition of the lignocellulosic precursors mostly influenced the final properties of the board. Seagrass-based cement boards provide novel possibilities to use new environmentally friendly materials for construction applications.

1. Introduction

Cement-lignocellulosic composites have been on the market for nearly a century. They are referred to as reinforced materials bonded by an inorganic binder such as ordinary Portland cement. Compared to the organically bonded composites they possess numerous advantages. As a binding agent, cement provides a durable surface revealing high fire and termite/decay resistance and the ability to withstand various weather conditions [1-5]. In addition, cement can be easily colored and brought into shape. Its relatively high density, however, makes it heavier and thus more difficult to handle and transport, which counteracts the low production costs.

The usage of cement-bonded particleboards (CBPB) in industrial applications started in the mid-1930s and was gradually improved in the following decades. The Elmendorf Research, Inc (ENRI) developed a concept to improve the properties of CBPB by focusing on the size and orientation of particles, which also has led to the later development of oriented strand boards (OSB). Great efforts were made to compare wood particles and fibers with other reinforcement fibers such as glass, steel, Kevlar, or asbestos. Overall, wood showed the highest suitability for industrial production because of its good processability, strength, temperature, and alkali resistance as well as low raw material costs [3].

With the increasing rate of cement-panel production and the rising demand for raw wood materials, new alternatives to wood-based products have emerged. Natural fibers and various other agricultural residues have been utilized in the production of lignocellulosic-cement panels [6-11]. Thereby, the use of local natural fibers (e.g., seagrass) has been catalyzed not only by their widespread availability in particular areas but also because of their individual properties, often resulting in enhanced composite properties.

The seagrass *Posidonia oceanica* is a flowering plant native to the Mediterranean Sea forming large underwater meadows at depths from 1 to 40 m. After windy storms, seagrass leaves break off the plant, are carried away by wave action, and settle on the seashores. Owing to their interesting properties such as fire and moisture resistance, seagrass leaves are regarded as an ecological alternative for wood composite production [12,13]. The spherical aggregates of seagrass form in submarine hollows as a result of leaf decomposition, followed by an intense entanglement process generated by the dynamic movement of waves [14]. Seagrass balls often referred to as aegagropila or commercially as Neptune balls, have been widely studied over the last decade due to their appealing characteristics. It has already been found that the addition of small amounts of seagrass can enhance the mechanical properties of cement composites while reducing their density, resulting in lightweight

Corresponding author.

E-mail address: cmai@gwdg.de (C. Mai).

¹ These authors contributed equally to this work.

<https://doi.org/10.1016/j.compositesa.2022.106864>

Received 2 July 2021; Received in revised form 1 February 2022; Accepted 4 February 2022

Available online 7 February 2022

1359-835X/© 2022 Elsevier Ltd. All rights reserved.

construction products [15-17]. Gypsum-seagrass composites exhibited interesting properties, especially in terms of insulation and their ability to absorb more mechanical energy before total failure occurs [18,19]. In previous studies, however, the amount of added fibers (by weight) was very low due to the low bulk density of loose seagrass fibers. Moreover, the common production technique was cement slurry-fiber mixing with subsequent molding. In this study, a dry process is applied to prepare panels containing large amounts of fibers, followed by pressing at elevated temperatures. The aim of the study is to compare seagrass fibers and pine wood particles in terms of their compatibility with cement, considering mechanical and physical properties. In addition, structural characterization of the composites was performed using imaging techniques to examine the bonding and failure mechanism of the cement boards.

2. Materials and methods

2.1. Materials

The seagrass *Posidonia oceanica* was randomly collected in the coastal area of Durrës, Albania (Adriatic Sea) in September 2020. The fibers were interconnected with each other forming balls with various equivalent diameters, varying from 4 to 15 cm. A mobile sawdust suction collector (Holzkraft ASA 163, Stürmer Maschinen GmbH, Hallstadt, Germany) was used to unravel the fibers in a loose form without shortening them and changing their morphological features.

In terms of morphological characteristics, the seagrass fibers have a long fibrous structure (Fig. 1, a). Two batches of coarse and fine industrial wood particles (Fig. 1, b) provided by the Swiss Krono Group AG (Luzern, Switzerland) were mixed in a ratio of 70% to 30% w/w. The cumulative distribution of the geodesic length of seagrass fibers and wood particles was determined by FibreShape PRO (X-shape, IST, Vilters, Switzerland). Significant differences regarding the length of the lignocellulosic materials were observed (Fig. 2). Although the median geodesic lengths slightly differ to each other (2.9 mm for seagrass fibers and 3.2 mm for wood particles), their length at P₁₀ and P₉₀ (10th and 90th percentile) of wood particles was visibly higher compared to seagrass fibers. For the former the maximum length was 45.3 mm while for the latter it was 32.2 mm. The obtained results of seagrass fibers size distribution are consistent with the results of previous studies [18].

The used cement was the commercial curing variant CEM I 52,5R-HS/NA Su (Holcim GmbH, Sehnde, Germany). This cement is commonly used for concrete in the building sector and fulfills the characteristics stated in the DIN EN 197-1 [20].

The acceleration agents utilized in the mixing process were water glass solution (K₂SiO₃, 30% solid content) and aluminum sulfate powder

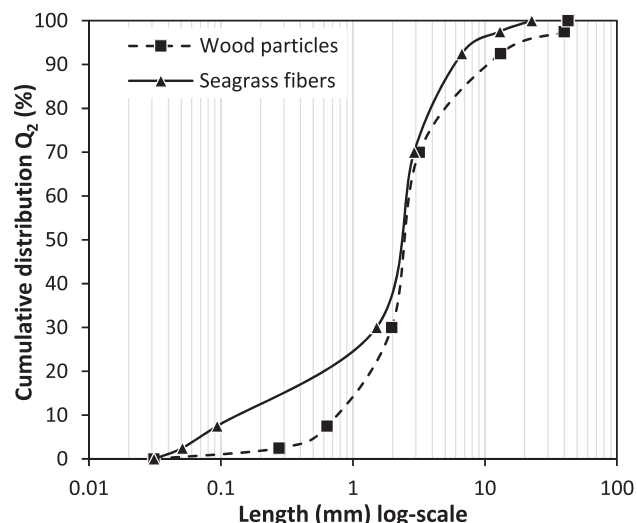


Fig. 2. Length distribution of seagrass fibers and wood particles.

(Al₂(SO₄)₃) provided by Isolbau (Isolbau e.K., Markersdorf, Germany; WHC GmbH, Hilgertshausen, Germany).

2.2. Chemical characterization of the lignocellulosic material

Laboratory analytical procedures (LAP) of the National Renewable Energy Laboratory (NREL), as well as the standards published by the Technical Association of the Pulp and Paper Industry (TAPPI), were used to determine the organic components of the biomasses. Prior to the analysis, the material was ground in a cutting mill (Retsch GmbH, Haan, Germany) with a 50-mesh screen. Each analysis step was performed in triplicates.

The first step of the cascading procedure was the hot water extraction. Oven-dried lignocellulosic material was transferred into extraction thimbles, which then were placed in Soxhlet extractors. After 5 h of hot water extraction, the thimbles were oven-dried at 103 °C in order to determine the dry mass.

Afterwards, an ethanol-cyclohexane extraction was conducted for 5 h followed by another drying step. The tests were performed according to T264 cm-97 [21]. The benzene was completely substituted by using cyclohexane in a ratio of 1:1.

Regarding the cell wall components, the NREL/TP-510-42618 LAP [22] was used to determine the lignin content of the extractive-free material. After the hydrolysis of the polysaccharides with sulfuric acid



Fig. 1. Seagrass balls and loose fibers (a), wood particles (b).

(72%), the remaining solids (lignin) were weighted after rinsing with demineralized water.

The holocellulose content was determined according to the procedure established by Wise [23]. Acetic acid and sodium chlorite were added to a suspension of extractive-free wood. The Erlenmeyer flasks were placed in a water bath at 80 °C. After completion of the reaction, the material was filtered and rinsed with cold water and acetone. Afterwards, the solids were dried and weighed again.

The evaluation of the ash content was conducted according to the TAPPI standard T211 om-02 [24].

To analyze the electrical conductivity (EC) of the organic material, a suspension of 100 cm³ of organic material and 360 ml of deionized water was prepared in a 500-ml laboratory flask. The flask was shaken for 1 h to solubilize the surface salts. Only the clear supernatant of the suspension was used to analyze the EC.

2.3. Hydration test

A preliminary investigation was conducted to assess the compatibility between seagrass fibers and pine wood particles with the cement. The hydration test was carried out as described by Hachmi [25]. The amounts of used Portland cement, water, and lignocellulosic material were based on experiments reported initially by Weatherwax and Tarkow [26] and later from Cabral [6]. For the paste preparation, the use of 2.7 ml water per gram of lignocellulosic material and an additional 0.25 ml of water per gram cement were used. Distilled water (90.5 ml) and lignocellulosic material (15 g oven-dry) were mixed with 200 g Portland cement and the paste was stirred manually for 2–3 min until a completely homogeneous mixture was formed. After the thorough mixing, the paste was taped with the tip of a type J temperature thermocouple (GMH 3250 Greisinger electronic, GHM Messtechnik GmbH, Remscheid, Germany) and put in a polyethylene bag to prevent loss of water and to keep constant moisture conditions.

A semi-adiabatic system was build using a stainless-steel vessel insulated by a vacuum wall, covered by glass wool, and placed in an insulating Styrofoam box. The sealed plastic bag was put in the insulation flask and left there for 24 h. The following equation was used to calculate the inhibitory index (I):

$$I = 100 \left[\left(\frac{t_2 - t_1}{t_2} \right) * \left(\frac{T_2' - T_2}{T_2'} \right) * \left(\frac{S_2 - S_2'}{S_2} \right) \right] \quad (1)$$

where I is the inhibition index (%); t_2 is the maximum temperature of the pure cement/water mixture (°C); t_1 is the maximum temperature of the lignocellulosic material/cement/water mixture (°C); T_2 is the time to reach maximum hydration temperature of the cement/water mixture (h); T_2' is the time to reach maximum hydration temperature of the lignocellulosic material/cement/water mixture (h); S_2 is the maximum slope/increment in the cement/water mixture (°C/h); S_2' is the maximum temperature slope/increment in the lignocellulosic material/cement/water mixture (°C/h). Two replicates were conducted for each mixture. The inhibition effect was classified in accordance with the grades presented in Table 1.

Another determinant factor for the inhibition index is the geometry, and especially the surface area of the fiber and particles. Therefore, a second series of tests was undertaken to examine the hydration characteristics of ground seagrass and wood particles. The raw fibers and particles were milled using a cutting mill (Retsch SM 2000, Retsch GmbH, Haan, Germany) with a 50-mesh screen. The further hydration test procedures of ground lignocellulosic material were the same as those described for the raw aggregates.

2.4. Production of cement boards

Target densities and compositions of seagrass-based and wood-based cement boards are presented in Table 2.

Cement boards with target densities varying from 1100 to 1400 kg m⁻³ and fiber contents (dry mass) varying from 22% to 52% based on the weight of cement were prepared using the dry process. Initially, the moisture content of seagrass fibers and wood particles was determined thermogravimetrically. The boards were pressed at 70 °C for 8 h with a pressing pressure of 18–24 MPa. Subsequently, their oven-dry mass was calculated along with the amount of water, cement, and accelerators.

However, the production processes of the corresponding cement boards slightly differed, due to the morphological dissimilarities of seagrass fibers and wood particles.

For wood particles, a 40 L vertical concrete mixer (Soroto action mixer 40 L, Soroto, Herstedorster, Denmark) was utilized. The mixing period lasted from 5 to 10 min depending on the amount of mixed raw materials.

First, water glass (K₂SiO₃) solution (1.5 wt% content to binder) and secondly aluminum sulfate (Al₂(SO₄)₃) solution (1 wt% content to binder) were sprayed onto the wood material using an air-actuated spray nozzle. By this means, a homogenous distribution of these accelerators and water was achieved. Afterwards, cement powder was steadily added to the mixture. The powder adhered with the wet particles (previously sprayed) forming a superficial layer of the mineral binder. In the last step, additional water (50% of total water amount) was sprayed, and the

Table 1
Grade of inhibition.

Inhibition index (%)	Grade of inhibition
$I < 10$	Low inhibition
$I = 10 - 50$	Moderate inhibition
$I = 50 - 100$	High inhibition
$I > 100$	Extreme inhibition

Table 2
Production variants of seagrass-based and wood-based cement boards.

Board type ^b	Target density (kg m ⁻³)	Aggregate content (wt%)	Binder content to the total mass (wt%)
SG 78/22	1400	22	78
SG 78/22	1250	22	78
SG 78/22	1100	22	78
SG 63/37	1400	37	63
SG 48/52	1400	52	48
WP 78/22	1400	22	78
WP 78/22	1250	22	78
WP 78/22	1100	22	78
WP 63/37	1400	37	63
WP 48/52	1400	52	48

^b Board type SG corresponds to seagrass-based cement boards, while WP corresponds to wood-based cement boards. The numbers indicate the binder to lignocellulosic aggregate ratio.

blend was mixed for a few additional minutes. The water amount added to the mixture was calculated using the equation applied by Simatupang and Okino et. al [27,28] as shown in Equation (2).

$$RW = 0.35C + (0.30 - M)W \quad (2)$$

where RW is the required water added to the mixture (L); C is the amount of Portland cement (kg); M is the moisture content of the lignocellulosic material (oven-dry basis) (wt%); W represents the oven-dry weight of the lignocellulosic material (kg).

Due to the high specific volume of seagrass fibers, a larger mixer was utilized for the mixing. The 80 L drum mixer (Atika, Altrad Lescha Atika GmbH, Burgau, Germany) was filled with the mass of fibers; the subsequent procedure was similar to that described above. During the spraying-mixing of seagrass fibers, agglomeration of fibers was induced resulting in the formation of small fiber balls. At the end of the process, the mixture consisted of the wet sphere-like clusters containing cement in their peripheral areas, whereas in the center they were in most cases cement-free. For a more homogeneous distribution of the binder in the fiber mass, mechanical mixing followed.

The mixture (balls) was put in a gasoline-powered shredder (Güde GH650, Güde GmbH & Co.KG, Wolpertshausen, Germany) equipped with a 25 mm sieve. After the untwisting process of fiber agglomerates, the homogenous mixture was adequate for the subsequent pressing operation.

In the last step, the consistent mass of the lignocellulosic material was weighted, initially pre-pressed, and then pressed at 70 °C for 8 h using a hot plate press (Joos HP-2000 lab, Gottfried Joos GmbH & Co. KG, Pfalzgrafenweiler, Germany). The bulk density of non-compacted seagrass fibers is lower than the bulk density of wood particles. As a consequence, a higher pressing force is required for the production of boards containing seagrass than for the corresponding boards containing wood particles. The formed cement boards were sealed in plastic bags and left for 27 d at 20 °C and 65% RH. The boards with dimensions of 450 × 450 × 17 mm³ were cut into various specimen dimensions. The specimens were left for an additional day to achieve equilibrium of moisture.

2.5. Density and mechanical characterization of cement-bonded boards

The following standard methods are included in the standard EN 634 [29] for testing and determination of physical-mechanical properties of cement particleboards. Evaluation of the raw density was conducted following the procedures described in the standard EN 323 [30]. Tetragonal specimens (50 × 50 × 17 mm³) were measured to determine density and selected for testing the subsequent internal bond strength (IB) and physical properties. Modulus of rupture (MOR), modulus of elasticity (MOE), and the work to maximal force F_{max} (W) were assessed by a three-point bending strength in accordance with the EN 310 standard [31]. Three test specimens were examined for each board (in total six replications for each variant), having nominal dimensions of 390 × 50 × 17 mm³. A universal testing machine (ZwickRoell Zmartpro, ZwickRoell, Ulm, Germany) with a 10 kN load cell was used with an applied crosshead speed of 6 mm min⁻¹ and a support span of 340 mm. In addition, for precise measurements of displacement and eventually MOE, an extensometer (Travel transducers for compression and 3- or 4-point flexure tests, Zwick Roell, Ulm, Germany) was employed.

The IB test was conducted in accordance with EN 319 [32]. Tetragonal samples obtained from the density measurements were bonded to metallic braces using a fast-curing polymer adhesive. The specimens were fitted to the testing machine (ZwickRoell Zmartpro, ZwickRoell, Ulm, Germany) component and a tensile stress perpendicular to the board plane was applied until failure having a continuous crosshead speed of 7 mm min⁻¹.

2.6. Cone calorimetry test, fire resistance

A mass loss calorimeter (MLC FTT, Fire Testing Technology, East Grinstead, UK) was used to evaluate the heat release rate (HRR), the mass loss rate (MLR) and the time to ignition (IT) according to ISO 5660-1 [33]. For further analysis, the total heat release (THR) in MJ m⁻² was calculated, which is the integral of the HRR curve over time. As stated in the standard, 100 × 100 mm² specimens with the given board thickness were used. One specimen per board was evaluated (two per variant). Prior to testing, the specimens were conditioned to constant mass at 23 ± 2 °C and 50 ± 5% RH. For the calorimetric measurements, the specimens were exposed to an irradiance of 50 kW m⁻² for 30 min. The arbitrary scale introduced by Petrella [34] was used to evaluate the risk level for these cement bonded boards. The four risk levels are defined in a common logarithm scale from 0.1 to 1000 MJ m⁻².

2.7. Determination of thickness swelling and water absorption

Swelling and water absorption were conducted after DIN EN 317 [35]. Three specimens per variant were tested. The specimens were completely submerged in water for 24 and 72 h. After the allotted time, they were removed and drained for 10 min to remove excess water. Subsequently, the thickness and the weight were measured.

2.8. Structural imaging of cement-bonded boards

Two imaging techniques (i.e., micro-CT and 3D-reflected light microscopy) were used to characterize wood- and seagrass-based cement boards (see above). Apart from cement boards, cement board specimens were imaged after applying bending stress.

For non-destructive examinations of wood-based and seagrass-based cement boards, X-ray micro-computed tomography (micro-CT) was employed with the commercial cone-beam system Nanotom s (phoenix|x-ray, GE Sensing & Inspection Technologies GmbH Wunstorf, Germany). The micro-CT is featured with a transmission molybdenum target and a stationary CMOS flat-panel detector. The image acquisitions were performed after cuboid samples measuring 10 × 10 × 15 mm³ and 15 × 15 × 20 mm³ (after bending stress) had been mounted onto a glass rod using a thermoplastic hot-melt adhesive. The samples were then scanned at a peak voltage of 60 keV and current of 100 µA. At each angular step, a projection image was saved with a 2000 ms X-ray exposure.

While being rotated through 360°, a series of 1800 or 2000 grayscale projection images were collected at an isotropic voxel size of 8 and 10 µm. After scanning, the projection images were transformed into a volumetric dataset using the phoenix datos|x reconstruction software (phoenix|x-ray, GE Sensing & Inspection Technologies GmbH, Wunstorf, Germany). The contrast in tomographic images is given by the natural X-ray attenuation of the samples. Thereby, the yielded grayscale projection images can be considered as a distribution map of X-ray attenuation values. In the reconstructed images, dark pixel/voxel characterizes regions of weak X-ray absorption (e.g. air), while X-ray opaque regions are represented by bright pixel/voxel

(e.g. cement). The 2D and 3D visualizations of the fiberboard samples

Table 3

Electric conductivity and chemical constituents of the lignocellulosic material used in this study.

Lignocellulosic Material	EC ^a (µS cm)	HWE ^a (%)	CEE ^a (%)	Lignin (%)	Holocellulose (%)	Ash (%)
Wood particles	107	9.3	3.2	30.0	74.1	0.4
Seagrass	1227	5.8	2.1	35.4	53.7	12.9

^a EC means electrical conductivity, HWE means hot water extractives and CEE means cyclohexane – ethanol extractives.

were realized using the analysis tools of the Avizo software (FEL, Thermo Fisher Scientific, Hillsboro, Oregon, USA).

Apart from micro-CT, cement boards after bending were imaged using the digital 3D-reflected light microscope Keyence VHX-5000 (Keyence, Neu-Isenburg, Germany). The use of this microscope makes it possible to obtain images with a high depth-of-field by combining different in-focus images along the z-axis. To achieve images with a high depth-of-field, the focus was manually set on the lowest and highest focus point of the region of interest. The acquired panorama images were captured at magnifications of $30 \times$.

3. Results and discussion

3.1. Chemical characterization

The two organic materials showed significant differences in their chemical composition (Table 3). Wood particles contained 5.8% hot water-soluble extractives (HWE), whereas the seagrass contained 9.3%. The content of extractives solubilized by cyclohexane-ethanol (CEE) was 3.2% and 2.1% for wood particles and seagrass fibers, respectively. Many authors have stated that the extractive content for different lignocellulosic materials vary heavily even in the same species. The reasons are that the extractive content is heavily related to the tree age, time of felling, bark content and many more [36,37]. The relatively high extractive content for wood particles obtained in this study could be explained with the use of industrial wood particles. Batches of industrial softwood particles can contain, apart from pine and spruce, proportions of other wood species as well as bark and recycled wood including binders.

The high content of HWE for seagrass is explained by the high proportion of soluble salts that comes from the seawater in which the *Posidonia oceanica* grows. It becomes obvious that the high amount of seawater salts results in a high electric conductivity (EC) of $1227 \mu\text{S cm}^{-1}$ of seagrass compared to the EC of $107 \mu\text{S cm}^{-1}$ found in wood particles (Table 3). Depending on the exposure to rain and the distance from the aggregates to the sea, the salinity and thus the EC can be reduced dramatically [38]. Khiari [39] reported similar extractive contents from *Posidonia oceanica* by using hot water and organic solvent extraction.

Contents of structural polymers were 30.0% and 35.5% for lignin and 74.1% as well as 53.7% for holocellulose for wood particles and seagrass, respectively.

The ash content revealed one of the biggest differences between the two organic materials. Pine wood exhibited an ash content of 0.4%, while it is 12.9% for seagrass. The dominating elements in pine wood are calcium and potassium, whereas the dominating elements in seagrass are silicon and calcium [36,40,41].

3.2. Compatibility assessed through hydration test

Hydration characteristics have been commonly used to evaluate the compatibility of cement with the lignocellulosic aggregate [26]. In order to assess the inhibition effect of cement from seagrass fibers and wood particles, the released heat (temperature) has been monitored through a period of 24 h. Fig. 3 displays the exothermic hydration curves of pure cement, seagrass fibers, and wood particles. As can be seen from the diagram, for pure cement, an increase of the temperature is noticed after 4 h and the maximal hydration temperature is reached within 8 h. On the other hand, seagrass, and wood aggregate-cement mixtures exhibit a delayed increase of maximal temperature of the exothermic hydration curve, at 10 and 16 h respectively.

The maximal hydration temperature of pure cement paste was greater than that of seagrass and wood aggregate mixtures. Still, in the case of the seagrass-cement paste a more intense exothermic reaction occurred compared to that with wood particles, indicating greater compatibility with cement.

The presence of several chemical constituents in the lignocellulosic material influences the degree of hydration (maximal temperature and

Table 4
Inhibition index of cement mixtures with seagrass fibers and wood particles.

Sample	Inhibition index (%)
Seagrass fibers	1.1
Wood particles	19.9
Seagrass fibers (milled)	2.7
Wood particles (milled)	31.3

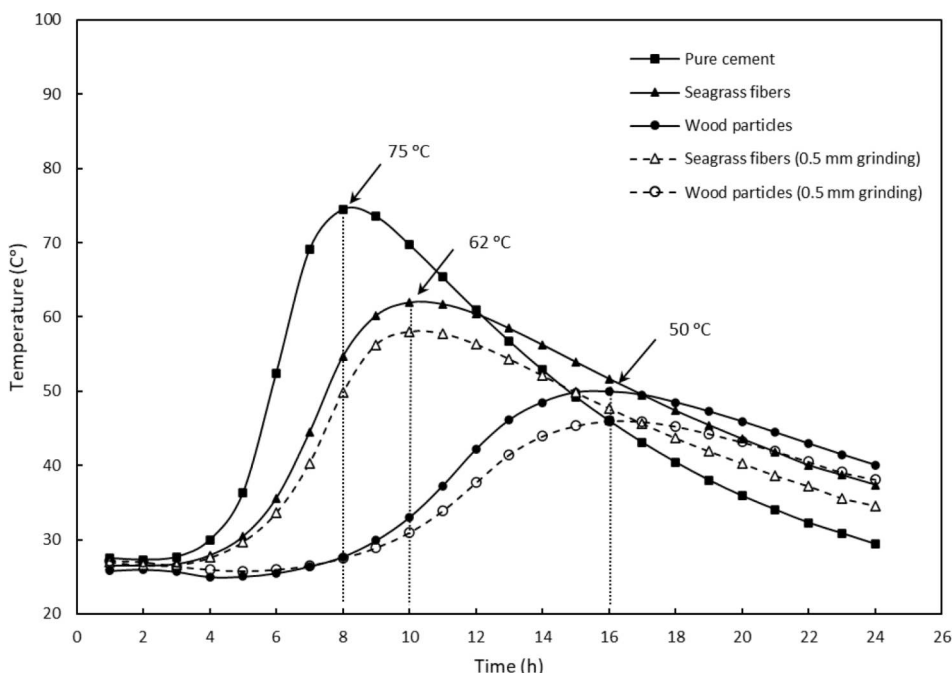


Fig. 3. Exothermic hydration diagrams for pure cement, seagrass fibers, wood particles, milled seagrass fibers, and milled wood particles.

time to reach this maximum). The higher the inhibition effect, *i.e.* relatively low maximal temperature and long time period to reach this maximum, the lower is the compatibility of pure cement with the lignocellulosic material.

Based on the calculations using Equation (1), the inhibition index (I) for seagrass fibers was 1.1%, whereas that for wood particles was 19.9%. Relating specifications given in Table 1 to our values, it can be asserted that seagrass fibers are low inhibitors while wood particles moderately inhibit cement hydration (Table 4).

The lower inhibition index of seagrass fibers compared to wood particles is directly associated with their chemical composition. Particularly, the content of extractives, polysaccharides, and specifically hemicelluloses can affect the formation of hydration products postponing the setting of cement paste. As stated by Thomas and Birchall, extractives can absorb calcium ions. The absence of calcium ions (Ca^{2+}) influences the process of cement hydration by generating alternative low mechanical performance products [42].

Further investigations showed that glucose and sucrose might be the main responsible agents for the retardation effect of cement hydration

[43]. While sucrose is present in negligible quantities in both lignocellulosic materials, the content of glucose, relative to the concentration of other monosaccharides, is much higher in *Pinus sylvestris* wood than in the seagrass *Posidonia oceanica* [36,44].

Additional studies reported that cement hydration is mostly affected by the wood extractive concentration rather than the species or the preparation method [45]. Referring to the results presented in Table 3, there is an obvious difference regarding the concentration of hot water (HWE) and cyclohexane-ethanol extractives (CEE), where seagrass exhibited lower amounts compared to pine wood particles.

The hydration degree of pastes prepared by mixing cement, water and fine (milled) lignocellulosic particles was slightly lower compared to that of pastes containing fibers and particles with the original shape. This is attributed to the increase in surface area generated by the grinding, which results in a higher quantity of leached sugars that can negatively affect hydration. A similar shift (decrease of 4 °C) of the maximal hydration temperatures was observed for both cement pastes containing milled seagrass and wood particles. In addition, the time needed to reach the highest temperature values was the same with raw

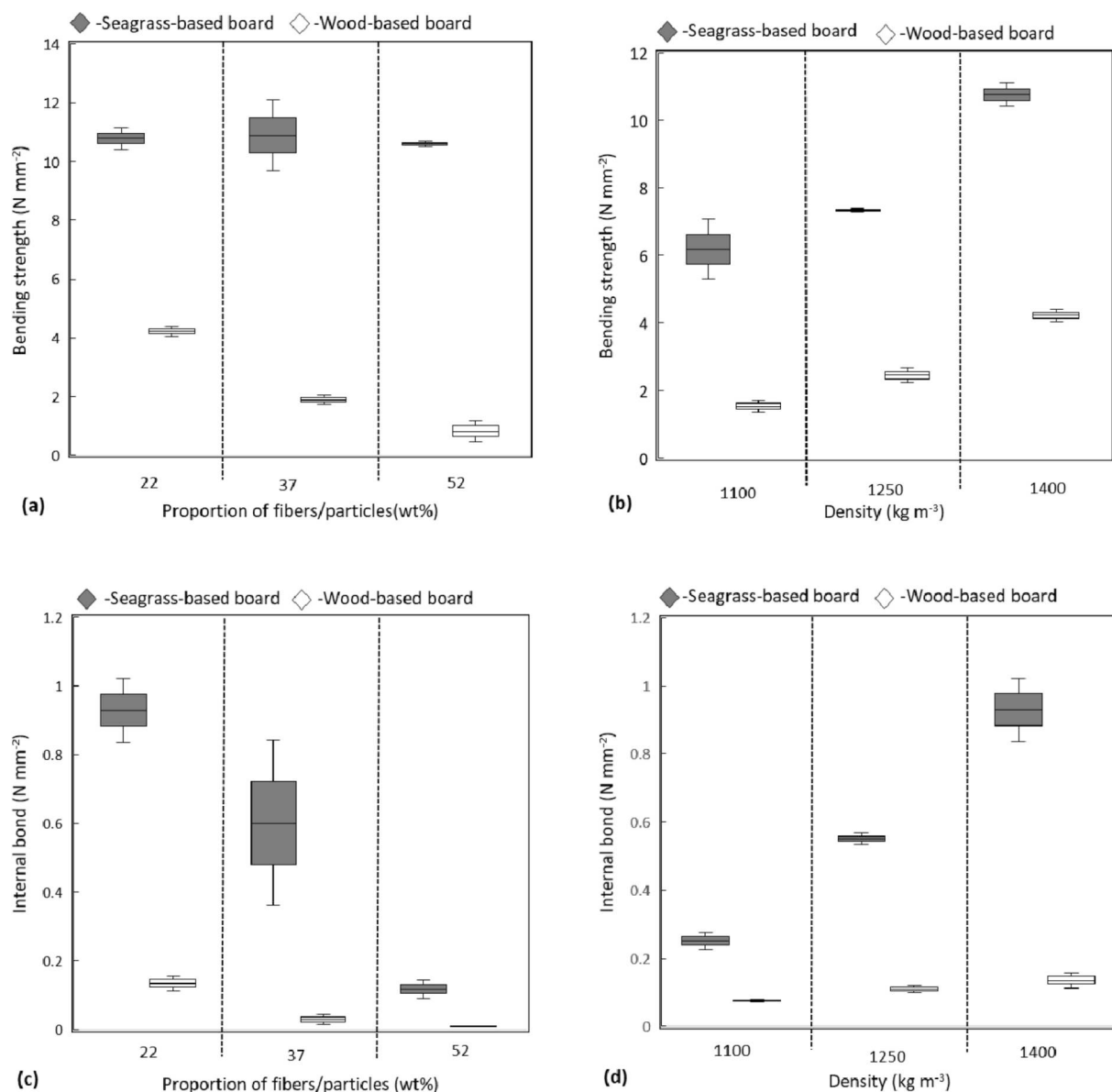


Fig. 4. Bending strength and internal bond strength of cement composites with various contents of seagrass fibers and pine wood particles (a, c) and various densities (b, d).

(non-milled) lignocellulosic material. The inhibition index, in this case, was slightly increased for both milled and non-milled materials. Their grade of inhibition, however, did not change (Tables 1 and 4).

3.3. Mechanical properties of seagrass fiber and wood particle boards

The boxplots of the flexural strength and internal bond of the prepared composite boards containing various amounts of lignocellulosic material and having various densities show clearly the superior mechanical performance of the seagrass-based cement boards (Fig. 4). The three-point bending strength for seagrass-based boards varied from 5.3 to 12.1 N mm⁻², whereas for wood-based boards those values were in the range of 0.5 to 4.4 N mm⁻². Comparing the values for the flexural test (Fig. 4 a, b), it appears that for seagrass composites density had a significant effect, while the content of the fibers in the board seems to have a minor effect. For wood boards, however, a considerable decrease in strength was observed, when both the content of fibers increased, or their density decreased.

Internal bond strength, similar to the bending strength, increased with density whereas it decreased with the addition of fibers and particles (Fig. 4 c, d). IB values vary from 0.22 to 1.05 N mm⁻² for seagrass-based cement boards and from 0.01 to 0.16 N mm⁻² for wood-based cement boards. In contrast to bending strength, IB is highly dependent on the proportion of cement serving as a binder and the compaction of fibers with each other. A higher proportion of cement implies that the possibility of direct bonding between various cement phases is higher, thus more tensile stress perpendicular to the plane is directly transmitted rather than through a phase involving fibers. Compaction or squeezing the fibers or particles with cement is more profound, when denser boards are prepared, ensuring that their entire surface is covered with the binder.

Modulus of elasticity for seagrass-based boards varied from 2.8 to 6.4 GPa and for the wood-based boards from 0.7 to 2.3 GPa (Table 5). It appears that MOE is significantly affected by the ratio of fibers-to-binder in the board. The higher the proportion of cement the higher is the MOE. The MOR and MOE results obtained for seagrass-based boards with high proportions of binder fulfil the requirements stated in the DIN EN 634 (MOR > 9 N mm⁻² and MOE > 4000 N mm⁻²). The IB of the seagrass-based boards were higher than the requirements stated in the DIN EN 634 (IB > 0.5 N mm⁻²). This applies to boards with 22% and 37% of lignocellulosic content as well as to the boards with densities over 1250 kg m⁻³.

Seagrass-based boards also attain higher values for work until F_{max} compared to equivalent wood-based composites (Table 5). The higher amount of energy required during bending implies that the material is more ductile and can therefore absorb more energy. In the case of wood-based cement boards, W varied from 105 to 225 N mm, whereas for seagrass these values were approximately ten times higher reaching up to 2452 N mm.

Table 5
Density and mechanical properties for seagrass-based and wood-based cement boards^a.

Board type ^b	Target density (kg m ⁻³)	Real density (kg m ⁻³)	Modulus of elasticity (N mm ⁻²)	Work until F _{max} (N mm)
SG 78/22	1400	1470 ± 11	6375 ± 375	1007 ± 6
SG 78/22	1250	1277 ± 5	3820 ± 100	879 ± 242
SG 78/22	1100	1180 ± 10	2845 ± 18	791 ± 108
SG 63/37	1400	1365 ± 36	4330 ± 260	1574 ± 77
SG 48/52	1400	1292 ± 10	2767 ± 103	2452 ± 22
WP 78/22	1400	1369 ± 21	2315 ± 20	225 ± 16
WP 78/22	1250	1246 ± 22	1264 ± 143	124 ± 2
WP 78/22	1100	1089 ± 8	789 ± 125	68 ± 12
WP 63/37	1400	1224 ± 70	892 ± 237	105 ± 7
WP 48/52	1400	1009 ± 95	429 ± 264	62 ± 33

^a Mean values and standard deviations (±) of 6 (2 sets × 3 samples) replicates for each type of composite.

^b Board type SG corresponds to seagrass-based cement boards, while WP corresponds to wood-based cement boards. The numbers indicate the binder to lignocellulosic aggregate ratio.

Under applied flexural stress, the fibers and particles in the outer layer of the composite are subjected to normal tensile stress. Under these conditions, either debonding (pull out) or cracking occurs in the fibers. Poor bonding can be developed from the presence of voids, lack of roughness of the fiber, and its surrounding area (interfacial transition zone) where a greater amount of water accumulates due to the hydrophilic nature of lignocellulosic material, ensuing in a lower degree of cement crystals aggregation. On the other hand, cracking or failure of the fiber is directly related to the tensile properties of the fiber itself and it is an indicator for good bonding. Both bending strength and internal bond strength considerably increased with increasing density. This increase is related to the proportion of the fibers that detach from the matrix or fail due to breaking. Observations of failed samples after testing showed that fibers in denser boards tended to break rather than de-bond. The failure mechanism of pine wood particleboards differed from the former one mainly because of the geometry and size and, secondarily, because of their chemical composition.

Particles, having a non-uniform geometry and a lower aspect ratio (length to diameter ratio), in contrast with seagrass fibers, not only encounter a shear resistance in the direction parallel to tensile stress (x-direction in Fig. 5), but also delamination resistance that is perpendicular to tensile strength. During the delamination process, cracking can occur in the interfacial transition zone (ITZ) or in the areas containing pores and voids where the probability of failure is high; in this case, the degree of friction between the ceramic matrix and the particle is insignificant, resulting thus in low mechanical strength [46,47].

Although target densities were set to range from 1100 kg m⁻³ to 1400 kg m⁻³, the obtained values, especially for variants with high proportions of lignocellulosic material, differed drastically (Fig. 6). The variation in density was attributed to the springback effect. The springback effect is an irreversible thickness swelling caused by compressive stress relief after the production of the board [48]. The aggregate geometry seems to be the reason why the springback effect of the seagrass-based boards is lower than the springback effect of wood-based boards. Even though the bulk density of seagrass fibers is lower than the one of wood particles, which leads to a higher volume before pressing, the irreversible stress relief seems much lower. The compression stress for seagrass-based cement boards is equally distributed in the panel plane and no stress “hot-spots” are created.

However, thicker particles and flakes tend to increase springback, whereas length has no influence on this effect. It is argued that the internal stresses incorporated into thicker flakes during pressing are the main reason for the dimensional instability [49].

3.4. Cone calorimetry test

The various variants of boards exhibited very low calorimetric values (Table 6). The mass loss (ML) for seagrass-based cement boards varied from 27 to 37%, while ML for wood-based cement boards varied from 24

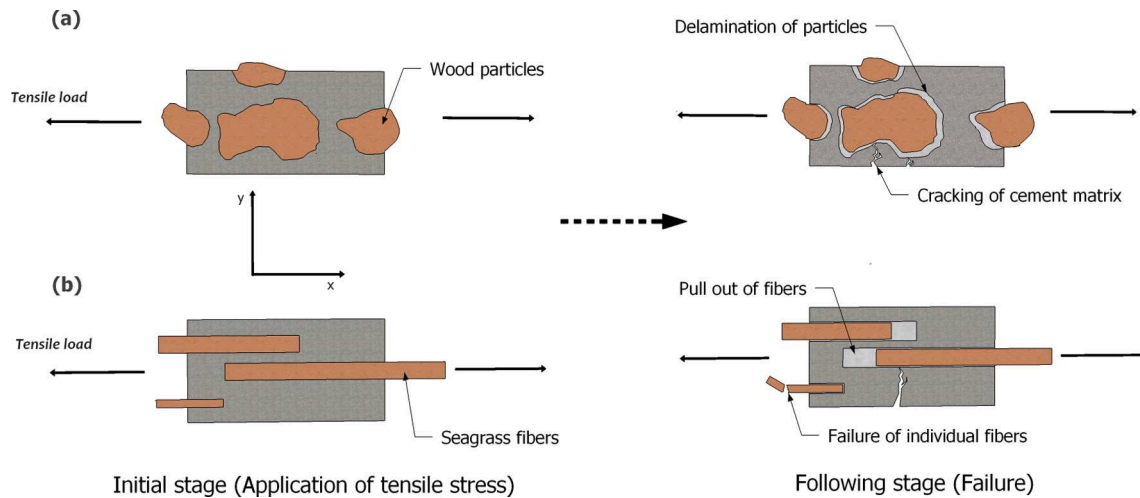


Fig. 5. Failure mechanism correlated with the applied tensile stress during bending of (a) wood-based and (b) seagrass-based cement board.

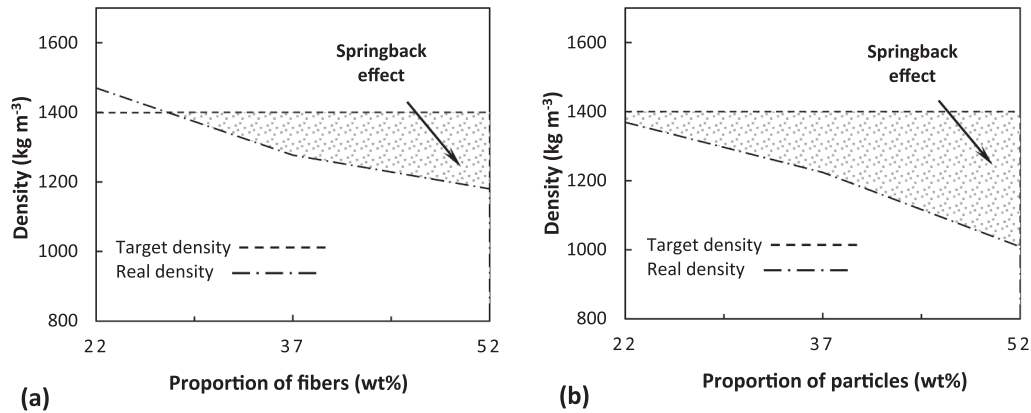


Fig. 6. The magnitude of springback effect with increasing proportion of fibers/particles for (a) seagrass-based cement boards and (b) wood-based cement boards.

Table 6
Results of calorimetric measurements.

Board type ^a	Density (kg m ⁻³)	ML ^b (%)	THR ^b (MJ m ²)	PHRR ^b (kW m ²)	IT ^b (s)	Risk level
SG 78/22	1315	27	55	40	–	Intermediate
SG 78/22	1288	27	53	40	–	Intermediate
SG 78/22	1181	29	52	40	–	Intermediate
SG 63/37	1253	32	48	43	–	Intermediate
SG 48/52	1163	37	59	46	1102	Intermediate
WP 78/22	1436	24	57	47	–	Intermediate
WP 78/22	1157	26	57	44	–	Intermediate
WP 78/22	1127	26	49	36	–	Intermediate
WP 63/37	1093	35	55	52	–	Intermediate
WP 48/52	831	38	45	83	58	Intermediate

^a Board type SG correspond to seagrass-based cement boards, while WP corresponds to wood-based cement boards. The numbers indicate the binder to lignocellulosic aggregate ratio.

^b ML is the mass loss, THR is the total heat release, PHRR is the peak heat release rate, IT is the ignition time

to 38%. For both organic materials, the decrease in density did not affect the ML, which is only dependent on the cement-lignocellulosic material ratio. The same applies to the peak heat release rate (PHRR). It increased when the content of lignocellulosic material increased. This trend was observed for both lignocellulosic materials. For wood-based cement boards, a decrease in density also reduces the PHRR (Table 6).

The total heat release was calculated as the integral below the heat

release rate over time. For both lignocellulosic materials, a reduction in density implies a reduction in THR, because the specimen as a whole consist of less organic material that can release heat. On the other hand, a relative increase in lignocellulosic material, due to a change in cement-lignocellulosic material ratio, increases the THR. Only the specimens containing the largest amount of lignocellulosic material (both seagrass and wood particles), ignited during the test. Seagrass fibers turned out to be superior to wood particles and have an ignition time approximately 20 times higher. Considering the risk level and the THR values, all panel types are classified in the “Intermediate risk” zone (Table 6).

Flame retardants for wood show different modes of action when exposed to fire. The most common ones are the mechanisms of dilution, char formation, ceramification, and alteration of thermal properties or inhibition of chain reactions [50]. Even though cement is not a conventional fire retardant, it operates in some of these ways when displayed to thermal action. The lignocellulosic material is covered with cement hydrate layers which prevent thermal degradation. The material is sealed and cannot emit volatile combustible gases, which may react with the atmospheric oxygen. Flaming combustion as well as flame spread is based on oxidation of these pyrolysis gases and are therefore prevented. A high cement-wood ratio means that a greater amount of organic material is covered by layers of cement hydrate, thus suppressing flammability [51].

Cement and other mineral binders / matrixes have a high amount of crystal water and chemically bound water. When these materials are exposed to higher temperatures, they are cooled by heat of evaporation [52]. Another effect of thermal properties that occurs, especially with

Table 7Thickness swelling (TS), water absorption (WA) and absolute water absorption (AWA)^a

Board type	Density (kg m ⁻³)	TS 24 h (%)	TS 72 h (%)	WA 24 h (%)	AWA 24 h (g)	WA 72 h (%)	AWA 72 h (g)
SG 78/22	1529	0.6	0.5	7.6	5.1	9.4	6.3
SG 78/22	1299	0.3	0.5	12.6	7.3	15.1	8.8
SG 78/22	1213	0.2	0.6	15.3	7.8	17.7	9.3
SG 63/37	1420	0.5	0.8	6.0	3.9	8.4	5.5
SG 48/52	1332	1.2	1.8	7.5	5.1	11.0	7.4
WP 78/22	1381	0.8	1.1	17.1	10.2	18.8	11.2
WP 78/22	1181	0.6	0.6	23.4	12.3	26.0	13.7
WP 78/22	993	0.7	0.8	32.9	14.6	34.9	15.4
WP 63/37	1242	7.8	8.4	22.0	13.0	24.3	14.4
WP 48/52	869	19.5	20.4	50.3	24.2	49.0	23.8

^a Mean values of 3 replicates for each type of composite

mineral binders with a high density, is the higher thermal conductivity of the mineral components compared to wood. The higher thermal conductivity dissipates heat from the point of thermal activity and alleviates the formation of hotspots [51]. None of the specimens tested in the cone calorimeter broke or cracked during the test. An absence of crack formation prevents the burn-through, which normally occurs when wood is burned. No new surface area is created for further pyrolysis and volatiles cannot escape from inside the tested specimen [52]. The very low PHRR also resembles the fact that ignition did not occur for most specimens, as well as the missing burn through. As shown in this study, the incombustibility does not depend on board density but on the cement-wood ratio, this was also proven by Namioka [53].

3.5. Water resistance and dimensional stability

Cement boards containing seagrass displayed lower water absorption (WA) and thickness swelling (TS) after submersion in water for 24 and 72 h than those containing wood particles (Table 7). The WA as an absolute value is also displayed, because it correlates with the density of the board. With the deviation of density, the absolute water absorption

(AWA) may lead to profoundly different relative values of WA. For both lignocellulosic materials, TS is not affected by density if the cement-lignocellulose ratio stays the same.

For boards containing seagrass fibers, significant TS after 24 and 72 h submersion occurred only for the variant with 52% fibers, reaching 1.2% and 1.8%, respectively. In contrast, boards containing 37% wood particles already showed significant maximum TS (72 h) (8.4%), while those with 53% wood particles revealed >20% maximum TS.

Even though TS is not influenced by the board density, WA increased for both lignocellulosic materials. For boards with seagrass fibers, the WA after 24 and 72 h increase with decreasing density from 7.6% and 9.4% to 15.3% and 17.7%. WA of boards with wood particles increased from 17.1% and 18.8% to 32.9% and 34.9%. The effect of the cement-lignocellulose ratio on the WA was not coherent. For boards with seagrass, WA after 24 h did not change with decreasing ratio, while the WA after 72 h increased from 9.4% to 11.0%.

For boards with wood particles, higher WA might be due to the springback effect. The WA of 50.3% and 49.0% can only partly be attributed to the change in cement-lignocellulose ratio, but also to the decrease in density.

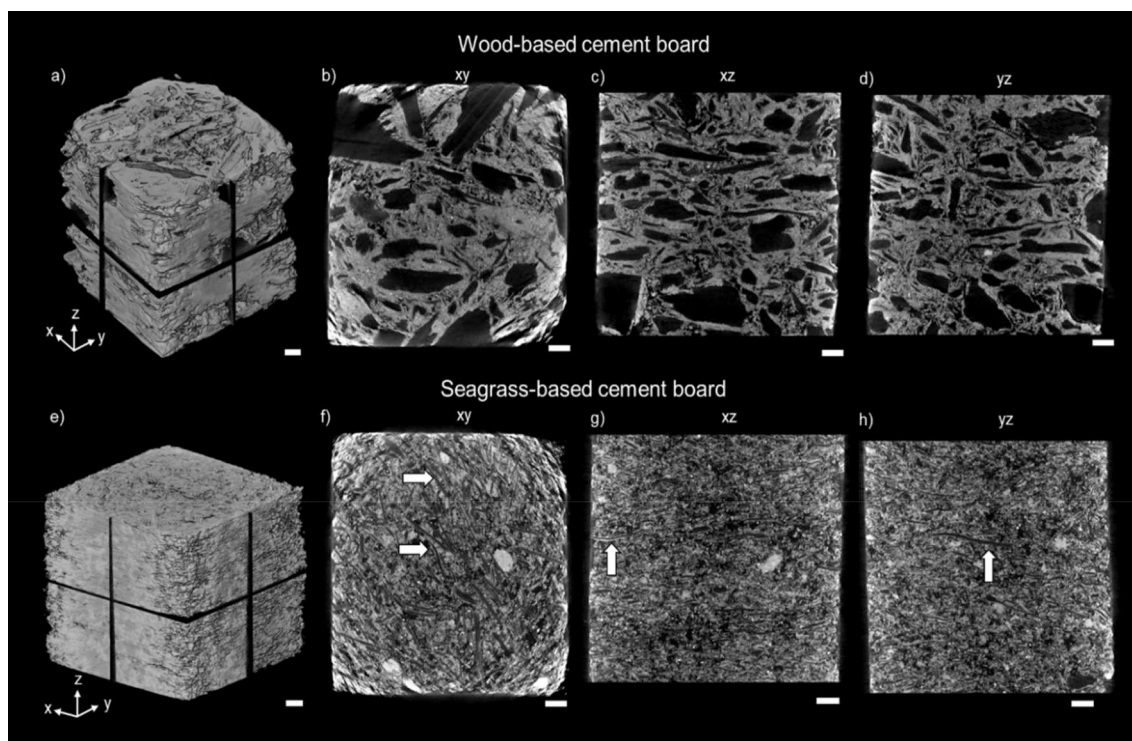


Fig. 7. Tomography images of native cement-bonded boards. The visualizations show the corresponding plane of sections (xy, xz, yz) of the internal board structure. Scale bars: 1 mm. Top: wood-based cement board (a, b, c, d) Bottom: Seagrass-based cement board (e, f, g, h).

Increased relative content of porous organic material, especially of wood particles increases the TS and WA and, thus, worsen the dimensional stability of the boards [54]. Furthermore, the increasing content of lignocellulosic material reduces MOE and Work until F_{max} (Table 5), indicating a weakening of the cement matrix. The latter is also reflected in TS and WA. Several researchers have found similar results when investigating cement-bonded particleboards [55-57]. The results for seagrass-based cement boards show that they are viable for exterior load-bearing use as they meet the requirements for the TS of 1.5% indicated in the standard DIN EN 634.

3.6. Structural imaging of cement-bonded boards

Structural imaging of the prepared seagrass-based and wood-based cement boards reveals their morphological differences. Tomography images show the cut sections of the prepared specimens in various directions (Fig. 7). Micro-CT is a powerful tool for the non-destructive characterization of wood materials and concrete materials [58]. However, the high X-ray opacity of cement makes it difficult to gain sufficient contrast between the air and the relatively fine organic material phase (i.e., wood particles and seagrass fibers). Nevertheless, dissimilarities can be easily observed, where the gray and black color shading correspond to the cement phase and the lignocellulosic aggregate, respectively. The cross-section images of wood-based cement boards show the continuation of the inorganic matrix, while particles are widely dispersed in it. Compared to the seagrass fibers, wood particles have visibly larger dimensions which might result in a higher degree of disruption of the tensile stress applied both in the longitudinal and lateral direction. On the other hand, seagrass fibers, because of their fineness and the adequate scale of mixing with cement, form a more compact structure than wood particles (Fig. 7, a).

In the case of seagrass-based boards, a thin layer of cement covers the fibers indicating a satisfactory distribution of stress in the internal structure. The orthotropic positioning of seagrass fibers is shown in Fig. 7, f (white arrows). In the xy-plane section of the seagrass board, which corresponds to the longitudinal direction, dark-grey color lineaments are noticeable, showing a preferential arrangement of fibers, in contrast to the lateral directions of the board, where fibers appear mostly as black dots manifesting their cross-sectional plane (Fig. 7, g, h). The preferred arrangement takes place during the pre-pressing and pressing of fibers in the production process. In this step, fibers that are randomly aligned in all directions are relocated to the horizontal direction (plane section xy), resulting in a material with orthotropic properties.

After applying tensile stress, the samples showed structural

deformation. The most apparent failure is the formation of cracks. The cracks extend relatively deep into the sample, as it is discernible in the micro-CT images of seagrass-based cement boards (Fig. 8) and the microscopy images of both wood-based and seagrass-based cement boards (Fig. 9). Size and shape differences of the raw material do not only affect the compactness and distribution of the inorganic binder in the composite but also its failure mode.

The vertical view of the fractured samples (Fig. 9 b, d) shows that in the case of seagrass composites, a higher amount of aggregates was involved in the transfer of tensile load, while in the case of the wood composites, the amplification of stress after the cracking initiation is higher resulting in a lower tensile resistance. The inclusion of a high fiber proportion is reflected in Fig. 9, d. The seagrass fibers were neither broken nor detached from the matrix, but transferred the tensile load to the cement matrix, dampening and inhibiting the initiation of the fracture. In addition, the 3D rendering of the crack in the seagrass board (colored in blue, Fig. 8, c) shows a high degree of crack propagation, demonstrating that more and more fibers are involved in the failure process. In the case of wood-based cement boards, on the other hand, the images show not only the cracks but also the distinct delamination of the individual wood particles (Fig. 9, a). Delamination of individual particles (Fig. 9, e) might be associated with the unsteady space known as Interfacial Transition Zone. The fractured area might have been caused by cutting the sample. Due to the unsteady ITZ, the stress applied during cutting might have caused the delamination of the wood particle.

ITZ is the region of the cement paste around the aggregate particles, which is perturbed by the presence of the aggregate. Previous studies confirmed that it arises due to the packing of the cement grains against the larger aggregate particles, leading to a more porous zone [59]. Along with the perturbation of the aggregates and the higher porosity, the inhibition effect described in section 3.2 could also occur in this region due to chemical constituents of lignocellulosic material, resulting in the formation of products with low mechanical strength.

Another notable difference in terms of the failure mechanism is the direction of fracture movement. While wood composites develop a crack that is directed perpendicular to the direction of tensile load (Fig. 9, a and f), in seagrass boards this movement, after the initial stage, is directed in the longitudinal direction parallel to the tensile load. In a hypothetical situation, the seagrass fibers would break or pull out if the direction were entirely perpendicular to the tensile load. However, the fracture seemed to be headed in the longitudinal direction because the fibers were more likely to delaminate rather than pull out in this direction. Still, in Fig. 9 c and d the pull-out is visibly indicated by an arrow.

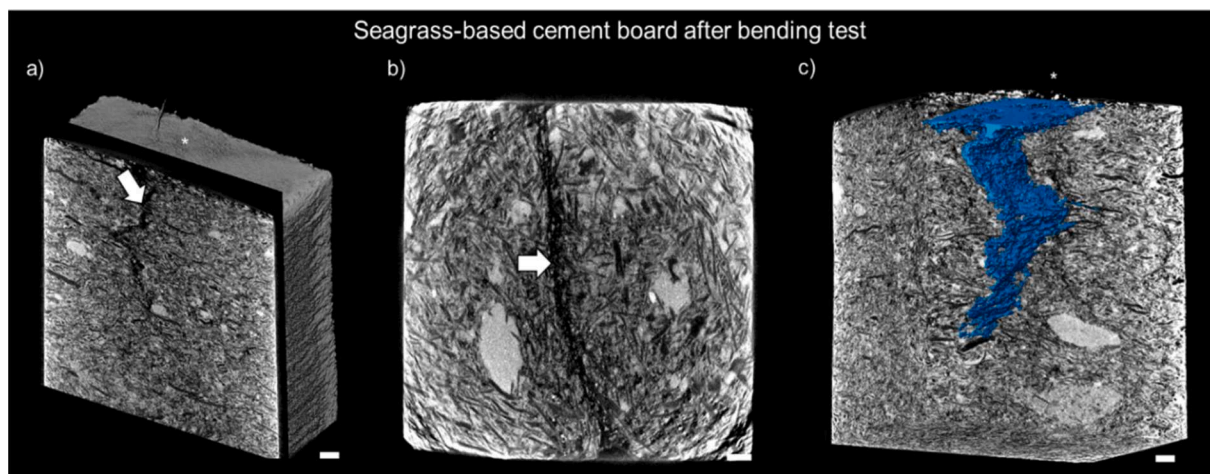


Fig. 8. Tomography images of a seagrass-based board after applied bending stress. Scale bars: 1 mm. The micro-CT images reveal a crack highlighted by an arrow in (a, b). The crack extends transversally through the entire sample. The 3D rendering of the crack colored in blue discloses that the crack extends from the surface (*) relatively deep (10.6 mm) into the sample (c).

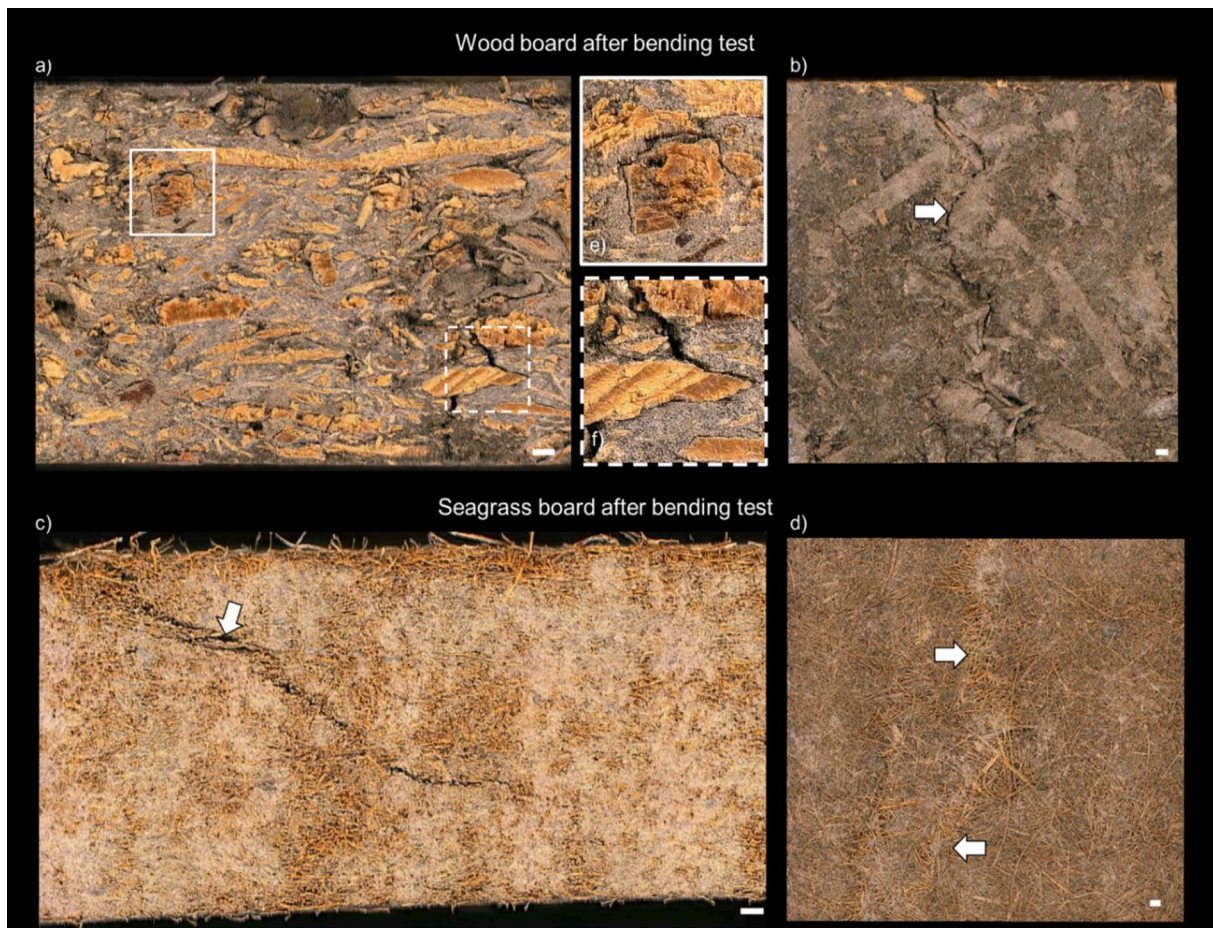


Fig. 9. Microscopy images of cement-bonded boards after applied bending stress. Scale bars: 1 mm. Top: Pine wood board (a, b). Close-ups (e, f) reveal delamination of wood particles as schematically shown in Fig. 5 a. Bottom: Seagrass board (c, d). The arrow highlights a crack and the involvement of fibers in the pull-out process.

4. Conclusion

In this study, the effect of two different lignocellulosic materials was examined. The effect of seagrass fibers (*Posidonia oceanica*) and pine wood particles (*Pinus sylvestris*), on the physico-mechanical properties as well as water and fire resistance of cement bonded boards was studied. Due to the higher chemical and physical compatibility of seagrass fibers compared to wood particles, seagrass-based cement boards reach higher mechanical strength and toughness than the comparable wood-based cement boards. The addition of up to 37 wt% seagrass fibers is suitable for standardized compliance. Increasing proportions of fibers (wt%) result in a loss of internal bond strength but do not influence the bending strength. Furthermore, seagrass-based cement boards exhibited better properties in both water resistance as well as flame resistance.

Microstructural analysis of the cement-bonded boards using X-ray micro-computed tomography and 3D-reflected light microscopy revealed that the seagrass-based boards exhibited a more homogeneous distribution of the cement and fibers. Seagrass-based cement boards transfer applied tensile stresses into the cement matrix instead of causing delamination and cracking caused in wood-based cement boards.

Taking the results of this study into account, seagrass-based cement boards present a sustainable and superior alternative to wood-based cement boards and can be used for the building sector, especially under the current wood scarcity.

CRedit authorship contribution statement

Aaron Kilian Mayer: Conceptualization, Methodology, Data

curation, Writing – original draft, Investigation, Visualization, Writing – review & editing. **Aldi Kuqo:** Conceptualization, Methodology, Data curation, Writing – original draft, Investigation, Visualization, Writing – review & editing. **Tim Koddenberg:** Investigation, Visualization. **Carsten Mai:** Supervision, Validation, Writing – review & editing.

Declaration of Competing Interest

The authors declare that they have no known competing financial interests or personal relationships that could have appeared to influence the work reported in this paper.

Acknowledgements

This research was supported by the Formas project 942-2016-2 (2017-21). Aldi Kuqo is grateful for funding from the German Academic Exchange Service (DAAD). We gratefully acknowledge the assistance by Christian Reck (Fraunhofer-Institut für Holzforschung, Wilhelm-Klauditz-Institut) who provided insights and useful discussions.

References

- [1] Frybort S, Mauritz R, Teischinger A, Müller U. Cement bonded composites—a mechanical review. *BioResources* 2008;3(2):602–26.
- [2] Wolfe WR, Gjinolli A. Cement-bonded wood composites as an engineering material. In: The use of recycled wood and paper in building applications. Forest Products Society, 1996. p.84-91.
- [3] Moslemi A. Inorganically bonded wood composites. *Chem Tech* 1988;18:504–10.

- [4] Mendes RF, Vilela AP, Farrapo CL, Mendes JF, Denzin Tonoli GH, Mendes LM. In: Sustainable and Nonconventional Construction Materials using Inorganic Bonded Fiber Composites. Elsevier; 2017. p. 3–16. <https://doi.org/10.1016/B978-0-08-102001-2.00001-2>.
- [5] Tittlein P, Cloutier A, Bissonnette B. Design of a low-density wood–cement particleboard for interior wall finish. *Cem Concr Compos* 2012;34(2):218–22.
- [6] Cabral MR, Nakanishi EY, dos Santos V, Palacios JH, Godbout S, Savastano Junior H, et al. Evaluation of pre-treatment efficiency on sugarcane bagasse fibers for the production of cement composites. *Arch Civil Mech Eng* 2018;18(4): 1092–102.
- [7] Cabral MR, Nakanishi EY, Mármol G, Palacios J, Godbout S, Lagacé R, et al. Potential of Jerusalem Artichoke (*Helianthus tuberosus* L.) stalks to produce cement-bonded particleboards. *Ind Crops Prod* 2018;122:214–22.
- [8] Wei YM, Tomita B. Effects of five additive materials on mechanical and dimensional properties of wood cement-bonded boards. *J Wood Sci* 2001;47(6): 437–44.
- [9] Rangavar H. Wood-cement board reinforced with steel nets and woven hemp yarns: physical and mechanical properties. *Wood Industry/Drvna Industrija* 2017;68(2): 121–8.
- [10] Diquélou Y, Gourlay E, Arnaud L, Kurek B. Impact of hemp shiv on cement setting and hardening influence of the extracted components from the aggregates and study of the interfaces with the inorganic matrix. *Cem Concr Compos* 2015;55: 112–21.
- [11] Ferrandez-García MT, Ferrandez-García CE, García-Ortuño T, Ferrandez-García A, Ferrandez-Villena M. Study of waste jute fibre panels (*Corchorus capsularis* L.) agglomerated with portland cement and starch. *Polymers* 2020;12(3):599.
- [12] Kuqo A, Korpa A, Dhano N. *Posidonia oceanica* leaves for processing of PMDI composite boards. *J Compos Mater* 2019;53(12):1697–703.
- [13] Rammou E, Mitani A, Ntalos G, Koutsianitis D, Taghiyari HR, Papadopoulos AN. The potential use of seaweed (*Posidonia oceanica*) as an alternative lignocellulosic raw material for wood composites manufacture. *Coatings* 2021;11(1):69.
- [14] Verhille G, Moulinet S, Vandenbergh N, Adda-Bedia M, Le Gal P. Structure and mechanics of aegagropilae fiber network. *Proc Natl Acad Sci* 2017;114(18): 4607–12.
- [15] Allègue L, Zidi M, Sghaier S. Mechanical properties of *Posidonia oceanica* fibers reinforced cement. *J Compos Mater* 2015;49(5):509–17.
- [16] Hamdaoui O, Limam O, Ibos L, Mazhoud A. Thermal and mechanical properties of hardened cement paste reinforced with *Posidonia-Oceanica* natural fibers. *Constr Build Mater* 2021;269:121339.
- [17] Kuqo A, Boci I, Vito S, Vishkulli S. Mechanical properties of lightweight concrete composed with *Posidonia Oceanica* fibres. *Zastita materijala* 2018;59(4):519–23.
- [18] Kuqo A, Mai C. Mechanical properties of lightweight gypsum composites comprised of seagrass *Posidonia oceanica* and pine (*Pinus sylvestris*) wood fibers. *Constr Build Mater* 2021;282:122714.
- [19] Jedidi M, Abroug A. Valorization of *Posidonia oceanica* Balls for the manufacture of an insulating and ecological material. *Jordan J Civil Eng* 2020;14:417–30.
- [20] DIN EN 197-1:2011, Cement - Part 1: Composition, specifications and conformity criteria for common cements.
- [21] TAPPI T 264 cm-97, Preparation of wood for chemical analysis.
- [22] NREL/TP-510-42618, Determination of Structural Carbohydrates and Lignin in Biomass.
- [23] Wise LE. Chlorite holocellulose, its fractionation and bearing on summative wood analysis and studies on the hemicelluloses. *Pap Trade J* 1946;122:35–43.
- [24] Tappi T211 om-02, Ash in wood, pulp, paper and paperboard: combustion at 525°C.
- [25] Hachmi H, Moslemi AA, Campbell AG. A new technique to classify the compatibility of wood with cement. *Wood Sci Technol* 1990;24:345–54.
- [26] Weatherwax RC. Effect of wood on the setting of ordinary Portland cement. *For Prod J* 1964;14:567–70.
- [27] Simatupang MH. Der Wasserbedarf bei der Herstellung zementgebundener Holzspanplattenwater requirement for the production of cement bonded particle board. Holz als Roh-und Werkstoff 1979;37(10):379–82.
- [28] Okino EYA, Souza MRD, Santana MAE, Alves MVdS, Sousa MED, Teixeira DE. Cement-bonded wood particleboard with a mixture of eucalypt and rubberwood. *Cem Concr Compos* 2004;26(6):729–34.
- [29] BS EN 634-2:2007. Cement-bonded particleboards. Specifications. Requirements.
- [30] BS EN 323:1993. Wood-based panels. Determination of density.
- [31] DIN EN 310:1993, Wood-based panels; determination of modulus of elasticity in bending and of bending strength.
- [32] BS EN 319:1993. Particleboards and fibreboards. Determination of tensile strength perpendicular to the plane of the board.
- [33] ISO 5660-1:2002-12, Reaction-to-fire tests - Heat release, smoke reduction and mass loss rate - Part 1 - Heat release rate (cone calorimeter method).
- [34] Petrella RV. The assessment of full-scale fire hazards from cone calorimeter data. *J Fire Sci* 1994;12(1):14–43.
- [35] DIN EN 317:1993, Particleboards and fibreboards; determination of swelling in thickness after immersion in water.
- [36] Rowell RM. Handbook of wood chemistry and wood composites. CRC Press; 2012.
- [37] Roffael E. Significance of wood extractives for wood bonding. *Appl Microbiol Biotechnol* 2016;100(4):1589–96.
- [38] Coccozza C, Parente A, Zaccone C, Mininni C, Santamaria P, Miano T. Chemical, physical and spectroscopic characterization of *Posidonia oceanica* (L.) Del. residues and their possible recycle. *Biomass Bioenergy* 2011;35(2):799–807.
- [39] Khiari R, Mhenni MF, Belgacem MN, Mauret E. Chemical composition and pulping of date palm rachis and *Posidonia oceanica* – a comparison with other wood and non-wood fibre sources. *Bioresour Technol* 2010;101(2):775–80.
- [40] Bettaieb F, Khiari R, Dufresne A, Mhenni MF, Putaux JL, Boufi S. Nanofibrillar cellulose from *Posidonia oceanica*: properties and morphological features. *Ind Crops Prod* 2015;72:97–106.
- [41] Dibdiakova J, Wang L, Li H. Characterization of ashes from *Pinus Sylvestris* forest biomass. *Energy Procedia* 2015;75:186–91.
- [42] Thomas NL, Birchall JD. The retarding action of sugars on cement hydration. *Cem Concr Res* 1983;13(6):830–42.
- [43] Kochova K, Schollbach K, Gauvin F, Brouwers HJH. Effect of saccharides on the hydration of ordinary Portland cement. *Constr Build Mater* 2017;150:268–75.
- [44] Ben Salem Y, Abdelhamid A, Mkdmini Hammi K, Le Cerf D, Bouraoui A, Majdoub H. Microwave-assisted extraction and pharmacological evaluation of polysaccharides from *Posidonia oceanica*. *Biosci Biotechnol Biochem* 2017;81(10): 1917–25.
- [45] Vaickelionis G, Vaickelioniene R. Cement hydration in the presence of wood extractives and pozzolan mineral additives. *Ceramics Silikaty* 2006;50:115–22.
- [46] De Luca A, Caputo F. A review on analytical failure criteria for composite materials. *Mater Sci* 2017;4:1165–85.
- [47] Dassios KG. A review of the pull-out mechanism in the fracture of brittle-matrix fibre-reinforced composites. *Adv Compos Lett* 2007;16(1):17–24.
- [48] Post PW. Relationship of flake size and resin content to mechanical and dimensional properties of flake board. *For Prod J* 1961;11:34–7.
- [49] Badejo SOO. Effect of flake geometry on properties of cement-bonded particleboard from mixed tropical hardwoods. *Wood Sci Technol* 1988;22(4): 357–69.
- [50] Sauerbier P, Mayer AK, Emmerich L, Militz H. Fire retardant treatment of wood – state of the art and future perspectives. *Wood Fire Saf* 2020;97–102.
- [51] Yu Y, Hou J, Dong Z, Wang C, Lu F, Song P. Evaluating the flammability performance of Portland cement-bonded particleboards with different cement–wood ratios using a cone calorimeter. *J Fire Sci* 2016;34(3):199–211.
- [52] Topf P. Brandverhalten von mineralisch gebundenen PlattenFire behaviour of mineral bonded boards. *Holz Als Roh- Werkst* 1989;47(10):415–9.
- [53] Namioka Y, Takahashi T, Anazawa T, Kitazawa M. Studies on the manufacturing of wood-based cement boards. *Rep Hokkaido Forest Prod Res Inst* 1976;65:88–142.
- [54] Sotannde OA, Oluwadare AO, Ogedoh O, Adeogun PF. Evaluation of cement-bonded particle boards produced from *Azelaia africana* wood residues. *J Eng Sci Technol* 2012;7:732–43.
- [55] Ogunjobi M, Gakenou O. Physical and mechanical properties of cement-bonded particle board produced from *Anogeissus leiocarpus* (DC.) Guill and Perr wood species. *African J Agri Technol Environ* 2019;8:192–9.
- [56] Ali IM, Nasr MS, Samir A. Enhancement of cured cement using environmental waste: particleboards incorporating nano slag. *Open Eng* 2020;10:273–81.
- [57] Marzuki AR, Rahim S, Hamidah M, Ruslan RA. Effects of wood: cement ratio on mechanical and physical properties of three-layered cement-bonded particleboards from *Leucaena Leucocephala*. *J Trop For Sci* 2011;23:67–121.
- [58] Van den Bulcke J, Biziks V, Andersons B, Mahnert K-C, Militz H, Van Loo D, et al. Potential of X-ray computed tomography for 3D anatomical analysis and microdensitometrical assessment in wood research with focus on wood modification. *Int Wood Prod J* 2013;4(3):183–90.
- [59] Scrivener KL, Crumie AK, Laugesen P. The interfacial transition zone (ITZ) between cement paste and aggregate in concrete. *Interface Sci* 2004;12(4):411–21.

Article 3

Use of dry mixing-spraying process for the production of geopolymer-bonded wood and seagrass fibreboards – Article 3

Aldi Kuqo, Tim Koddenberg, Carsten Mai *

*Corresponding author, email: cmai@gwdg.de

Wood Biology and Wood Products, Faculty of Forest Sciences and Forest Ecology, University of Göttingen, Büsgenweg 4, 37077, Göttingen, Germany

Authorship (according to Clement, 2014)

	Conceptualization (30%)	Practical work (30%)	Writing/Editing (30%)	Administration (10%)	Contribution
A. Kuqo	60%	90%	60%	20%	64%
T. Koddenberg	10%	10	15%	0%	10.5
C. Mai	30%	0%	25%	80%	24.5%

Ideas: Design of the investigation / Experimental planning / Interpretation of the data

Work: Execution of the experiment / Data collection and analysis

Writing: Drafting the article / Critical, substantive revision / Reviewing the final version

Administration: Resource management and ensuring scientific integrity before, during, and after publication

Published in Composites Part B: Engineering, 248, 110387.

Published in November 2022

DOI: <https://doi.org/10.1016/j.compositesb.2022.110387>



Use of dry mixing-spraying process for the production of geopolymer-bonded wood and seagrass fibreboards

Aldi Kuqo, Tim Koddenberg, Carsten Mai*

Wood Biology and Wood Products, Faculty of Forest Sciences and Forest Ecology, University of Goettingen, Büsingenweg 4, 37077, Göttingen, Germany

ARTICLE INFO

Keywords:

Seagrass fibres
Wood fibres
Geopolymer composites
Mechanical testing
X-ray microtomography

ABSTRACT

Mixing lignocellulosic fibres with a mineral binder to produce fibreboards is a challenging process due to their large volume per unit mass and their susceptibility to agglomeration (balling effect). The main objective in the dry mixing-spraying process presented in our study is the uniform distribution of the geopolymer binder in the lignocellulosic material. In this work, we compare the properties of two types of composites processed by implementing the abovementioned technique. Geopolymer-bonded fibreboards were produced using up to 50 wt % seagrass or wood fibres. Microscopy and X-ray micro-tomography investigations of the geopolymer composites indicated that their mechanical and physical properties depend on the size of incorporated fibres. Large seagrass fibres were appropriately mixed with the mineral binder matrix forming solid fibreboards that were able to reach the standard requirements for cement boards. More specifically, seagrass-based fibreboards exhibit up to 42% higher bending strength (up to 9.4 MPa) compared to fibreboards composed of wood fibres. In addition, their low thickness swelling and low mean heat release rate in a cone calorimeter (varying from 21.5 to 26.6 kW m⁻²) indicated a high resistance to water and fire. Considering the resulting properties of the produced fibreboards, the dry-mixing spraying process can be an appropriate technique for producing geopolymer composites containing large amounts of relatively long fibres.

1. Introduction

Owing to environmental awareness, manufacturers of building materials have been attentive to implementing new technologies and including new elements that ensure their products' sustainability and eco-friendliness. In the last century, ordinary Portland cement (OPC) has become one of the most significant building materials. Due to the high emission of carbon dioxide during lime burning and the immense amount of energy required in the manufacturing process, however, cement is considered a substantial contributor to global CO₂ emissions [1]. Geopolymers are regarded as a suitable alternative to Portland cement [2,3]. In terms of their composition, geopolymers are stable aluminium-silicate polymers formed by the reaction of aluminosilicate power with an appropriate activator [4]. The research on geopolymer concrete has shown an increasing trend in the last decade, with a particular focus on the properties of the obtained products [2,5]. In most of the studies conducted in the field of geopolymer composites, relatively small amounts of lignocellulosic or synthetic fibres have been incorporated, ranging from 0.5 to 10 wt% [6,7]. In other studies,

geopolymer has been regarded as an adhesive rather than concrete [8].

A high proportion of lignocellulosic fibres might have an undesirable effect on the overall performance of the inorganically bonded materials. Firstly, the increased interfacial volume between them and the geopolymer is a weakening factor resulting in a decrease of mechanical strength [9,10]. Furthermore, spherical agglomerates form during the mixing of vast volumes of fibrous aggregate with the viscous geopolymer paste, resulting in heterogeneous phases of matrix and unbonded aggregates (balling effect) [11]. The main challenge in the production of lignocellulosic fibreboards is the development of a homogeneous mixture that can ensure good mechanical and physical properties. The agglomeration (balling effect) of lignocellulosic and synthetic fibres has been regarded as one of the main factors influencing the properties of cementitious composites [11–15]. In particular, the balling of fibres in geopolymer composites has led to a reduction of workability during their production and eventually their compression strength and an increase in their water absorption [16]. For a wide range of composite systems, at high fractions of fibres, the occurrence of agglomeration leads to an increase in defects of composites and eventually loss of their

* Corresponding author.

E-mail address: cmai@gwdg.de (C. Mai).

<https://doi.org/10.1016/j.compositesb.2022.110387>

Received 17 January 2022; Received in revised form 25 August 2022; Accepted 29 October 2022

Available online 2 November 2022

1359-8368/© 2022 Elsevier Ltd. All rights reserved.

strength [17,18].

In previous research, various ways to avoid balling have been suggested. A low addition of fibres during the production of cementitious composites and the reduction of the size of fibres (especially their aspect ratio) could diminish the balling tendencies [11,12]. However, the cementitious composites containing a low proportion of fibres can be costly as a high amount of binder is required for their production. The reduction of fibre's aspect ratio (length to thickness ratio) can be another method to prevent the balling phenomenon. In many cases, however, reducing the fibres' length (by trimming or milling) can lessen their reinforcing effect, as they have lower anchorage lengths. Many authors have also adapted various techniques in order to avoid the balling effect by combining the mixing order of the raw materials [19]. In terms of mixing, geopolymer and Portland cement composites have many similarities.

Three primary processes are used in the industry to manufacture cement particleboards and fibreboards: the dry process, the semi-dry process, and the wet process [19]. The most common technique is the Hatschek (wet) process, in which a cement slurry with an excess of water is mixed with the fibres or particles forming a pulp. In the consequent stages, the pulp is placed in a special screen equipped with a vacuum chamber and the excess water is drained off [11,19]. In the semi-dry process, a viscous mixture is formed, which is then compacted and/or vibrated to form the cement boards. In the dry process, the moisture required for hydration of the cement is released by the particles or fibres themselves. This process is followed by hot-pressing so that hardening can take place.

In this study, an innovative technique is presented in analogy to the dry process utilized in the production of cement boards to ensure homogeneous distribution of the geopolymer precursor and alkaline activator in the lignocellulosic fibre material. Due to the homogeneous mixture, the inclusion of high proportions (up to 50 wt%) of fibres is attainable, reducing the cost of the composite boards. The term "dry process" for the production of geopolymer concrete has been used by several authors in recent research, signifying the mixing of dry alkaline activator with the precursor and adding water in the last phase [20]. However, the following dry mixing-spraying technique, intended for the production of composite boards, represents the mixing of fibres in a dry state without the formation of geopolymer paste or slurry. Though researchers have investigated various approaches to produce geopolymer composites containing high proportions of wood fibres, the mechanical properties of the composites obtained tend to deteriorate worsen at high fibre contents [21]. In our study, we aim to manipulate the mixing process in such a way that the "balling" of the relatively long fibres (high aspect ratio) is avoided and a suitable mixing of raw materials is attained. As a result, a high strength-to-bulk-density ratio of the composites is achievable at low cost. Compared with synthetic fibres, natural lignocellulosic fibres provide several advantages in terms of biodegradability, light weight, low price, life-cycle superiority, and satisfactory mechanical properties [22]. *Posidonia oceanica* fibres are found on the Mediterranean shores in the form of brownish-coloured balls. They are agglomerates of fibres generated by the decomposition of seagrass leaves in combination with the movement of waves. Their morphological features and chemical composition make them suitable candidates for application in the building sector [23]. Previous reports have shown that including small amounts of fibres into the ceramic matrices can improve their strength and toughness [24]. Wood fibres also referred to as lignocellulosic fibres, are derivatives of the wood refining process. They have been widely used in the production of insulation and cement fibreboards.

The objective of our study is the production of geopolymer fibreboards by using the dry mixing-spraying process and their characterization. In this manner, the effect of the size and morphology of the seagrass and wood fibres on the adequacy of mixing and the resulting properties of the produced fibreboards are also investigated. The geopolymer-bonded fibreboards are characterized and compared in

terms of their mechanical and physical properties. In addition, visual examinations of the microstructure of the produced geopolymer fibreboards are carried out.

2. Materials and methods

2.1. Materials

Seagrass spheres (*Posidonia oceanica*) were collected from the coast of Durrës (Albania, Adriatic Sea). The seagrass fibres were untwisted from the spherical agglomerates by using a mobile suction machine (Holzkraft ASA 163, Stürmer Maschinen GmbH, Hallstadt, Germany). After disentangling, the fibres obtained their loose form. The brownish seagrass fibres have a lignocellulosic composition consisting of 7.9% extractives, 35.4% lignin, 53.9% holocellulose and 12.9% ash [25]. Wood fibres (*Pinus sylvestris*) were provided by STEICO SE (Feldkirchen, Germany). The industrial STEICO wood fibres are composed of 6.2% extractives, 23.2% lignin, 31.5% hemicellulose and 39.4% cellulose [26]. A hammermill (Electra SAS VS1, Poudenas, France) was utilized to separate the fibres until they gained their uncompacted volume. The used metakaolin powder was Metamax (BASF, Ludwigshafen, Germany). The mean particle size of the metakaolin was 1.3 μm (particle size <2 μm : 68%). Its mineralogical composition comprised silica (SiO_2) and alumina (Al_2O_3) (Table 1) primarily. A mixture of sodium silicate Na_2SiO_3 (Carl Roth GmbH + Co. KG, Karlsruhe, Germany) and sodium hydroxide (NaOH) technical grade 98% (AppliChem GmbH, Darmstadt) was utilized for the preparation of the alkaline activator.

2.2. Methods

2.2.1. Uncompacted bulk density and fibre size distribution

The uncompacted bulk density of wood and seagrass fibres was determined according to BS EN 1097-3:1998 [27]. The oven-dried material was carefully poured into a metal vessel of a specified volume until it was completely filled. The weight of the poured material was divided by the volume of the vessel.

The size distribution of the fibres was determined using dynamic image analysis (Qicpic, Sympatec, Clausthal-Zellerfeld, Germany). The fibres of representative samples were placed in the feeder unit, accelerated by the compressed air jet, and scanned with the image analysis sensor. Due to their size differences, seagrass was determined using the dispersion system Qicpic Gradis for an extensive dispersion range, while wood fibres were measured using the Qicpic Rodos dry disperser (small dispersion range).

2.2.2. Production of geopolymer-bonded fibreboards

The production of geopolymer-bonded seagrass fibreboards (GSF) and geopolymer-bonded wood fibreboards (GWF) consisted of several steps (Fig. 1). For the preparation of the alkaline activator with a specific composition (Table 2), sodium hydroxide (NaOH) pellets were initially dissolved in water (exothermic reaction). Afterwards, Na_2SiO_3 solution with a solids content of $\sim 36\%$ (7.80–8.50% Na_2O , 25.80–28.50% SiO_2 , $\sim 64\%$ H_2O) also referred to as water glass, was poured into the sodium hydroxide solution, stirred, and left for 24 h. Before mixing, the solution was again stirred intensively for 5 min.

An 80-Litre drum mixer (Atika, Altrad Lescha Atika GmbH, Burgau, Germany) was used for the dry mixing-spraying process. The drum mixer (50 rpm) was equipped with a modified agitator (3 metal rods were placed in the body of the mixing tank) to avoid the movement of the whole mass of fibres and instead increase the efficiency of mixing by facilitating the movement of the fibres towards each other in the mixer. First, the mass of the fibres was calculated along with the amount of metakaolin and alkaline activator (Table 2). After the mixer was filled with the fibres, a plastic cover with a small circular window was attached to the drum to prevent the fibres from flowing out. During the spraying process, the drum was shifted to a horizontal position (60° – 90°)

Table 1
Chemical composition of metakaolin (wt%)^a.

SiO ₂	Al ₂ O ₃	Na ₂ O	K ₂ O	TiO ₂	Fe ₂ O ₃	CaO	MgO	P ₂ O ₅	LOI
52.3%	45.2%	0.22%	0.15%	1.74%	0.42%	0.04%	0.04%	0.08%	0.79%

^a According to provider.

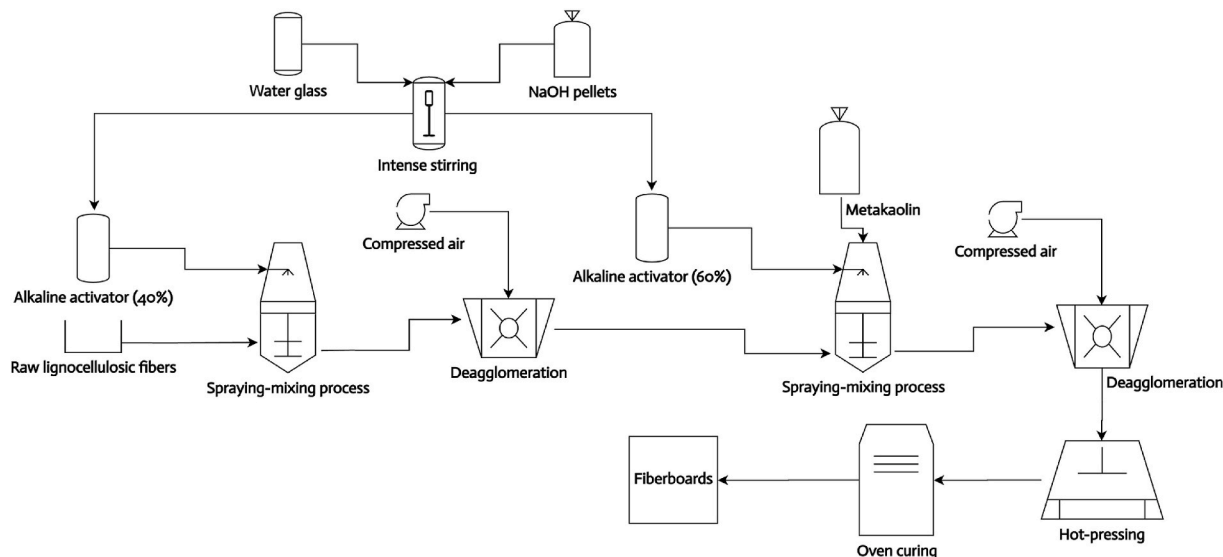


Fig. 1. Schematic flow diagram of geopolymer-bonded fibreboards production.

Table 2
Formulations of mixtures for the production of geopolymer fibreboards.

Type of board	Proportion of fibres (wt%)	Amount of fibres-dry (g)	Volume of fibres (L)	Amount of metakaolin (g)	Amount of alkaline activator		
					Na ₂ SiO ₃ -dry (g)	NaOH-dry (g)	Total H ₂ O (g)
GWF-30	30	1167	49	1744	667	310	1554
GWF-40	40	1560	66	1495	572	266	1554
GWF-50	50	1945	82	1246	477	221	1554
GSF-30	30	1167	47	1744	667	310	1554
GSF-40	40	1560	64	1495	572	266	1554
GSF-50	50	1945	79	1246	477	221	1554

^a The volume of uncompacted fibres was calculated from their weight and uncompacted density.

so that the fibres could pass in front of the circular window and be sprayed.

In the first phase, which lasted 5 min, 40% of the alkaline activator was sprayed onto the fibres with a spray nozzle. Due to the agglomeration of the lignocellulosic fibres, small spherical fibre clusters were formed. In the first deagglomeration step, the mass of sprayed fibres was gradually fed into a gasoline-powered shredder (Güde GH650, Güde GmbH & Co. KG, Wolpertshausen, Germany). Compressed air was used to intensify the unravelling of the fibres and move them quickly out of the shredder, reducing the risk of shredding (breaking fibres). Following the deagglomeration process (3–5 min), the loose, homogeneous mixture was again placed in the drum mixer and metakaolin powder was gradually added. After 2 min of further mixing, the remaining alkaline activator (60%) was sprayed onto the fibre mass. Again, the formation of fibre agglomerates occurred. The agglomerates were put into the shredder for a second cycle until a homogeneous mixture of fibres, metakaolin and activator had formed. Finally, the mixture was weighed, prepressed, and placed in a metal tetragonal frame attached to the hot press (Joos HP-2000 lab, Gottfried Joos GmbH & Co. KG, Pfalzgrafeweiler, Germany). The fibre mixture was pressed at 70 °C for 6 h using a specific pressure (20 MPa). After hot pressing, the produced

boards (with dimensions 450 × 450 × 16 mm³) were oven-cured at 50 °C for 72 h. The 72-h curing ensured the complete setting of the geopolymer binder. The duration of hot-pressing and the temperature were crucial factors for the production of geopolymer fibreboards. As a large volume of fibres was pressed, the expansive stress of fibres in the board also increased. As a result, lower temperatures and shorter pressing times than the parameters stated above could result in low initial strength, which increases the risk of springback and fibres popping out of the boards. In addition, it has been reported that elevated temperatures can induce geopolymerization [28]. Before testing, the prepared boards were conditioned at 23 °C and 65% relative humidity for another 25 days and cut into specific specimen sizes. A total of 12 boards were produced (2 boards per variant).

2.2.3. Determination of bulk density and mechanical properties of geopolymer-bonded fibreboards

The determination of the bulk density and the mechanical properties was carried out according to the specifications of the standard BS EN 634-2:2007 for the testing and determination of the physical-mechanical properties of cementitious boards [29]. Initially, the dimensions of the specimens (50 × 50 × 16 mm³) were measured to

determine the bulk density. Then, they were randomly selected for further testing of interfacial bond strength (IBS) and water absorption test. The specimens were bonded to metallic braces for IBS testing with a fast-curing polymer. They were then fitted in the universal testing machine ZwickRoell Zmartpro 10 kN (ZwickRoell, Ulm, Germany) and subjected to tensile loading at a continuous crosshead speed of 7 mm min⁻¹ perpendicular to the plane of the plate until failure. The screw pull-out strength (SPS) test was performed according to DIN EN 320:2007 [30]. An axial force perpendicular to the surface of the specimen (75 × 75 × 16 mm³) was applied using the universal testing machine with a crosshead speed of 10 mm min⁻¹. The maximum force required to extract the screw was recorded.

Bending strength, modulus of elasticity (MOE), and work to maximum load (W) were assessed by a three-point bending test with specimen dimensions of 370 × 50 × 16 mm³. A universal testing machine (ZwickRoell Zmartpro 10 kN, ZwickRoell, Ulm, Germany) with a crosshead speed of 6 mm min⁻¹ was employed for the tests, while the support span was 320 mm.

2.2.4. Water uptake and thickness swelling

Thickness swelling and water absorption were tested according to DIN EN 317:1993 [31]. The specimens were completely immersed in water for 24 and 72 h. After the specified time, they were removed and allowed to drain to remove excess water. Subsequently, the thickness and weight were measured. Further, to comment on the magnitude of diffusion of fibreboards, a set of specimens were immersed in water for shorter periods. Subsequently, they were weighted, and the correlation of water uptake with time was investigated.

2.2.5. Cone-calorimetry test and fire resistance

The heat release rate (HRR), mass loss rate (MLR), and time to ignition (IT) were evaluated following ISO 5660-1:2002-12 [32]. A mass loss calorimeter (MLC FTT, Fire Testing Technology, East Grinstead, UK) was employed for cone calorimetry testing. Tetragonal specimens (100 × 100 mm²) with a given thickness were exposed to a heat flux of 50 kW m⁻² for 30 min. In addition, the total heat release (THR) was calculated (integration of the HRR vs time curve).

2.2.6. FT-IR and XRD analysis

Fourier transform infrared spectroscopy (FT-IR) was performed using the FT-IR ATR spectrometer ALPHA II (Bruker, Bremen, Germany) in a frequency range of 4000–400 cm⁻¹ at a spectral resolution of 4 cm⁻¹ and 24 scans per sample to identify the nature of bonding exhibited by metakaolin, and the ground geopolymer-bonded composites. For the preparation of the samples (grinding), a Herzog HSM (HERZOG Maschinenfabrik GmbH & Co. KG, Osnabrück, Germany) grinder was utilized.

X-ray diffraction (XRD) (PANalytical Empyrean, Almelo, Netherlands) diffractometer equipped with a Cu LFF HR X-ray tube, programmable anti-scatter slit and a PIXcel^{3D} detector was employed to determine the phase of the samples (metakaolin and geopolymer-bonded composites). The scanning degrees, i.e., the 2θ range, was 5–60° and the step size was 0.026°. A scanning speed of 1°/min was applied for the measurement. The accelerating voltage and current were 45 kV and 40 mA, respectively. The COD (Crystallography Open Database) and database of Zeolite structures reference library were used for the qualitative identification of the crystalline phases.

2.2.7. Structural imaging of geopolymer-bonded fibreboards

The structural characterization of geopolymer fibreboards was performed by 3D-reflected light microscopy and X-ray micro-computed tomography (micro-CT). For the microscopy investigation, specimens were imaged using the Keyence VHX-5000 digital 3D reflected light microscope (Keyence, Neu-Isenburg, Germany). Images with a high depth-of-field were obtained with this microscope by combining different in-focus images. The acquired images were captured at

magnifications of 50 × and 100 ×. Specimens with the higher modulus of elasticity (MOE) from the two variants were selected for the analysis (GSF-30 and GWF-40).

The non-destructive examination of the fibreboards was accomplished by the commercial micro-CT system Nanotom s (phoenix|x-ray, GE Sensing & Inspection Technologies GmbH Wunstorf, Germany). Therefore, the cuboid specimens measuring 14 × 16 × 32 mm³ were scanned at a peak tube voltage of 60 keV, a current of 120 μA, and a 2500 ms X-ray exposure. For each scan, a stack of 1800 greyscale projection images was collected at a voxel size of 10 μm. The captured stacks of images were then converted into volumetric datasets using the phoenix datos|x reconstruction© software (phoenix|x-ray, GE Sensing & Inspection Technologies GmbH, Wunstorf, Germany). The structural visualizations of the specimens, provided in 2D and 3D, were realized using the Avizo software (FEI, Thermo Fisher Scientific, Hillsboro, Oregon, USA).

A further analysis investigating the bonding of lignocellulosic fibres with the geopolymer matrix was conducted using scanning electron microscopy (SEM). First, the samples obtained from the interfacial bond test (section 2.2.3) were cut into smaller dimensions. Then, their broken, delaminated area was investigated with a ZEISS EVO LS 15 electron scanning microscope (Carl Zeiss Microscopy GmbH, Jena, Germany). The working parameters were set to an accelerating voltage of 5 kV and 10 kV for GSF-30 and GWF-40, respectively, while the acquired images were captured at magnifications of 160 × and 63 ×.

3. Results and discussion

3.1. Bulk density and size distribution of lignocellulosic fibres

The difference in terms of the uncompacted bulk density between seagrass and wood fibres was not significant. For seagrass fibres, it was 24.5 kg m⁻³, while for wood fibres, it reached 23.7 kg m⁻³. The bulk density of fibres fluctuates and depends on the process used to generate their loose form. The volume-weighted cumulative distributions of seagrass and wood fibres exhibited a significant difference in their size (Fig. 2). The mean length of seagrass fibres was 11.1 mm, while their length at 90th percentile-P₉₀ can be up to 22.3 mm. In contrast, the mean length of wood fibres was 3.0 mm, while their P₉₀ length was 4.6 mm. The thickness of most seagrass fibres (percentiles P₁₀–P₉₀) varied from 0.08 to 0.3 mm; in contrast, most wood fibres ranged from 0.05 to 0.2 mm thickness. On average, seagrass fibres were up to 3–4 times longer and 1–2 times thicker than wood fibres. Referring to the obtained results, the aspect ratio (ratio of length to thickness) of seagrass fibres appears to be ~95 while the aspect ratio of wood fibres is ~40.

The smaller the fibres' size, the greater is their specific surface area [33]. The fibres' outer surface area per unit mass is of particular importance, as a high quantity of binder and a homogeneous distribution was required to bond them completely.

3.2. Density and mechanical properties of fibreboards

The mean density of geopolymer bonded fibreboards varied from 1038 to 1217 kg m⁻³ (Table 3). With the increasing fibre content, the density of the fibreboards tended to decrease. This behaviour might be attributed to the replacement of the geopolymer binder by the lignocellulosic fibres, which resulted in a slight thickness expansion of the fibreboards. Compared to commercial cement boards (typical density: 1300–1500 kg m⁻³), geopolymer fibreboards can be considered lightweight.

In terms of mechanical properties, seagrass fibreboards (GSF) achieved a higher MOE (up to 4039 MPa) than the corresponding wood fibreboards (GWF), which reached up to 2625 MPa.

Like density, MOE is highly dependent on the binder content in the fibreboard. In terms of the standard, GSF-30 satisfies the requirements of BS EN 634-2:2007 (>4000 MPa).

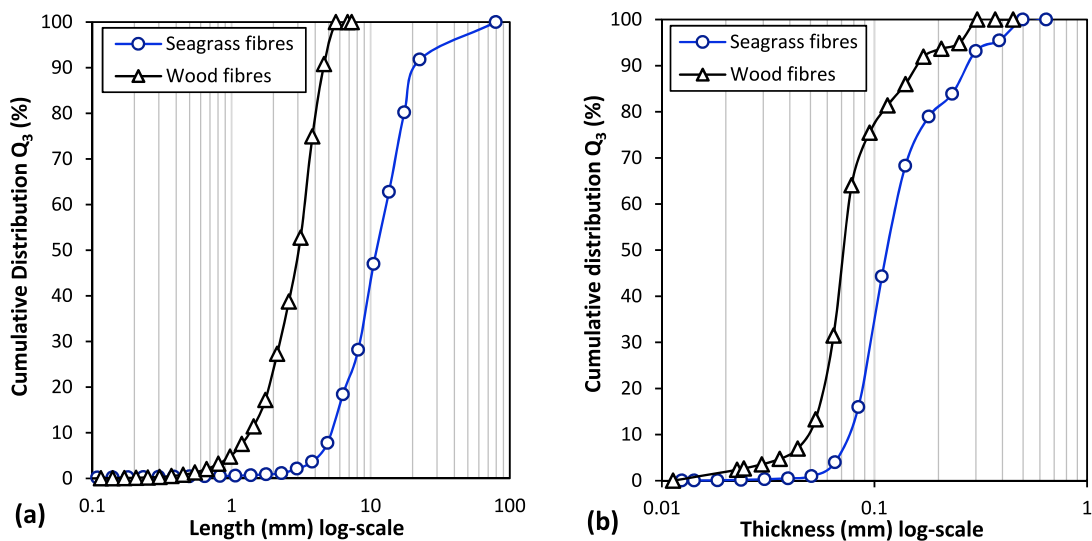


Fig. 2. Cumulative distribution of fibre length (a) and thickness (b) for seagrass and wood fibres.

Table 3

Bulk density and mechanical properties of geopolymer-based fibreboards. GWF: Geopolymer-bonded wood fibreboards. GSF: geopolymer-bonded seagrass fibreboards.

Type of board	Density (kg m ⁻³)	Modulus of elasticity (MPa)	Bending strength (MPa)	Interfacial bond strength (MPa)	Work to maximum load (N mm)	Screw pull-out strength (N)
GWF-30	1217 ± 34	2516 ± 356	5.22 ± 0.25	0.06 ± 0.03	597 ± 214	864 ± 107
GWF-40	1130 ± 26	2625 ± 117	7.59 ± 0.33	0.14 ± 0.10	1131 ± 149	1028 ± 133
GWF-50	1070 ± 24	1449 ± 85	5.31 ± 0.21	0.05 ± 0.02	1154 ± 160	1086 ± 78
GSF-30	1172 ± 47	4039 ± 529	8.96 ± 1.01	0.25 ± 0.08	917 ± 325	1421 ± 112
GSF-40	1152 ± 41	3273 ± 310	9.43 ± 0.86	0.14 ± 0.05	1313 ± 376	1293 ± 138
GSF-50	1038 ± 43	1948 ± 333	6.01 ± 1.02	0.04 ± 0.03	878 ± 252	1135 ± 133

Mean values ± standard deviations of 8 (2 sets × 4 samples) replicates for each type of fibreboard.

Regarding bending strength, a crucial property of boards intended for construction application, GSB performed significantly better than the corresponding GWF. Within one board type, the bending strength initially increased with the fibre content up to 40 wt% and decreased thereafter. This increase might be attributed to the ability of the fibres to distribute the applied stress across the board. Fibres have a high effective surface area to withstand the shear stress and can bridge the area where the bending moment is greatest. If the fibre content is increased further (50 wt%), the amount of binder is no longer sufficient to bind and transfer the applied stress, resulting in a deterioration of the strength. The bending strength of GSF-40 surpassed the BS EN 634-2:2007 standard value of 9 MPa, while the GSF-30 reached up to 8.96 MPa, which is close to the standard requirement.

The IBS of boards containing 30 wt% seagrass fibres was notably higher compared to those containing wood fibres. Unlike bending strength, IBS is highly dependent on the proportion of geopolymer and the compaction of fibres with each other. The stress applied perpendicular to the board during the IBS test is affected by the magnitude of disruptions of the fibres arranged parallel to the plane of the board. A higher binder content implies a higher probability of direct bonding through the bulk mineral matrix rather than the turquoise phase disrupted by the fibres.

The work to maximum load (W) represents the area below the strain-stress diagram and is an indicator of the toughness of the board. GSF required more energy to reach the Fmax compared to GWF, especially with lower fibre content. At a high fibre content (50 wt%), the lack of bonding sites results in effortless pull-out of seagrass fibres, reflected in low W and eventually low toughness. On the other hand, the W of GWF constantly increased with the increase in fibre content. The increase in

toughness of the boards can be associated with replacing the brittle binder with fibres. In this case, the fibres are still interlocked and have the ability to dissipate the applied stress.

The screw pull-out strength (SPS) of fibreboards with low seagrass content was up to 40% higher compared to the corresponding GWF. The more continuous solid mineral phase in the GSF compared to GWF might be responsible for high performance. The force required to withdraw the screw tended to decrease with the content of seagrass fibres. In the case of boards containing wood fibres, however, the SPS increased with increasing content of lignocellulosic material.

3.3. Water absorption resistance and thickness swelling

Geopolymer-bonded fibreboards containing seagrass displayed lower thickness swelling (TS) than those containing wood fibres after 24- and 72-h immersion in water (Table 4). The significantly lower TS-24 h of GSF compared to GWF might be associated with the adequate distribution of geopolymer binder in the board and its ability to cover and protect the seagrass fibres. The TS increased with the fibre content of the board. The addition of the relative content of porous organic material results in an increase in TS and water absorption (WA), deteriorating the dimensional stability of the boards. Some of the variants (GSF-30, GSF-40, and GWF-30) comply with the BS EN 634-2:2007 standard (TS<1.5%), indicating that they can be used in exterior applications. The WA of boards containing seagrass was slightly higher than that of wood fibres. The main reason for this difference might be the lower densities and, thus, the higher porosity of GSF compared to GWF. Regarding the water sorption (uptake) kinetics, the water saturation capability for both types of boards containing 30 and 40 wt%

Table 4

Thickness swelling (TS), water absorption (WA) of geopolymer-based fibreboards after 24 and 72 h of immersion in water.

Type of board	Density (kg m ⁻³)	TS-24 h (%)	TS-72 h (%)	WA-24 h (%)	WA-72 h (%)
GWF-30	1250	0.6 ± 0.3	0.9 ± 0.4	19.6 ± 0.7	18.6 ± 1.0
GWF-40	1126	2.7 ± 0.9	4.1 ± 1.3	23.9 ± 1.2	23.7 ± 1.1
GWF-50	1047	12.7 ± 3.3	21.0 ± 4.9	37.0 ± 5.2	44.7 ± 4.6
GSF-30	1202	0.4 ± 0.2	0.5 ± 0.3	23.1 ± 1.4	23.1 ± 1.4
GSF-40	1077	1.3 ± 1.0	2.5 ± 0.9	28.3 ± 1.3	28.8 ± 1.2
GSF-50	1010	10.5 ± 2.1	15.0 ± 2.7	39.7 ± 2.7	41.4 ± 0.8

Mean values ± standard deviations of 6 (2 sets × 3 samples) replicates for each type of fibreboard.

lignocellulosic fibres was attained much earlier compared to the fibreboards containing 50 wt% of fibres. The results are consistent with the previous literature [34]. When comparing GSF with GWF, no significant differences were noticed in terms of diffusion. In the first 4 h, the water uptake reached up to 98% of the saturation capability. Further analysis revealed that the diffusion mechanism is pseudo-Fickian. According to the literature, the main factors affecting the water absorption of wood material composites include the fibre volume fraction, orientation of fibres, exposed surface area, and temperature [35]. In addition to the large amount of the hydrophilic fibres, another possible cause of high water absorption is the conveyance of water molecules into voids and micro cracks present in the geopolymer matrix.

3.4. Cone calorimetry and fire resistance

Geopolymers are known to have very high thermal resistance [36]. Calorimetric measurements showed geopolymer-bonded fibreboards exhibited very low calorific values (Table 5). The mean heat release rate (HRR) of GWF was significantly higher (up to 30%) compared to GSB. Similar to HRR, the total heat release (THR) was considerably higher for fibreboards containing wood fibres. Both HRR and THR tended to increase with the increasing proportion of fibres. While two of the GWF ignited at approx. 1260 s, GSF boards did not ignite at all. Mass loss rate, along with other thermal properties, increased with the increase of the combustible lignocellulosic material. GSF containing seagrass were thermally degraded at a slower rate compared to the corresponding GWF based on wood fibres.

The difference between GSF and GWF in terms of their ability to withstand heat flux can be attributed to the degree of encapsulation with the geopolymer matrix and, eventually, the protection of fibres. Seagrass fibres having a larger size and smaller specific surface area than wood fibres required a lower amount of binder to be covered with the geopolymer matrix, resulting in more fire-resistant composites. The fibres were sealed and emitted less volatile combustible gases that could react with atmospheric oxygen delaying ignition. Another important reason

Table 5

Results of calorimetric measurements.

Type of board	Mean heat release rate (kW m ⁻²)	Total heat release (MJ m ⁻²)	Ignition time (s)	Mass loss rate (10 ⁻² g s ⁻¹)
GWF-30	30.4	43.4	1259	3.7
GWF-40	36.7	66.1	–	4.0
GWF-50	34	55.6	1262	4.4
GSF-30	21.5	38.7	–	3.4
GSF-40	26.6	48.2	–	3.4
GSF-50	26.6	46.1	–	3.5

for the good performance of GSF compared to GWF might be attributed to their different chemical composition. Previous reports have confirmed that seagrass fibres consist of a large amount of inorganic minerals (high ash content), implying high fire resistance [25].

3.5. FT-IR and XRD analysis

The FT-IR spectrum of metakaolin shows prominent characteristic bands (Fig. 3). Two of the bands at 1075 cm⁻¹ and 805 cm⁻¹ are assigned to T–O–Si bonds (T: Si or Al) [37]. The third band (450 cm⁻¹) might be related to Si–O–Si in-plane bending vibration [37,38]. For geopolymer composites, its main band was shifted from 1075 cm⁻¹ up to 989 cm⁻¹, whereas the band present at 805 cm⁻¹ for metakaolin had disappeared. According to previous studies, the extent (magnitude) of the band at 1075 cm⁻¹ indicates the occurrence of geopolymerization. The position of the T–O–Si asymmetric stretching vibration is affected by the bond angle and length in the silicate network. In other words, the higher the shift and the increase in peak area is, the higher the degree of cross-linking and the larger the aluminosilicate polymers formed [37,39,40]. The spectra show that the degree of shift depended on the proportion of fibres, as the displacement was significant for GSF-30 and GWF-30. However, at high fibre proportions, the peak only shifted to 1017 cm⁻¹ and 1022 cm⁻¹ for GSF-50 and GWF-50, respectively. The bands of the boards containing seagrass fibres (GSF) were further shifted towards lower wavenumbers compared to the corresponding boards with wood fibres (GWF). The degree of geopolymerization tended to decrease with the increase in the proportion of lignocellulosic material. Another band in the range of 1590–1625 cm⁻¹ can be assigned to the water bending vibration (O–H), while the slight peak at ~ 3400 cm⁻¹ is assigned to stretching and deformations of H–O–H [37,38].

In terms of crystallinity, both metakaolin and geopolymer composite samples (GWF-30 and GSF-30) appear predominantly amorphous (Fig. 4). The obtained X-Ray Diffraction (XRD) patterns of metakaolin reveal a broad hump between 16 and 28° 2θ, indicating the amorphous phase. Accordingly, the broad hump also appeared in the case of geopolymer composite samples at 2θ 18–31°. The slight displacement of the hump on the pattern of the latter samples indicates the formation of the amorphous geopolymer phase and the development of geopolymerization [41]. The shift or the slight increase of the amorphous phase has also been observed for other types of geopolymers which originated from the most commonly used precursors such as fly ash and slag [21,38].

The main crystalline phases identified in metakaolin are quartz (SiO₂) and anatase (TiO₂). The presence of anatase is confirmed by the chemical composition of metakaolin (TiO₂ = 1.7 wt%). Traces of these crystalline phases have also been obtained in previous research, where

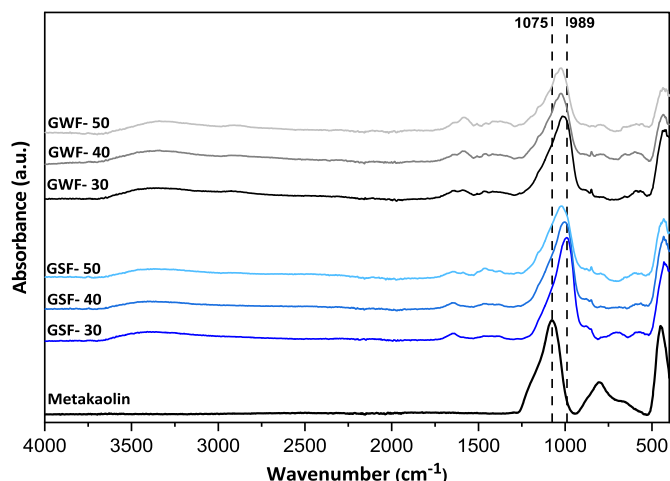


Fig. 3. FT-IR spectra of metakaolin and geopolymer-bonded composites.

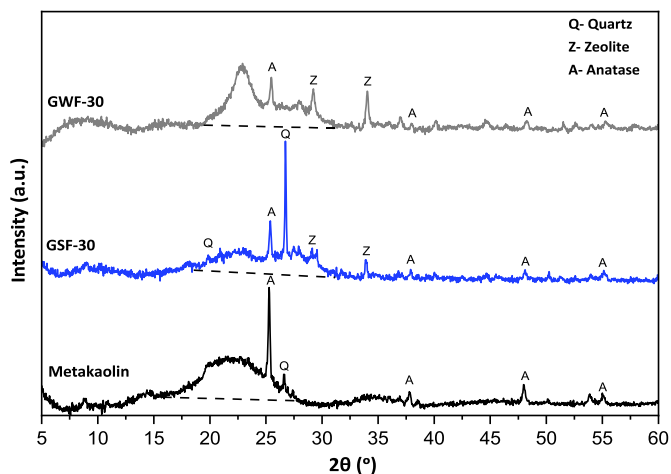


Fig. 4. XRD pattern of metakaolin and geopolymer-bonded composites.

the same type of metakaolin (MetaMax) was used [42,43]. In both geopolymer composite samples (GSF-30 and GWF-30), peaks indicated the formation of a new crystalline zeolitic phase, Zeolite A ($\text{Na}_9\text{Al}_9\text{Si}_9\text{O}_{384}\cdot 216\text{H}_2\text{O}$). The formation of this phase is enhanced in systems with thermal curing and containing higher amounts of alkali in the activator [42]. On the other hand, compared to the metakaolin sample pattern, some of the peaks detected in the geopolymer composites (quartz and anatase) tended to reduce their intensity, indicating

their participation in the geopolymerization.

A significant difference observed in the geopolymer composite samples was the intensity of the quartz phase (at $\sim 2\theta 27^\circ$) compared to the parent metakaolin precursor. The peak indicating quartz in the GWF-30 sample diffractogram disappeared completely, implying that it might have been involved in geopolymerization, which can lead to geopolymer gel formation [2]. In the case of GSF-30, however, the peak indicating the crystalline phase of quartz is much higher. The main cause for the increase of the quartz peak might be associated with the small amount of sea sand settled on the surface of seagrass fibres.

In previous works, the addition of sand as an aggregate to prepare geopolymer concrete has also led to the appearance of quartz peaks [44]. The crystalline phases (existing and neofomed) observed in geopolymer materials are mostly related to the mineral composition of the precursor. The crystalline phase of quartz is often observed in fly ash-based geopolymers, usually accompanied by other phases such as mullite and hematite [21,44]. In the case of metallurgical slag, apart from zeolitic structures, a common obtained phase is C-S-H (associated with the high CaO composition) [38].

3.6. Microstructural characterization and homogeneity of geopolymer-bonded fibreboards

The images obtained from the 3D reflected light microscopy reveal the compactness and the degree of encapsulation of the lignocellulosic fibres (Fig. 5 a, b). Significant differences can be seen between the two types of fibreboards. The brownish circular spots in the cross-section of

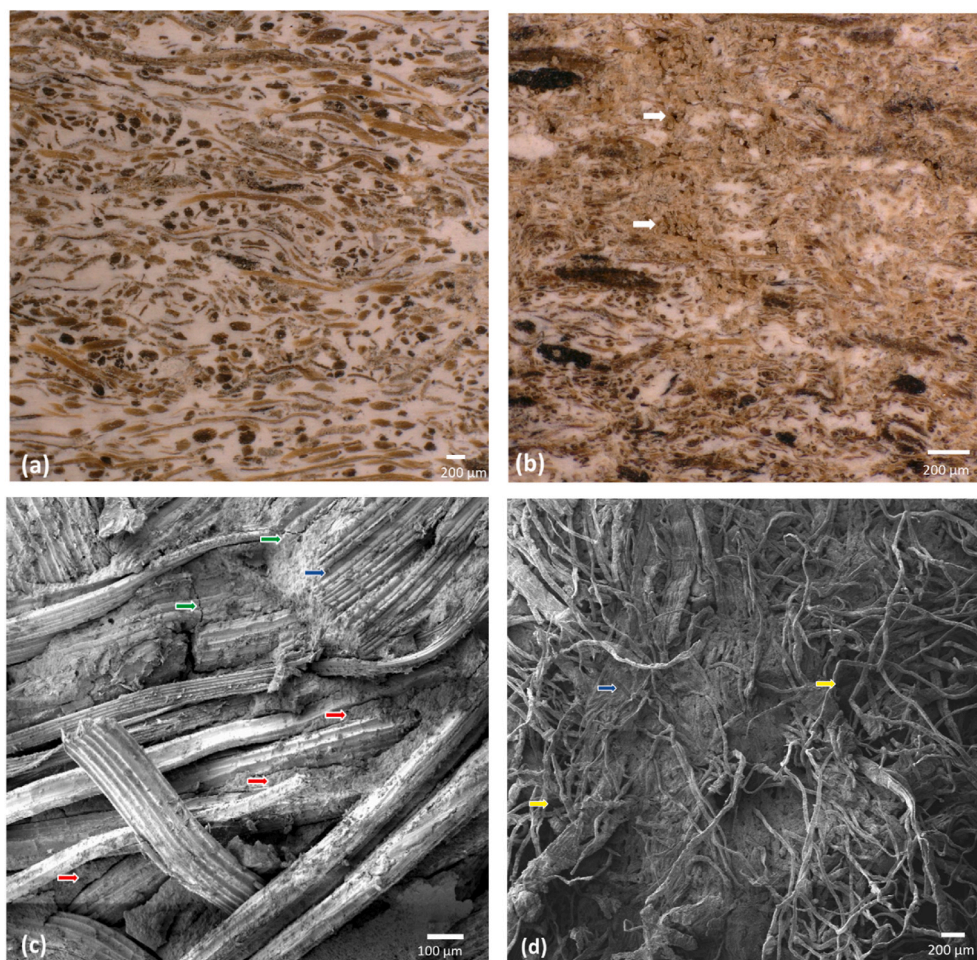


Fig. 5. Microscopy images of GSF-30 magnified $50\times$ (a) and GWF-40 magnified $100\times$ (b) conducted with a 3D-reflected digital microscope. Microscopy images of GSF-30 magnified $160\times$ (c) and GWF-40 magnified $63\times$ (d) conducted with scanning electron microscope (SEM).

GSF represent the seagrass fibres cut perpendicular to their longitudinal direction (Fig. 5, a). The elongated, curved shapes that appear along with the circular spots show the tangential cuts of the seagrass fibres. The presence of the elongated shapes indicates that the fibres are preferentially arranged during the hot-pressing.

Further examination of the images shows that the fibres are well covered by the geopolymer mineral, suggesting a high degree of coverage, compaction, and continuity of the mineral phase. The high degree of coverage can result in high durability and good mechanical properties, as the entire fibre surface area is bridged with the matrix and loads can be easily transferred and distributed. In contrast, the boards containing smaller wood fibres form geopolymer-binder agglomerates that are no longer bonded together (Fig. 5, b). The disruption of the geopolymer matrix (agglomeration) negatively affects the mechanical properties of the board (Table 3). In addition, a porous, non-bonded structure is observed in the GWF board (white arrows), indicating the lack of binder distribution during mixing.

Images obtained by means of SEM show the geopolymer binder distribution as well as the seagrass and wood fibres characteristics (Fig. 5 c, d). During the interfacial bond test, transversal stress is applied perpendicular to the plane of the specimen. As a result of the applied force, the mineral matrix breaks, while a portion of lignocellulosic fibres de-bond from it. The large seagrass fibres have a unique surface shape (channel-like form). The clear-cut channel-like marks (indicated by the blue arrow), which represent the delaminated areas, indicate an adequate contact between them and the matrix (Fig. 5 c). The presence of the thin layer, which covers the seagrass fibres in the GSF (red arrows), indicates that the binder is well distributed. The well-bonded fibre-matrix structure results in an effective transfer of stress. The appearance of tiny cracks (green arrows) in the matrix of the GSF is evidence that the stress is adequately distributed. In the case of GWF, the SEM image shows a typical matrix agglomerate surrounded by wood fibres (Fig. 5 d). A large number of pores and un-bonded fibres (yellow arrows) can also be seen. The absence of visible cracks on the surface of the fractured sample indicates that the geopolymer matrix is intact as the fibres are in contact with each other rather than with the matrix. The heterogeneous distribution of fibre agglomerates (or regions where their

proportion is much higher compared to their target proportion) results in the formation of ‘weak’ areas. During the application of mechanical stress, these areas are the first to fail rather than the geopolymer matrix. Delamination of wood fibres also seemed to have taken place in the case of GWF, as tiny marks are noticed in the mineral phase (blue arrow). However, the hardly distinct marks indicate a poor contact between the fibres and the mineral phase.

Micro-CT (X-ray micro-computed tomography) is a powerful tool that has been used for the non-destructive characterization of lignocellulosic and cementitious materials [45–47]. Using three dimensional reconstructions of the mineral phases (high density) sub-volumes from geopolymer-bonded boards, the morphological differences between GSF and GWF could be easily attained (Fig. 6 a, c). GSF have a seemingly continuous mineral phase and homogeneously distributed fibres, forming a network of reinforcing fibres (emerging as capillary tubes). On the other hand, the morphology of the internal GWF structure indicates the presence of geopolymer agglomerates appearing as spherical mineral clusters rather than a well-interconnected binding system (Fig. 6 c). The tomography images show the cut-sections of the prepared specimens in various directions (Fig. 6 b, d). The dissimilarities between the fibreboards can be easily identified. The bright grey colour corresponds to the mineral phases, while the dark grey/black colour is assigned to the lignocellulosic fibres and pores. The cross-section images of the GSF show the continuation of the inorganic matrix, while fibres are widely dispersed in it. A significant portion of seagrass fibres is completely incorporated within the geopolymer matrix. The black phases in GSF indicate the presence of voids and pores. The primary reason for the formation of voids in the fibreboards is the manual handling during the moulding process. After the fibre deagglomeration process, the mixture of fibres and geopolymer paste was carefully dispersed into the mould by hand. Unavoidably, fibres tend to agglomerate mainly due to the adhesive forces of geopolymer paste (mixture of alkaline activator and metakaolin), resulting in the fluctuation of material density. This issue, however, can be avoided in a continuous process, as the mixture can pass directly from de-agglomeration to hot-pressing. In GWF, dispersed agglomerates of geopolymer phases occur instead of a continuous mineral phase (Fig. 6 d). The white spots in the images (planes of sections xy ,

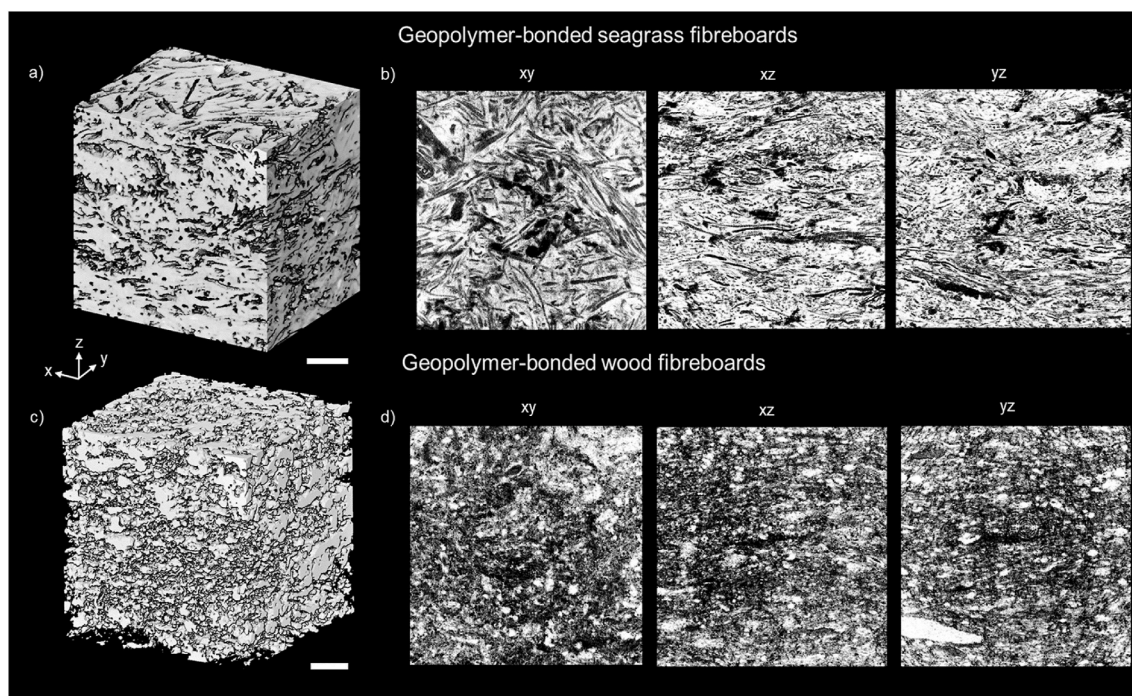


Fig. 6. X-ray tomography images of native geopolymer-bonded fibreboards. Three-dimensional illustration of binder distribution (a, c) The visualizations show the corresponding plane of sections (xy , xz , yz) of the internal board structure. Scale bars: 1 mm. Top: GSF (b) Bottom: GWF (d).

xz, yz) represent geopolymer, whereas the dark grey phase is assigned to wood fibres and the pores.

Here, the geopolymer was not properly distributed, leading thus to the formation of mineral agglomerates rather than bonding the fibres together. Due to the high specific surface area, wood fibres are not covered with the geopolymer phase, resulting in poor mechanical and physical properties.

3.7. The efficiency of the dry mixing-spraying process

Mixing a large volume (ranging from 47 to 82 L) of fibres with a small amount of binder is a challenging process. The homogeneous distribution of the binder onto the lignocellulosic mass played an essential role in obtaining compact and dimensionally stable fibreboards. An initial layer of alkaline activator wetted the surface of fibres after the first mixing-spraying step. This step was of great significance because it affected the distribution of metakaolin particles. During the intense mixing (deagglomeration), the fibres were untwisted and, at the same time, collided with each other to further wet and distribute the alkaline solution. When metakaolin powder was added, its microscopic particles attached to the wet surface of the fibres creating a secondary superficial layer (Fig. 7 a). During the final addition of the alkaline activator, the tiny droplets of alkaline solution adhered to the ‘dry’ metakaolin surface of the fibres. The third outer layer of the alkaline activator ensured that metakaolin was fully wetted and increased the adherence of the fibres to each other.

During hot-pressing, the fibres approached each other and the geopolymer paste (mixture of alkaline activator and metakaolin) was further mixed and ‘squeezed’, ensuring saturation of internal voids and pores. The heat of the hot press induced the geopolymerization reaction forming a solid binder that held fibres together. Due to the thin ‘microlayer’ formation, the amount of binder required to bind a specific amount of lignocellulosic material was minimal. This was the case for the relatively large seagrass fibres. When the very fine wood fibres were processed with this technique, however, they tended to agglomerate, covering the alkaline activator’s droplets (Fig. 7, b). The added metakaolin settled in the outer part of the wood agglomerates. After the second deagglomeration process, a major proportion of metakaolin

adhered to the “wet” wood fibres forming geopolymer matrix (agglomerates) areas, while a small portion of it was deposited on the “dry” non-sprayed (alkaline activator) areas (FT-IR results confirmed the presence of unreacted metakaolin, Fig. 3).

4. Conclusion

The dry mixing-spraying process followed by deagglomeration and hot-pressing is an effective method to produce geopolymer-bonded fibreboards. The uniform distribution of the geopolymer binder, forming a thin ‘microlayer’ that binds the aggregates, can increase the performance of fibreboards while reducing their cost, as only a small proportion of the adhesive is required for the mixing process. There are some limitations, however, as tiny fibres with a large specific surface area are not adequately mixed and binder agglomerates form instead. The seagrass fibres, which are larger than wood fibres, are successfully encapsulated with the geopolymer matrix forming a solid composite structure. GSF have significantly higher (up to 42%) bending strength compared to GWF. Likewise, the modulus of elasticity (MOE), interfacial bond strength (IBS) and screw pull-out strength (SPS) were considerably higher for the former. Adequate sealing of seagrass fibres leads to high water and fire resistance; on the other hand, the incompletely covered and unbonded wood fibres are more susceptible to heat flux and water ingress. As a result, none of the GSF ignites, while the total heat release (THR) is up to 37% lower compared to GWF. The thickness swelling (TS) of the former is up to two times lower compared to the latter.

This technique could be utilized for the mixing of lignocellulosic aggregates of various sizes and geometries. When mixing materials that are not prone to agglomeration (e.g. particles), the process can become much more straightforward as no deagglomeration step is required. In addition to wood by-products (wood wool, particles, strands), this method can be used to mix a wide variety of materials, including natural fibres and agro-industrial residues.

CRedit

Conceptualization: Aldi Kuqo, Carsten Mai.

Investigation: Aldi Kuqo, Tim Koddenberg.

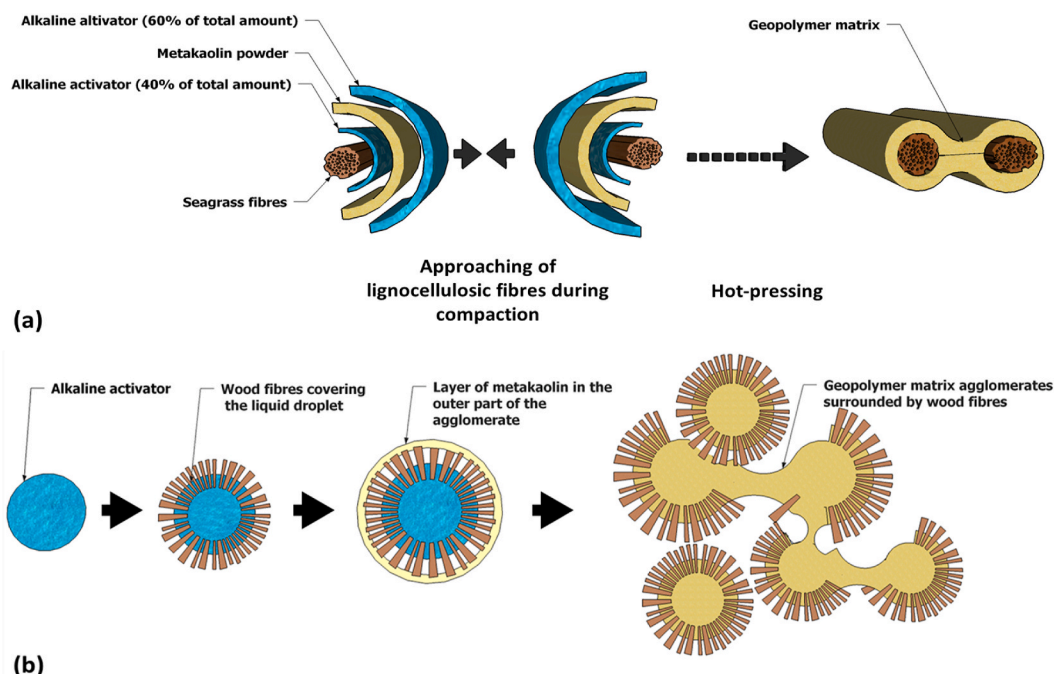


Fig. 7. Formation of the geopolymer matrix by a dry mixing-spraying process for seagrass fibres (a), and for wood fibres (b).

Supervision: Carsten Mai.

Visualization: Aldi Kuqo, Tim Koddenberg.

Writing-Original draft: Aldi Kuqo, Tim Koddenberg.

Writing - review & editing: Aldi Kuqo, Tim Koddenberg, Carsten Mai.

Declaration of competing interest

The authors declare that they have no known competing financial interests or personal relationships that could have appeared to influence the work reported in this paper

Data availability

Data will be made available on request.

Acknowledgments

This work was supported by DAAD (German Academic Exchange Service). Funding was provided through the funding programme: Research Grants - Doctoral Programmes in Germany, DAAD.

References

- [1] Olivier JG, Schure KM, Peters JAHW. Trends in global CO₂ and total greenhouse gas emissions, 5. PBL Netherlands Environmental Assessment Agency; 2017.
- [2] Provis JL, Van Deventer JSJ, editors. Geopolymers: structures, processing, properties and industrial applications. Elsevier; 2009.
- [3] Zhang P, Zheng Y, Wang K, Zhang J. A review on properties of fresh and hardened geopolymer mortar. *Compos B Eng* 2018;152:79–95.
- [4] Davidovits J. Geopolymers. Ceramic-like inorganic polymers. *J. Ceram. Sci. Technol* 2017;8(3):335–50.
- [5] Part WK, Ramli M, Cheah CB. An overview on the influence of various factors on the properties of geopolymer concrete derived from industrial by-products. *Construct Build Mater* 2015;77:370–95.
- [6] Ma CK, Awang AZ, Omar W. Structural and material performance of geopolymer concrete: a review. *Construct Build Mater* 2018;186:90–102.
- [7] Masi G, Rickard WDA, Bignozzi MC, van Riessen A. The effect of organic and inorganic fibres on the mechanical and thermal properties of aluminate activated geopolymers. *Compos B Eng* 2015;76:218–28.
- [8] Shalbafan A, Welling J, Hasch J. Effect of aluminosilicate powders on the applicability of innovative geopolymer binders for wood-based composites. *Eur. J. Wood Wood Prod.* 2017;75:893–902.
- [9] Guo L, et al. Sulfate resistance of hybrid fibre reinforced metakaolin geopolymer composites. *Compos B Eng* 2020;183:107689.
- [10] Alomayri T, Shaikh FUA, Low IM. Synthesis and mechanical properties of cotton fabric reinforced geopolymer composites. *Compos B Eng* 2014;60:36–42.
- [11] Lima PRL, Roque AB, Fontes CMA, Lima JMF, Barros JA. Potentialities of cement-based recycled materials reinforced with sisal fibers as a filler component of precast concrete slabs. In: Savastano HJ, Fiorelli J, Dos Santos SF, editors. Sustainable and nonconventional construction materials using inorganic bonded fiber composites duxford. Woodhead Publishing; 2017. p. 399–428.
- [12] Wafa FF. Properties & applications of fiber reinforced concrete. *Eng Sci* 1990:1.
- [13] Alyousef R, Alabduljabbar H, Mohammadhosseini H, Mohamed AM, Siddika A, Alrshoudi F, Alaskar A. Utilization of sheep wool as potential fibrous materials in the production of concrete composites. *J Build Eng* 2020;30:101216.
- [14] Akinyemi BA, Dai C. Development of banana fibers and wood bottom ash modified cement mortars. *Construct Build Mater* 2020;241:118041.
- [15] Mohammadhosseini H. Production of sustainable green concrete composites comprising industrial waste carpet fibres. In: Thomas S, Balakrishnan P, editors. Green composites Singapore. Springer; 2019. p. 25–52.
- [16] Farhan KZ, Johari MAM, Demirboğa R. Impact of fiber reinforcements on properties of geopolymer composites: a review. *J Build Eng* 2021;44:102628.
- [17] Khandelwal S, Rhee KY. Recent advances in basalt-fiber-reinforced composites: tailoring the fiber-matrix interface. *Compos B Eng* 2020;192:108011.
- [18] Zhu C, Su Y, Wang X, Sun H, Ouyang Q, Zhang D. Process optimization, microstructure characterization and thermal properties of mesophase pitch-based carbon fiber reinforced aluminum matrix composites fabricated by vacuum hot pressing. *Compos B Eng* 2021;215:108746.
- [19] Şahin HT, Kaya Aİ, ÖÜ Yalcin, Kılınçarslan Ş, Şimşek Y, Mantanis Gİ. A study on the production process and properties of cement-based wood composite materials. *Mehmet Akif Ersoy Üniversitesi Fen Bilimleri Enstitüsü Dergisi* 2019;10(2):219–28.
- [20] Abdel-Gawwad HA, Abo-El-Enein SA. A novel method to produce dry geopolymer cement powder. *HBRC j.* 2016;12(1):13–24.
- [21] Furtos G, Molnar L, Silaghi-Dumitrescu L, Pascuta P, Korniejenko K. Mechanical and thermal properties of wood fiber reinforced geopolymer composites. *J Nat Fibers* 2021:1–16.
- [22] Li M, et al. Recent advancements of plant-based natural fiber-reinforced composites and their applications. *Compos B Eng* 2020;200:108254.
- [23] Maciá A, Baeza FJ, Saval JM, Ivorra S. Mechanical properties of boards made in biocomposites reinforced with wood and *Posidonia oceanica* fibres. *Compos B Eng* 2016;104:1–8.
- [24] Kuqo A, Mai C. Mechanical properties of lightweight gypsum composites comprised of seagrass *Posidonia oceanica* and pine (*Pinus sylvestris*) wood fibres. *Construct Build Mater* 2021;282:122714.
- [25] Mayer AK, Kuqo A, Koddenberg T, Mai C. Seagrass-and wood-based cement boards: a comparative study in terms of physico-mechanical and structural properties. *Compos Appl Sci Manuf* 2022;156:106864.
- [26] Robles E, Czubak E, Kowaluk G, Labidi J. Lignocellulosic-based multilayer self-bonded composites with modified cellulose nanoparticles. *Compos B Eng* 2016;106:300–7.
- [27] BS EN 1097-3. Tests for mechanical and physical properties of aggregates Part 3: determination of loose bulk density and voids. 1998.
- [28] Görhan G, Kürklü G. The influence of the NaOH solution on the properties of the fly ash-based geopolymer mortar cured at different temperatures. *Compos B Eng* 2014;58:371–7.
- [29] BS EN 634-2. Cement-bonded particleboards - Specifications - Part 2: Requirements for OPC bonded particleboards for use in dry, humid and external conditions. 2007.
- [30] DIN EN 320. Particleboards and fibreboards - determination of resistance to axial withdrawal of screws. 2007.
- [31] DIN EN 317:1993, Particleboards and fibreboards; determination of swelling in thickness after immersion in water.
- [32] ISO 5660-1:2002-12, Reaction-to-fire tests - heat release, smoke reduction and mass loss rate - Part 1 - heat release rate (cone calorimeter method).
- [33] Ko FK, Yang H. Functional nanofiber: enabling material for the next generations smart textiles. *J Fiber Bioeng Inf* 2008;1(2):81–92.
- [34] Luthfi N, Wang X, Kito K. Effect of drying temperature on the physical properties of binderless fiberboard from bagasse: study of water absorption. *Sci Technol Aliment* 2021;26:30–8.
- [35] Klyosov AA. Wood-plastic composites. John Wiley & Sons; 2007.
- [36] Zhang P, Han X, Hu S, Wang J, Wang T. High-temperature behavior of polyvinyl alcohol fiber-reinforced metakaolin/fly ash-based geopolymer mortar. *Compos B Eng* 2022:110171.
- [37] Król M, Rożek P, Chlebda D, Mozgawa W. Influence of alkali metal cations/type of activator on the structure of alkali-activated fly ash-ATR-FTIR studies. *Spectrochim Acta Mol Biomol Spectrosc* 2018;198:33–7.
- [38] Cao R, Zhang S, Banthia N, Zhang Y, Zhang Z. Interpreting the early-age reaction process of alkali-activated slag by using combined embedded ultrasonic measurement, thermal analysis, XRD, FTIR and SEM. *Compos B Eng* 2020;186:107840.
- [39] Rasouli HR, Golestani-Fard F, Mirhabibi AR, Nasab GM, Mackenzie KJD, Shahraki MH. Fabrication and properties of microporous metakaolin-based geopolymer bodies with polylactic acid (PLA) fibres as pore generators. *Ceram Int* 2015;41(6):7872–80.
- [40] Bai C, Li H, Bernardo E, Colombo P. Waste-to-resource preparation of glass-containing foams from geopolymers. *Ceram Int* 2019;45(6):7196–202.
- [41] Du FP, et al. Microstructure and compressive properties of silicon carbide reinforced geopolymer. *Compos B Eng* 2016;105:93–100.
- [42] Longhi MA, Rodriguez ED, Walkley B, Zhang Z, Kirchheim AP. Metakaolin-based geopolymers: relation between formulation, physicochemical properties and fluorescence formation. *Compos B Eng* 2020;182:107671.
- [43] Moro D, et al. Thermal, X-ray diffraction and oedometric analyses of silt-waste/NaOH-activated metakaolin geopolymer composite. *J. Compos. Sci.* 2021;5(10):269.
- [44] Korniejenko K, Kejzlar P, Louda P. The influence of the material structure on the mechanical properties of geopolymer composites reinforced with short fibers obtained with additive technologies. *Int J Mol Sci* 2022;23(4):2023.
- [45] Koddenberg T, Militz H. Morphological imaging and quantification of axial xylem tissue in *Fraxinus excelsior* L. through X-ray micro-computed tomography. *Micron* 2018;111:28–35.
- [46] Chen YX, Klima KM, Brouwers HJH, Yu Q. Effect of silica aerogel on thermal insulation and acoustic absorption of geopolymer foam composites: the role of aerogel particle size. *Compos B Eng* 2022;242:110048.
- [47] Chung SY, Kim JS, Stephan D, Han TS. Overview of the use of micro-computed tomography (micro-CT) to investigate the relation between the material characteristics and properties of cement-based materials. *Construct Build Mater* 2019;229:116843.

Article 4

Enhancement of physico-mechanical properties of geopolymer particleboards through the use of seagrass fibers – Article 4

Aldi Kuqo^a, Aaron Kilian Mayer^a, Stephen O. Amiandamhen^b, Stergios Adamopoulos^c, Carsten Mai^a

*Corresponding author, email: cmai@gwdg.de

^a Department of Wood Biology and Wood Products, Faculty of Forest Sciences and Forest Ecology, University of Goettingen, Büsgenweg 4, 37077 Göttingen, Germany

^b Department of Forestry and Wood Technology, Linnaeus University, Lückligs Plats 1, 351 95 Växjö, Sweden

^c Department of Forest Biomaterials and Technology, Swedish University of Agricultural Sciences, Box 7008, 750 07 Uppsala, Sweden

Authorship (according to Clement, 2014)

	Conceptualization (30%)	Practical work (30%)	Writing/Editing (30%)	Administration (10%)	Contribution
A. Kuqo	50%	60%	50%	0%	48%
A. K. Mayer	10%	20%	10%	0%	12%
S.O. Amiandamhen	0%	10%	10%	0%	6%
S. Adamopoulos	0%	10%	0%	0%	3%
C. Mai	40%	0%	30%	100%	31%

Ideas: Design of the investigation / Experimental planning / Interpretation of the data

Work: Execution of the experiment / Data collection and analysis

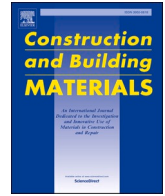
Writing: Drafting the article / Critical, substantive revision / Reviewing the final version

Administration: Resource management and ensuring scientific integrity before, during, and after publication

Published in Construction and Building Materials, 374, 130889.

Published in February 2023

DOI: <https://doi.org/10.1016/j.conbuildmat.2023.130889>



Enhancement of physico-mechanical properties of geopolymer particleboards through the use of seagrass fibers

Aldi Kuqo^a, Aaron Kilian Mayer^a, Stephen O. Amiamdamhen^b, Stergios Adamopoulos^c, Carsten Mai^{a,*}

^a Department of Wood Biology and Wood Products, Faculty of Forest Sciences and Forest Ecology, University of Goettingen, Büsingenweg 4, 37077 Göttingen, Germany

^b Department of Forestry and Wood Technology, Linnaeus University, Lückligs Plats 1, 351 95 Växjö, Sweden

^c Department of Forest Biomaterials and Technology, Swedish University of Agricultural Sciences, Box 7008, 750 07 Uppsala, Sweden

ARTICLE INFO

Keywords:

Geopolymer particleboards
Mechanical properties
Posidonia oceanica fibers
Sandwich boards
Seagrass

ABSTRACT

Two types of geopolymer-bonded boards were produced using initial wetting of lignocellulosic aggregates followed by dry mixing and hot-pressing. Boards were prepared by incorporating large fractions of lignocellulosic material (up to 50 wt%). Geopolymer particleboards (GP) were produced using wood particles whereas geopolymer sandwich boards (GSB) were produced from wood particles and seagrass fibers, with the latter allocated in the outer layers. Inclusion of seagrass fibers was found to enhance bending strength and toughness of GSB by up to 20 and 40 % respectively. The bending strength tended to increase with the addition of lignocellulosic aggregates, reaching up to 8.9 N mm⁻². Fire resistance of GSB was slightly higher compared to GP. Further investigations such as FT-IR, XRD analysis and visual examination by digital microscopy showed an adequate degree of geopolymerization and mixing of the precursor and alkaline activator, indicating the high effectiveness of the mixing technique.

1. Introduction

The production of ordinary Portland cement releases about 0.8 tons of CO₂ for every ton of clinker produced, making it one of the major contributors of CO₂ emissions, which can account for up to 8 % of the total CO₂ emissions worldwide [1–2]. On the other hand, other inorganic binders such as geopolymer can be seen as a more viable and sustainable solution to the highly energy-intensive conventional Portland cement. Applications of geopolymers (alkali-activated cements) involve concrete for structural performance, coatings, binders for high fire resistance of composites, and even toxic waste encapsulation materials [3,4]. In recent decades, geopolymer composites have been widely studied to find new, environmentally friendly perspectives for replacing unsustainable Portland cement. In particular, it has previously been reported that the final construction products made from geopolymer such as prefabricated facade panels are generally more environmentally friendly than other technically competitive (i.e. cement) products [5].

The use of prefabricated construction materials is a growing trend in the building sector, not only because of time and cost efficiency but also

because of their ease of construction and their ability to be cast at large scale, enabling extensive facade covering with fewer joints and allowing for larger vertical spaces between supports than most facade systems [6]. Prefabricated panels such as cement-bonded composites containing wood aggregates present several benefits compared to conventional wood products. Fire, termite, and water resistance are the major advantages implying their use for interior and exterior purposes [7]. In addition, cement-bonded boards display a relatively lower density compared to reinforced concrete, inferring low transport costs and easy handling [8]. In spite of the numerous benefits of cement particleboards, their relatively low bending strength has limited their possible applications.

Structural sandwich boards, mainly used as insulation materials, have been heavily exploited as they can improve the energy efficiency of the building while, at the same time, having the necessary structural capacity [9]. This type of structural solution has been widely applied in precast structural panels, where the outer layer also provides protection against mechanical damage, weather sheltering, and acts as a vapor barrier [6]. Reinforcement of the outer layer, where the tensile stress during bending between aggregates is high and the possibility of

* Corresponding author.

E-mail address: cmai@gwdg.de (C. Mai).

<https://doi.org/10.1016/j.conbuildmat.2023.130889>

Received 28 February 2022; Received in revised form 14 December 2022; Accepted 27 February 2023

Available online 8 March 2023

0950-0618/© 2023 Elsevier Ltd. All rights reserved.

fracture formation exists, could be an effective approach to improve mechanical performance. The mechanism of debonding of wood-cement particleboards is mainly related to the failure of the interfacial bond between the wood phase and the spiky cement crystals. On the other hand, replacement of wood particles (low aspect ratio) with thinner and longer lignocellulosic aggregates, such as fibers, can lead to a high friction pull-out process, which requires more energy to create a fracture and break. In this way, a stronger and stiffer board can be produced [7,10].

Natural fibers have gained substantial attention because their inclusion can enhance toughness and, in many cases, the bending strength of composite materials. In addition, no energy-intensive process is required to refine them, as they are available in fibrous form [11]. Fibers derived from *Posidonia oceanica* seagrasses can be easily found in coastal areas of the Mediterranean Sea. *Posidonia oceanica* fibers are agglomerated and interconnected to form spherical clusters called seagrass balls but also referred to as aegagropila. Seagrass balls are formed by the detachment of small fibers in seagrasses' rhizomes and the decomposition of their leaves in combination with the intense entanglement process generated by the dynamic movement of the waves. It has already been reported that the addition of small amounts of seagrass fibers can enhance the mechanical properties of cement composites while reducing their density, resulting in lightweight construction products [12–14]. Previously, seagrass fibers have been found to be more compatible with Portland cement and to have higher fire resistance than wood by-products (particles) [15,16]. Much research has been undertaken on geopolymer-bonded composites with incorporated natural aggregates, or wood by-products [4,17,18]. However, most researchers have focused on the production of reinforced concrete blocks containing relatively small proportions of aggregates prepared by molding, while the cylinder compression test and beam test have been the most frequently adopted assessing methods [19]. Geopolymers-wood composites are regarded as a promising material for construction [20–22]. Geopolymer as a binder in wood composite manufacturing would be a potentially important class of formaldehyde-free wood composites [22]. However, previous reports have shown that an extensive addition of wood aggregates can worsen the mechanical properties of the composites. It has been recommended that an addition of 5 to 20 wt% could, in some cases, increase the flexural or compression strength of composites [20,21,23,24]. On the other hand, the addition of a large amount of wood aggregates can have a beneficial impact on the resulting material as it can improve the insulation properties and make it lightweight [20]. In other cases, geopolymer-bonded boards containing relatively high proportion of lignocellulosic aggregates (5–50 %) have shown promising results [25–28]. Yet, although the mechanical strength is fairly high in some cases, the strength to proportion of lignocellulosic aggregates is still low.

A higher proportion of lignocellulosic aggregates in the prefabricated boards would result in a more cost-effective and environmentally friendly (high carbon storage capacity) material, as a lower amount of binder is required. The objective of this study was to produce geopolymer reinforced composite boards containing up to 50 wt% lignocellulosic aggregates while maintaining high mechanical strength. The metakaolin-based geopolymer-bonded boards were produced using the non-conventional technique of wetting lignocellulosic aggregates followed by dry mixing and hot pressing. In contrast to the previous reported techniques [20,21,23,24,29], in which metakaolin is first mixed with aggregates and in the second step alkaline activator is added, in this work a specific amount of alkaline activator is added to wet particles in the first step, while metakaolin is added thereafter. Geopolymer particleboards (GP) consisting of wood particles and seagrass-reinforced geopolymer sandwich boards (GSB) containing wood particles (middle layer) and seagrass fibers (seagrass substituted an equal mass of wood particles, 12.5 % wt/wt on each outer layer) were compared in terms of their mechanical and physical properties. In addition, the boards were visually examined with a digital 3D light microscope to examine the

adequacy of the mixing process, and with other techniques such as XRD and FT-IR to investigate the degree of geopolymerization and the formed minerals.

2. Experimental

2.1. Materials

The wood particles (a mixture of fresh cut and recycled wood particles) were provided by the Swiss Krono Group AG (Luzern, Switzerland). Their moisture content was 8.1 %. *Posidonia oceanica* fibers were collected in the seashore of Durrës (Albania, Mediterranean Sea) in September 2020. In their original form, the fibers are twisted into spherical clusters forming balls. To separate the fibers, the seagrass balls were initially processed in a suction machine (Holzkraft ASA 163, Stürmer Maschinen GmbH, Hallstadt, Germany). The rotor blade of the suction machine has a minimal effect on the morphology and length of seagrass fibers. The moisture content of seagrass fibers was 13.9 %.

The commercial metakaolin MetaMax (BASF, Ludwigshafen, Germany) was utilized as a precursor for the production of geopolymer boards. In terms of the particle size of metakaolin powder, more than 68 % of particles have a size smaller than 2 µm. As regards chemical composition, metakaolin is constituted of 52.3 % SiO₂, 45.2 % Al₂O₃, 1.7 % TiO₂, 0.4 % Fe₂O₃, traces of Na₂O and K₂O and LOI of 0.8 % (supplier specifications). Sodium silicate (Na₂SiO₃, extra pure 38/40 °Bé) provided by Carl Roth GmbH + Co. KG (Karlsruhe, Germany) and sodium hydroxide (NaOH, technical grade 98 %, AppliChem GmbH, Darmstadt, Germany) were used for the preparation of the alkaline activator. The chemical composition of sodium silicate (Na₂SiO₃) solution, also referred to as water glass, was 7.80–8.50 % Na₂O, 25.80–28.50 % SiO₂, and ~ 64 % H₂O. The commercial cement boards (Amroc Panel B1), purchased by Amroc Baustoffe GmbH (Magdeburg, Germany), were used as reference boards.

2.2. Morphological characterization of particles and fibers

The length and thickness density distribution weighted by surface area (q₂), as well as the aspect ratio of the lignocellulosic aggregates, were measured using FibreShape PRO (X-shape, IST, Vilters, Switzerland). Representative samples of wood particles (3.50 g) and seagrass fibers (0.25 g) were manually dispersed on a transparent film of A4 size. Fibers and particles were scattered in such a way that they do not overlap with each other. High-resolution images were created using a flatbed scanner (Epson Perfection V850 Pro, Epson, Tokyo, Japan) in transmitted light mode. The scans were then loaded to the FiberShape software and fiber dimensions were assessed by static image analysis.

2.3. Production of geopolymer boards

The production of geopolymer boards consisted of mixing raw materials, hot-pressing and curing at elevated temperatures. The alkaline activator was initially prepared by dissolving sodium hydroxide pellets in water (exothermic process). After the alkaline solution had cooled down to room temperature, it was mixed with the sodium silicate solution at a specific ratio (Table 1).

Table 1
Geopolymer binder mix design.

Parameter	Value
Alkaline activator to precursor ratio	1.6
Na ₂ SiO ₃ /NaOH ratio (dry)	2.15
SiO ₂ /Na ₂ O ratio of geopolymer binder	3.97
Water/binder ratio	0.4
Si/Al ratio	3.27
Na/Al ratio	0.65

The solution was then left to stand for 24 h and was thoroughly stirred before being used for the subsequent mixing procedure. A 40-l vertical concrete mixer (Soroto action mixer 40 L, Soroto, Herstedorster, Denmark) was used for mixing. During the continuous mixing of the lignocellulosic aggregates, all the undermentioned operations took place.

For the production of the geopolymer-bonded wood particleboard (GP), a specified amount of wood particles was first sprayed with 40 % of the total alkaline activator using a spraying nozzle so that they were completely covered with the liquid (Table 2).

Subsequently, the metakaolin powder was gradually dispersed on the wood particles with the help of a sieve. The fine grains of metakaolin powder adhered to the moist surface of the particles. The mixture was blended until the entire surface of the particles was covered with mineral powder. In the last step, the additional amount of alkaline activator (60 %) was sprayed on, wetting the outer “dry” layer of metakaolin. After the mixing process, which lasted from 15 to 20 min, the mixture of geopolymer binder and lignocellulosic aggregates were placed on a metal plate and pre-pressed in order to obtain the desired shape. A tetragonal metallic frame with a thickness of 16 mm was attached to the metal plate, and the mixture was pressed until the target thickness was reached (upper pressing plate attached to the metallic frame). A hydraulic press (Joos HP-2000 lab, Gottfried Joos GmbH & Co.KG, Pfalzgrafenweiler, Germany) was employed for the hot-pressing. The mixture was pressed at 70 °C for 6 h. The solid boards have a compact structure and a pale cream to brownish color (Fig. 1).

To produce the geopolymer sandwich boards reinforced with seagrass fibers (GSB), the lignocellulosic aggregates (seagrass fibers and wood particles), metakaolin, and alkaline activator were mixed following the same procedure as the one described above. Then, a specific amount of fibers was added in the top and bottom layer (12.5 % wt/wt each side, as indicated by white arrow) replacing wood particles (Fig. 1 b). In total, 12 boards (2 boards per variant) containing 30, 40, and 50 wt% lignocellulosic aggregates were produced. The dimensions of each board were 450 × 450 × 16 mm³, while their target density was 1150 kg m⁻³. The prepared boards were then oven-cured at 50 °C for 72 h. After thermal curing, the boards were left to cure for another 25 days under standard conditions (23 °C, 65 % RH). After cutting to the specified dimensions, their mechanical and physical properties were determined. The produced geopolymer-based boards were compared with commercial cement boards in terms of mechanical and physical properties. The latter were designated as REF.

2.4. Density and mechanical characterization

Mechanical properties such as bending strength otherwise known as modulus of rupture (MOR), modulus of elasticity (MOE), internal bond strength (IB), and various physical properties were determined after standardized procedures. The majority of the undermentioned standard methods are included in the standard EN 634-2:2007 for the determination of physical-mechanical properties of cement-bonded particleboards [30].

The bulk density of the geopolymer bonded boards was determined

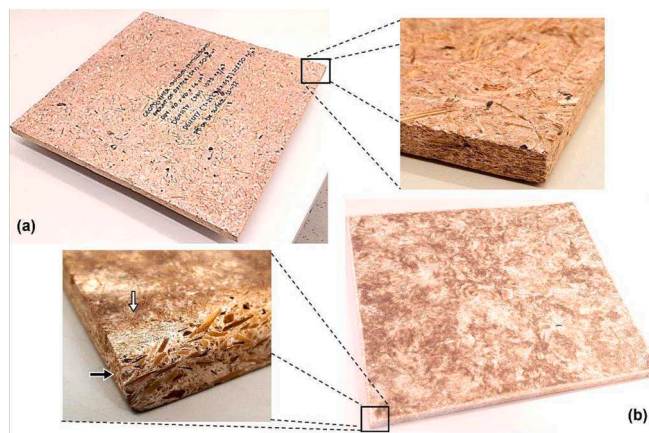


Fig. 1. GP containing 50 wt% wood particles (a) and GSB containing 30 wt% wood particles (indicated by black arrow) and seagrass fibers (indicated by white arrow) in the outer layers (b).

following the standard DIN EN 323:1993 [31]. Initially, the exact dimensions and weight of the specimens (4 specimens per board, 8 specimens per variant) with nominal dimensions of 50 × 50 × 16 mm³ were assessed to determine the density of the board. The samples were then used to test the internal bond strength (IB), water absorption (WA), and thickness swelling (TS). Modulus of rupture (MOR), modulus of elasticity (MOE) and work to maximum force (W), were determined in accordance with the standard DIN EN 310:1993 [32]. The three-point bending test was conducted using a universal testing machine (Zwick-Roell Zmartpro, ZwickRoell, Ulm, Germany) with a 10 kN load cell, an applied crosshead speed of 6 mm min⁻¹, and a support span of 320 mm. The specimens had nominal dimensions of 370 × 50 × 16 mm³.

Internal bond strength (IB) was tested according to DIN EN 319:1993 [33]. Tetragonal samples measuring 50 × 50 × 16 mm³ were bonded to metallic braces using a fast-curing polymer adhesive. Afterwards, they were clamped in the testing machine ZwickRoell Zmartpro (ZwickRoell, Ulm, Germany) and a tensile stress perpendicular to the plane of the board was applied at a continuous crosshead speed of 7 mm min⁻¹ until failure.

As an indicator of the toughness of the prepared boards, work to F_{max} (W) and impact resistance (IR) were evaluated in accordance with the EN 310:1993 and DIN EN ISO 179-2:2012, respectively. While W was computed along with the MOR, the impact resistance (Charpy unnotched impact strength) was determined using a swinging pendulum impact tester (Resil Impact, CEAST, Martinsried, Germany) following a slight variation of the procedure described in DIN EN ISO 179-2:2012 [34]. For this test, a 2-J-hammer was utilized and the support span for the bending test was 60 mm. The specimen dimensions were 10 × 15 × 100 mm³.

The screw withdrawal resistance was tested according to EN 320:2011-07 [35] using the universal testing machine ZwickRoell Zmartpro (ZwickRoell, Ulm, Germany). Tetragonal specimens

Table 2

Formulations of mixtures for the production of geopolymer boards. GP: geopolymer-bonded particleboard, GSB: geopolymer-bonded seagrass sandwich board.

Type of board	Proportion of lignocellulosic aggregates (wt%)	Amount of wood particles -dry (g)	Amount of seagrass fibers-dry (g)	Amount of metakaolin (g)	Amount of alkaline activator		
					Na ₂ SiO ₃ -dry (g)	NaOH-dry (g)	Total H ₂ O (g)
GP	30	1167	–	1744	667	310	1813
	40	1560	–	1495	572	266	1554
	50	1945	–	1246	477	221	1295
GSB	30	878	293	1744	667	310	1813
	40	1167	389	1495	572	266	1554
	50	1458	486	1246	477	221	1295

measuring $75 \times 75 \times 16 \text{ mm}^3$ were drilled and then screwed in the center of the face (surface) and in the side (edge). The axial force perpendicular to the surface and the edge of geopolymer boards was determined. The displacement rate for screw withdrawal was 10 mm min^{-1} .

The statistical differences between the mean values obtained from the mechanical and physical characterization (all mechanical and physical tests) were assessed by ANOVA and Tukey's (HSD) using a p-value of under 0.05 as the threshold of statistical significance.

2.5. Determination of thickness swelling and water absorption

Thickness swelling (TS) and water absorption (WA) were conducted following DIN EN 317:1993 [36]. The specimens were completely submerged in water ($20 \text{ }^\circ\text{C}$). After 24 and 72 h, they were removed and drained for a few minutes to remove excess water. Afterwards, their thickness and weight were measured. The percentage increase in thickness and weight after submersion was measured as TS and WA, respectively. The statistical differences between the mean values were assessed by ANOVA and Tukey's (HSD) using a p-value of under 0.05 as the threshold of statistical significance.

2.6. Cone calorimetry test

The heat release rate (HRR), the total heat release (THR) and the time to ignition were evaluated using a mass loss calorimeter (MLC FTT, Fire Testing Technology, East Grinstead, UK) following ISO 5660-1:2002-12 [37]. Tetragonal specimens ($100 \times 100 \text{ mm}^2$) with a given thickness were exposed to heat flux of 50 kW m^{-2} for 30 min.

2.7. Characterization of geopolymerization degree by FT-IR and XRD

Specimens were selected from the original boards and cut to smaller dimensions using a circular saw. Then they were ground using a cutting mill (Retsch SM 2000, Retsch GmbH, Haan, Germany) until a coarse powder was formed. In order to obtain the fine powder samples, a Herzog HSM mill (HERZOG Maschinenfabrik GmbH & Co. KG, Osnabrück, Germany) was employed. Fourier transform infrared spectroscopy (FT-IR) was performed using an ALPHA II device (Bruker, Bremen, Germany) with attenuated total reflectance (ATR) technique in a frequency range of $4000\text{--}400 \text{ cm}^{-1}$ to assess the mineral part of the geopolymer-bonded composites and to identify the bonds exhibited by metakaolin and the ground composites. An X-ray diffraction (XRD) diffractometer (PANalytical Empyrean, Almelo, The Netherlands) equipped with a Cu LFF HR X-ray tube, programmable anti-scatter slit, and a PIXcel3D detector was employed to determine the phase of the samples (metakaolin and geopolymer-bonded composites). The scanning degrees, i.e. 2θ range, was 5 to 60° with a scanning speed of $1^\circ/\text{min}$ at 45 kV and 40 mA .

2.8. Microstructural characterization of the boards and the mixing efficiency

For the structure analysis (arrangement of particles and fibers in the board), cut samples were cleaned with compressed air to remove dust on their surface. The samples were scanned using the digital 3D-reflected light microscope VHX-5000 (Keyence, Neu-Isenburg, Germany). With this microscope, images with a high depth-of-field were obtained by combining different in-focus images. The captured images were taken with $50\times$ magnification (images showing wood cells (Fig. 7 e) were magnified $1500\times$). In order to investigate the mixing degree of alkaline activator and metakaolin, an additional colored geopolymer-bonded particleboard (GP) was produced. In this case, the alkaline activator was colored by adding a red mineral pigment (Bayferrox Rot 130 M, Harold Scholz, and Co. GmbH, Recklinghausen, Germany). The bright, red-colored alkaline activator was mixed with the lignocellulosic

aggregates and white-colored metakaolin following the same procedure as the one described above (Section 2.3).

3. Results and discussion

3.1. Fiber length distribution

The results of the imaging technique FiberShape revealed major size differences between seagrass fibers and wood particles (Fig. 2). In terms of geodesic length, wood particles were larger, reaching a maximum length up to 42.7 mm , while seagrass fibers could be up to 33.6 mm long. A wide distribution of the wood particles was expected as these were composed of a mixture of fine (30 \% wt/wt) and coarse (70 \% wt/wt) aggregates. On the other hand, a large amount of seagrass fines with less than 0.1 mm in length generated by the unraveling process was also noticed (Fig. 2 a). In line with these results, previous studies have also reported a similar geodesic length for seagrass fibers [16]. Although the distribution of the geodesic length for both aggregates is comparable, an obvious difference is observed in the thickness range (Fig. 2 b). Seagrass fibers are clearly thinner than the wood particles, with a mean thickness of 0.13 mm , whereas the latter ones can be 0.70 mm thick on average (Table 3).

The aspect ratio (ratio of the minimum to the maximum Feret diameter according to ISO 9276-2:2014 [38]) of the lignocellulosic aggregates also revealed further morphological details. It was higher for wood particles compared to seagrass fibers; however, their difference was relatively low. The high aspect ratio (in contrast with the traditional definition of length to thickness ratio) of seagrass fibers was considerably high, even though they have a long and thin structure. This implies that the minimum Feret diameter was also high. As the minimum Feret diameter is specified as the minimal distance between the two parallel planes bounding the object perpendicular to that direction, it can be stated that seagrass fibers possess a curved shape, and their straightness may be disproportionate to the aspect ratio.

3.2. Density and mechanical properties of geopolymer boards

The densities of the prepared GP and GSB boards varied from 1120 to 1190 kg m^{-3} (Fig. 3) and did not deviate more than 4 \% from the target density. Compared to commercial Portland cement particleboard (REF) (1410 kg m^{-3}), the density of GP and GSB is about 20 \% lower due to the higher content of lignocellulosic materials in the board.

The MOR of the GP and GSB (cured for 28 days) varied from 5.9 to 8.9 N mm^{-2} (Fig. 4 a). MOR increased with the increasing lignocellulosic aggregate content. Boards containing 50 wt\% lignocellulose had the highest MOR, while boards with a content of up to 30 wt\% were the weakest. The increase of MOR among boards with different aggregate proportions can be attributed to the ability of wood particles and seagrass fibers to distribute the stress applied during bending. As the proportion of lignocellulosic aggregates increases, the regions of stress concentration around adjacent aggregates become more diffuse, resulting in an increased resistance to the stresses applied. Larger quantities of aggregates distribute internal stresses over a larger specific surface per unit volume, reducing areas of high stress concentration where critical failure is more likely to occur. Boards containing a high proportion of geopolymer matrix are brittle and prone to fracture. Because of the presence of irregularities (small voids and pores) in the outer face of the board (where the tensile stress is high), microcracks can form and begin to propagate shaping a large crack which grows along the depth of the board resulting in failure. In contrast, wood particles and especially seagrass fibers can transmit localized forces to regions with lower stress, leading to multiple cracking.

In terms of the MOR between boards with the same proportion of aggregates, the addition of seagrass fibers in the outer layer of the GP boards seemed to significantly improve their performance (ANOVA, $p \leq 0.05$). GSB exhibited on average $15\text{--}20 \text{ \%}$ higher strength than GP. The

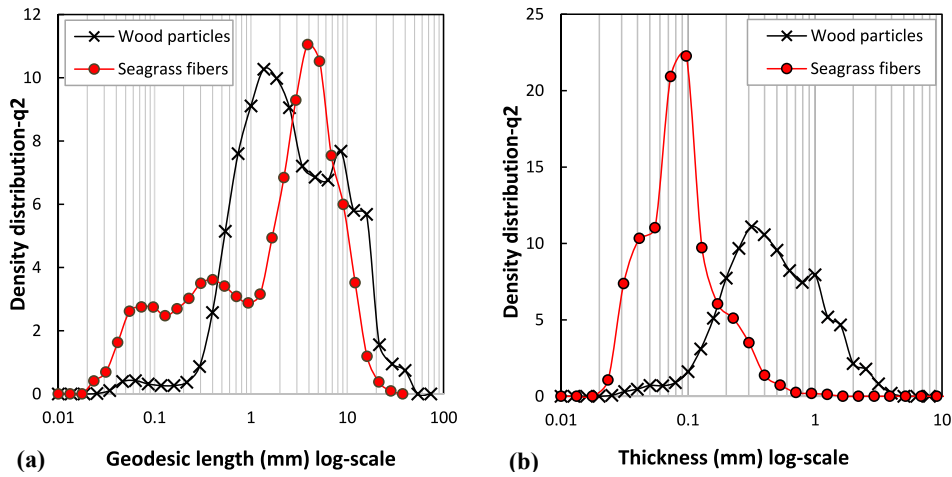


Fig. 2. Geodesic length (a) and thickness (b) size distribution of seagrass fibers and wood particles.

Table 3

Size characteristics of seagrass fibers and wood particles.

Parameters	Seagrass fibers	Wood particles
Counted objects	154,425	111,250
Mean geodesic length (mm)	3.22	5.63
Maximal geodesic length (mm)	33.55	42.67
Mean thickness (mm)	0.13	0.70
Maximal thickness (mm)	1.50	3.99
Aspect ratio	0.29	0.37

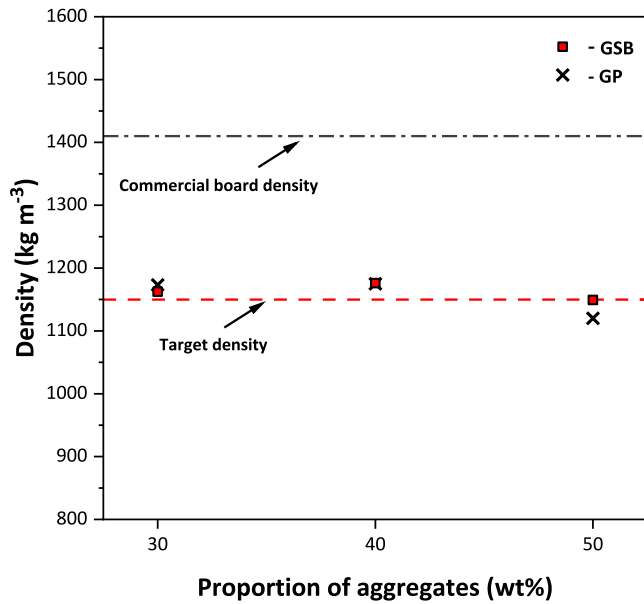


Fig. 3. The density of produced boards, their target density and density of commercial cement boards.

differences in the mechanical performance are not only related to the single fiber/particle strength of seagrass and wood, but also to their physical interaction with the geopolymer matrix. It is known that flake geometry is highly correlated with board key properties, including MOR, MOE, IB, and TS. The longer and thinner the strands or particles, i. e. the higher the aspect ratio, the stronger, stiffer, and more dimensionally stable the boards [7]. Compared to wood particles, long and thin seagrass fibers have a large surface area, which is effectively involved in the load transfer to the matrix. Fibers with longer anchorage

lengths have a greater effective surface area to withstand shear stress and can bridge the area where the bending moment is greatest. Compared to the standard MOR according to EN 634-2:2007, GSB containing 40 and 50 wt% aggregates attained a MOR slightly below the value of 9 N mm^{-2} . The commercial cementitious structural panels (REF) performed well in terms of modulus of rupture, reaching about 10 N mm^{-2} . The high bending strength was expected as their density is very high. The strength-to-weight ratio, however, is lower compared to GSB.

The modulus of elasticity (MOE) showed a decreasing trend and ranged from 3680 N mm^{-2} for GP containing 30 wt% and 2820 N mm^{-2} for GSB containing 50 wt% aggregates (Fig. 4 b). The decrease in MOE could be due to the reduction of binder proportion in the board. When comparing the MOE of GP and GSB, it was found that the inclusion of seagrass fibers also slightly reduced the MOE of the prepared boards (though not statistically significant, ANOVA, $p \leq 0.05$). A major cause for the slight reduction could be attributed to the manual fabrication. In the molding process before pre-pressing, a large volume of seagrass fibers substituted an equal mass of wood particles in the outer layer (Fig. 1 b, indicated by white arrow). During the pre-pressing of GP, wood particles were in direct contact with the pre-pressing plate and thus had favorable conditions to reorganize and fill the voids to form a compact structure. In the case of GSB, however, the pre-pressing plate came in contact with the voluminous seagrass fibers, resulting in a lack of uniformity and compaction of the middle wood particles layer. Thus, although a certain amount of reinforcing fibers was attached to the middle layer containing wood particles, the layers were not aligned. As a result, the thickness of each layer fluctuated a lot, resulting in the discontinuation of compactness, especially in the area between the layers. Although the MOE of GSB did not meet the standard MOE value of 4000 N mm^{-2} for commercial cement boards according to EN 634-2:2007, it reached an adequate value of $\sim 3700 \text{ N mm}^{-2}$. On the other hand, the REF exceeded the standard MOE and reached 6500 N mm^{-2} . The very high MOE is closely related to its high density. It should be noted that a similar MOE was achieved when the target density was above 1400 kg m^{-3} [25].

The load-deformation diagram shows the ductile and brittle response of the boards under flexural loading (Fig. 5 a). GSB not only withstand a higher load before fracture compared to GP, but also absorb a large amount of energy (area under the curve). GP appear to be more brittle compared to the corresponding GSB. At about 30 % deformation, the reaction becomes plastic (ductile), indicating the formation of cracks, delamination of particles, and failure or pull-out of fibers. During plastic deformation, the fibers break or detach, followed by a loud cracking sound. The load-deformation behavior of REF is significantly different from GSB and GP. REF is much stiffer and more brittle compared to GSB. REF shows elastic behavior, while the load drops drastically to failure

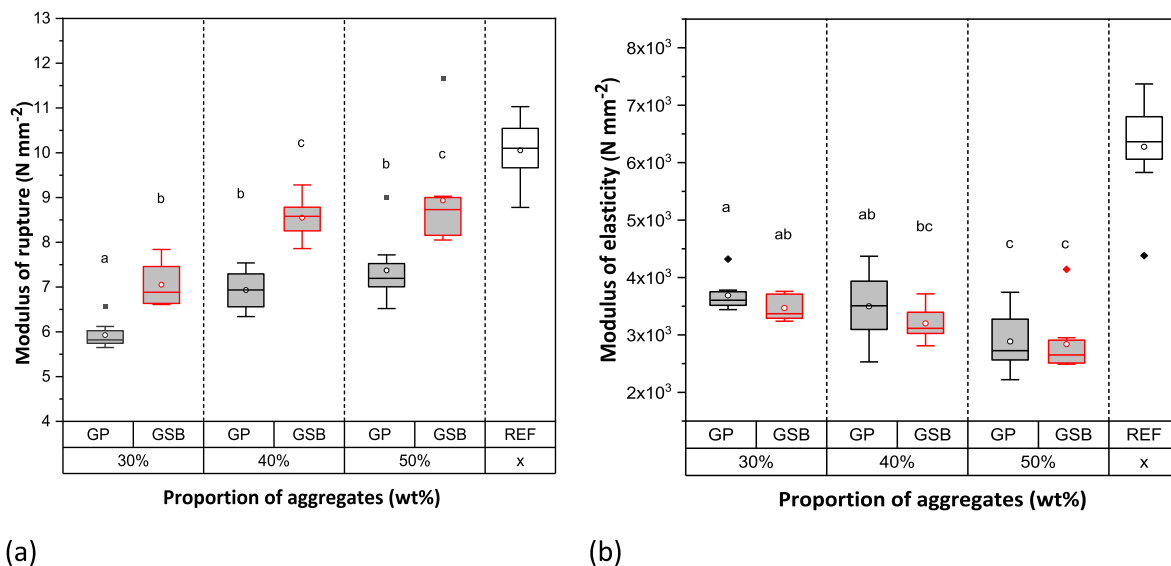


Fig. 4. The modulus of rupture (a) and modulus of elasticity (b) of GP, GSB and reference board (REF). Boxplots show results of 8 replicates per variant. The whiskers indicate the minimum to the maximum; the box represents the 25 %, 50 % and 75 % quartile; the mean value of each data set is depicted as quadrangle inside the box. Values denoted with different letters are significantly different ($p \leq 0.05$) as determined by ANOVA and Tukey's HSD test.

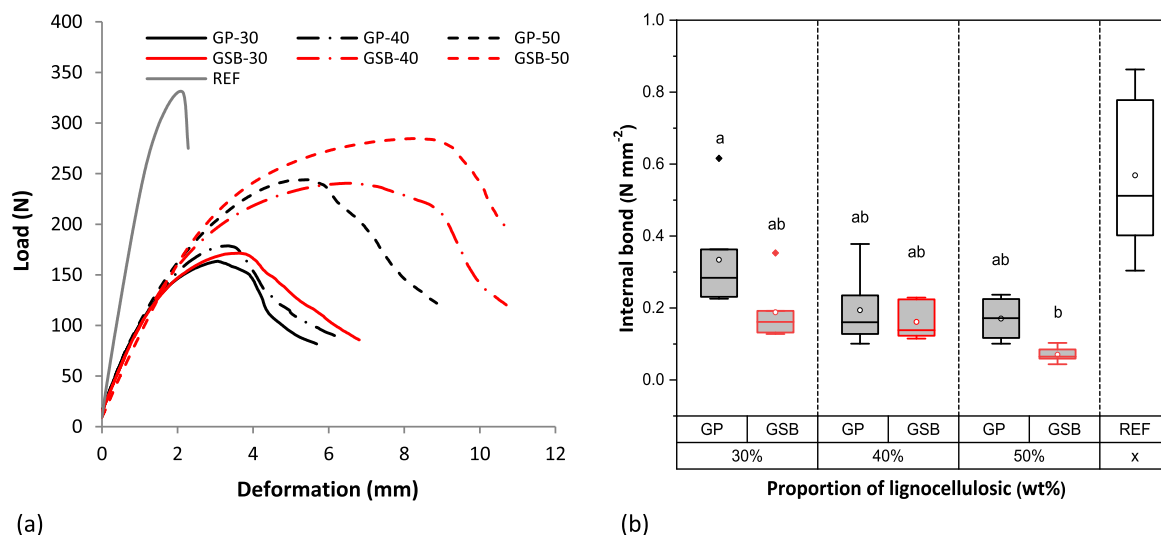


Fig. 5. The load – deformation plot for a series of specimens of GP, GSB and REF obtained by the three-point bending test (a). The internal bond strength of GP, GSB and REF. Boxplots show results of 8 replicates per variant. The whiskers indicate the minimum to the maximum; the box represents the 25 %, 50 % and 75 % quartile; the mean value of each data set is depicted as quadrangle inside the box. Values denoted with different letters are significantly different ($p \leq 0.05$) as determined by ANOVA and Tukey's HSD test.

when deformed further.

As with the MOE, boards with a higher binder content performed better in terms of internal bond strength (IB) than those with a low content (Fig. 5 b). IB varied from 0.36 N mm⁻² for GP containing 30 wt% aggregates to 0.09 N mm⁻² for GSB with 50 wt% aggregates. Between the variants, the significant decrease of IB is related to the insufficient adhesion of seagrass fibers with wood particles (ANOVA, $p \leq 0.05$). While in the bending test the seagrass fibers were successfully involved in distributing the stress longitudinally, in the IB test of GSB boards, where a perpendicular force was applied, one of the outer fiber layers was easily delaminated from the core wood particle layer. The lack of mechanical interlocking between the seagrass fibers and the wood particles located in the middle layer is the major cause of low IB strength. Another basis for the low IB might be the insufficient binder

distribution on the voluminous seagrass fibers, which have a high surface area. As a result of the insufficient mixing, the distribution of the binder is partial and leads to easy delamination. As for the REF, the high internal bond could be related not only to the high density of the board specimens, but also to the high content of the cement phase and the other additives used in the board production to improve their properties.

Impact resistance (dynamic bending) and work to F_{max} (static bending) indicate the toughness of the geopolymer (Fig. 6). Both impact resistance (IR) and work to F_{max} (W) indicated that the toughness of the geopolymer-bonded boards was increased with the amount of lignocellulosic aggregates. Mean values of IR varied from 2.4 kJ m⁻² for GP containing 30 wt% aggregates to 6.6 kJ m⁻² for GSB with 50 wt% aggregates. GSB were more capable to absorb energy than the corresponding GP; their toughness was increased from 24 to 38 % related to

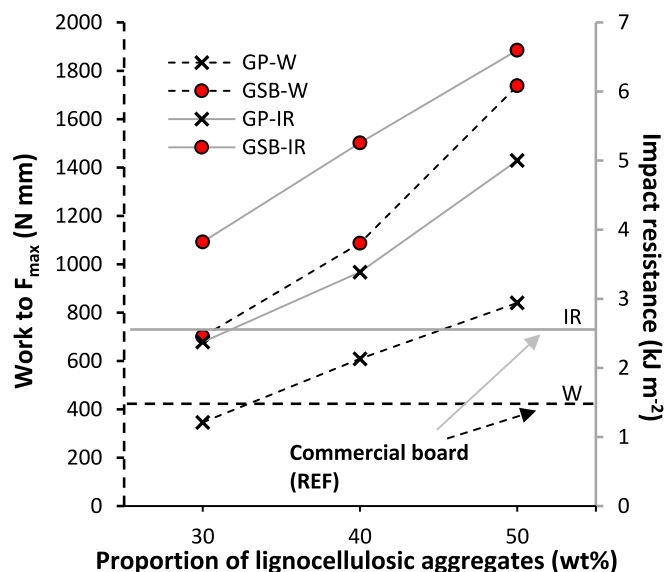


Fig. 6. Work to F_{max} (W) and impact resistance (IR) of GP, GSB and commercial cement board. Mean values of 4 specimens per board (8 replicates per variant).

the respective GP. The W was also increased in the same way as the IR. For GP, W varied between 346 and 840 N mm, whereas for GSB it varied between 700 and 1737 N mm. The inclusion of reinforcing fibers seemed to be much more effective in static than in dynamic bending. The tendency of increased toughness with the increasing proportion of lignocellulosic material could be explained by its ability to hinder and stop the crack propagation and movement of fractures through the geopolymer phase [15–17]. As it was demonstrated earlier in the load-deformation graph (Fig. 5 a), REF absorbs much lower amounts of energy compared to GSB and GP. Both impact resistance and work to F_{max} for REF are very low, being 2.6 kJ m^{-2} and 420 N mm respectively. This is a negative characteristic for commercial boards (REF) as it indicates that in an event of failure, boards can break unexpectedly.

Screw withdrawal resistance (SWR) is an indirect indicator of mechanical strength and shear modulus. The edge-SWR values of the boards were lower compared to surface-SWR values (Table 4). The tensile force applied to pull-out the standardized screws ranged from 1176 to 1484 N for SWR at the surface and from 693 to 1105 N for SWR at the edge of the specimens.

In particular, there were no significant differences in surface-SWR, except for the boards with 50 wt% of aggregates, where a 10 % decrease in SWR occurred for GSB (ANOVA, $p \leq 0.05$). In the case of edge-SWR, however, GSB exhibited higher values. The cracks formed during the screwing process of GP boards might have affected their performance. GSB, on the other hand, did not develop cracks and

Table 4
Screw withdrawal resistance (SWR) of GP and GSB.

Type of board	Proportion of aggregates (wt%)	Surface-SWR	Edge-SWR
GP	30	1484 ± 174 ^a	839 ± 108 ^{ac}
	40	1375 ± 119 ^a	824 ± 152 ^{ac}
	50	1320 ± 105 ^{ab}	818 ± 141 ^{ac}
GSB	30	1433 ± 36 ^a	1105 ± 83 ^b
	40	1368 ± 90 ^a	1040 ± 196 ^a
	50	1176 ± 107 ^b	693 ± 175 ^c
REF	x	1423 ± 47	1282 ± 114

Mean values ± standard deviations of 8 (2 variants × 4 samples) replicates for each type of board. Values denoted with different letters are significantly different ($p \leq 0.05$) as determined by ANOVA and Tukey's HSD test.

therefore performed relatively better than the corresponding GP. In terms of surface-SWR, both GSB and GP containing 30 %wt lignocellulosic aggregates perform slightly better than REF. On the other hand, the edge-SWR of REF is higher compared to the former.

3.3. Thickness swelling and water resistance of GP and GSB

The geopolymer composites displayed fairly similar water absorption (WA) and thickness swelling (TS) after submersion in water for 24 and 72 h, with some exceptions (Table 5). TS for boards containing low proportions of aggregates was 1.3 % for both types of boards. In the case of GP, a 10 wt% increase in wood particles resulted in a 1.1 % increase in TS, while WA did not seem to be affected as no changes were observed. On the other hand, the TS of GSB containing 40 % aggregates increased to 3.8 %. The higher increase (though not statistically significant, ANOVA, $p \leq 0.05$) in TS of GSB compared to GP can be attributed to the lack of compactness in the sandwich board. With the further increase of the lignocellulosic content, both TS and WA increased reaching the maximum values. It is well known that increased relative content of porous organic material, especially of wood particles, increases TS and WA and thus deteriorates the dimensional stability of the boards [39].

Initially, it was expected that TS and WA would be higher for GP compared to GSB because a finer and uniform fiber-geopolymer phase in GSB could protect the inner structure. GP, however, performed very well in terms of water resistance. A possible reason for the low TS of GP could be the “glassy” geopolymer layer that covers the wood particles, preventing water from entering the wood pores and expanding. The effect of initial wetting of the particles with the alkaline activator and subsequent mixing with metakaolin in the dry state and hot-pressing is explained by the conceptual mechanisms presented in Fig. 7.

In the first phase of mixing, the alkaline activator consisting of a mixture of sodium hydroxide and sodium silicate (water glass) was sprayed onto the hydrophilic lignocellulosic material. As a result, a portion of the liquid may fill the cells of the lignocellulosic aggregates (Fig. 7 b). Afterwards, two scenarios are possible. In the first scenario, the fine particles of metakaolin, added in the second phase, attach to the wet wood aggregates, and migrate through the liquid alkaline solution entering into the microscopic cells and starting to geopolymerize, thus forming a well incorporated layer in their pores (Fig. 7 c).

The high pressure might incite the migration process of the alkaline activator liquid and metakaolin particles during pressing or the particle diffusion through the liquid. In the second possible scenario, metakaolin

Table 5
Thickness swelling (TS) and water absorption (WA) of GP and GSB.

Type of board	Proportion of aggregates (wt%)	TS (%)		WA (%)	
		-24 h	-72 h	-24 h	-72 h
GP	30	1.3 ± 0.4 ^a	1.8 ± 0.5 ^a	22.5 ± 0.9 ^{a*}	22.9 ± 1.0 ^{a*}
	40	2.4 ± 0.8 ^a	3.6 ± 1.4 ^a	21.7 ± 2.8 ^{a*}	22.6 ± 2.9 ^{a*}
	50	7.6 ± 0.5 ^b	9.5 ± 0.6 ^b	24.3 ± 0.5 ^{ab*}	26.1 ± 0.5 ^{ab*}
GSB	30	1.3 ± 0.4 ^a	1.9 ± 0.6 ^a	23.0 ± 0.5 ^{a*}	23.1 ± 0.6 ^{a*}
	40	3.6 ± 0.6 ^a	5.8 ± 1.2 ^a	23.7 ± 0.8 ^{ab*}	24.7 ± 0.9 ^{a*}
	50	8.1 ± 4.5 ^b	12.1 ± 4.9 ^b	26.6 ± 0.8 ^{b*}	28.7 ± 1.3 ^{b*}
REF	x	0.4 ± 0.1	0.8 ± 0.4	11.8 ± 0.7	13.5 ± 0.6

Mean values ± standard deviations of 6 (2 variants × 3 samples) replicates for each type of board. Values denoted with different letters (letter followed by * for WA-24 h and WA-72 h) are significantly different ($p \leq 0.05$) as determined by ANOVA and Tukey's HSD test.

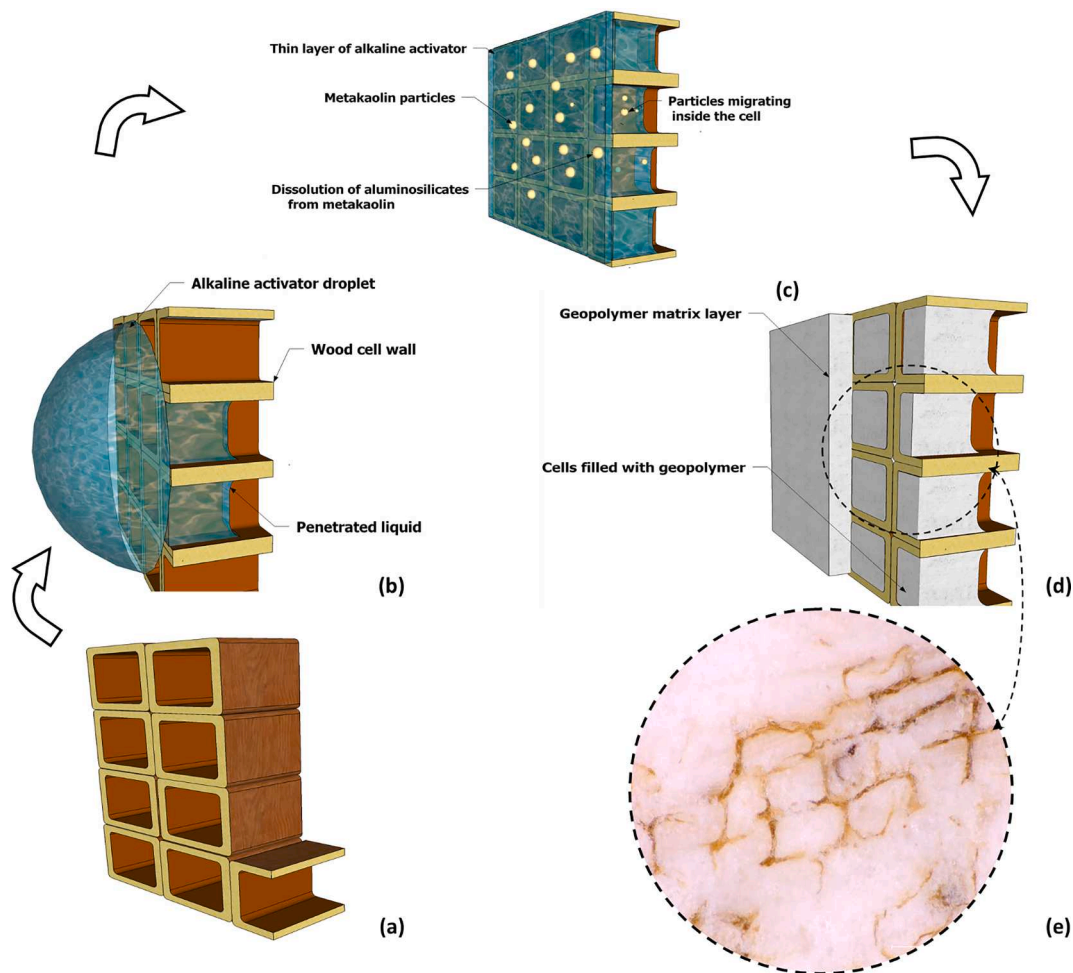


Fig. 7. Proposed mechanism of filling the tracheids with geopolymer during wetting of particles in the first phase, followed by dry mixing and hot-pressing. The wood cell before spraying (a), an alkaline activator droplet wetting the cells after spraying (b), dissolution of aluminosilicates from metakaolin and migration inside the tracheid and/or metakaolin particles migrating inside the wood cell (c), the geopolymerization occurs inside the cells of wood (d), image (magnified 1500 \times) showing wood tracheids filled with geopolymer (e).

particles that settled on the surface of the particles are wetted from the alkaline activator and start to dissolve. The aluminosilicates (dissolved from activated metakaolin) are the ones that migrate inside the tracheid and start to polymerize.

The high temperature accelerates the geopolymerization, resulting in geopolymer formation inside the wood cell (Fig. 7 d, e). The well-attached geopolymer matrix not only serves as a protective layer but can also enhance and distribute stress transfer, thus increasing the mechanical properties. It should also be noted that the above mechanisms are only possible in the cross-sectional (axial) direction of wood particles. In the longitudinal direction of the wood particles, tracheids are cut in the tangential direction forming channel-like structures.

As expected, REF shows lower TS and WA values compared to the geopolymer-based boards. Besides the high density, the main reason for the low TS and WA values could be the very low proportion of lignocellulosic aggregates in the board.

3.4. Cone calorimetry

The cone calorimetry tests show that at irradiance levels of 50 kW m⁻², typical of the heat flux in a well-developed fire, both types of boards displayed high fire resistance (Table 6). In previous research has been reported that geopolymer composites are flame resistant and exhibit negligible heat release values [40]. The mean heat release rate (HRR) and the total heat release (THR) increased with the increasing

Table 6

Mean heat release rate (HRR), total heat release (THR), and mass loss rate of GP and GSB determined in a cone calorimetry.

Type of board	Proportion of aggregates (%)	Mean heat release rate (kW m ⁻²)	Total heat release (MJ m ⁻²)	Mass loss rate (10 ⁻² g s ⁻¹)
GP	30	28	50	3.6
	40	31	56	3.6
	50	35	63	5.0
GSB	30	28	51	3.5
	40	30	54	4.1
	50	31	57	4.2
REF	x	21	37	3.3

proportion of lignocellulosic aggregate. Correspondingly, the mass loss rate increased ranging from 0.035 to 0.050 g s⁻¹. GP and GSB containing 30 and 40 wt% lignocellulosic aggregates did not display significant differences in terms of THR. On the other hand, GSB containing a high proportion of lignocellulosic aggregates (50 wt%) exhibited approximately 10 % lower THR than the corresponding GP.

The geopolymer successfully sealed the wood particles and seagrass fibers, preventing thermal degradation. In the first phase, as a result of

heat exposure (50 kW m^{-2} or $790 \text{ }^\circ\text{C}$), the boards began to change color and the bound water in the lignocellulosic materials started to evaporate, thus preventing a rapid temperature increase (latent energy). In the next phase, the lignocellulosic aggregates started to pyrolyze ($500 \text{ }^\circ\text{C}$) with the further increase of temperature and char began to form. Pyrolysis resulted in the emission of gases and a considerable contraction of the boards. In the final phase, when the concentration of combustible gases and the temperature was high enough, the gases ignited, and the boards started to burn. Interestingly, the flames mainly spread along the edges of the boards. The flames were generated from the char that settled in the aluminum foil, which was used to seal the specimens. The char formed because the gases and fumes generated during pyrolysis had a free path from the cut section of the board rather than from the upper surface of the board.

Slight differences in terms of ignition time were noticed when comparing GP with GSB. The variants containing 30 wt% lignocellulosic aggregates did not ignite. With the increase in the organic material, however, the boards started to ignite from approximately 1050 s onward (Fig. 8). GP exhibit an earlier time of ignition than the GSB. This is a positive feature for GSB, which seem to be even more fire-resistant compared to the former. Both types of lignocellulosic material were successfully encapsulated by the geopolymer matrix, forming a solid structure. However, large individual wood particles had a greater volume and organic mass than small and thin seagrass fibers. While these “single protective shells” were smaller for small seagrass fibers, they were much larger for wood particles, implying a high probability of combustible gas accumulation. REF did not ignite and had a lower THR compared to GSB and GP. The very low HRR and mass loss rate of REF indicate the low content of wood particles in the board.

3.5. FT-IR and XRD analysis

FT-IR spectra of metakaolin and geopolymer-bonded boards revealed phase transformations and the degree of the geopolymerization (Fig. 9). In the spectrum of metakaolin, bands at 1075 cm^{-1} and 805 cm^{-1} are assigned to T–O–Si (T represents Al or Si) bonds [41]. Another band at 450 cm^{-1} might represent Si–O–Si in-plane bending vibration [41–44]. For geopolymers, the band at 805 cm^{-1} representing metakaolin disappeared, while its main band was shifted from 1075 cm^{-1} up to 989 cm^{-1} . Previous studies have reported that the shift of these bands corresponds to the geopolymerization reaction [42–44], as the position of the asymmetric T–O–Si stretching vibrations is affected by the bonding angle and length in the silicate network. The shift in the wavenumber and the increase of peak height and area indicates a higher degree of crosslinking (larger molecules of aluminosilicate polymers), a higher degree of polymerization, which results in better mechanical properties

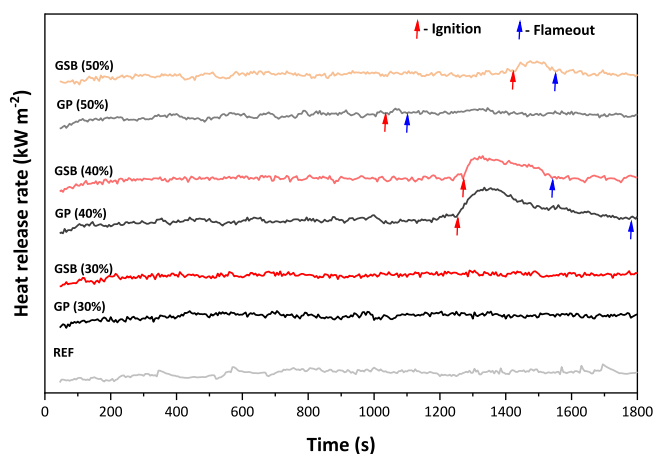


Fig. 8. Heat release rate as a function of time for GP and GSB (with various proportions wt%).

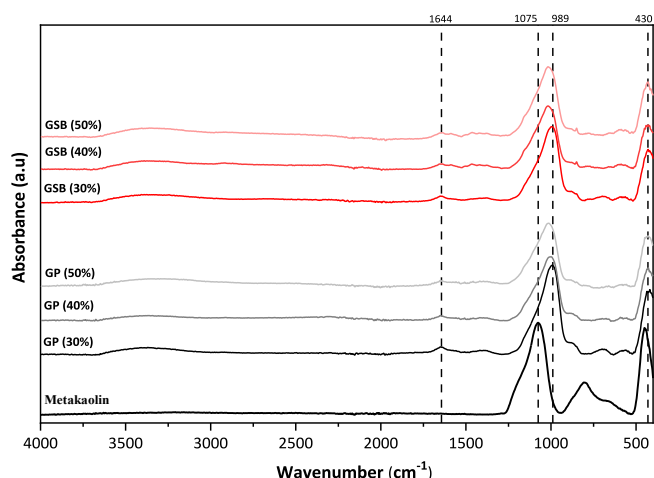


Fig. 9. FT-IR spectra of metakaolin and geopolymer-bonded boards (with various proportions wt%).

[44–46]. As a result of the alkaline activation process of metakaolin, the Al–O asymmetric stretch band shifts towards lower frequencies at around 989 cm^{-1} , indicating the formation of an alkaline aluminosilicate gel [44]. In addition, it was observed that the relocation of this peak was affected by the amount of organic aggregates on the board.

While the band for boards with 30 wt% aggregates was at 989 cm^{-1} , the peaks for a higher proportion of wood particles and seagrass fibers were at 999 and 1014 cm^{-1} for the 40 and 50 wt%, respectively. The band around 1623 cm^{-1} was attributed to water bending (O–H), while the slight peak at $\sim 3400 \text{ cm}^{-1}$ is related to stretching and deformations of H–O–H [41–46].

X-ray diffraction (XRD) patterns of metakaolin and geopolymer boards (GP and GSB) containing a low amount of lignocellulosic aggregates (30 wt%) show that the samples consist mainly of an amorphous phase (Fig. 10). The XRD pattern of metakaolin powder indicates a typical amorphous broad hump centered at 2θ of 16 to 32° with superimposed peaks of crystalline quartz (SiO_2) and anatase (TiO_2) impurities. The presence of anatase is confirmed by the chemical composition of metakaolin ($\text{TiO}_2 = 1.7\%$). In the geopolymer boards, a broad non-symmetric hump appeared in a range of 2θ from 16 to 37° . The presence of the amorphous neoformed geopolymer phase in the aforementioned range indicates the development of the geopolymerization reaction [47,48]. Quartz (at $\sim 2\theta$ of 27°), that appeared in the metakaolin, is completely diminished in the geopolymer board

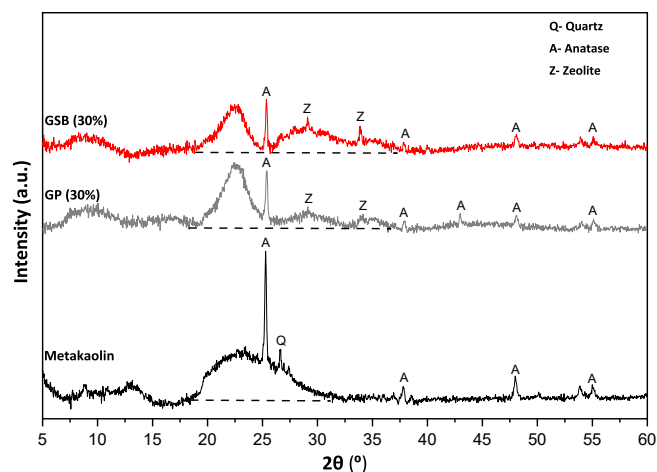


Fig. 10. XRD pattern of metakaolin and geopolymer-bonded composites (with the specified proportions wt%).

samples, indicating that it might have been involved in the geopolymerization. In both geopolymer composite sample patterns, traces of a newly formed crystalline phase were noticed at a 2θ of 29° and 34° . The peak is associated with Zeolite A ($\text{Na}_{96}\text{Al}_{96}\text{Si}_{96}\text{O}_{384}\cdot 216\text{H}_2\text{O}$) phase. The formation of this phase is enhanced in systems with thermal curing and containing higher amounts of alkali in the activator. As geopolymer is considered to be an amorphous gel matrix containing zeolite agglomerates, its presence indicates geopolymerization [3].

3.6. Structural characterization and the effectiveness of mixing

Microscopic 3D-reflected light images of the cut specimens of the GSB indicated an appropriate distribution of the geopolymer binder (Fig. 11 a).

The images show a clear difference between the two layers (indicated with white dashed arrows). In the middle layer, the much larger wood

particles are entirely covered with a geopolymer binder. The particles are oriented in a horizontal orthotropic position during the pressing process (Fig. 11 a). In the outer layers, the cut sections of seagrass fibers are also visible as tiny brownish spots. These fibers are also entirely covered with geopolymer binder, thus ensuring high mechanical strength and good physical properties.

Micrographs of colored GP boards containing 50 wt% wood particles show a fine mixing of metakaolin with the alkaline activator (Fig. 11 b). The red-colored phase represents the geopolymer matrix, while the brownish-gold-colored phase represents the wood particles. The presence of bark is also noticed (dark black color objects). The intensity of the red-colored (color adjusted) phase is generally uniform, with minor exceptions. Small white spots can be seen in the scan (white arrows), indicating an area of unmixed metakaolin with alkaline activator. The white spots, also, might appear due to the fact that the colorant was not completely soluble in the high alkaline environment (agglomeration of

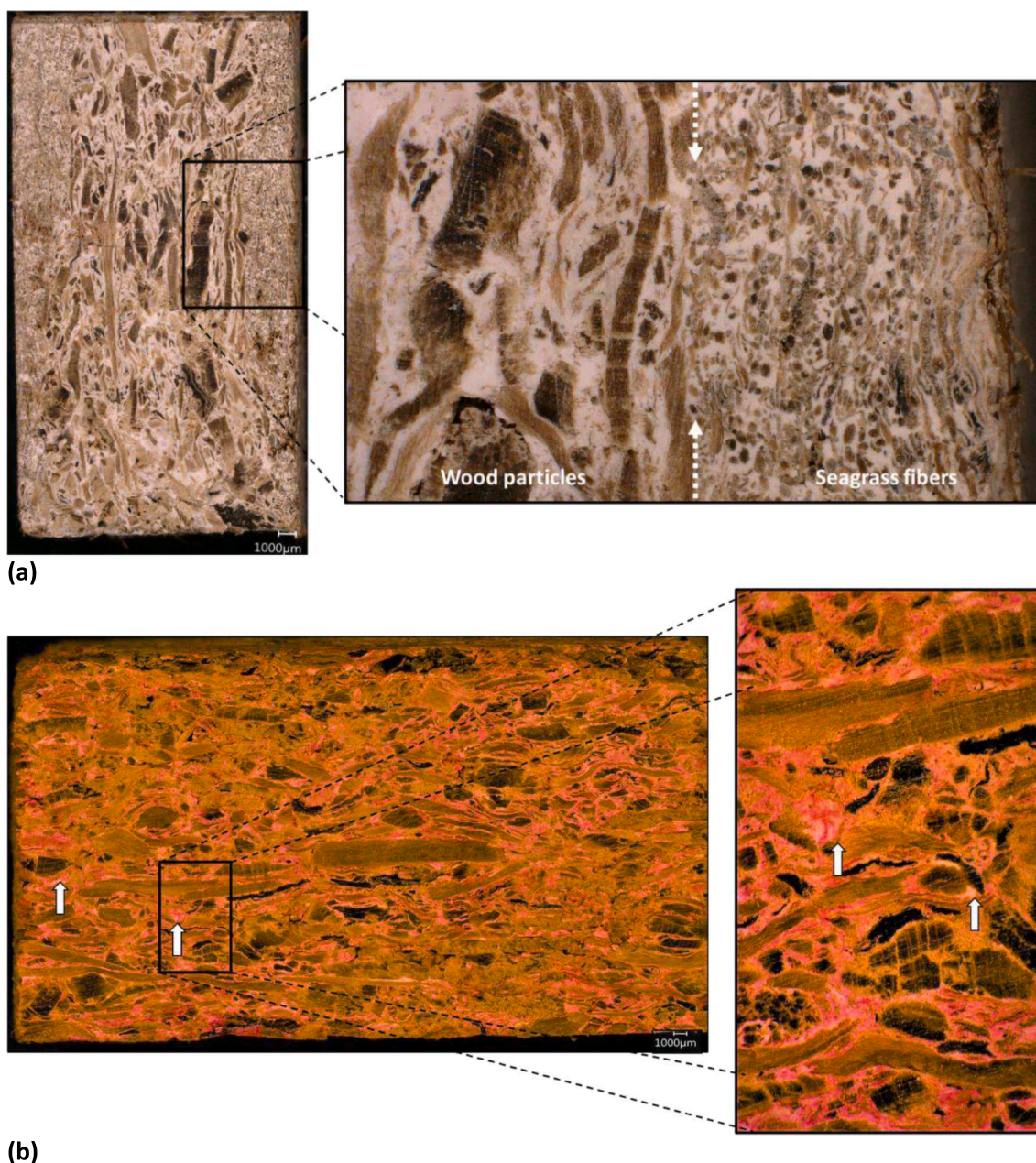


Fig. 11. Side view micrograph of cut cross-section of geopolymer-bonded seagrass sandwich board (GSB) (a), color adjusted microscopic images of geopolymer-bonded particleboard (GP) prepared with a mixture of alkaline activator and a colorant (b).

colorant particles occurred). Dispersion could be further improved by increasing the mixing time and the proportion of the binder to the board. In addition, mixing metakaolin with alkaline activator might depend on the movement of liquid caused by compression (squeezing) of the mixed mass during the pressing operation.

4. Conclusion

Increasing the proportion of lignocellulosic aggregates in GP and GSB improves the MOR of both types of boards. The replacement (25 % wt/wt) of wood particles in the outer layers, with seagrass fibers (GSB) results in a 15 to 20 % increase in MOR and toughness compared to GP. Although commercial boards exhibit higher mechanical strength, still, their strength-to-weight ratio is lower compared to GSB containing 40 and 50 wt% aggregates. For GP and GSB, other properties such as internal bond, modulus of elasticity, and screw withdrawal resistance decrease with increasing lignocellulose content. Fire and water resistance show no significant differences compared to each other. The very low total heat release indicates that geopolymer acts as a protective coating to lignocellulosic material. FT-IR and XRD data as well as 3D-reflected light microscopy images reveal a high degree of geopolymerization and sufficient mixing of metakaolin with the alkaline activator justifying the good mechanical properties of the boards. Considering that a large amount of lignocellulosic aggregates can be incorporated, it is possible to produce a low-cost and environmentally friendly geopolymer-bonded composites suitable for indoor and in some cases for outdoor use. Both types of boards can be regarded as substitutes for cement and organically bonded particleboards to be used for construction purposes. The allocation of fibers in the outer layers appears to be a viable solution to produce boards with high bending strength. Seagrass fibers, being abundant in coastal areas, present an attractive alternative for the reinforcement of construction panels. It is suggested that future work should focus on optimizing the properties of geopolymer-bonded boards depending on their application and, in particular, on reducing energy consumption during their manufacture and curing.

CRedit authorship contribution statement

Aldi Kuqo: Conceptualization, Investigation, Validation, Methodology, Visualization, Writing – original draft, Writing – review & editing. **Aaron Kilian Mayer:** Investigation, Validation, Visualization, Writing – review & editing. **Stephen O. Amiandamhen:** Investigation, Validation, Visualization, Writing – review & editing. **Stergios Adamopoulos:** Validation, Funding acquisition, Supervision, Visualization, Writing – review & editing. **Carsten Mai:** Conceptualization, Validation, Supervision, Funding acquisition, Visualization, Writing – review & editing.

Declaration of Competing Interest

The authors declare that they have no known competing financial interests or personal relationships that could have appeared to influence the work reported in this paper.

Data availability

Data will be made available on request.

Acknowledgments

This research was supported by the Formas project 942-2016-2 (2017-21). Aldi Kuqo is grateful for the support of the German Academic Exchange Service (DAAD).

References

- [1] C. Argiz, A. Moragues, E. Menéndez, Use of ground coal bottom ash as cement constituent in concretes exposed to chloride environments, *J. Clean. Prod.* 170 (2018) 25–33, <https://doi.org/10.1016/j.jclepro.2017.09.117>.
- [2] J. Lehne, Johanna, F. Preston, Making concrete change: Innovation in low-carbon cement and concrete. UK: Chatham House Report, Energy Environment and Resources Department; 2018.
- [3] J.L. Provis, J.S.J. VanDeventer, Geopolymers, structure, processing, properties and application. UK: Woodhead Publishing Limited; 2009.
- [4] O.U. Emmanuel, A. Kuqo, C. Mai, Non-conventional mineral binder-bonded lignocellulosic composite materials: A review, *BioResources*. 16 (2021) 4606–4648.
- [5] D. Kvočka, A. Lešek, F. Knez, V. Ducman, M. Panizza, C. Tsoutis, A. Bernardi, Life Cycle Assessment of Prefabricated Geopolymeric Façade Cladding Panels Made from Large Fractions of Recycled Construction and Demolition Waste. *Materials*, 13 (2020) 3931. .
- [6] R. O'Hegarty, R., Kinnane, O. (2020). Review of precast concrete sandwich panels and their innovations. *Construction and building materials*, 233, 117145. 10.1016/j.conbuildmat.2019.117145.
- [7] S. Frybort, R. Mauritz, A. Teischinger, U. Müller, Cement bonded composites—A mechanical review, *BioResources* 3 (2008) 602–626.
- [8] L. Bejó, P. Takáts, N. Vass, "Development of cement bonded composite beams, *Acta Silv. Lign. Hung.* 1 (2005) 111-119. <http://publicatio.nyme.hu/id/eprint/139>.
- [9] J. Vervloet, T. Tysmans, M. El Kadi, M. De Munck, P. Kapsalis, P. Van Itterbeeck, D. Van Hemelrijck, Validation of a numerical bending model for sandwich beams with textile-reinforced cement faces by means of digital image correlation, *Appl. Sci.* 9 (2019) 1253, <https://doi.org/10.3390/app9061253>.
- [10] S. O. J. Badejo, Effect of flake geometry on properties of cement-bonded particleboard from mixed tropical hardwoods, *Wood Sci. Technol.* 22 (1988) 357-370. 10.1007/BF00353325.
- [11] F.A. Silva, N. Chawla, R.D. Toledo Filho, Mechanical behavior of natural sisal fibers, *J. Biobased Mater. Bio Energy* 4 (2010) 1–8, <https://doi.org/10.1166/jbmb.2010.1074>.
- [12] L. Allegue, M. Zidi, S. Sghaier, Mechanical properties of Posidonia oceanica fibers reinforced cement. *J. Compos. Mater.* 49 (2015) 509-517. 10.1177%2F0021998314521254.
- [13] O. Hamdaoui, O. Limam, L. Ibos, A. Mazioud, Thermal and mechanical properties of hardened cement paste reinforced with Posidonia-Oceanica natural fibers, *Constr. Build. Mater.* 269 (2021), 121339, <https://doi.org/10.1016/j.conbuildmat.2020.121339>.
- [14] A. Kuqo, C. Mai, Mechanical properties of lightweight gypsum composites comprised of seagrass Posidonia oceanica and pine (*Pinus sylvestris*) wood fibers, *Constr. Build. Mater.* 282 (2021), 122714, <https://doi.org/10.1016/j.conbuildmat.2021.122714>.
- [15] A.K. Mayer, A. Kuqo, T. Koddenberg, C. Mai, Seagrass-and wood-based cement boards: A comparative study in terms of physico-mechanical and structural properties, *Compos. Part A: Appl. Sci. Manuf.* 156 (2022), 106864, <https://doi.org/10.1016/j.compositesa.2022.106864>.
- [16] A. Kuqo, T. Koddenberg, C. Mai, Use of dry mixing-spraying process for the production of geopolymer-bonded wood and seagrass fibreboards, *Compos. Part B: Eng.* 248 (2023), 110387, <https://doi.org/10.1016/j.compositesb.2022.110387>.
- [17] T. Alomayri, F.U.A. Shaikh, I.M. Low, Synthesis and mechanical properties of cotton fabric reinforced geopolymer composites, *Compos. Part B: Eng.* 60 (2014) 36–42, <https://doi.org/10.1016/j.compositesb.2013.12.036>.
- [18] B. Asante, G. Schmidt, R. Teixeira, A. Krause, H.S. Junior, Influence of wood pretreatment and fly ash particle size on the performance of geopolymer wood composite, *Eur. J. Wood Wood Prod.* 79 (2021) 597–609, <https://doi.org/10.1007/s00107-021-01671-9>.
- [19] C.K. Ma, A.Z. Awang, W. Omar, Structural and material performance of geopolymer concrete: A review, *Constr. Build. Mater.* 186 (2018) 90–102, <https://doi.org/10.1016/j.conbuildmat.2018.07.111>.
- [20] G. Furtos, L. Molnar, L. Silaghi-Dumitrescu, P. Pascuta, K. Korniejenko, Mechanical and thermal properties of wood fiber reinforced geopolymer composites, *J. Nat. Fibers* (2021) 1–16, <https://doi.org/10.1080/15440478.2021.1929655>.
- [21] G. Furtos, L. Silaghi-Dumitrescu, P. Pascuta, C. Sarosi, K. Korniejenko, Mechanical properties of wood fiber reinforced geopolymer composites with sand addition, *J. Nat. Fibers* 18 (2021) 285–296, <https://doi.org/10.1080/15440478.2019.1621792>.
- [22] S.N. Sarmin, J. Welling, A. Krause, A. Shalbafan, Investigating the possibility of geopolymer to produce inorganic-bonded wood composites for multifunctional construction material—a review, *BioResources* 9 (2014) 7941–7950.
- [23] S.N. Sarmin, J. Welling, Lightweight geopolymer wood composite synthesized from alkali-activated fly ash and metakaolin, *J. Teknologi* 78 (2016).
- [24] H. Ye, Y. Zhang, Z. Yu, Wood flour's effect on the properties of geopolymer-based composites at different curing times, *BioResources* 13 (2018) 2499–2514.
- [25] H.O. Olayiwola, S.O. Amiandamhen, M. Meincken, L. Tyhoda, Investigating the suitability of fly ash/metakaolin-based geopolymers reinforced with South African alien invasive wood and sugarcane bagasse residues for use in outdoor conditions, *Eur. J. Wood Wood Prod.* 79 (2021) 611–627, <https://doi.org/10.1007/s00107-020-01636-4>.
- [26] Berzins, A., Morozovs, A., Gross, U., & Iejavs, J. (2017). Mechanical properties of wood-geopolymer composite. *Eng. Rural Dev.* 16 (2017) 1167-1173. 10.22616/ERDev2017.16.N251.

- [27] P. Duan, C. Yan, W. Zhou, W. Luo, Fresh properties, mechanical strength and microstructure of fly ash geopolymer paste reinforced with sawdust, *Constr. Build. Mater.* 111 (2016) 600–610, <https://doi.org/10.1016/j.conbuildmat.2016.02.091>.
- [28] P. Feltz, P. Balaguru, J. Giancaspro, R. Lyon, Mechanical properties of wood-based particle board utilizing geopolymer. *Soc. for the Advancement of Material and Process Engineering.* 50 (2005) 651–663.
- [29] B. Asante, G. Schmidt, R. Teixeira, A. Krause, H. Savastano Junior, Influence of wood pretreatment and fly ash particle size on the performance of geopolymer wood composite, *Eur. J. Wood Wood Prod.* 79 (2021) 597–609, <https://doi.org/10.1007/s00107-021-01671>.
- [30] -9BS EN 634-2:2007. Cement-bonded particleboards. Specifications. Requirements.
- [31] BS EN 323:1993. Wood-based panels. Determination of density.
- [32] DIN EN 310:1993. Wood-based panels; determination of modulus of elasticity in bending and of bending strength.
- [33] BS EN 319:1993. Particleboards and fibreboards. Determination of tensile strength perpendicular to the plane of the board.
- [34] DIN EN ISO 179-1:2010. Kunststoffe – Bestimmung der Charpy-Schlageigenschaften – Deutsche Fassung.
- [35] DIN EN 320:2007. Particleboards and fibreboards - Determination of resistance to axial withdrawal of screws.
- [36] DIN EN 317:1993. Particleboards and fibreboards; determination of swelling in thickness after immersion in water.
- [37] ISO 5660-1:2002-12, Reaction-to-fire tests - Heat release, smoke reduction and mass loss rate - Part 1 - Heat release rate (cone calorimeter method).
- [38] ISO 9276-2:2014. Representation of results of particle size analysis — Part 2: Calculation of average particle sizes/diameters and moments from particle size distributions.
- [39] O.A. Sotandde, A.O. Oluwadare, O. Ogedoh, P.F. Adeogun, Evaluation of cement-bonded particle boards produced from *Azelia africana* wood residues, *J. Eng. Sci. Technol.* 7 (2012) 732–743.
- [40] G. Roviello, L. Ricciotti, C. Ferone, F. Colangelo, O. Tarallo, Fire resistant melamine based organic-geopolymer hybrid composites, *Cem. Concr. Compos.* 59 (2015) 89–99, <https://doi.org/10.1016/j.cemconcomp.2015.03.007>.
- [41] H.R. Rasouli, F. Golestani-Fard, A.R. Mirhabibi, G.M. Nasab, K.J.D. Mackenzie, M. H. Shahraki, Fabrication and properties of microporous metakaolin-based geopolymer bodies with polylactic acid (PLA) fibers as pore generators, *Ceram. Int.* 41 (2015) 7872–7880, <https://doi.org/10.1016/j.ceramint.2015.02.125>.
- [42] H. Assaedi, F.U.A. Shaikh, I.M. Low, Characterizations of flax fabric reinforced nanoclay-geopolymer composites, *Compos. Part B: Eng.* 95 (2016) 412–422, <https://doi.org/10.1016/j.compositesb.2016.04.007>.
- [43] H.T. Kouamo, A. Elimbi, J.A. Mbey, C.N. Sabouang, D. Njopwouo, The effect of adding alumina-oxide to metakaolin and volcanic ash on geopolymer products: A comparative study, *Constr. Build. Mater.* 35 (2012) 960–969, <https://doi.org/10.1016/j.conbuildmat.2012.04.023>.
- [44] C.A. Rosas-Casarez, S.P. Arredondo-Rea, A. Cruz-Enríquez, R. Corral-Higuera, M.D. J Pellegrini-Cervantes, J.M. Gómez-Soberón, T.D.J. Medina-Serna, Influence of Size Reduction of Fly Ash Particles by Grinding on the Chemical Properties of Geopolymers. *Applied Sciences.* 8(2018):365. 10.3390/app8030365.
- [45] C. Bai, H. Li, E. Bernardo, P. Colombo, Waste-to-resource preparation of glass-containing foams from geopolymers, *Ceram. Int.* 45 (2019) 7196–7202, <https://doi.org/10.1016/j.ceramint.2018.12.227>.
- [46] M. Król, P. Rožek, D. Chlebda, W. Mozgawa, W. Influence of alkali metal cations/ type of activator on the structure of alkali-activated fly ash–ATR-FTIR studies. *Spectrochimica Acta Part A: Molecular and Biomolecular Spectroscopy*, 198 (2018) 33–37. 10.1016/j.saa.2018.02.067.
- [47] F.P. Du, S.S. Xie, F. Zhang, C.Y. Tang, L. Chen, W.C. Law, C.P. Tsui, Microstructure and compressive properties of silicon carbide reinforced geopolymer, *Compos. Part B-Eng.* 105 (2016) 93–100, <https://doi.org/10.1016/j.compositesb.2016.08.036>.
- [48] J. He, Y. Jie, J. Zhang, Y. Yu, G. Zhang, Synthesis and characterization of red mud and rice husk ash-based geopolymer composites, *Cem. Concr. Compos.* 37 (2013) 108–118, <https://doi.org/10.1016/j.cemconcomp.2012.11.010>.

Article 5

Seagrass Leaves: An Alternative Resource for the Production of Insulation Materials – Article 5

Aldi Kuqo *, Carsten Mai

* Corresponding author, email: akuqo@uni-goettingen.de

Department of Wood Biology and Wood Products, Faculty of Forest Sciences and Forest Ecology, University of Goettingen, Büsgenweg 4, 37077 Göttingen, Germany

Authorship (according to Clement, 2014)

	Conceptualization (30%)	Practical work (30%)	Writing/Editing (30%)	Administration (10%)	Contribution
A. Kuqo	60%	100%	70%	20%	71%
C. Mai	40%	0%	30%	80%	29%

Ideas: Design of the investigation / Experimental planning / Interpretation of the data

Work: Execution of the experiment / Data collection and analysis

Writing: Drafting the article / Critical, substantive revision / Reviewing the final version

Administration: Resource management and ensuring scientific integrity before, during, and after publication

Published in Materials 15.19 : 6933.

Published in October 2022

DOI: <https://doi.org/10.3390/ma15196933>

Article

Seagrass Leaves: An Alternative Resource for the Production of Insulation Materials

Aldi Kuqo *  and Carsten Mai 

Department of Wood Biology and Wood Products, Faculty of Forest Sciences and Forest Ecology,
University of Goettingen, Büsungenweg 4, 37077 Göttingen, Germany

* Correspondence: akuqo@uni-goettingen.de

Abstract: Seagrass wracks, the remains of dead leaves accumulated on seashores, are important ecosystems and beneficial for the marine environment. Their presence on the touristic beaches, however, is a problem for the tourism industry due to the lack of aesthetics and safety reasons. At the present time, seagrass leaves are landfilled, although this is not considered an ecological waste management practice. Among other proposed practices for more sustainable and environmentally friendly management, such as composting and biogas or energy generation, in this study we aim to use seagrass leaves for the production of insulation materials. Insulation boards from two types of seagrass leaves (*Posidonia oceanica* and *Zostera marina*) at densities varying from 80 to 200 kg m⁻³ were prepared and their physical and mechanical properties were examined and compared to those of wood fiber insulation boards. The thermal conductivity of seagrass-based insulation boards varied from 0.042 to 0.050 W m⁻¹ K⁻¹, which was up to 12% lower compared to the latter. The cone calorimetry analysis revealed that seagrass-based insulation boards are more fire resistant than those from wood fibers, as they release very low amounts of heat during combustion and do not ignite when exposed to a single flame (Bunsen burner). A simplified cost analysis showed that insulation boards made from seagrass leaves can be up to 30% cheaper compared to those made from wood fibers. After their end of life, seagrass leaves can again be considered a valuable resource and be further utilized by adopting other management strategies.

Keywords: fire properties; *Posidonia oceanica*; seagrass wracks; thermal insulation; waste valorization; *Zostera marina*



Citation: Kuqo, A.; Mai, C. Seagrass Leaves: An Alternative Resource for the Production of Insulation Materials. *Materials* **2022**, *15*, 6933. <https://doi.org/10.3390/ma15196933>

Academic Editors: Ilze Irbe,
Christian Brischke and Miha Humar

Received: 14 September 2022

Accepted: 4 October 2022

Published: 6 October 2022

Publisher's Note: MDPI stays neutral with regard to jurisdictional claims in published maps and institutional affiliations.



Copyright: © 2022 by the authors. Licensee MDPI, Basel, Switzerland. This article is an open access article distributed under the terms and conditions of the Creative Commons Attribution (CC BY) license (<https://creativecommons.org/licenses/by/4.0/>).

1. Introduction

Seagrasses are marine flowering plants that can form underwater meadows. Their presence can extend up to 90 m below sea level [1]. The global distribution of seagrass is estimated at 177,000–600,000 km² [2]. Seagrass species come in many different shapes and sizes. Their leaf size can vary from several cm up to 7 m. The largest amount of seagrass is found on the shores of Australia, but also on the continental coasts of the Americas, northern Europe, and more abundantly in the Mediterranean area [2]. According to Cebrian and Duarte [3], a moderately wide belt of seagrass may yield more than 125 kg of dry material per square meter of the coastline each year. Although seagrasses are crucial habitats for many marine organisms [4], their leaves break off after their growing season and are moved by wave currents, settle on the shores, and start decomposing. The seagrass leaves undergo microbial breakdown, emitting greenhouse gases such as carbon dioxide (CO₂) and methane (CH₄) into the atmosphere [5,6]. Apart from the release of greenhouse gases and unpleasant smells due to natural degradation, the effects of seagrass wrack lying on beaches include the impairment of tourism in the affected areas. Seagrass wrack is therefore removed from the shoreline and disposed of in landfills [7–10].

Landfilling is considered the least effective way to manage this waste biomass according to the European Union (EU) Waste Framework Directive [11]. For sustainable

management, a paradigm shift should be made by no longer considering seagrass wrack as a waste, but as a resource. Thus, much research has been carried out to study the various ways of valorizing seagrass wrack. A current study conducted by Mainardis et al. [12] indicated that composting is one of the most effective ways to utilize organic seagrass residues. In another work, the material has been studied to unveil its potential for biogas production in the anaerobic digestion process [8,13]. Other researchers have taken different approaches to solving the problem of seagrass waste utilization. Khiari and Belgacem [14] studied the possibility of producing cellulose pulps and paper. It has already been confirmed that this raw material has potential for paper production. The high content of mineral components, however, might have a negative effect on the chemical recovery process in the papermaking industry [14]. Another potential use of seagrass reported in the literature is its conversion into energy [15]. Converting the waste into a carbon-neutral biocoal is also a viable alternative [16].

The conversion of seagrass waste (leaves) into a functional material for the construction sector is one of the most frequent approaches for its utilization. Much work has focused on the use of seagrass leaves bonded with organic binders (pMDI, UF, etc.) to produce medium-density fiber/particleboards [17,18]. In other cases, researchers have used mineral binders such as cement for the production of insulation composites [19]. Although the relatively high-density organically or minerally bonded seagrass-based materials seem to be an interesting alternative to conventional wood fiberboards/particleboards; their low mechanical properties are a major drawback that limits their application. The aim of our study is to investigate the use of seagrass leaves extracted from seagrass wracks for the production of low-density, organically bonded insulation materials, and to compare them with those made from wood fibers. It should be noted that one of the seagrass types investigated in this study, *Posidonia oceanica*, which occurs in the Mediterranean area, is subdivided into seagrass fibers and leaves. Seagrass fibers have been extensively studied and are already commercialized as an insulation material [10,20,21]. Leaves, however, are less investigated in this regard. Along with *Posidonia oceanica* leaves (POL), the second species of seagrass studied is *Zostera marina* (ZM). ZM seagrass is widely distributed in the Northern Hemisphere [22]. ZM leaves were applied in their loose form as insulation material (Cabot's Quilt) at the beginning of the 20th century [23]. Rather than a loose-fill or a blow-in insulation material, our objective is to produce and characterize rigid boards intended for partition walls, ceilings, and roofing. Our motive for conducting this research was not only to investigate a feasible approach to seagrass waste management, but also to produce a low-cost building product that can be applied for insulation.

A well-insulated building is a precondition for an economically viable use of energy. Driven by governmental measures to reduce greenhouse gas emissions, improve cost efficiency, and adopt new regulations for energy-efficient buildings, global demand for thermal insulation materials in building applications is projected to increase. Wood fiber insulation boards have been trending lately and are regarded as laudable alternatives to synthetic insulation materials [24,25]. However, the high energy demand for refining wood fibers and the scarcity of raw wood in particular areas have initiated research into substitute resources.

Apart from the initial morphological and chemical characterization of raw materials and the examination of the physico-mechanical properties of the boards produced, a simplified cost analysis was carried out to estimate the economic profitability of using seagrass leaves compared to wood fibers for the production of insulation boards.

2. Materials and Methods

2.1. Materials

Zostera marina seagrass leaves were provided by Seegrashandel GmbH (Westerau, Germany). The raw material had been collected in the East Sea. After natural drying under ambient conditions, leaves with a length of 5 to 60 cm were cut to shorter lengths to avoid problems during the spraying process. Leaves of the Mediterranean seagrass

Posidonia oceanica were collected on the shore of Durrës, Albania. The relatively freshly washed-up seagrass was collected in December 2021. The leaves were dried and shaken several times to remove excess sand before further processing. Wood fibers (a mixture of spruce and pine wood fibers) for the production of reference boards were provided by GUTEX GmbH (Waldshut-Tiengen, Germany). A low-temperature curing polymeric methylene diphenyl diisocyanate (pMDI) resin (I-Bond WFI 4370, Huntsman, Everberg, Belgium) was used as a binder.

2.2. Methods

2.2.1. Determination of Morphological Characteristics

The geodesic length and thickness density distribution weighted by surface area (q_2) of seagrass leaves and wood fibers were measured using FibreShape PRO (X-shape, IST, Vilters, Switzerland). Representative samples of *Posidonia oceanica* leaves (3.5 g), *Zostera marina* leaves (2.0 g), and wood fibers (0.1 g) were manually dispersed on a transparent film of A4 size. The raw leaves and fibers were scattered in such a way that they did not overlap. High-resolution images were created using a flatbed scanner (Epson Perfection V850 Pro, Epson, Tokyo, Japan) in transmitted light mode. The object dimensions were assessed by the static image analysis of the FiberShape software. The internal structure of seagrass leaves was scanned using a digital 3D-reflected light microscope VHX-5000 (Keyence, Neu-Isenburg, Germany).

2.2.2. Chemical Analysis

The laboratory analytical procedures (LAP) of the National Renewable Energy Laboratory (NREL) and the standards published by the Technical Association of the Pulp and Paper Industry (TAPPI) were used to determine the chemical composition of the raw lignocellulosic materials. Initially, the material (seagrass leaves and wood fibers) was ground in a cutting mill (Retsch GmbH, Haan, Germany) with a 0.5 mm screen. Each analysis step was performed in duplicates. The first step of the cascading procedure was the hot-water extraction. The oven-dried lignocellulosic material was extracted for 5 h in a Soxhlet extractor and then dried at 103 °C. Afterward, an ethanol–cyclohexane (1:2) extraction was conducted for another 5 h. The tests were performed according to T264 cm-97 [26]. NREL/TP-510-42618 LAP [27] was used to determine the lignin content of the extractive free material. After the hydrolysis of the polysaccharides with sulfuric acid (72%), the remaining solids (lignin) were weighed after rinsing with demineralized water and drying. The holocellulose content was determined according to the procedure established by L. E. Wise [28]. The evaluation of the ash content was conducted according to the procedure described in TAPPI T 211 [29].

2.2.3. Production of Insulation Boards

The boards were produced by using a dry process. The raw material was vigorously stirred in a gluing drum and the adhesive sprayed through a nozzle at a flow rate of approximately 0.1 to 0.15 g s⁻¹. Before further processing, the moisture content was determined thermogravimetrically. The moisture content of naturally dried *Zostera marina* leaves was 13.9%; for *Posidonia oceanica* leaves it was 15.5%, while for wood fibers it was as high as 9.2%. The adhesive proportion for the boards produced was 6 wt%. The sprayed material was cold pre-pressed and then hot-pressed at 190 °C. Before hot-pressing, 30 g of water was sprayed onto each side of pre-pressed boards to allow steam to form and activate the binder. The dimensions of the boards were 450 × 450 × 40 mm³. In total, 24 boards (8 boards for each type of raw material for 4 different target densities) were prepared (Figure 1, Table 1). The boards were cut to test specimen dimensions and conditioned to constant mass at 20 ± 2 °C and 50 ± 5% RH prior to testing.

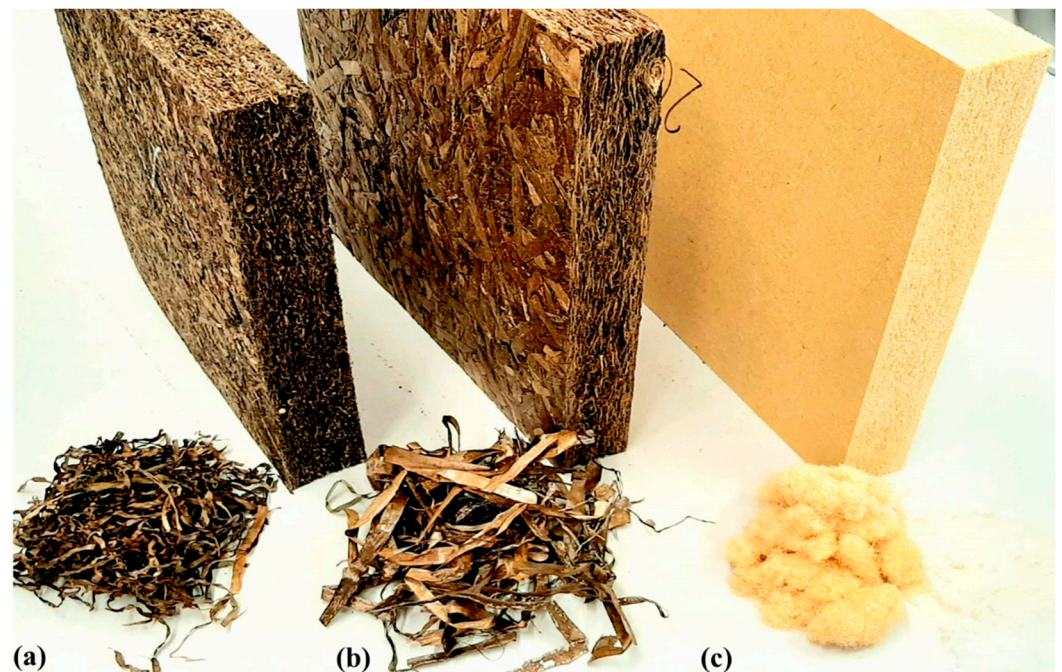


Figure 1. Seagrass boards and the respective raw materials. Boards produced from *Zostera marina* leaves (a), *Posidonia oceanica* leaves (b), and wood fibers (c).

Table 1. Production variants and the respective abbreviations.

Raw Material	Amount of Raw Material (g)	Amount of Binder (g)	Target Density (kg m ⁻³)	Type of Composite
<i>Zostera marina</i> leaves	818	43	80	ZM-80
	1023	54	100	ZM-100
	1534	82	150	ZM-150
	2045	109	200	ZM-200
<i>Posidonia oceanica</i> leaves	837	43	80	POL-80
	1046	54	100	POL-100
	1569	82	150	POL-150
	2092	109	200	POL-200
Wood fibers	789	43	80	WF-80
	989	54	100	WF-100
	1479	82	150	WF-150
	1973	109	200	WF-200

2.2.4. Mechanical Testing

Specimens whose density was within $\pm 10\%$ of the target density were selected for the mechanical tests. For the compression test, a compressive force was applied perpendicular to the faces of the test specimen at a constant speed ($0.1 \text{ d min}^{-1} \pm 25\%$, in which d is the thickness of the test specimen in mm) using a universal testing machine (ZwickRoell Zmartpro, ZwickRoell, Ulm, Germany) with a 10 kN load cell. The tests were conducted according to DIN EN 826 [30]. Four specimens per variant with nominal dimensions of $50 \times 50 \times 40 \text{ mm}^3$ were tested. The internal bond strength (tensile strength perpendicular to the faces) was evaluated following DIN EN 1607 [31]. The test specimens (with nominal dimensions of $50 \times 50 \times 40 \text{ mm}^3$) were glued between two stiff boards with a fast-curing polymer adhesive and then inserted into the universal testing machine. Tensile stress was applied at a constant speed of 10 mm min^{-1} . Four specimens were tested for each variant.

2.2.5. Thermal Conductivity Measurements

Thermal conductivity was determined following the procedure described in the standard DIN EN 12667 [32]. The Heat Flow Meter HFM 446 Lambda Eco-Line (NETZSCH Group, Selb, Germany) was used for the measurement. Two specimens for each variant (target density) measuring $250 \times 250 \times 40 \text{ mm}^3$ were tested at 5 different temperatures (10, 15, 20, 25, and $30 \text{ }^\circ\text{C}$). The equipment quantifies the steady-state heat flow through a test specimen placed between two plates with thermal sensors. The difference between the hot and cold plates was $20 \text{ }^\circ\text{C}$. The thermal conductivity for $23 \text{ }^\circ\text{C}$ (λ_{23}) was calculated by applying linear regression.

2.2.6. Cone Calorimetry and Single Flame Tests

The procedure described in ISO 5660-1 [33] was adopted for the cone calorimetry test. Tetragonal specimens ($100 \times 100 \text{ mm}^2$) with a given thickness were exposed to a heat flux of 50 kW m^{-2} for 30 min. The peak heat release (PHR), the total heat release after 1800 s (THR), and the mass loss rate at the first 300 s (MRL) were evaluated using a mass loss calorimeter (MLC FTT, Fire Testing Technology, East Grinstead, UK). In addition, the ignition and the flameout times were assessed. Three specimens were tested for each variant.

The single flame test was conducted according to DIN EN ISO 11925-2 [34]. Specimens sized $250 \times 90 \times 40 \text{ mm}^3$ were clamped to the fire chamber device (Taurus Instruments AG, Weimar, Germany). Their surface was exposed to fire for 15 s. The flame of the Bunsen burner had a flame height of 20 mm. The direction of flame was 45° to the direction of the specimen. After flame exposure, the pyrolytic behavior of the sample was evaluated by observing whether ignition took place and if the flame reached a height of 150 mm above the burning point in the specified time span; the soot cone height (height of burned area) was measured. An additional set of specimens was tested following the same procedure, with the lower edges of the specimens exposed to the flame for 30 s. Two specimens were tested for each variant.

2.2.7. Water Absorption Test

The water absorption test was determined following the standard EN 1609 [35] with minor modifications. Specimens measuring $100 \times 100 \times 40 \text{ mm}^3$ were placed in the empty water vessel and remained partially submerged as water was added. The water was carefully filled into the container until the underside of the specimen was $(10 \pm 2) \text{ mm}$ below the water level. After 24 h immersion in water, the specimens were weighed and the increase in weight per square meter after submersion was calculated. In total, 3 specimens were tested for each variant.

3. Results and Discussion

3.1. Morphological Considerations and Chemical Composition

Seagrass has long, flattened leaves that are thin and blade-like. Wood fibers, in contrast, have a fibrous, structure with irregular (ideally round) cross-sectional shapes. Assuming that wood fibers have a cylinder-like structure, their shape can be easily examined as the thickness of the analyzed object corresponds to their diameter. During the test, seagrass leaves were preferentially positioned in the scan bed. The length and width of seagrass leaves can be easily determined. Their thickness (third dimension), however, cannot be measured from the 2D scan. The thickness of seagrass leaves was measured by examining the microscopy images. The POL leaves exhibited a thickness that varied from 100 to $200 \text{ }\mu\text{m}$, while ZM leaves appeared to be slightly thinner, having a thickness of 80 to $150 \text{ }\mu\text{m}$. The static image analysis showed the major differences between seagrasses and WF in terms of geodesic length and width (thickness for fibers) (Table 2).

Table 2. Geodesic length and thickness distribution of seagrass *Zostera marina* (ZM), seagrass *Posidonia oceanica* (POL), and wood fibers (WF).

Percentile (%)	POL (Leaves)		ZM (Leaves)		WF (Fibers)	
	Geodesic Length (mm)	Width (mm)	Geodesic Length (mm)	Width (mm)	Geodesic Length (mm)	Thickness (mm)
0	5.23	1.03	0.10	0.04	0.05	0.02
10	48.39	3.68	13.48	0.78	0.63	0.05
50	78.97	5.71	36.74	1.56	2.12	0.06
90	94.32	7.04	72.22	3.10	4.61	0.27
100	99.68	8.09	86.01	4.29	16.61	1.65

The geodesic length of POL leaves varied from 5.2 to 99.7 mm. ZM leaves were slightly shorter compared to the former, reaching up to 86.01 mm. WF were seemingly short, up to 16.61 mm long, while their median geodesic length was 2.1 mm. It must be noted that wood fibers might contain a large proportion of fines, which differs greatly from the median geodesic length of seagrass leaves (Table 2). As indicated by FiberShape, POL leaves were wider compared to ZM. It is worth noting that some seagrass leaves may fold, resulting in reduced dimensions.

In terms of their chemical composition, seagrass leaves contain a higher content of extractives compared to wood fibers (Table 3). A high content of extractives in POL leaves has also been reported in previous studies [14]. In the case of ZM leaves, it has previously been reported that their content of polysaccharides is high while their lignin content is low. ZM leaves' composition is comparable to sisal and jute [36]. A significant difference in lignin content was found between seagrasses and wood fibers. The latter contained 28.3% lignin, which is significantly higher compared to the former. According to Khiari and Belgacem, the differences in terms of lignin and holocellulose content are likely related to climate conditions and the chemical composition of the soil [14]. The ash content of seagrasses was considerably high and similar to that of rice and flax shives [37,38]. The high ash content is attributed to the chemical composition of the marine environment in which the plants grow and/or to their contamination by sand. Further elemental analysis showed that the main element of ash is silicon [14].

Table 3. Chemical composition of raw lignocellulosic materials.

Raw Material	HWE ^a (%)	CEE ^b (%)	Lignin (%)	Holocellulose (%)	Ash (%)
ZM (leaves)	17.9	1.0	17.5	44.6	22.0
POL (leaves)	10.9	4.2	18.7	54.7	13.9
WF (fibers)	9.0	2.1	28.3	66.0	0.5

^a HWE indicates hot-water extractives, ^b CEE indicates cyclohexane–ethanol extractives.

3.2. Mechanical Properties of Insulation Boards

Owing to the different chemical composition and morphological features of the lignocellulosic materials, different internal bond and compression strengths of the respective boards were obtained (Table 4). The internal bond strength tended to increase with increasing target density for all variants. ZM and POL boards displayed three to four times lower internal bond strength compared to WF boards.

During the pressing process, the long seagrass leaves tend to position themselves preferentially in a horizontal direction. The flat and wide surfaces of leaves are attached, forming a compact, multilayer structure. When transversal stress is applied, the bonded leaves can break, resulting in mechanical failure. At high densities, as a result of high compaction, increasingly more leaves are attached and glued to each other, increasing the bonded surface. In the case of WF boards, along with the chemical bonding provided by

the pMDI binder, the wood fibers are interlocked with each other to form a stable structure. In addition, shorter and thinner fibers usually provide high internal bond strength [39].

Table 4. Internal bond strength and compression strength of produced composite boards.

Type of Composite	Actual Density (kg m ⁻³)	Internal Bond Strength (kPa)	Compression at 10% Deformation, σ_{10} (kPa)
ZM-80	86 ± 5	2.8 ± 1.2	17.5 ± 6.3
ZM-100	103 ± 4	5.1 ± 1.0	24.1 ± 9.4
ZM-150	151 ± 4	8.0 ± 0.9	42.6 ± 12.1
ZM-200	206 ± 9	9.4 ± 3	102.7 ± 48.4
POL-80	83 ± 8	2.6 ± 1.3	13.9 ± 3.6
POL-100	103 ± 6	4.5 ± 1.4	15.9 ± 1.2
POL-150	152 ± 7	6.7 ± 4.3	38.4 ± 3.1
POL-200	209 ± 13	21.0 ± 6.0	95.4 ± 15.0
WF-80	81 ± 3	10.6 ± 1.4	35.4 ± 2.6
WF-100	104 ± 2	16.4 ± 1.5	56.2 ± 2.1
WF-150	154 ± 5	29.5 ± 4.7	151.0 ± 5.8
WF-200	202 ± 6	42.8 ± 6.1	254.4 ± 17.3

Mean values and (±) standard deviations.

The compression strengths at 10% deformation showed a similar trend with the internal bond strength as the target density increased. WF boards exhibited higher compression strength compared to the corresponding POL and ZM boards. In the case of the former, wood fibers are interlocked with each other and positioned in various directions on the board. The bundles of the randomly directed wood fibers “resist” the applied vertical force, leading to high compression strengths. During the production of seagrass boards, seagrass leaves lay horizontally. A portion of the leaves, however, tended to fold, resulting in the formation of large voids within the POL and ZM board structure. These large voids are responsible for the low compression strength. The higher compression strength of WF boards can be explained by the higher glue effectiveness as well. Short and thin wood fibers have a great surface area and glue is utilized to a high extent [39].

3.3. Thermal Conductivity of Insulation Boards

Thermal conductivity λ (TC) is a measure of the effectiveness of a material in conducting heat. The investigation of this property allows a quantitative comparison between the effectiveness of different thermal insulation materials. The TC of produced boards depended on their actual density (Figure 2). POL boards exhibited the lowest TCs, varying from 0.042 to 0.050 W m⁻¹ K⁻¹. ZM boards had slightly higher values of TC compared to POL boards but were still within the same range. WF boards seem to conduct thermal energy better, as TC was higher in their case and varied from 0.044 to 0.057 W m⁻¹ K⁻¹. The fitted curves associated with TC values illustrate the differences between the produced boards (Figure 2). It is evident that POL boards have a substantially lower TC at relatively high densities, ranging from 150 to 228 kg m⁻³, compared to other variants. For WF boards, there is a strong increase in TC with density (stronger than that of the other variants).

The amount and volume of voids between the lignocellulosic aggregates in the boards decrease considerably with increasing board density. The heat flow is transferred through the solid material (conduction) and air voids (convection). The TC of air within the voids is lower than that of solid material; thus, the resulting material has low TC at decreasing density. Apart from the chemical composition, another cause for the low TC of seagrass-based boards might be the shape and size of seagrass leaves. During the pressing operation, the seagrass leaves lie longitudinally. Both seagrass-based boards are composed of multiple individual layers that are bonded with each other. Heat is conducted through the solid material mainly in the longitudinal direction, but it can be also transferred from one layer to another through conduction (if the layers are attached to one another). Many voids are also

present between the layers of seagrass leaves. In this case, the heat is transferred through convection. Overall, the heat transfer in the vertical direction is low. WF boards, on the other hand, contain fiber bundles that are extended and a large proportion of which are also vertically directed. The heat is effectively conducted through the wood fibers, which eventually leads to high TC.

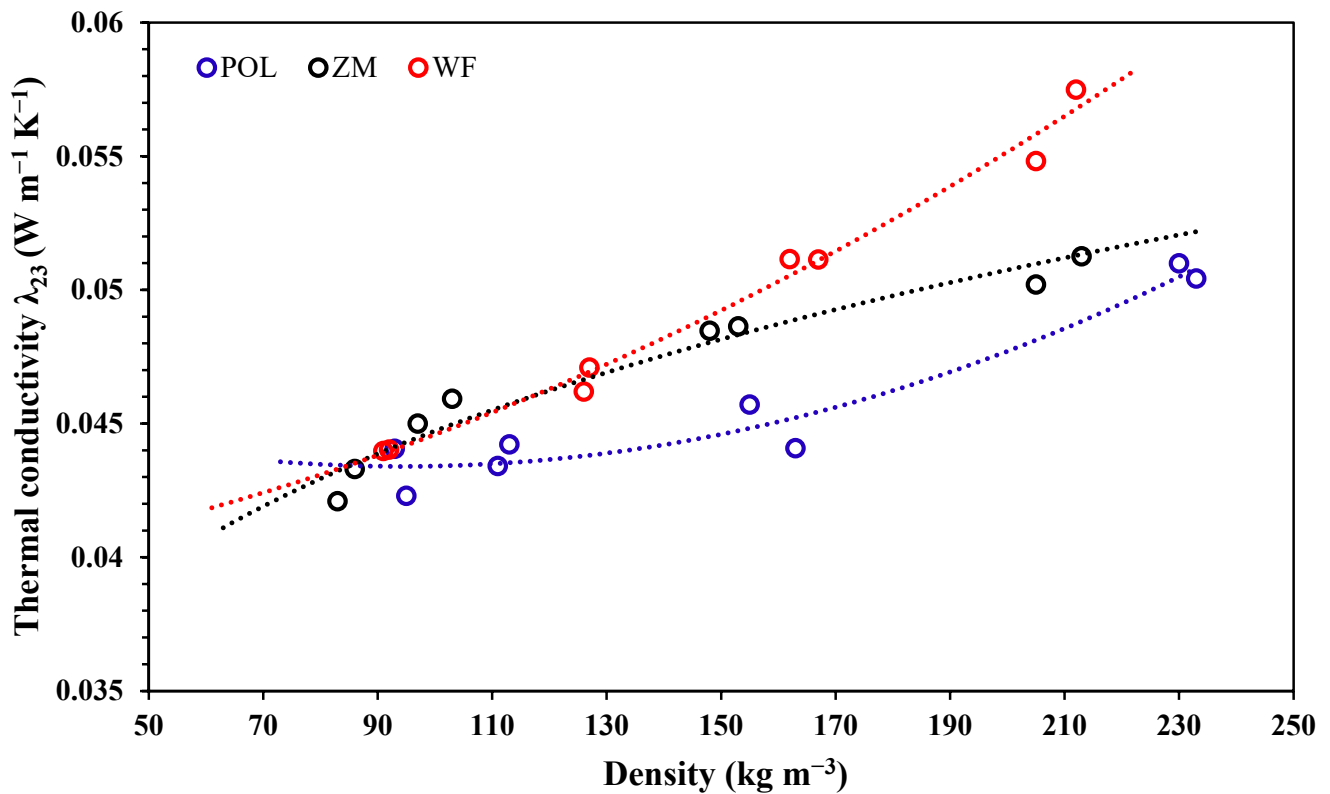


Figure 2. Thermal conductivity of seagrass-based boards (POL and ZM) and wood fiber-based boards (WF) at 23 °C for actual densities varying from 80 to 228 kg m⁻³.

Another cause for the low TC of POL and ZM boards is the internal porous and spongy structure of seagrass leaves. *Posidonia oceanica* seagrass leaves contain a high number of pores of various sizes (Figure 3a). The internal structure can also act as an insulation layer. *Zostera marina* leaves have a very similar structure to the former; the size of their pores, however, is much larger (Figure 3b). In the case of wood fibers (Figure 3c), heat flow takes place by conduction through the single fibers and through convection (air). The high porosity in the wood fiberboard structure results in a relatively low TC.

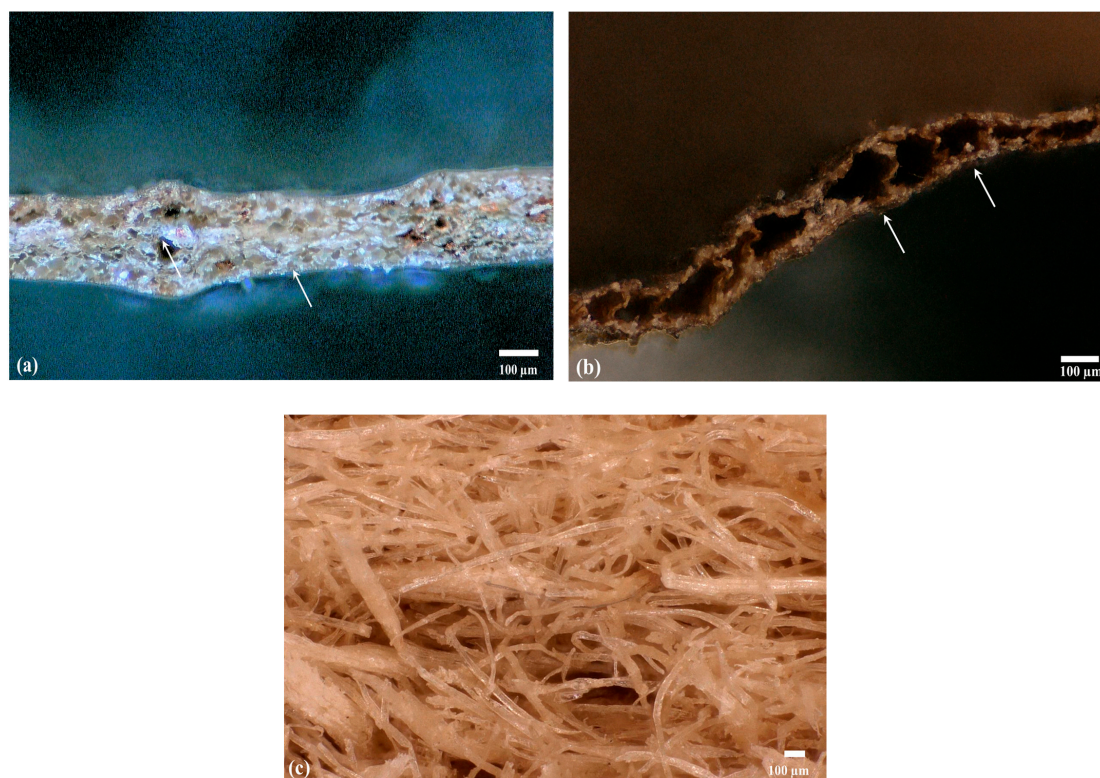


Figure 3. Microscopy images showing the internal structure of seagrass leaves. Cross-section view of *Posidonia oceanica* seagrass (a), *Zostera marina* seagrass (b), and wood fibers (c). The white arrows indicate the porous structure of leaves (closed cells).

3.4. Fire Resistance

Cone calorimetry, a method used in the field of fire safety engineering, showed that seagrass-based boards are much more resistant to fire compared to WF boards (Figure 4). Organic-based insulation materials are known to be susceptible to fire. All boards ignited within the first 10 s of being exposed to the heat. However, significant differences were noticed in terms of heat released during combustion, duration, and characteristics of the flame generated. The peak heat release (PHR) of POL and ZM boards was considerably lower compared to WF boards (Figure 4a). Specifically, WF boards had up to 70% higher PHR compared to POL and more than 110% higher compared to ZM boards. There was no visible change in PHR with increasing density. Similarly, the total heat release (THR) was twice as high for WF boards compared to seagrass boards (Figure 4b).

In contrast with PHR, the THR of WF boards increased with density. At high board densities, a large amount of the combustible organic mass is burned, resulting in high THR. Interestingly, no variance of THR with density was observed for seagrass-based boards. These were much more difficult to burn and exhibited a very weak flame after ignition. The mass loss rates at 300 s (MLR) were consistent with the THR and PHR (Figure 4c). A slight difference was observed between boards of POL and ZM. Although in the case of ZM boards the flame extinguished very quickly (after approximately 30 s), the MLR was higher compared to POL boards. For POL boards, MLR tended to decrease with density even though they develop a flame for a relatively long period (Figure 4d). The POL boards sustained the flame for long periods, but this did not seem to affect their mass. With increasing density, the lignocellulosic mass tended to burn for long periods. As density increases, the absence of large voids affects the MLR by decreasing it. In the case of the ZM boards, the lignocellulosic mass burned for only a few seconds; yet still a mass loss was observed even though there was no flame.

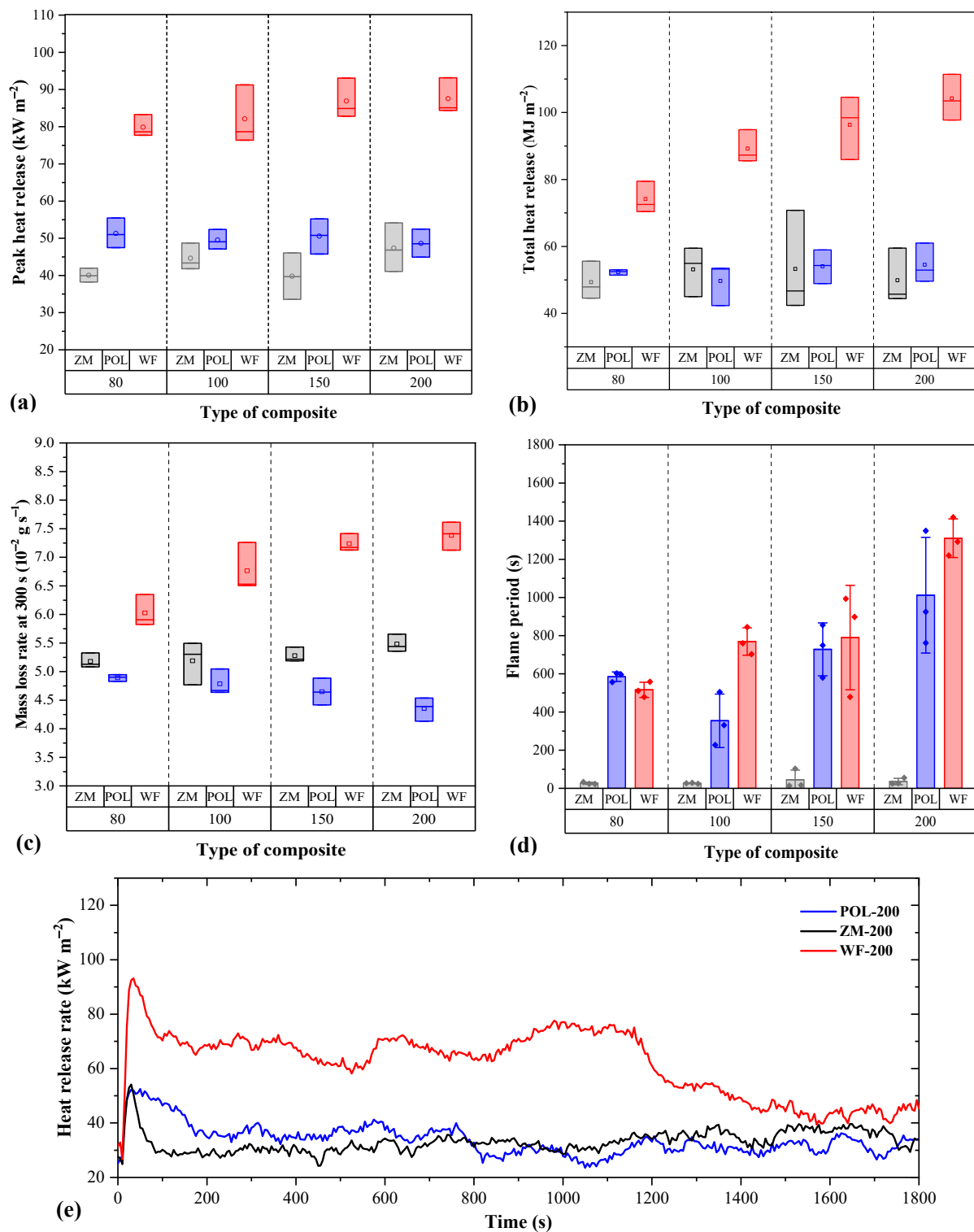


Figure 4. Fire properties of insulation boards of various densities determined with cone calorimetry. Peak heat release (a), total heat release for 1800 s (b), mass loss rate at the initial periods (300 s) (c), flame period (difference between ignition and flameout) (d), heat release rate for specimens with the target density of 200 kg m⁻³ (e). In plots (a–c), each box represents the standard deviation, the horizontal lines within the box represent the median, and the dots represent the mean value. In plot (d), the height of the column represents the mean value, the vertical line on each column represents the standard deviation, and the dots represent individual data.

MRL of WF boards was significantly higher compared to seagrass-based boards, and increased with density. Tiny wood fibers are very susceptible to fire and burn easily followed by a great mass loss rate. In the case of the WF boards, a major portion of the heat was released in the first 300 s (Figure 4e).

The single flame test was carried out for two different periods, for 15 and 30 s at the surface and the edge, respectively. None of the seagrass-based boards ignited when the flame was applied (Table 5). On the other hand, all of the WF boards were ignited. The burned area (soot cone height) of seagrass-based boards varied from 27 to 35 mm when the flame was applied to the surface for 15 s. For the longer period of flame application, the cone height slightly increased. All WF board specimens ignited regardless of density. When the flame was applied on the edge of the specimen for 30 s, the burnt area was very large and exceeded the limit of 150 mm within a short period (less than 30 s after the burner is removed), resulting in failure of the test.

Table 5. Single flame test results for produced seagrass-based and WF insulation boards.

Type of Composite	Bunsen Burner Analysis at the Surface for 15 s				Bunsen Burner Analysis at the Edge for 30 s			
	Ignition	Time to Flameout (s)	Soot Cone Height (mm)	Pass/Fail *	Ignition	Time to Flameout (s)	Soot Cone Height (mm)	Pass/Fail **
ZM-80	No	n/a	35	Pass	No	n/a	32	Pass
ZM-100	No	n/a	27	Pass	No	n/a	30	Pass
ZM-150	No	n/a	27	Pass	No	n/a	41	Pass
ZM-200	No	n/a	28	Pass	No	n/a	41	Pass
POL-80	No	n/a	35	Pass	No	n/a	47	Pass
POL-100	No	n/a	32	Pass	No	n/a	55	Pass
POL-150	No	n/a	31	Pass	No	n/a	51	Pass
POL-200	No	n/a	31	Pass	No	n/a	38	Pass
WF-80	Yes	19	118	Pass	Yes	>60	All ***	Fail
WF-100	Yes	60	110	Pass	Yes	>60	All ***	Fail
WF-150	Yes	28	90	Pass	Yes	44	112	Pass
WF-200	Yes	49	All ***	Pass	Yes	>60	All ***	Fail

Each measurement was performed in duplicate. * The test is regarded as pass when the flame extinguishes within 15 s after burner is removed without passing the cone height of 150 mm. ** The test is regarded as pass when the flame extinguishes within 30 s after burner is removed without passing the cone height of 150 mm. *** The entire surface of the specimen is burned.

The high performance as related to flame and heat resistance of seagrass boards might be associated either with the structure or their chemical composition. The chemical analysis (Table 3) showed that seagrass leaves contain high amounts of mineral constituents (ash). Ash itself can be composed of silica (SiO₂), sodium chloride (NaCl), and other trace minerals. As the flame of intense heat is applied to the specimens, a protective layer forms on their surface, which acts as an insulation layer for the inner organic material. Similar behavior has been observed in rice husk-based materials. The silica layer present in these materials can reradiate heat from an external heat source while insulating the unburnt mass, thus providing a sufficient shielding effect [40]. Owing to the flame-shielding effect, a possible application of seagrass leaves could be a fire protection coating. Owing to the broad leaf structure and the capability to insulate and protect against fire, layers of seagrass leaves can be attached to existing wooden structures to protect them from thermal flux. Additionally, their pleasant brownish appearance could be attractive for interior decoration.

Based on the results of the single flame test, we can estimate that the fire resistance class of seagrass-based insulation boards is B, C, or D. On the other hand, some of the WF boards did not pass the single flame tests, which means that they can be classified as class E. Hakkarainen [41] proposed that the fire class can be predicted based on the ignitability and the cone calorimetry results. Hakkarainen suggested that materials releasing less than 50 kW m⁻² are predicted to be class A2/B. Most of the seagrass-based boards exhibited

low-peak heat release (even lower than 50 kW m^{-2}). However, Hakkarainen also stated that if the ignition time is shorter than 5 s or longer than 60 s, the specimens are outside the range of the index approach. Owing to the high uncertainty of the class prediction, this procedure was not applied in our case; in some of our samples, ignition occurred earlier than 5 s.

3.5. Water Absorption

The water absorption of seagrass-based boards appears to be higher than that of WF boards (Figure 5). The latter differed slightly from POL and was considerably lower compared to ZM boards. The water absorption tended to increase with the density of the boards. The water-related properties of the boards depend on the morphological characteristic and chemistry of raw materials. Water can wet the surface of wood fibers in the WF board specimen. After the specimens are removed from the water container, the adhesive forces holding the water to the wood fibers are weaker than the gravity forces, so that the water flows downward and leaches out of the specimen. The pMDI binder can further hydrophobize the fiber surface, thereby reducing the adhesion forces of water to the fibers.

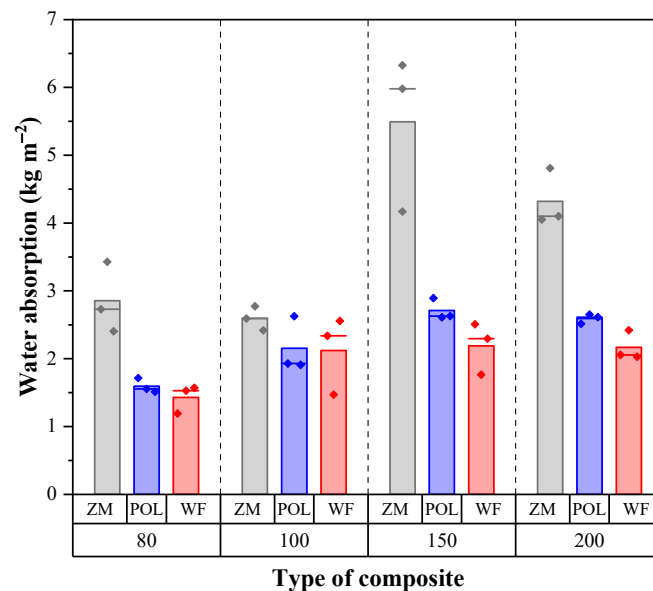


Figure 5. Water absorption of insulation boards of various densities. The height of the column represents the mean value, the vertical line on each column represents the standard deviation, and the dots represent individual data.

On the other hand, even though seagrass fibers have a smaller surface area, they contain pores (Figure 3). POL seagrass leaves contain many pores with a wide size distribution, while ZM leaves have few large pores. ZM boards absorbed far more water compared to POL boards. This difference might be associated with the capillary forces keeping water out of the pores. The far larger pores in ZM leaves have low capillary forces, so that much more water can be absorbed, resulting in high water absorption. Another factor that influences the water absorption is the chemical composition of the raw materials. Wood fibers contain higher amounts of lignin than seagrass (Table 3). Lignin is known to be a hydrophobic component, implying low water absorption.

3.6. A Simplified Cost Analysis and Comparison with Other Natural Resources

A simplified cost analysis was undertaken to estimate and compare the costs for the production of insulation boards from seagrass leaves and wood fibers. The economic analysis was carried out considering a target density of the insulation board of 200 kg m^{-3} . For this analysis, we referred to the data of a previous study, conducted by Rocchi et al. [42].

The authors studied the use of pruning remains from *Tilia* wood to produce insulation boards. The cost data were adapted to our study. The individual costs were calculated for the year 2021, taking into account inflation rates (inflation rates of Germany). Prices for electricity prices (EUR kWh⁻¹) and natural gas (EUR m⁻³) were estimated for July 2021, and the data were obtained from the European Commission and Ycharts, respectively [43,44]. As seagrass is a waste material, we did not include any initial cost for the raw material. The total cost of seagrass leaves consists of collection costs, transportation, cleaning operation, and processing of insulation boards. The cost of seagrass collection was obtained by Mainardis et al. [12]. The transport costs of the raw materials are assumed to be identical as they depend on the location of the processing plant. The binder cost, the fixed costs, and labor costs are also assumed to be similar as the same amount of binder can be used for spraying. The operating costs are also similar for the two types of raw materials. In terms of energy requirement, seagrass leaves do not need to be pre-heated and refined, which accounts for 40% of the total energy required for the production of insulation/MDF fiberboards [45,46]. These costs are excluded from seagrass processing as leaves might be used to produce insulation boards in their original form. Energy is only required for the initial drying and hot-pressing of the boards along with other side operations. Seagrass leaves might also need to be cleaned from sand particles by using a horizontal-vibrating sieving machine. To optimize this operation, the conveyor can be adapted (conveyor belt with holes), making it even more cost-effective. The costs for cleaning were estimated at 2 EUR m⁻³. Considering the high fire resistance of seagrass-based boards, the cost of adding fire retardants is eliminated. After calculating of the abovementioned single costs, the total cost of seagrass-based boards is estimated at 66.4 EUR m⁻³, while the cost of WF-based boards reaches 95.1 EUR m⁻³ (Figure 6). The obtained costs are within the range of estimated costs (37–145 EUR m⁻³, excluding the logistics) for wood-based insulation materials, mentioned in previous work [42].

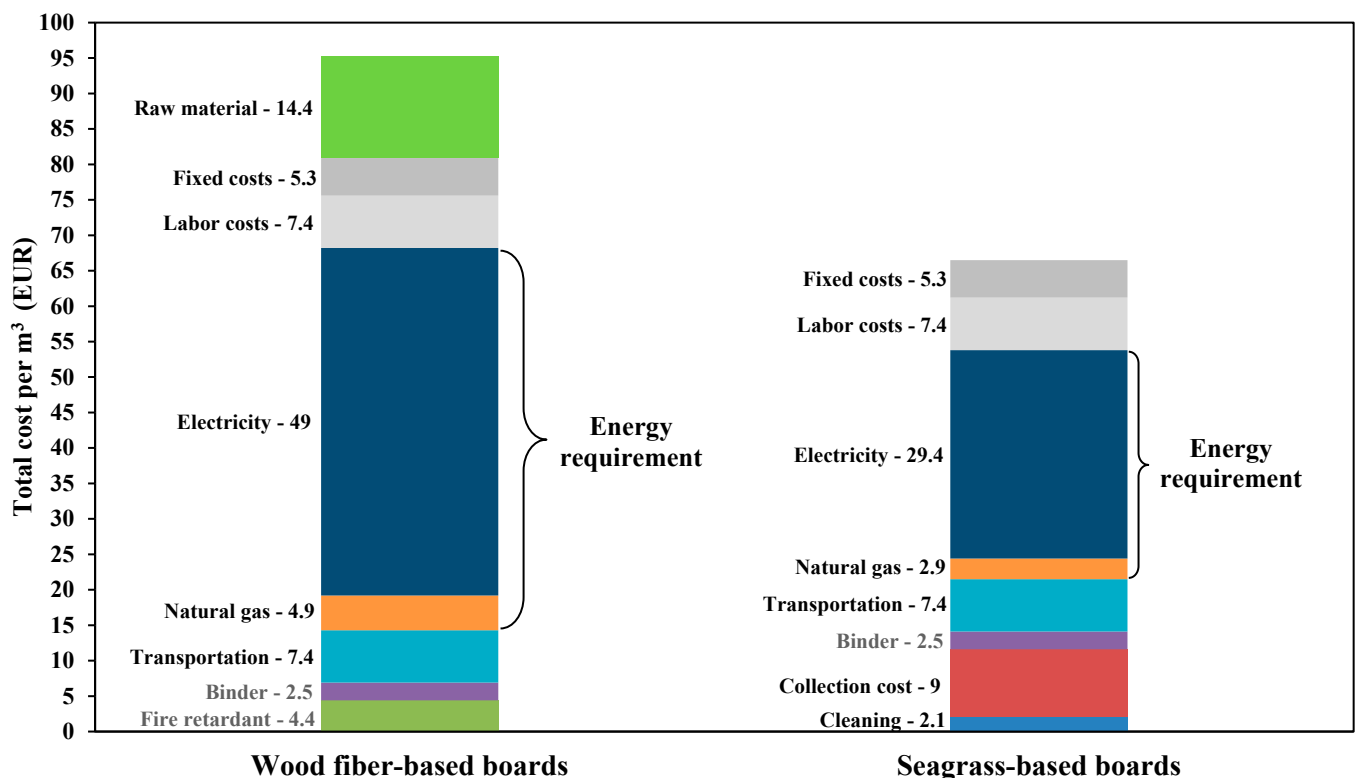


Figure 6. A simplified cost analysis of the insulation boards from seagrass leaves and wood fibers.

Apart from the economical profitability, a comparison of seagrass with other natural fibers (and synthetic materials) shows the advantages of seagrass materials (Table 6).

Comparing our results with those of other natural fibers, it seems that the TC is better (lower) or similar within the same density range. Some of the natural fibers reportedly have lower TC compared to seagrass. However, the densities of other fibers are very low, which might be an indication of the low mechanical properties of the respective composites. In terms of fire resistance, most of the other natural fibers are classified as class E. Rice husk and flax seem to be the most fire-resistant materials. Both flax and rice husk, however, have a relatively high TC (up to two times higher than seagrass) at high densities. The embodied (gray) energy is associated with the sum of the impacts of all greenhouse gas emissions attributed to the material during its life cycle. Some of the natural fibers mentioned are highly insulating materials, but generally require a high amount of energy to be harvested, processed, transported, etc. Seagrass leaves do not need to be heavily processed and therefore can potentially have low embodied energy. However, additional studies need to be conducted to verify this hypothesis.

Table 6. The thermal conductivity, resistance to fire, and the embodied energy for various types of insulation at a specific range of densities.

Insulation Type	Density (kg m ⁻³)	Thermal Conductivity (W m ⁻¹ K ⁻¹)	Resistance to Fire	Embodied Energy (MJ kg ⁻¹)	References
EPS	18–50	0.029–0.041	E	80.8–127	[47]
Flax	20–100	0.033–0.090	C	39.5	[47,48]
Hemp	25–100	0.039–0.123	E	18.7	[48]
Kenaf	30–180	0.026–0.044	E	22.7–39.1	[48]
Rice husk	130–170	0.048–0.080	C	1.4	[48,49]
Date palm	187–389	0.072–0.085	n/a	n/a	[50]
Coir fibers	50–160	0.040–0.050	D-E	0.55	[48]
Cotton stalks	150–450	0.058–0.082	E	44–48	[47,51]
Wood fibers	50–270	0.040–0.052	E	20.3	[47,52]
Seagrass POF *	70–130	0.037–0.043	n/a	n/a	[52]
Wood fibers	92–212	0.044–0.057	E	n/a	Current study
Seagrass POL *	95–233	0.042–0.050	B-D	n/a	Current study
Seagrass ZM *	83–213	0.042–0.051	B-D	n/a	Current study

* POF indicates *Posidonia oceanica* fibers (balls), POL indicates *Posidonia oceanica* leaves, and ZM indicates *Zostera marina* leaves.

4. Conclusions

The utilization of seagrass leaves from wracks in the manufacturing of insulation boards not only reduces greenhouse gas emissions but is also an effective measure to avoid costly landfilling. From the technical point of view, the boards comprising seagrass appear to be better thermal insulators than the corresponding WF boards. More specifically, the TC of WF boards is 5 to 12% higher than that of seagrass-based boards. The heat release during the combustion of the latter is twice as low compared to the former, indicating a very high fire resistance. In terms of mechanical properties, seagrass-based boards have lower compression and internal bond strength compared to boards made of wood fibers at the same range of densities. However, with seagrass boards, the strength requirements of building insulation materials can be met at densities varying between 150 and 200 kg m⁻³. The simplified cost analysis shows that seagrass leaves are an inexpensive and ecological alternative to wood fibers due to the low raw material costs, the low energy required for their processing, and the fact that they might require none to very low amounts of fire retardants. The use of seagrass leaves as an insulation material is one of the most effective practices in the management of seagrass wracks and does not compete with other management scenarios. Instead, this strategy can be an intermediate link in the waste management chain. After the end of their life as an insulation material, seagrass leaves can

still be considered a valuable resource and could be further exploited for biogas production, composting, or energy generation.

Author Contributions: Conceptualization, A.K. and C.M.; Methodology, A.K. and C.M.; Investigation, A.K.; Writing—Original Draft Preparation, A.K.; Writing—Review and Editing, A.K. and C.M.; Visualization, A.K. and C.M.; Supervision, C.M. All authors have read and agreed to the published version of the manuscript.

Funding: We acknowledge support by the Open Access Publication Funds of the Göttingen University.

Data Availability Statement: The data presented in this study are available upon request from the corresponding author.

Acknowledgments: Aldi Kuqo is grateful for the support of the German Academic Exchange Service (DAAD).

Conflicts of Interest: The authors declare no conflict of interest.

References

- Duarte, C.M. Seagrass depth limits. *Aquat. Bot.* **1991**, *40*, 363–377. [CrossRef]
- McKenzie, L.J.; Nordlund, L.M.; Jones, B.L.; Cullen-Unsworth, L.C.; Roelfsema, C.; Unsworth, R.K.F. The global distribution of seagrass meadows. *Environ. Res. Lett.* **2020**, *15*, 074041. [CrossRef]
- Cebrian, J.; Duarte, C.M. Detrital stocks and dynamics of the seagrass *Posidonia oceanica* (L.) Delile in the Spanish Mediterranean. *Aquat. Bot.* **2001**, *70*, 295–309. [CrossRef]
- Vacchi, M.; Falco, G.D.; Simeone, S.; Montefalcone, M.; Morri, C.; Ferrari, M.; Bianchi, C.N. Biogeomorphology of the Mediterranean *Posidonia oceanica* seagrass meadows. *Earth Surf. Process. Landf.* **2017**, *42*, 42–54. [CrossRef]
- Misson, G.; Mainardis, M.; Marroni, F.; Peressotti, A.; Goi, D. Environmental methane emissions from seagrass wrack and evaluation of salinity effect on microbial community composition. *J. Clean. Prod.* **2021**, *285*, 125426. [CrossRef]
- Liu, S.; Trevathan-Tackett, S.M.; Lewis, C.J.E.; Ollivier, Q.R.; Jiang, Z.; Huang, X.; Macreadie, P.I. Beach-cast seagrass wrack contributes substantially to global greenhouse gas emissions. *J. Environ. Manag.* **2019**, *231*, 329–335. [CrossRef]
- Corraini, N.R.; de Souza de Lima, A.; Bonetti, J.; Rangel-Buitrago, N. Troubles in the paradise: Litter and its scenic impact on the North Santa Catarina island beaches, Brazil. *Mar. Pollut. Bull.* **2018**, *131*, 572–579. [CrossRef] [PubMed]
- Misson, G.; Mainardis, M.; Incerti, G.; Goi, D.; Peressotti, A. Preliminary evaluation of potential methane production from anaerobic digestion of beach-cast seagrass wrack: The case study of high-adriatic coast. *J. Clean. Prod.* **2020**, *254*, 120131. [CrossRef]
- Pfeifer, L. “Neptune Balls” Polysaccharides: Disentangling the Wiry Seagrass Detritus. *Polymers* **2021**, *13*, 4285. [CrossRef]
- Zannen, S.; Halimi, M.T.; Hassen, M.B.; Abualsauod, E.H.; Othman, A.M. Development of a Multifunctional Wet Laid Nonwoven from Marine Waste *Posidonia oceanica* Technical Fiber and CMC Binder. *Polymers* **2022**, *14*, 865. [CrossRef]
- European Parliament. Directive 2008/98/EC of the European Parliament and of the Council of 19 November 2008 on Waste and Repealing Certain Directives. 2008. Available online: <https://eur-lex.europa.eu/legal-content/EN/TXT/PDF/?uri=CELEX:02008L0098-20180705&from=EN> (accessed on 12 July 2022).
- Mainardis, M.; Magnolo, F.; Ferrara, C.; Vance, C.; Misson, G.; De Feo, G.; Speelman, S.; Murphy, F.; Goi, D. Alternative seagrass wrack management practices in the circular bioeconomy framework: A life cycle assessment approach. *Sci. Total Environ.* **2021**, *798*, 149283. [CrossRef] [PubMed]
- Balata, G.; Tola, A. Cost-opportunity analysis of the use of *Posidonia oceanica* as a source of bio-energy in tourism-oriented territories. The case of Alghero. *J. Clean. Prod.* **2018**, *172*, 4085–4098. [CrossRef]
- Khiari, R.; Belgacem, M.N. Potential for using multiscale *posidonia oceanica* waste: Current status and prospects in material science. In *Lignocellul. Fibre Biomass Based Compos. Mater*; Jawaid, M., Md Tahir, P., Saba, N., Eds.; Woodhead Publishing: Duxford, UK, 2017; pp. 447–471. [CrossRef]
- Ntalos, G.; Sideras, A. The usage of *Posidonia oceanica* as a raw material for wood composite and thermal energy production. *J. Int. Sci. Publ. Mater. Methods Technol.* **2014**, *8*, 605–611.
- Chubarenko, B.; Woelfel, J.; Hofmann, J.; Aldag, S.; Beldowski, J.; Burlakovs, J.; Schubert, H. Converting beach wrack into a resource as a challenge for the Baltic Sea (an overview). *Ocean. Coast. Manag.* **2021**, *200*, 105413. [CrossRef]
- Kuqo, A.; Korpa, A.; Dhano, N. *Posidonia oceanica* leaves for processing of PMDI composite boards. *J. Compos. Mater.* **2019**, *53*, 1697–1703. [CrossRef]
- Rammou, E.; Mitani, A.; Ntalos, G.; Koutsianitis, D.; Taghiyari, H.R.; Papadopoulos, A.N. The potential use of seaweed (*Posidonia oceanica*) as an alternative lignocellulosic raw material for wood composites manufacture. *Coatings* **2021**, *11*, 69. [CrossRef]
- Mehrez, I.; Hachem, H.; Gheith, R.; Jemni, A. Valorization of *Posidonia-Oceanica* leaves for the building insulation sector. *J. Compos. Mater.* **2022**, *56*, 1973–1985. [CrossRef]
- Mayer, A.K.; Kuqo, A.; Koddenberg, T.; Mai, C. Seagrass-and wood-based cement boards: A comparative study in terms of physico-mechanical and structural properties. *Compos. Part A Appl. Sci. Manuf.* **2022**, *156*, 106864. [CrossRef]

21. Ayadi, M.; Zouari, R.; Segovia, C.; Baffoun, A.; Msahli, S.; Brosse, N. Development of Airlaid Non-Woven Panels for Building's Thermal Insulation. In *Construction Technologies and Architecture*; Trans Tech Publications Ltd.: Bäch, Switzerland, 2022; Volume 1, pp. 772–781. [CrossRef]
22. Short, F.T.; Frederick, T. *World Atlas of Seagrasses*; University of California Press: California, CA, USA, 2003; p. 16.
23. Wyllie-Echeverria, S.; Alan Cox, P. The seagrass (*Zostera marina* [zosteraceae]) industry of Nova Scotia (1907–1960). *Econ. Bot.* **1999**, *53*, 419–426. [CrossRef]
24. Segovia, F.; Blanchet, P.; Auclair, N.; Essoua Essoua, G.G. Thermo-mechanical properties of a wood fiber insulation board using a bio-based adhesive as a binder. *Buildings* **2020**, *10*, 152. [CrossRef]
25. Richter, M.; Horn, W.; Juritsch, E.; Klinge, A.; Radeljic, L.; Jann, O. Natural building materials for interior fitting and refurbishment—What about indoor emissions? *Materials* **2021**, *14*, 234. [CrossRef] [PubMed]
26. TAPPI T 264 cm-97, Preparation of Wood for Chemical Analysis. 1997. Available online: <https://imisrise.tappi.org/TAPPI/Products/01/T/0104T264.aspx> (accessed on 5 July 2022).
27. NREL/TP-510-42618, Determination of Structural Carbohydrates and Lignin in Biomass. 2008. Available online: <https://www.nrel.gov/docs/gen/fy13/42618.pdf> (accessed on 5 July 2022).
28. Wise, L.E. Chlorite holocellulose, its fractionation and bearing on summative wood analysis and on studies on the hemicelluloses. *Pap. Trade* **1946**, *122*, 35–43.
29. TAPPI T211 om-02, Ash in Wood, Pulp, Paper and Paperboard: Combustion at 525 °C. 2002. Available online: <https://imisrise.tappi.org/TAPPI/Products/01/T/0104T211.aspx> (accessed on 5 July 2022).
30. DIN EN 826, Thermal Insulating Products for Building Applications-Determination of Compression Behaviour. German Version EN 826:2013, Berlin. 2013. Available online: <https://www.beuth.de/de/norm/din-en-826/172014993> (accessed on 5 July 2022). German version EN 826:2013, Berlin.
31. DIN EN 1607, Thermal Insulating Products for Building Applications-Determination of Tensile Strength Perpendicular to Faces. German Version EN 1607:2013, Berlin. 2013. Available online: <https://www.beuth.de/de/norm/din-en-1607/171957716> (accessed on 5 July 2022).
32. DIN EN 12667, Thermal Performance of Building Materials and Products-Determination of Thermal Resistance by Means of Guarded Hot Plate and HEAT flow Meter Methods-Products of High and Medium Thermal Resistance. German Version EN 12667:2001, Berlin. 2001. Available online: <https://www.beuth.de/de/norm/din-en-12667/33692201> (accessed on 5 July 2022).
33. ISO 5660-1, Reaction-to-Fire Tests-Heat Release, Smoke Reduction and Mass Loss Rate-Part 1-Heat Release Rate (Cone Calorimeter Method). ISO 5660-1:2002-12. 2002. Available online: <https://www.iso.org/standard/35351.html> (accessed on 5 July 2022).
34. DIN EN ISO 11925-2, Reaction to Fire Tests-Ignitability of Products Subjected to Direct Impingement of flame-Part 2: Single Flame Source Test (ISO 11925-2:2010). German Version EN ISO 11925-2:2010, Berlin. 2011. Available online: <https://www.iso.org/standard/45782.html> (accessed on 5 July 2022).
35. DIN EN 1609, Thermal Insulating Products for Building Applications-Determination of Short Term Water Absorption by Partial Immersion. German Version EN 1609:2013, Berlin. 2013. Available online: <https://www.beuth.de/de/norm/din-en-1609/171957791> (accessed on 5 July 2022).
36. Davies, P.; Morvan, C.; Sire, O.; Baley, C. Structure and properties of fibres from sea-grass (*Zostera marina*). *J. Mater. Sci.* **2007**, *42*, 4850–4857. [CrossRef]
37. Ross, K.; Mazza, G. Characteristics of lignin from flax shives as affected by extraction conditions. *Int. J. Mol. Sci.* **2010**, *11*, 4035–4050. [CrossRef]
38. Jongpradist, P.; Homtragoon, W.; Sukkarak, R.; Kongkitkul, W.; Jamsawang, P. Efficiency of rice husk ash as cementitious material in high-strength cement-admixed clay. *Adv. Civ. Eng.* **2018**, *2018*, 8346319. [CrossRef]
39. Bütün Buschalsky, F.Y.; Mai, C. Repeated thermo-hydrolytic disintegration of medium density fibreboards (MDF) for the production of new MDF. *Eur. J. Wood Wood Prod.* **2021**, *79*, 1451–1459. [CrossRef]
40. Zhao, Q.; Zhang, B.; Quan, H.; Yam, R.C.; Yuen, R.K.; Li, R.K. Flame retardancy of rice husk-filled high-density polyethylene ecomposites. *Compos. Sci. Technol.* **2009**, *69*, 2675–2681. [CrossRef]
41. Hakkarainen, T. Rate of heat release and ignitability indices in predicting SBI test results. *J. Fire Sci.* **2001**, *19*, 284–305. [CrossRef]
42. Rocchi, L.; Paolotti, L.; Fagioli, F.F.; Boggia, A. Production of insulating panel from pruning remains: An economic and environmental analysis. *Energy Procedia* **2018**, *147*, 145–153. [CrossRef]
43. Eurostat, European Commission. Gas Prices for Non-Household Consumers-bi-Annual Data (from 2007 Onwards). 2021. Available online: https://ec.europa.eu/eurostat/web/energy/data/database?node_code=nrg_price (accessed on 3 August 2022).
44. Ycharts.com. Germany Natural Gas Border Price. 2022. Available online: https://ycharts.com/indicators/germany_natural_gas_border_price (accessed on 3 August 2022).
45. Li, J.; Pang, S.; Scharpf, E.W. Modeling of thermal energy demand in MDF production. *For. Prod. J.* **2007**, *57*, 97–104.
46. Adeeb, E.; Kim, T.W.; Sohn, C.H. Cost-benefit analysis of medium-density fiberboard production by adding fiber from recycled medium-density fiberboard. *For. Prod. J.* **2018**, *68*, 414–418. [CrossRef]
47. Kumar, D.; Alam, M.; Zou, P.X.; Sanjayan, J.G.; Memon, R.A. Comparative analysis of building insulation material properties and performance. *Renew. Sustain. Energy Rev.* **2020**, *131*, 110038. [CrossRef]
48. Schiavoni, S.; Bianchi, F.; Asdrubali, F. Insulation materials for the building sector: A review and comparative analysis. *Renew. Sustain. Energy Rev.* **2016**, *62*, 988–1011. [CrossRef]

49. Battezzore, D.; Alongi, J.; Duraccio, D.; Frache, A. Reuse and Valorisation of Hemp Fibres and Rice Husk Particles for Fire Resistant Fibreboards and Particleboards. *J. Polym. Environ.* **2018**, *26*, 3731–3744. [[CrossRef](#)]
50. Agoudjil, B.; Benchabane, A.; Boudenne, A.; Ibos, L.; Fois, M. Renewable materials to reduce building heat loss: Characterization of date palm wood. *Energy Build.* **2011**, *43*, 491–497. [[CrossRef](#)]
51. Zhou, X.Y.; Zheng, F.; Li, H.G.; Lu, C.L. An environment-friendly thermal insulation material from cotton stalk fibers. *Energy Build.* **2020**, *42*, 1070–1074. [[CrossRef](#)]
52. Fachagentur Nachwachsende Rohstoffe e.V. (FNR). Dämmstoffe aus Nachwachsenden Rohstoffen. Gülzow-Prüzen. Abteilung Kompetenz-und Informationszentrum Wald und Holz (KIWUH). 2019. Available online: https://www.fnr.de/fileadmin/allgemein/pdf/broschueren/Brosch%C3%BCre_Baustoffe_Web.pdf (accessed on 5 July 2022).

Article 6

Flexible Insulation Mats from *Zostera marina* Seagrass – Article 6

Aldi Kuqo, Carsten Mai*

*Corresponding author, email: cmai@gwdg.de

a Department of Wood Biology and Wood Products, Faculty of Forest Sciences and Forest Ecology, University of Goettingen, Büsgenweg 4, 37077 Göttingen, Germany

Authorship (according to Clement, 2014)

	Conceptualization (30%)	Practical work (30%)	Writing/Editing (30%)	Administration (10%)	Contribution
A. Kuqo	50%	100%	70%	10%	67%
C. Mai	50%	0%	30%	90%	33%

Ideas: Design of the investigation / Experimental planning / Interpretation of the data

Work: Execution of the experiment / Data collection and analysis

Writing: Drafting the article / Critical, substantive revision / Reviewing the final version


Administration: Resource management and ensuring scientific integrity before, during, and after publication

Published in Journal of Natural Fibers 20.1: 2154303.

Published in December 2022

DOI: <https://doi.org/10.1080/15440478.2022.2154303>

Flexible Insulation Mats from *Zostera marina* Seagrass

Aldi Kuqo  and Carsten Mai 

Department of Wood Biology and Wood Products, Faculty of Forest Sciences and Forest Ecology, University of Goettingen, Göttingen, Germany

ABSTRACT

The dead seagrass leaves accumulated on the seashores, also known as beach (seagrass) wracks, can be considered a sustainable and ecologically beneficial source for application in the construction sector. An innovative thermal insulation material composed of *Zostera marina* seagrass leaves was developed using bicomponent fibers as a binding agent. The bicomponent fibers consisted of polypropylene in the core and polyethylene in the sheath. This work aimed to investigate the effect of mat density on mechanical properties (compression and internal bond strength), thermal conductivity and fire properties. The seagrass-based (SG) mats were compared to reference mats consisting of wood fibers (WF). The digital and scanning electron microscopy investigation revealed the differences in the bonding mechanism between the two types of mats. Although slightly higher than WF mats, the thermal conductivity of SG mats still varied from 0.039 to 0.051 W m⁻¹ K⁻¹ and is comparable to those of other natural fiber-based boards with the same density range. The low peak heat release of SG mats (up to 63% lower than wood fiber-based mats) indicates their high resistance to fire. SG mats provide novel possibilities for using new environmentally friendly materials intended for ceiling and partition applications.

摘要

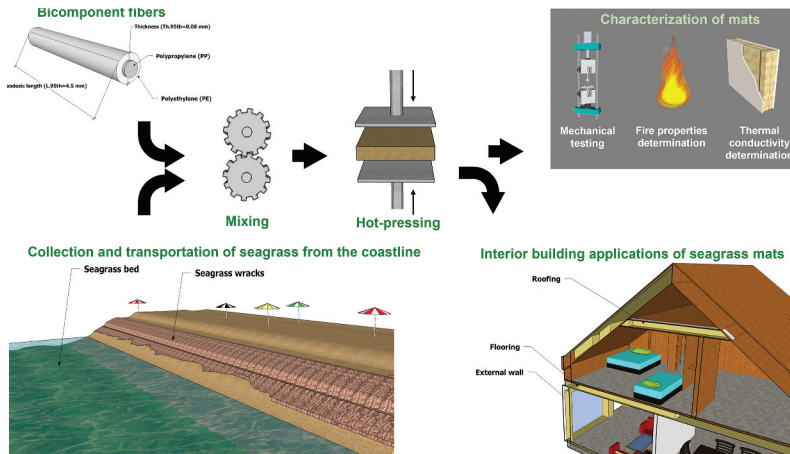
堆积在海边的死海草叶,也被称为海滩(海草)残骸,可以被认为是建筑领域应用的可持续和生态有益的来源。使用双组分纤维作为粘合剂开发了一种由 *Zostera marina* 海草叶组成的创新隔热材料。双组分纤维由芯中的聚丙烯和外皮中的聚乙烯组成。这项工作旨在研究垫子密度对机械性能(压缩和内部结合强度)、导热性和防火性能的影响。将基于海草的(SG)垫子与由木纤维(WF)组成的参考垫子进行了比较。数字和扫描电子显微镜研究揭示了两种垫子之间粘合机制的差异。虽然略高于WF垫,但SG垫的导热系数仍然在0.039至0.051 Wm⁻¹ K⁻¹之间变化,与具有相同密度范围的其他天然纤维基板相当。SG垫的低峰值热释放(比木质纤维垫低63%)表明它们具有高防火性。SG垫子为使用用于天花板和隔断应用的新型环保材料提供了新的可能性。

KEYWORDS

Flexible mats; fire resistance; seagrass; thermal conductivity; wood fibers

关键词

弹性垫; 防火性能; 海草; 导热系数; 木纤维



Introduction

The building sector in the EU is responsible for 40% of the energy consumption and 36% of greenhouse gas emissions, which mainly stem from construction, usage, renovation and demolition (Tsemekidi-Tzeiranaki et al. 2019). Nowadays, intelligent solutions and sustainable development efforts in construction are gaining high significance. One of the most effective measures for implementing green technology is the utilization of natural resources and agro-industrial wastes.

Other than natural or waste lignocellulosic resources, products derived from wood have also been trending over the last years. Wood fibers have been widely used in construction as they are considered a sustainable and eco-friendly alternative for the production of insulation materials (Imken, Kraft, and Mai 2021; Schulte et al. 2021). Apart from being environmentally friendly, wood fiberboards are excellent thermal insulators; they are breathable, soundproofing and can be installed and handled easily. However, despite their advantages, they also seem to have some drawbacks. In some cases, the raw materials might not be widely available. Their high cost is another factor that might affect their commercial application. In particular, the production of wood fibers requires a high energy input, which increases their cost (Schulte et al. 2021). Another common problem of organic insulation materials is their relatively low fire resistance. Most of them are classified as highly combustible and possess low resistance to fire (Graupner and Müssig 2010; Kumar et al. 2020; Zou et al. 2021).

Along with other resources, seagrasses have emerged as an attractive alternative solution for their application in construction. Seagrasses are aquatic flowering plants native to marine environments. As a result of the windy weather conditions, seagrass leaves break, and moved by the force of the waves are washed onto the shore creating an unpleasant view, which is a problem, especially during the tourist season. Therefore, local authorities are usually compelled to clean these shores. Although it is considered a waste product, seagrass is a functional raw material (Kuqo, Korpa, and Dharmo 2019). Among the various seagrasses, *Posidonia oceanica* (Mediterranean seagrass) is one of the most extensively studied species. Specifically, fiberboards composed of *Posidonia oceanica* have been regarded as adequate alternatives to other thermal insulation materials, as they display a very low thermal conductivity (Ayadi et al. 2022; Hamdaoui et al. 2018; Kuqo and Mai 2022; Zannen et al. 2022). In other cases, incorporating seagrass fibers and leaves into mineral matrixes (gypsum, cement) has led to the improvement of thermal insulation (Jedidi and Abroug 2020; Mehrez et al. 2022). However, only a few studies deal with the investigation of *Zostera marina* seagrass species to be used for building insulation. *Zostera marina* leaves have been considered an effective insulation material since the 20th Century due to the high demand for energy-saving products (Wyllie-Echeverria and

Alan Cox 1999). Cabot's Quilt has been a popular commercial building material from the 1900s to the 1940s. The "blanket type" seagrass covered with the paper was advertised as a lightweight, heat- and sound-insulating, cost-effective material for loose-fill application in walls (Wyllie-Echeverria and Alan Cox 1999). The low energy requirements for the processing energy (typically about 10 times less than conventional materials) implies low production costs and makes seagrass an ecologically friendly building solution (Teppand, Jones, and Brischke 2017).

Although some of the characteristics of *Zostera marina* seagrass are already known from the past, no research has yet been carried out in the area of flexible insulation composites and their mechanical and physical characterization. Thus, the purpose of this paper is to fill this gap by examining the properties of flexible mats produced from the *Zostera marina* and comparing them with those of wood fiber mats. In addition to the mechanical and thermal properties, we studied the fire resistance and discussed the leaf/fiber size, the vertical density profile and their effect on the material's major properties.

Experimental part

Materials

Zostera marina seagrass leaves were provided by Seegrashandel GmbH (Westerau, Germany). The raw material was collected in the Baltic Sea. The dried, brownish leaves were from 5 to 60 cm long. They were cut into shorter pieces to avoid problems in the mixing process. For the production of reference mats, we used pine wood fibers (*Pinus sylvestris*) provided by Steico SE (Feldkirchen, Germany). Bi-component fibers (Bico), provided by (AL-Adhesion C, FiberVisions, Varde, Denmark), were utilized as a binding agent. Bico fibers consisted of two distinct raw polymeric components (Polypropylene in the inner layer and Polyethylene in the outer layer). Figure 1 shows the shape and size of the raw materials and the structure of the binder.

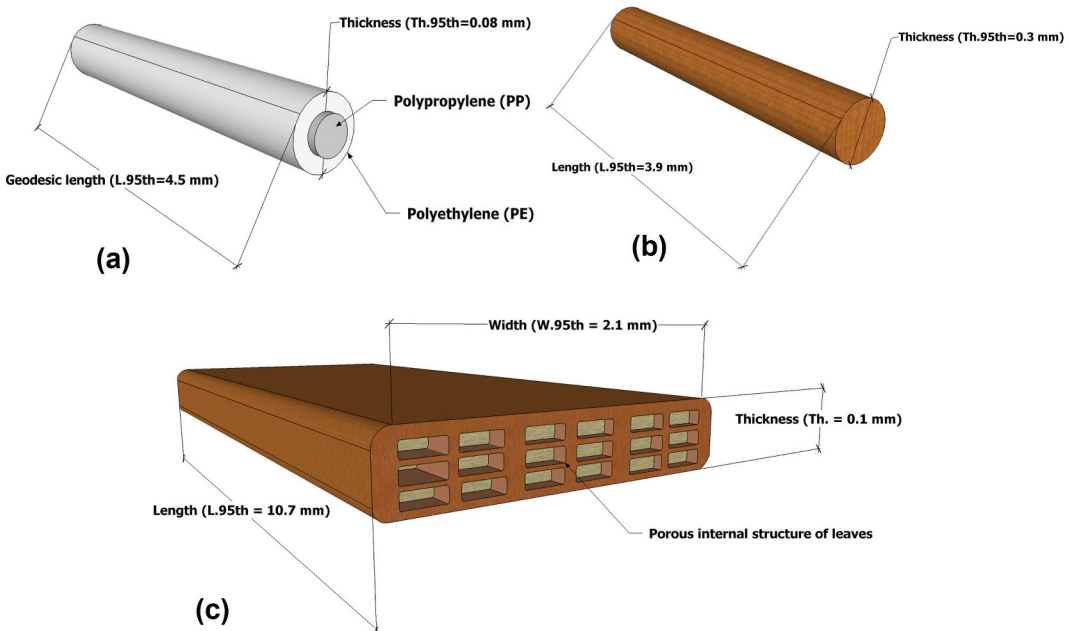


Figure 1. Geodesic size (95th percentile) and structure of Bico fibers (a), wood fibers (b) and seagrass leaves (c).

Methods

Size distribution of raw materials and binder

The size distribution (geodesic length) of seagrass leaves, wood and Bico fibers was determined using FibreShape PRO (X-shape, IST, Vilters, Switzerland). Representative samples of processed (after passing the mixing process) seagrass leaves (2 g), wood fibers (0.15 g) and Bico fibers (0.05 g) were manually dispersed on a transparent film and scanned using a flatbed scanner (Epson Perfection V850 Pro, Epson, Tokyo, Japan) in transmitted light mode. High-resolution images were created and scans were then loaded to the FiberShape software.

Production of insulation mats

The mats were produced by mixing 90 wt% raw material and 10 wt% Bico fibers followed by hot-pressing. The raw materials and Bico fibers were initially vigorously mixed using a hammer mill (Electra SAS VS1, Poudenas, France). The mixture was pre-pressed and then hot-pressed at 190°C. The hot-pressing time was 640 s (16 s mm⁻¹ thickness). A hot press (Joos HP-2000 lab, Gottfried Joos GmbH & Co.KG, Pfalzgrafenweiler, Germany) was utilized for the pressing operation. Two mats for each variant (in total, 16 mats) were prepared. The mats had 4 different target densities (80, 100, 150, and 200 kg m⁻³) and their dimensions were 450 × 450 × 40 mm³. The abbreviations of the produced boards are shown in Table 1.

Mechanical characterization

Before the determination of the physico-mechanical properties, the mats were cut into various specimen sizes and were conditioned at 50 ± 5% RH and 23 ± 2°C. Specimens whose density was within ±10% of the target density were selected for the following mechanical tests. For the compression test, a compressive force was applied perpendicular to the faces of the test specimen at a constant speed (0.1 d min⁻¹ ±25%, in which d is the thickness of the test specimen in mm) using a universal testing machine (ZwickRoell Zmartpro, ZwickRoell, Ulm, Germany) with a 10 kN load cell. The tests were conducted according to EN 826 (2013). The internal bond (tensile strength perpendicular to the faces) was evaluated following EN 1607 (2013). The test specimens (with nominal dimensions of 50 × 50 × 40 mm³) were glued with a fast-curing polymer adhesive between two stiff boards and thereafter were installed in the universal testing machine. Tensile stress was applied at a constant speed of 10 mm min⁻¹. An additional test was performed to determine the flexibility (or bendability) when a bending force is applied. Specimens were tested in a three-point bending test set up using a universal testing machine (ZwickRoell Zmartpro, Ulm, Germany), with the load applied to the specimen midway between the two supports. Specimens with dimensions of 300 × 50 × 40 mm³ were used for this test. The support span was 200 mm. The diameter of the load and support rollers was 15 mm. The specimens were bent to an elongation of 20 mm (or 0.5 d, where d is the thickness of the specimen in mm), and the applied force was recorded at a rate of 10 mm min⁻¹. After reaching the target elongation of 20 mm, the load was reversed at the same speed (10 mm min⁻¹) and the applied force

Table 1. Abbreviations for seagrass-based (SG) mats and wood fiber-based (WF) mats with various densities.

Type of mat	Raw material	Density (kg m ⁻³)
SG-80	Seagrass leaves	80
SG-100		100
SG-150		150
SG-200		200
WF-80	Wood fibers	80
WF-100		100
WF-150		150
WF-200		200

was recorded until the loading roll reached its initial position. The flexibility of the material was expressed as elongation (mm) divided by the applied force (N).

Density profile measurements

The X-ray density profile was determined using a Grecon Density profiler (Fagus-GreCon Greten GmbH & Co., Alfeld, Germany). For the density profile measurements we selected representative specimens with target densities of 100 and 200 kg m⁻³ for each type of mat. Specimens with dimensions 50 × 50 × 40 mm³ were inserted into the machine so that the X-ray ran in the vertical direction. The X-ray scanning speed was 2 mm s⁻¹.

Microscopy investigation

The cross-section part of mats' specimens was imaged using the Keyence VHX-5000 digital 3D reflected light microscope (Keyence, Neu-Isenburg, Germany). The acquired images were captured at magnifications of 50× and 150×. Scanning electron microscope (SEM) images were taken using a Zeiss EVO LS 15 Microscope (Carl Zeiss Microscopy GmbH, Jena, Germany). The acquired SEM images were captured at magnifications of 164× and 430× for seagrass- and wood-based mats specimens respectively.

Thermal conductivity measurements

A 446 Lambda Eco-Line Heat Flow Meter (NETZSCH Group, Selb, Germany) was utilized to determine thermal conductivity. The test procedure was in accordance with the standard EN 12667 (2001). One specimen per board (in total 8 specimens for each type of mat) measuring 250 × 250 × 40 mm³ were tested at mean temperatures varying from 10 to 30 °C. The thermal conductivity at 23 °C (λ_{23}) was calculated by applying linear regression.

Cone calorimetry tests and thermogravimetric analysis

The procedure described in the standard ISO 5660-1 (2002) was adopted for the cone calorimetric measurements using a mass loss calorimeter (MLC FTT, Fire Testing Technology, East Grinstead, UK). Tetragonal specimens (100 × 100 mm²) with a given thickness were exposed to a heat flux of 50 kW m⁻² for 30 min. The thermogravimetric analysis was performed using a NETZSCH TG 209F1 Iris (Erich NETZSCH GmbH & Co. Holding KG, Selb, Germany). The test was carried out using an oxidative environment (a mixture of 4 mL min⁻¹ oxygen and 16 mL min⁻¹ nitrogen) to imitate the combustion of raw materials under natural conditions. The samples were placed in open alumina crucibles. The heating rate for the test was 20 K min⁻¹ starting from 50 to 1000 °C.

Results and discussion

Size distribution and morphological considerations

Static image analysis revealed the significant size differences between the raw aggregates in terms of geodesic length (Figure 2). Seagrass leaves were much larger compared to wood fibers, reaching a maximum length (95th percentile) of up to 10.7 mm, while wood fibers could be up to 3.9 mm long. During the mixing process, some of the leaves were chopped and their size was decreased. In the case of seagrass leaves, the curve showing the geodesic length density distribution skewed toward the maximum values. A wide length distribution representing wood fibers indicates that a high amount of fines (possibly caused by the intense mixing) is also present in the batch of fibers. The binding agent (Bico fibers) and wood fibers have fairly similar mean geodesic lengths of 1.2 and 1.5 mm, respectively. In addition to their size distribution, seagrass leaves differ from wood fibers in terms of shape. Wood and Bico fibers have a cylindrical structure, whereas seagrass leaves display a prismatic form (Figure 1). Along with the size, the shape plays a vital role in the bonding mechanism and, more specifically, in the ability of Bico fibers to bridge with the raw lignocellulosic material.

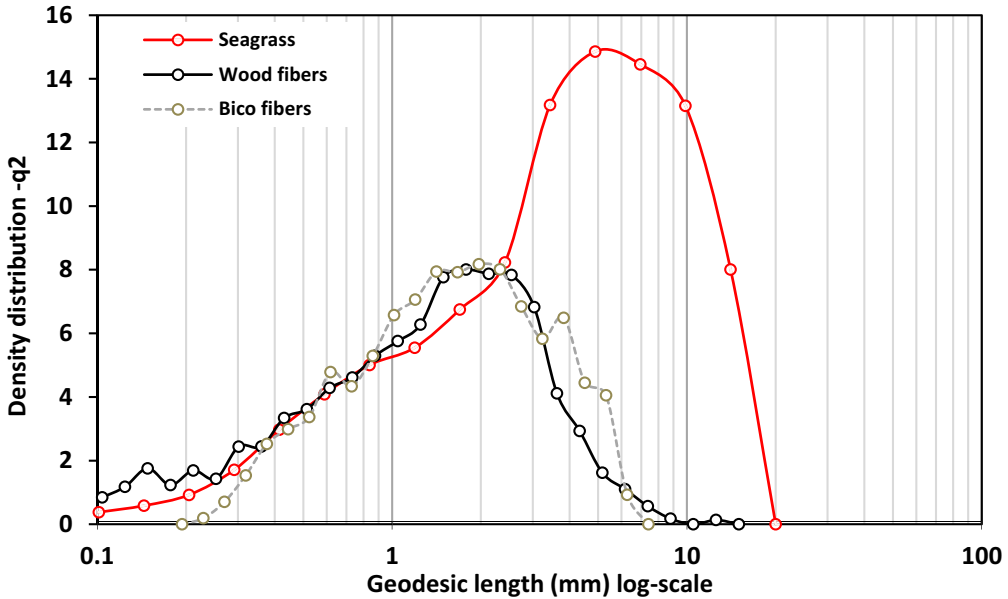


Figure 2. Geodesic length size distribution of seagrass *Zostera marina*, wood fibers and Bico fibers.

Density profile

The vertical density profiles of SG and WF based mats are shown in Figure 3(a,b), respectively. The vertical density profile highly depends on the compressibility of the mats and the processing method used to prepare them. The variants with a density of 100 kg m^{-3} (SG-100 and WF-100) are pretty similar. Their density profiles are even, indicating a uniform density distribution. The roughness (magnitude of local oscillations of density) of the density profile curves is another significant dissimilarity between these mats. The curve in the SG-100 is rougher compared to the one of WF-100. The roughness indicates the number and the size of voids and pores in the mat. The rougher the curve, the larger the air voids.

The differences in roughness were also observed in the curves representing the density profiles of the samples with the higher target density (SG-200 and WF-200). However, significant differences can be seen when comparing the shape of high-density with low-density mats (Figure 3(a,b)). The density close to the faces reached up to 430 kg m^{-3} . The higher the target density, the more uneven is the vertical density profile (Benthien and Ohlmeyer 2017). The “U-shaped” density profile indicates that the board can be better glued, laminated and exhibit a high bending strength (Shi et al. 2005; Wang et al. 2001). On the other hand, a low density in the middle of the profile curve (transversal direction) implies a weak area with low compaction and, eventually, low internal bond strength.

Mechanical properties

The mean compression force at 10% strain (σ_{10}) is shown in Table 2. The compression strength increased with the target density. This was to be expected, as a large amount of material per unit volume results in a low number of air voids and a more compact material. Regarding the differences between the two types, the SG mats appeared to have slightly lower compression strengths except for the variant having a target density of 100 kg m^{-3} (SG-100). The compression strength is firmly associated with the bonding mechanism of the mats. More specifically, bonding is related to the mechanical interlocking, the morphology of the lignocellulosic aggregates and the number of bridging points between them and the Bico fibers. In terms of compression strength, wood fibers have a lower

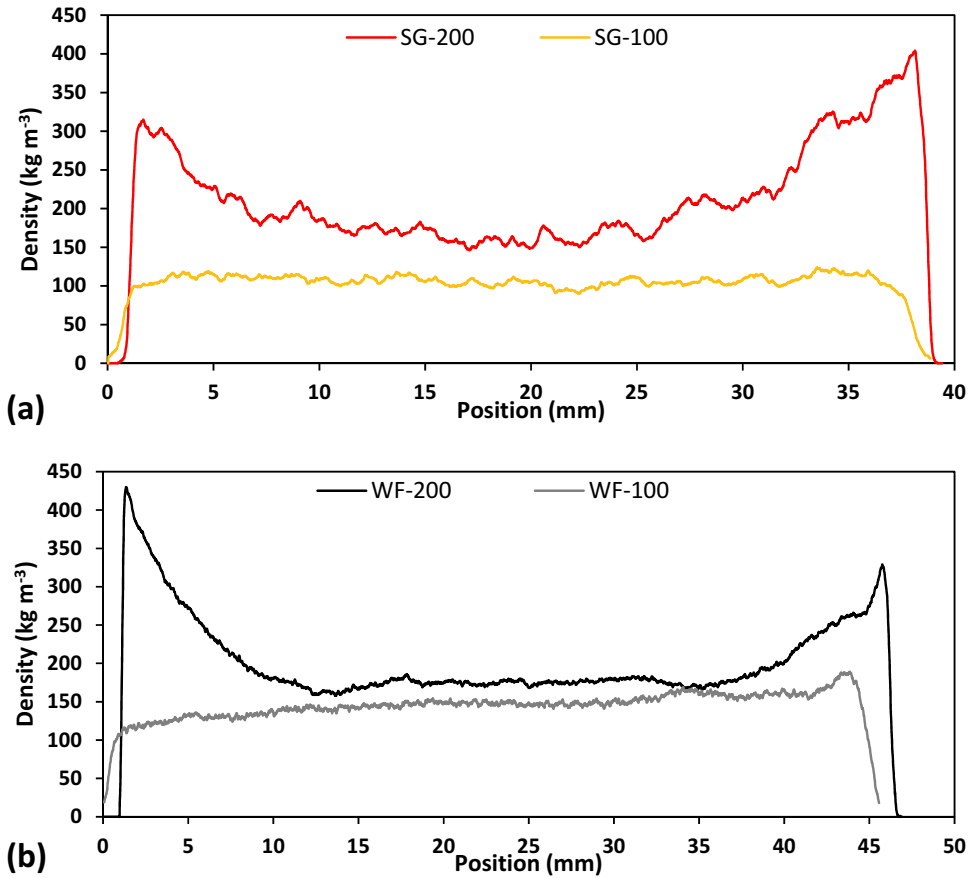


Figure 3. Density profile of seagrass-based (SG) mats (a) and wood fiber-based (WF) mats (b).

Table 2. Mechanical properties of prepared seagrass (SG) and wood fiber (WF) mats.

Type of mat	Compression strength (kPa)	Internal bond strength (kPa)	Flexibility (mm N ⁻¹) *
SG-80	2.6 ± 0.1	5.1 ± 0.7	6.7
SG-100	4.5 ± 0.7	5.1 ± 0.2	6.6
SG-150	6.5 ± 1.0	5.7 ± 0.9	1.2
SG-200	15.0 ± 3.0	7.1 ± 0.1	0.7
WF-80	2.7 ± 0.1	1.5 ± 0.2	5.9
WF-100	3.7 ± 0.2	2.6 ± 0.6	2.1
WF-150	6.8 ± 1.0	2.9 ± 0.7	0.7
WF-200	19.8 ± 2.3	8.1 ± 0.6	0.3

Mean values and standard deviations (±) of 4 (2 sets × 2 samples) replicates for each type of mat. *Mean values of 2 replicates for each type of mat.

uncompacted bulk density and thus greater specific volume than seagrass leaves, forming bundles (agglomerates of wood fibers) that require high stress to compress them. In contrast, the compression strength of the SG-100 mat is higher compared to the corresponding WF mat. This behavior might be related to the better distribution of the raw material in the pre-pressed seagrass leaves-Bico fibers mixture. The mats exhibited much higher compression strengths at high densities (SG-200 and WF-200). As previously mentioned, density in the faces of prepared mats was substantially high (Figure 3). The high density of the surfaces implies that the Bico fibers, consisting of PE and PP, are entirely melted, as both have lower melting temperatures than the hot press (190 °C). As this layer of the

premixed blend is in direct contact with the hot press, a semi-plastic compact and stable layer is formed. This layer might have contributed to the high compression strength of the mats. There are several parameters which affect the

With the exception of the specimen with the highest target density (SG-200), the mats comprised of seagrass displayed up to 240% higher internal bond strength than wood-based mats (Table 2). As shown in the standard force – strain graph shown in Figure 4(a), along with internal bond strength values, SG mats displayed a higher toughness compared to the corresponding WF mats. The deformation at the maximum standard force for the former was 2 to 4 times higher than the latter, indicating a high degree of elasticity of SG mats. During the internal bond test, the mats made of seagrass developed small fractures, while the specimen itself contracted in the directions perpendicular to the specific loading direction (higher Poisson ratio). In the case of WF mats, however, the development of fractures occurred much earlier, while their size was much larger than the fractures that appeared in the SG mats (Figure 4(a)). With further increase in density, the internal bond of WF mats seems to increase much faster compared to SG mats (Figure 4(b)). Still, at low densities, SG mats seem to be superior.

The microscopy images presented in Figure 5 show the cut cross-sectional side of the produced mats. The dissimilarities in terms of stretchability and high internal bond strength for the two types of mats are associated with the ability of the single Bico fibers (indicated by blue arrows) to bond with the raw material and, most importantly, to bond with each other. Seagrass leaves are larger aggregates compared to wood fibers, and, as a result, their corresponding mats have large voids and pores as reflected in density fluctuations (Figure 3). The presence of large voids can facilitate the bonding (white arrows) of Bico fibers with each other (Figure 5(a,c), white arrows), constructing a three-dimensional network of plastic fibers with seagrass leaves incorporated into their structure. In addition, some Bico fibers are also bonded with the seagrass leaves, resulting in an even more sturdy structure.

In the case of WF mats, Bico fibers tended to predominately bond to wood fibers rather than with other Bico fibers (Figure 5(b,d)), red arrows). As the proportion of binding fibers is only 10 wt%, and they are well dispersed in the mixture, it might be presumed that they are surrounded by wood fibers forming tiny wood fiber agglomerates (fibers interlocked with each other). The strength of the bond (degree of adhesion) between two plastic Bico fibers seemed to be higher than the Bico-wood fiber

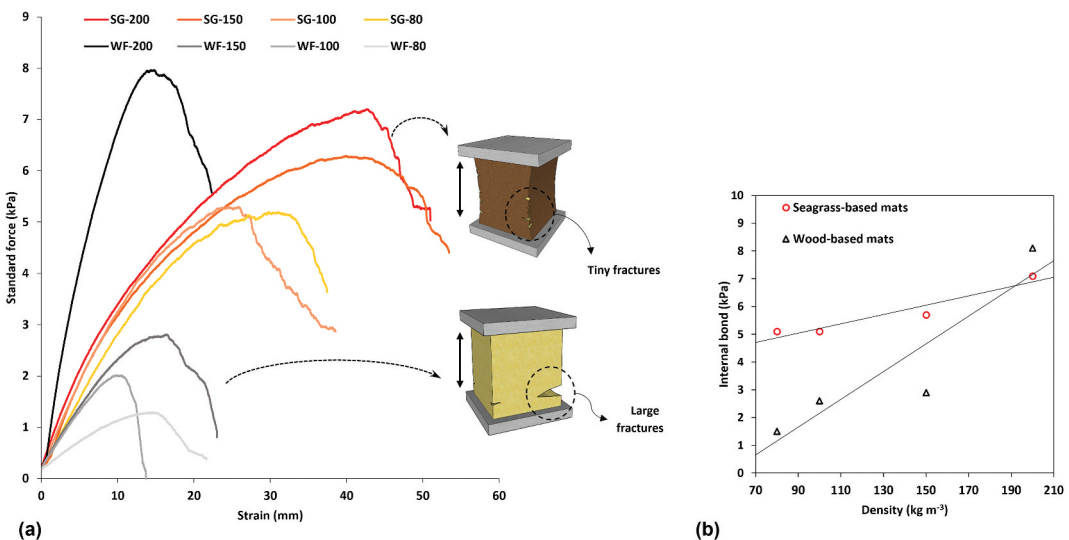


Figure 4. Standard force vs. strain during the internal bond test of seagrass-based (SG) and wood fiber-based (WF) mats at various target densities (a), and the internal bond values as a function of density (b).

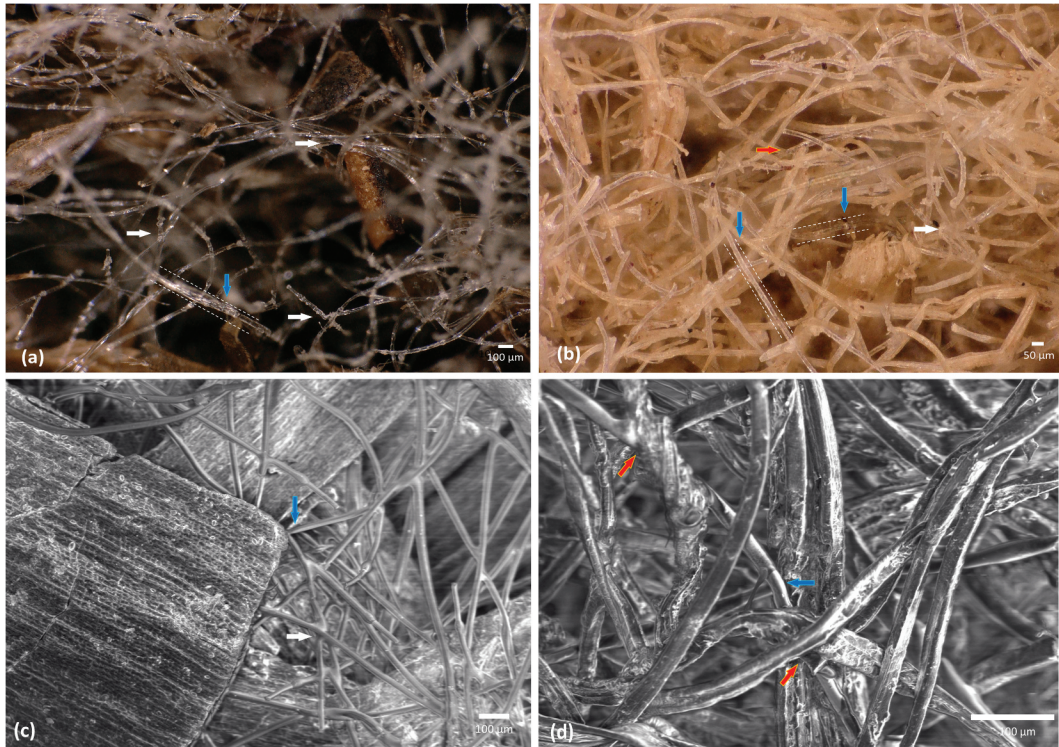


Figure 5. Digital micrographs and images obtained by scanning electron microscopy of seagrass-based (SG) mats (a, c), and wood-based fiber (WF) mats (b, d). Blue arrows indicate the Bico fibers, white arrows indicate the bond between two Bico fibers and red arrows indicates the bond between Bico and wood fiber.

bond. During the hot-pressing process, the applied heat partially melts the outer layer of Bico fibers. Sintering acts to bond fibers together into a strong network. As for the Bico-wood fiber bond, the degree of sintering is lower. As a result, the wood fibers can de-bond easier when subjected to transversal stress, resulting in lower internal bond strength and stretchability (elasticity).

Similar studies have reported that the type of binder affects the strength of the insulation material (Imken, Kraft, and Mai 2021). Both compressive and internal bond strength of materials bonded with bico fibers appear to be lower than when other binders such as pMDI are used (Imken, Kraft, and Mai 2021). Higher strength values were obtained when using other natural fibers such as flax, jute, and hemp compared to our results (Korjenic, Zach, and Hroudová 2016). However, it should be noted that the proportion of bico fibers in the aforementioned study was twice as high as in our study, which might lead to strength increase.

Compared to the corresponding WF mats, the SG mats appear to be more flexible (Table 2). For both types of mats, flexibility tends to decrease with increasing density. The lower the density, the less compact the mats and the lower the resistance to deformation. Flexibility (the opposite of stiffness) was particularly high for the low-density mats, reaching up to 6.7 mm N^{-1} .

The ability of the mat to return to its original shape (elasticity) was measured by determining the bending force during release of the load cell. As can be seen in Figure 6, the bending resistance of the mat drops sharply after the strain reaches 20 mm and the load cell is released back, and then stabilizes when the strain is reduced to 0. At a strain of about 2 to 4 mm, the bending resistance force is 0, which means that the load cell is no longer in contact with the specimen. This behavior indicates that after bending the mat can recover its initial position up to 90%. The low strain at which the bending resistance force becomes 0 N indicates a high ability of the mat to return to its original position (high

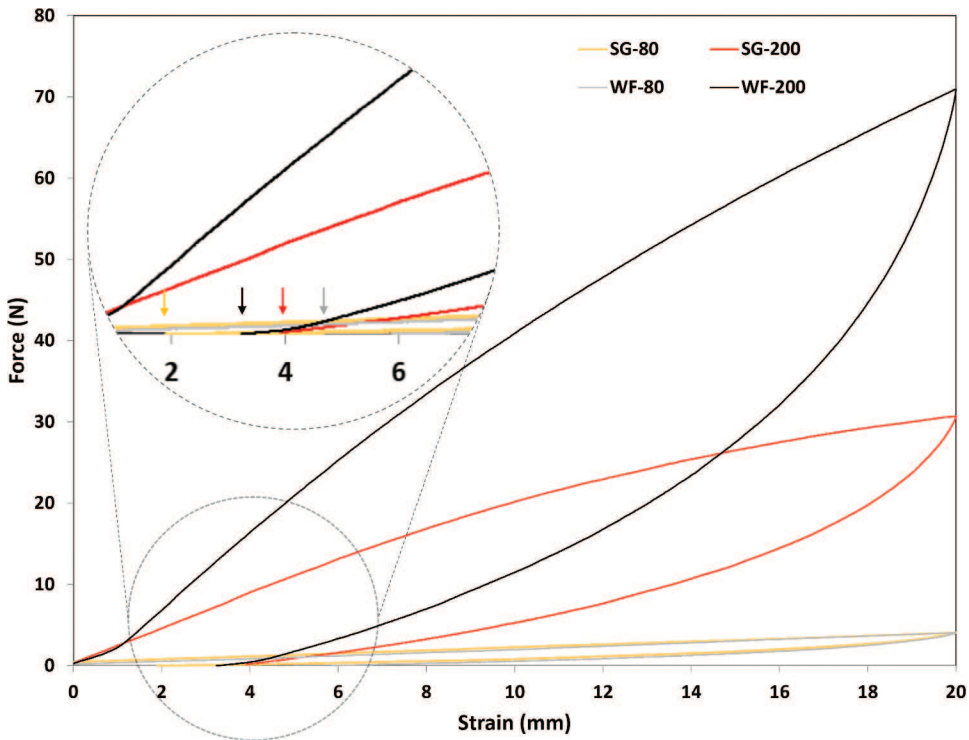


Figure 6. The applied force vs strain plot (1 full cycle) indicating the bending flexibility of mats.

elasticity). On the other hand, the leaf-like structure formed (hysteresis) indicates that the mats have partial plastic deformation. It should be noted that the larger the area within the leaf-like structure, the higher the plastic behavior of the mat. Conversely, the larger the area below the leaf-like structure, the more elastic the behavior. **Figure 6** clearly shows that low density mats (SG-80 and WF-80) are more elastic than high density mats. An easily bendable mat, contrarily to stiff boards, can be used to insulate irregular areas in the building.

Thermal conductivity

Figure 7 shows the thermal conductivity for various densities. For target densities starting at 80 to 200 kg m^{-3} , thermal conductivity initially decreased and then tended to increase. Its values varied from 0.0390 to 0.0510 $\text{W m}^{-1} \text{K}^{-1}$ for SG mats and from 0.0389 to 0.0465 $\text{W m}^{-1} \text{K}^{-1}$ for WF mats. It should also be noted that the real densities of SG mats have deviated from the target density and are considerably higher than WF mats. Therefore, thermal conductivities are expected to be significantly higher for the former. Still, SG mats exhibit similar or even lower thermal conductivities than boards prepared by other natural resources. Previous research has reported that the thermal conductivity of most mineral and lignocellulosic materials varies from 0.030 to 0.070 $\text{W m}^{-1} \text{K}^{-1}$ (Hung Anh and Pásztor 2021; Kumar et al. 2020). Other natural non-conventional fibers used to produce flexible materials (nonwovens) have shown promising results in terms of thermal conductivity. Thilagavathi et al. (2020), Samanta et al. (2021) and Kumar et al. (2021) reported very low thermal conductivity values of 0.02 to 0.05 $\text{W m}^{-1} \text{K}^{-1}$, which are comparable or even better than those of synthetic insulation materials. However, due the low density, it would be expected that the mechanical properties would also be low. In another study using Bico-bonded mats with lower or similar densities to ours, thermal conductivities vary between 0.04 and 0.05 $\text{W m}^{-1} \text{K}^{-1}$ (Korjenic, Zach, and Hroudová (2016). From

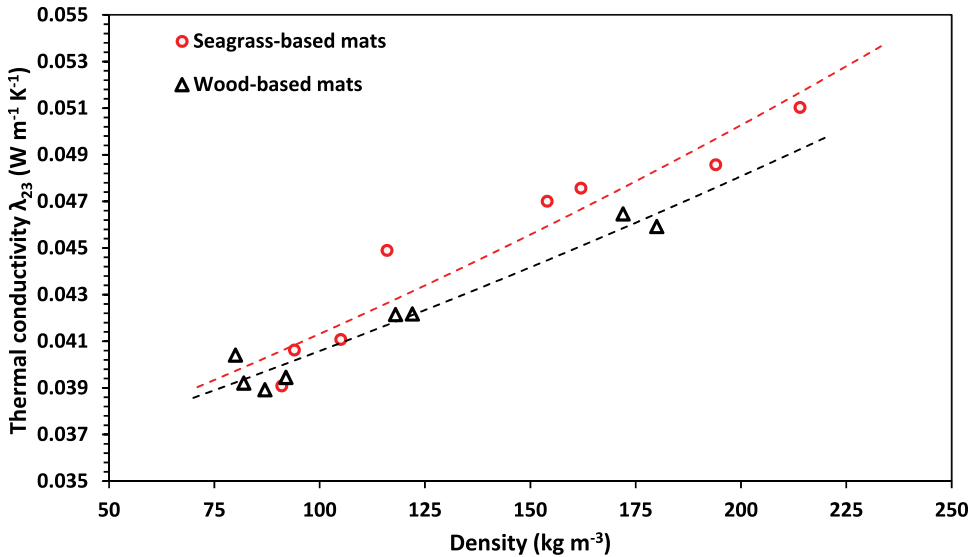


Figure 7. Thermal conductivity at 23 °C (λ_{23}) of seagrass-based (SG) and wood fiber-based (WF) mats at various densities.

Figure 7, it appears that materials based on seagrass leaves have similar thermal conductivities to the natural fibers (hemp, flax and jute) from the study mentioned above.

The predominant mechanisms of heat transfer in the case of indoor insulation materials are convection and conduction. Convection is the movement of heat by the actual motion of air molecules through the air voids of the mats. Conversely, conduction can occur through the raw lignocellulosic aggregates and the Bico fibers. The slightly higher thermal conductivity of SG mats compared to WF mats is mainly associated with the thermal conductivity of seagrass leaves and their arrangement in the mat (presence of large voids). Materials with the same density but larger pore sizes can transfer heat better via convection because the air can flow more easily (Hung Anh and Pásztor 2021; Xie et al. 2011). Another reason for the high thermal conductivity of SG compared to WF mats could be related to the ability of bico fibers to bond and transfer heat to each other. Since Bico fibers are plastic materials, they have higher thermal conductivity than lignocellulosic materials (Ebadi-Dehaghani and Nazempour 2012). In the case of SG mats, the Bico fibers tend to predominantly interconnect and form a three-dimensional network. Heat is thus transferred (conduction) through the net-like structure, resulting in higher thermal conductivity of SG compared to WF mats.

Fire resistance

Insulation boards made of natural or synthetic organic materials have been shown to be problematic when it comes to resistance to fire (Graupner and Müssig 2010; Kumar et al. 2020; Zou et al. 2021). Seagrass leaves may contain high amounts of minerals (sand, salts) as they are collected from the seashores. Previous studies have confirmed that composites containing seagrass fibers (species: *Posidonia oceanica*) do not burn quickly and are nonflammable (Mayer et al. 2022). Cone calorimetry data are presented in Figure 8 and Table 3. Results showed that SG mats displayed higher fire resistance than WF mats. All of the specimens ignited within the first 10 seconds. Initially, a major heat peak was noticed for both types of mats. However, the peak intensity was significantly different for the two types. The peak heat release (PHR) was not dependent on the density of the mats. WF mats had a PHR value approximately twice as high as SG mats (Table 3). The total heat release (THR), which represents the total amount of energy released during the test period (1800 s), was again considerably higher for the WF mats compared to SG mats. The THR values depended on the density

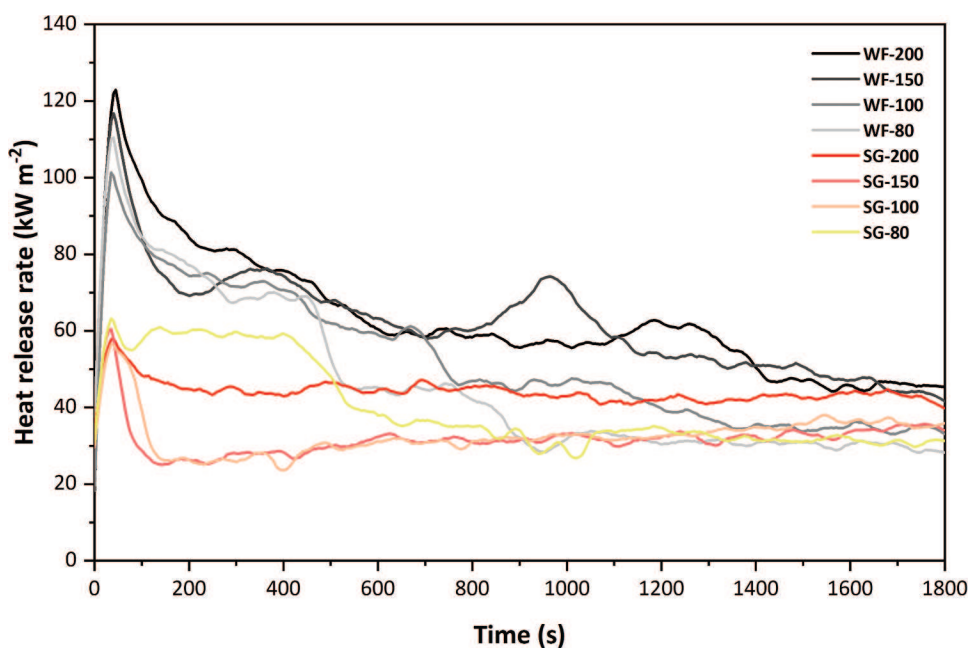


Figure 8. The heat release rate of seagrass-based (SG) and wood fiber-based (WF) mats.

Table 3. Results of cone calorimetry tests.

Type of mat	Peak heat release (kW m^{-2})	Total heat release (MJ m^{-2})	Flame period (s)	Mass loss rate at 300 s (10^{-2} g s^{-1})	Mass lost during the flame period (%)
SG-80	64.3	72.0	518	5.5	76.8
SG-100	56.2	58.9	89	5.2	10.9
SG-150	60.1	57.3	41	5.1	3.4
SG-200	58.7	79.3	1790	5.1	70.8
WF-80	109.6	83.0	494	6.1	80.8
WF-100	99.1	93.8	693	5.6	86.0
WF-150	114.9	111.9	1056	9.8	85.0
WF-200	121.5	113.7	1387	8.7	86.3

of WF mats. With increasing density, the mass of organic material per unit volume increased, leading to the increment of the energy released during combustion. The THR for seagrass-based mats, on the other hand, did not seem to be affected by density but rather by the duration of flaming. For all SG mat specimens, the flame intensity was very low. Only tiny flames appeared during the combustion process. Nevertheless, the flame period observed for SG-80 and SG-200 was much longer than for SG-100 and SG-150. The mass-loss rate (MLR) at 300 s varied from 0.051 to 0.055 g s^{-1} for SG mats and 0.056 to 0.098 g s^{-1} for WF mats. It is evident that the former burn and degrade more slowly compared to the latter.

The predominant parameters affecting the combustion of raw materials might be their chemical composition and morphological characteristics. A subsequent thermogravimetric analysis (TGA) was conducted to better understand the effect of these parameters. The TGA can reveal the impact of the chemical composition of the lignocellulosic material on the combustion process of the insulation mats.

The TGA curves (Figure 9) showed that after moisture release, thermal degradation of seagrass and wood fibers went through two different processes: the devolatilization step occurred between 250 and 350°C, and char formation took place above 350°C. The release of volatiles is attributed to the decomposition of three main constituents (hemicelluloses, cellulose and lignin), while the last step is assigned only to the combustion of previously formed char residues (Rowell 2005). There are two

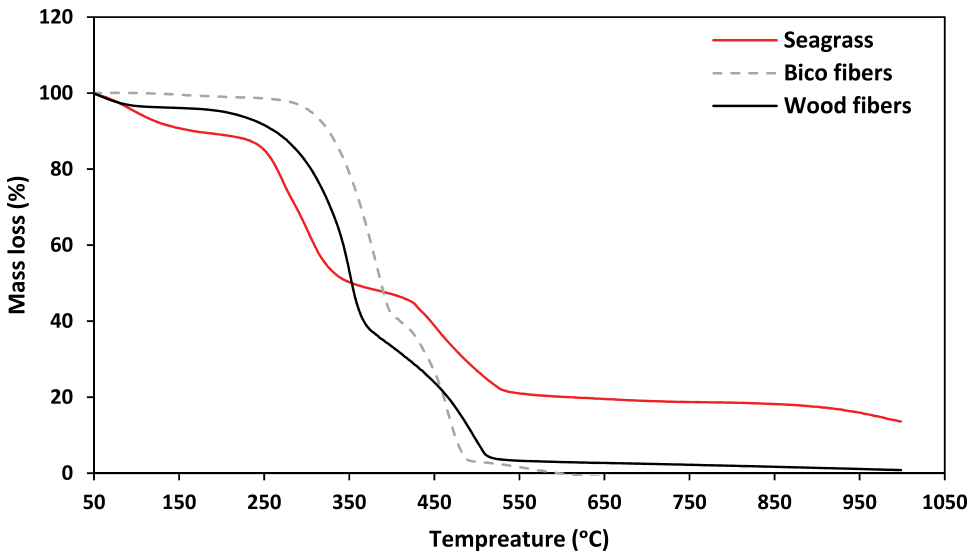


Figure 9. Thermogravimetric analysis of seagrass leaves, wood fibers and Bico fibers.

possible mechanisms associated with the higher fire resistance of seagrass compared to wood fibers. Firstly, due to the chemical composition of seagrass, the chemicals released in the first stages of oxidation alter fuel production by increasing the amount of char and reducing the amount of volatile combustible vapors and lowering the temperature at which pyrolysis begins. The pyrolysis/oxidation reactions are altered so that the thermal composition occurs at lower temperatures than wood fibers. As a result of this alteration, the amount of levoglucosan is reduced, leading to a reduction in the amount of volatile, combustible gases. This is similar behavior to fire-retardant-treated materials (LeVan and Winandy 1990; Rowell 2005). Secondly, another possible mechanism for the fire-retardancy of seagrass might be associated with salts such as sodium chloride (NaCl) on its surface. The presence of the salts might affect the vapor-phase reactions, as they may inhibit the chain reactions that involve the recombination of oxygen ions with halides (Cl⁻). The residual mass of burned seagrass is significantly higher compared to that of wood fibers (approximately 14%). It indicates the presence of high ash content in seagrass (sand particles, salts and other minerals).

The mass lost during the flame period in the cone calorimeter was considerably low for seagrass-based mats. This value can be as low as 24% of the total weight of the specimen (Table 3). The chemical composition of seagrass plays a determining role in the fire resistance of the respective SG mats. Regarding the Bico fibers, the TGA shows two major deviations of the TG curve. In the first period, from ~270 to 360°C, PE apparently oxidizes, implying a reduction in mass, while oxidation of PP occurs at higher temperatures (~360 to 480°C). The plastic Bico fibers are entirely oxidized at 600 °C.

Conclusion

Wood-based insulation boards have been already known as an ecological alternative to synthetic materials because of their ability to sequester carbon. Still, considering the scarce availability of wood and the high energy input for the production of wood fibers (refining process), other resources should also be taken into consideration. The seagrass leaves could be a potential candidate for fabricating insulation materials. The Mats composed of seagrass exhibit lower compression strength but higher internal bond than the reference WF mats. In terms of flexibility, SG mats are very elastic, especially at low target densities, as the binding fibers adhere to one another to form a stable three-dimensional network. The thermal conductivity of SG mats varies from 0.039 to 0.051 W m⁻¹ K⁻¹ and is correlated

with the mats' density. Mats comprised of seagrass have slightly higher thermal conductivity compared to those of wood, which is comparable to other known natural fibers. Regarding fire resistance, the low heat release rate of SG mats shows that seagrass leaves are an adequate and cost-effective resource for increasing the fire safety of buildings as no fire retardant needs to be applied. The difficulty in the combustion of SG mats is attributed to the chemical composition of seagrass leaves. The produced mats are adequate for interior wall partitions and roofing applications and are easy to install as they are flexible. The insulation products made from abundant waste material such as seagrass *Zostera marina* can be a sustainable and cost-effective solution for the building sector.

Highlights

- The thermal conductivity of produced mats varied from 0.039 to 0.051 W m⁻¹ K⁻¹.
- Seagrass-based mats possess exceptional fire resistance.
- Seagrass-based mats exhibit higher internal bond compared to wood fiber-based mats.
- Low-density mats are more flexible compared to those having high density.
- Flexible seagrass-based mats can be used for building insulation, particularly in irregular areas around the building.

Acknowledgments

The authors acknowledge support by the Open Access Publication Funds of the Göttingen University. This work was also supported by DAAD (German Academic Exchange Service). Funding was provided through the funding programme: Research Grants - Doctoral Programmes in Germany, DAAD.

Disclosure statement

No potential conflict of interest was reported by the author(s).

ORCID

Aldi Kuqo  <http://orcid.org/0000-0002-2698-1682>
 Carsten Mai  <http://orcid.org/0000-0002-1540-4185>

References

- Ayadi, M., R. Zouari, C. Segovia, A. Baffoun, S. Msahli, and N. Brosse. 2022. Development of airlaid non-woven panels for building's thermal insulation. *Construction Technologies and Architecture* 1:772–81. www.scientific.net/CTA.1.772.
- Benthien, J. T., and M. Ohlmeyer. 2017. Influence of face-to-core layer ratio and core layer resin content on the properties of density-decreased particleboards. *European Journal of Wood and Wood Products* 75 (1):55–62. doi:10.1007/s00107-016-1059-5.
- DIN EN 12667. 2001. *Thermal performance of building materials and products - determination of thermal resistance by means of guarded hot plate and heat flow meter methods - products of high and medium thermal resistance*. In *German version EN*, Vol. 12667, 2001. Berlin, Germany.
- DIN EN 1607. 2013. *Thermal insulating products for building applications - determination of tensile strength perpendicular to faces*. In *German version EN 1607:2013*. Berlin, Germany.
- DIN EN 826. 2013. *Thermal insulating products for building applications - determination of compression behaviour*. In *German version EN*, Vol. 826, 2013. Berlin, Germany.
- Ebadi-Dehaghani, H., and M. Nazempour. 2012. *Thermal conductivity of nanoparticles filled polymers*. London, UK: INTECH Open Access Publisher.
- Graupner, N., and J. Müssig. 2010. Technical applications of natural fibres: An overview Müssig, J. In *Industrial applications of natural fibres: Structure, properties and technical applications*. West Sussex, UK: John Wiley & Sons, Ltd 73–86.
- Hamdaoui, O., L. Ibos, A. Mazioud, M. Safi, and O. Limam. 2018. Thermophysical characterization of posidonia oceanica marine fibers intended to be used as an insulation material in mediterranean buildings. *Construction and Building Materials* 180:68–76. doi:10.1016/j.conbuildmat.2018.05.195.

- Hung Anh, L. D., and Z. Pásztor. 2021. An overview of factors influencing thermal conductivity of building insulation materials. *Journal of Building Engineering* 44:102604. doi:10.1016/j.job.2021.102604.
- Imken, A. A., R. Kraft, and C. Mai. 2021. Production and characterisation of wood-fibre insulation boards (WFIB) from hardwood fibres and fibre blends. *Wood Material Science & Engineering* 1–7. doi:10.1080/17480272.2021.1958919.
- ISO 5560-1. 2002. *Reaction-to-fire tests - heat release, smoke reduction and mass loss rate - part 1 - heat release rate (cone calorimeter method)*, 5660–1. Geneva, Switzerland.
- Jedidi, M., and A. Abroug. 2020. "Valorization of Posidonia oceanica Balls for the Manufacture of an Insulating and Ecological Material." *Jordan Journal of Civil Engineering* 14.3.
- Korjenic, A., J. Zach, and J. Hroudová. 2016. The use of insulating materials based on natural fibers in combination with plant facades in building constructions. *Energy and Buildings* 116:45–58. doi:10.1016/j.enbuild.2015.12.037.
- Kumar, D., M. Alam, P. X. Zou, J. G. Sanjayan, and R. A. Memon. 2020. Comparative analysis of building insulation material properties and performance. *Renewable and Sustainable Energy Reviews* 131:110038. doi:10.1016/j.rser.2020.110038.
- Kumar, N. M., T. G. P. S., and V. V. 2021. Development of needle punched nonwovens from natural fiber waste for thermal insulation application. *Journal of Natural Fibers* 19 (14):1–9. doi:10.1080/15440478.2021.1990175.
- Kuqo, A., A. Korpa, and N. Dharmo. 2019. Posidonia oceanica leaves for processing of PMDI composite boards. *Journal of Composite Materials* 53 (12):1697–703. doi:10.1177/0021998318808024.
- Kuqo, A., and C. Mai. 2022. Seagrass leaves: An alternative resource for the production of insulation materials. *Materials* 15 (19):6933. doi:https://doi.org/10.3390/ma15196933.
- LeVan, S. L., and J. E. Winandy. 1990. Effects of fire retardant treatments on wood strength: A review. *Wood and Fiber Science* 22:113–31.
- Mayer, A. K., A. Kuqo, T. Koddenberg, and C. Mai. 2022. Seagrass-and wood-based cement boards: A comparative study in terms of physico-mechanical and structural properties. *Composites Part A, Applied Science and Manufacturing* 156:106864. doi:10.1016/j.compositesa.2022.106864.
- Mehrez, I., H. Hachem, R. Gheith, and A. Jemni. 2022. Valorization of Posidonia-Oceanica leaves for the building insulation sector. *Journal of Composite Materials*. 56:1973–1985. doi:10.1177/2F00219983221087793
- Rowell, R. M. 2005. *Handbook of wood chemistry and wood composites*. London, UK: CRC press.
- Samanta, K. K., I. Mustafa, S. Debnath, E. Das, G. Basu, and S. K. Ghosh. 2021. Study of thermal insulation performance of layered jute nonwoven: A sustainable material. *Journal of Natural Fibers* 19 (11):1–14. doi:10.1080/15440478.2020.1856274.
- Schulte, M., I. Lewandowski, R. Pude, and M. Wagner. 2021. Comparative life cycle assessment of bio-based insulation materials: Environmental and economic performances. *GCB Bioenergy* 13 (6):979–98. doi:10.1111/gcbb.12825.
- Shi, J. L., S. Y. Zhang, B. Riedl, and G. Brunette. 2005. Flexural properties, internal bond strength, and dimensional stability of medium density fiberboard panels made from hybrid poplar clones. *Wood and Fiber Science* 37:629–37.
- Teppand, T. G., D. Jones and C. Brischke. 2017. *Performance of bio-based building materials*. Duxford, UK: Woodhead Publishing.
- Thilagavathi, G., N. Muthukumar, S. Neela Krishnanan, and T. Senthilram. 2020. Development and characterization of pineapple fibre nonwovens for thermal and sound insulation applications. *Journal of Natural Fibers* 17 (10):1391–400. doi:10.1080/15440478.2019.1569575.
- Tsemekidi-Tzeiranaki, S., N. Labanca, B. Cuniberti, A. Toleikyte, P. Zangheri, and P. Bertoldi. 2019. Analysis of the annual reports 2018 under the energy efficiency directive—summary report. Publications Office of the European Union: Luxembourg.
- Wang, S., P. M. Winistorfer, T. M. Young, and C. Helton. 2001. Step-closing pressing of medium density fiberboard; part 1. Influences on the vertical density profile. *Holz als roh-und Werkstoff* 59 (1–2):19–26. doi:10.1007/s001070050466.
- Wyllie-Echeverria, S., and P. Alan Cox. 1999. L'industrie de l'aileul (zostera marina zosteraeae) de la nouvelle-Écosse (1907–1960). *Economic Botany* 53 (4):419–26. doi:10.1007/BF02866721.
- Xie, Y., Q. Tong, Y. Chen, J. Liu, and M. Lin. 2011. Manufacture and properties of ultra-low density fibreboard from wood fibre. *BioResources* 6:4055–66.
- Zannen, S., M. T. Halimi, M. B. Hassen, E. H. Abualsauod, and A. M. Othman. 2022. Development of a multifunctional wet laid nonwoven from marine waste posidonia oceanica technical fiber and CMC binder. *Polymers* 14 (5):865. doi:10.3390/polym14050865.
- Zou, S., H. Li, L. Liu, S. Wang, X. Zhang, and G. Zhang. 2021. Experimental study on fire resistance improvement of wheat straw composite insulation materials for buildings. *Journal of Building Engineering* 43:103172. doi:10.1016/j.job.2021.103172.

